NUREG/IA–0186

International Agreement Report

Analysis of the RELAP5/MOD3.2.2beta Critical Flow Models and Assessment Against Critical Flow Data From the Marviken Tests

Prepared by

C. Queral, J. Mulas, C. G. de la Rúa

Energy Systems Department
School of Mining Engineering
Polytechnic University of Madrid
SPAIN

Office of Nuclear Regulatory Research
U.S. Nuclear Regulatory Commission
Washington, DC 20555–0001

July 2000

Prepared as part of
The Agreement on Research Participation and Technical Exchange
under the International Code Application and Maintenance Program (CAMP)

Published by
U.S. Nuclear Regulatory Commission

AVAILABILITY OF REFERENCE MATERIALS IN NRC PUBLICATIONS

NRC Reference Material

As of November 1999, you may electronically access NUREG-series publications and other NRC records at NRC's Public Electronic Reading Room at www.nrc.gov/NRC/ADAMS/index.html. Publicly released records include, to name a few, NUREG-series publications; *Federal Register* notices; applicant, licensee, and vendor documents and correspondence; NRC correspondence and internal memoranda; bulletins and information notices; inspection and investigative reports; licensee event reports; and Commission papers and their attachments.

NRC publications in the NUREG series, NRC regulations, and *Title 10, Energy*, in the Code of *Federal Regulations* may also be purchased from one of these two sources.

1. The Superintendent of Documents
   U.S. Government Printing Office
   P. O. Box 37082
   Washington, DC 20402–9328
   www.access.gpo.gov/su_docs
   202–512–1800
2. The National Technical Information Service
   Springfield, VA 22161–0002
   www.ntis.gov
   1–800–553–6847 or, locally, 703–605–6000

A single copy of each NRC draft report for comment is available free, to the extent of supply, upon written request as follows:

Address: Office of the Chief Information Officer,
Reproduction and Distribution
Services Section
U.S. Nuclear Regulatory Commission
Washington, DC 20555-0001
E-mail: DISTRIBUTION@nrc.gov
Facsimile: 301–415–2289

Some publications in the NUREG series that are posted at NRC's Web site address www.nrc.gov/NRC/NUREGS/indexnum.html are updated regularly and may differ from the last printed version.

Non-NRC Reference Material

Documents available from public and special technical libraries include all open literature items, such as books, journal articles, and transactions, *Federal Register* notices, Federal and State legislation, and congressional reports. Such documents as theses, dissertations, foreign reports and translations, and non-NRC conference proceedings may be purchased from their sponsoring organization.

Copies of industry codes and standards used in a substantive manner in the NRC regulatory process are maintained at—

The NRC Technical Library
Two White Flint North
11545 Rockville Pike
Rockville, MD 20852–2738

These standards are available in the library for reference use by the public. Codes and standards are usually copyrighted and may be purchased from the originating organization or, if they are American National Standards, from—

American National Standards Institute
11 West 42nd Street
New York, NY 10036–8002
www.ansi.org
212–642–4900

The NUREG series comprises (1) technical and administrative reports and books prepared by the staff (NUREG–XXXX) or agency contractors (NUREG/CR–XXXX), (2) proceedings of conferences (NUREG/CP–XXXX), (3) reports resulting from international agreements (NUREG/IA–XXXX), (4) brochures (NUREG/BR–XXXX), and (5) compilations of legal decisions and orders of the Commission and Atomic and Safety Licensing Boards and of Directors' decisions under Section 2.206 of NRC's regulations (NUREG–0750).

DISCLAIMER: This report was prepared under an international cooperative agreement for the exchange of technical information. Neither the U.S. Government nor any agency thereof, nor any employee, makes any warranty, expressed or implied, or assumes any legal liability or responsibility for any third party's use, or the results of such use, of any information, apparatus, product or process disclosed in this publication, or represents that its use by such third party would not infringe privately owned rights.

NUREG/IA–0186

International Agreement Report

Analysis of the RELAP5/MOD3.2.2beta Critical Flow Models and Assessment Against Critical Flow Data From the Marviken Tests

Prepared by

C. Queral, J. Mulas, C. G. de la Rúa

Energy Systems Department
School of Mining Engineering
Polytechnic University of Madrid
SPAIN

Office of Nuclear Regulatory Research
U.S. Nuclear Regulatory Commission
Washington, DC 20555–0001

July 2000

Prepared as part of
The Agreement on Research Participation and Technical Exchange
under the International Code Application and Maintenance Program (CAMP)

Published by
U.S. Nuclear Regulatory Commission

Abstract

In this report the critical flow models of RELAP5/MOD3.2.2beta have been analized. Firstly, an analysis of the implementation of the RELAP5/MOD3.2.2beta models have been performed in which it has been proved that the transition from the critical to the non-critical flow model is not well done for the Ransom-Trapp model. Secondly, a sensitivity analysis of both models (Ransom-Trapp and Henry-Fauske) in subcooled, two-phase and vapor conditions has been taken with respect to temperature, pressure, void-fraction, discharge coefficients, energy loss coefficient and disequilibrium parameter. Finally, seven Marviken tests have been simulated and compared with the experimental data in order to validate both models. As a part of this assessment, an adjustment of the discharge coefficients for the Ransom-Trapp model with different nodalizations has been done and also it has been checked which are the best values of the disequilibrium parameter for the Henry-Fauske model in subcooled and two-phase conditions.

Conclusions indicate that the behaviour of the Henry-Fauske model is better than that of the Ransom-Trapp. In this sense, the new model is an improvement with respect to the Ransom-Trapp.

Contents

1 Introduction **1**

2 Analysis of RELAP5/MOD3.2 Critical Flow Model **3**

2.1 Problems with the transition from CFM to Non-CFM. Logic of JCHOKE subroutine 4

3 Sensitivity Analysis of RELAP5/MOD3 CFM **7**

3.1 Sensitivity Analysis of Ransom-Trapp Model 7

3.1.1 Sensitivity Analysis of Subcooled CFM to Temperature, Pressure, MDC and Forward Energy Loss Coefficient 9

3.1.2 Sensitivity Analysis of Two-phase CFM to Void-fraction and TDC 30

3.1.3 Sensitivity Analysis of Steam CFM to Temperature, Pressure and SDC 38

3.2 Sensitivity Analysis of Henry-Fauske Model 47

3.2.1 Sensitivity Analysis of Subcooled CFM to Temperature, Pressure, Disequilibrium Parameter and Forward Energy Loss Coefficient 49

3.2.2 Sensitivity Analysis of Two-phase CFM to Void-fraction and Disequilibrium Parameter 50

3.3 Discussion and Conclusions of the Sensitivity Results 56

4 Assessment of RELAP5/MOD3 CFM against Marviken Tests **57**

4.1 Facility and Test Description 58

4.2 Models Description 64

4.3 Review of the Marviken Tests Simulation Bibliography 67

4.4 Results and Discussion of Boundary Condition Model (BCM). Ransom-Trapp Model 81

4.4.1 Comparison of Critical and Non-critical Flow Models 93

4.4.2 Selection of Model Options 99

4.4.3 Discharge Coefficient Adjustment 106

4.5 Results and Discussion of the Initial Condition Model (ICM). Ransom-Trapp Model 125

4.5.1 Discharge Coefficient Adjustment 125

4.5.2 Comparison between TRAC-BF1 and RELAP5/MOD3.2 Results 132

4.6 Results and Discussion of Boundary Condition Model (BCM). Henry-Fauske Model 132

5 Conclusions **139**

Bibliography **145**

I Appendix: Subroutine JCHOKE flow logic **148**

II Appendix: Modified JCHOKE Subroutine **163**

List of Figures

2.1 Selection model block diagram. JCHOKE Subroutine. 5

2.2 Transition from CFM to Non-CFM block diagram. JCHOKE subroutine. 6

3.1 Sensitivity nodalization model. 8

3.2 Pressure at the last node (Temperature sensitivity of the subcooled model, with increasing temperature). CFM on. 12

3.3 Pressure at the last node (Temperature sensitivity of the subcooled model, with increasing temperature). CFM off. 12

3.4 Temperature at the last node (Temperature sensitivity of the subcooled model, with increasing temperature). CFM on. 13

3.5 Temperature at the last node (Temperature sensitivity of the subcooled model, with increasing temperature). CFM off. 13

3.6 Mass flow at the last node (Temperature sensitivity of the subcooled model, with increasing temperature). CFM on. 14

3.7 Mass flow at the last node (Temperature sensitivity of the subcooled model, with increasing temperature). CFM off. 14

3.8 Mass flow at the last node (Temperature sensitivity of the subcooled model, with increasing temperature). Comparison of CFM on with CFM off. 15

3.9 Temperature at the last node (Temperature sensitivity of the subcooled model, with decreasing temperature). CFM on. 16

3.10 Temperature at the last node (Temperature sensitivity of the subcooled model, with decreasing temperature). CFM off. 16

3.11 Mass flow at the last node (Temperature sensitivity of the subcooled model, with decreasing temperature). CFM on. 17

3.12 Mass flow at the last node (Temperature sensitivity of the subcooled model, with decreasing temperature). CFM off. 17

3.13 Mass flow at the last node (Temperature sensitivity of the subcooled model, with decreasing temperature). Comparison of CFM on with CFM off. 18

3.14 Transition at temperature from CFM to Non-CFM. Subcooled region. 19

3.15 Subcooling. Transition from CFM to Non-CFM. Subcooled region. . . 19

3.16 Liquid temperature at the last node (Pressure sensitivity of the subcooled model, with increasing pressure). CFM on. 20

3.17 Liquid temperature at the last node (Pressure sensitivity of the subcooled model, with increasing pressure). CFM off. 20

3.18 Pressure at the last node (Pressure sensitivity of the subcooled model, with increasing pressure). CFM on. 21

3.19 Pressure at the last node (Pressure sensitivity of the subcooled model, with increasing pressure). CFM off. 21

3.20 Mass flow at nozzle exit (Pressure sensitivity of the subcooled model, with increasing pressure). CFM on. 22

3.21 Mass flow at nozzle exit (Pressure sensitivity of the subcooled model, with increasing pressure). CFM off. 22

3.22 Mass flow at nozzle exit (Pressure sensitivity of the subcooled model, with increasing pressure). Comparison of CFM on with CFM off. . . 23

3.23 Pressure at the last node (Pressure sensitivity of the subcooled model, with decreasing pressure). CFM on. 24

3.24 Pressure at the last node (Pressure sensitivity of the subcooled model, with decreasing pressure). CFM off. 24

3.25 Mass flow at nozzle exit (Pressure sensitivity of the subcooled model, with decreasing pressure). CFM on. 25

3.26 Mass flow at nozzle exit (Pressure sensitivity of the subcooled model, with decreasing pressure). CFM off. 26

3.27 Mass flow at nozzle exit (Pressure sensitivity of the subcooled model, with decreasing pressure). Comparison of CFM on with CFM off. . . 26

3.28 Pressure at the last node. MDC sensitivity of the subcooled model. . 27

3.29 Temperature at the last node. MDC sensitivity of the subcooled model. 27

3.30 Mass flow at nozzle exit. MDC sensitivity of the subcooled model. . . 28

3.31 Mass flow at nozzle exit. Energy loss coefficient sensitivity of the subcooled model. 28

3.32 Pressure at the last node. Energy loss coefficient sensitivity of the subcooled model. 29

3.33 Pressure at the last node. Void-fraction sensitivity of the two-phase model. Homogeneous and non-homogeneous models. 31

3.34 Void-fraction at nozzle exit. Void-fraction sensitivity of the two-phase model. Homogeneous model. 32

3.35 Mass flow at nozzle exit. Void-fraction sensitivity of the two-phase model. Homogeneous model. 32

3.36 Critical mass flux. Ransom-Trapp model. 33

3.37 Critical mass flux. Homogeneous model (Taken from [LAH-93] pp 444). 34

3.38 Void-fraction at nozzle exit. Void-fraction sensitivity of the two-phase model. Non-homogeneous model. 35

3.39 Mass flow at nozzle exit. Void-fraction sensitivity of the two-phase model. Non-homogeneous model. 35

3.40 Pressure at the last node. TDC sensitivity of the two-phase model. . 36

3.41 Void-fraction at nozzle exit. TDC sensitivity of the two-phase model. 36

3.42 Mass flow at nozzle exit. TDC sensitivity of the two-phase model. . . 37

3.43 Pressure at the last node (Temperature sensitivity of the steam model). CFM on. 40

3.44 Pressure at the last node (Temperature sensitivity of the steam model). CFM off. 40

3.45 Temperature at the last node (Temperature sensitivity of the steam model). CFM on. 41

3.46 Temperature at the last node (Temperature sensitivity of the steam model). CFM off. 41

3.47 Mass flow at nozzle exit (Temperature sensitivity of the steam model). CFM on. 42

3.48 Mass flow at nozzle exit (Temperature sensitivity of the steam model). CFM off. 42

3.49 Liquid temperature at the last node (Pressure sensitivity of the steam model). CFM on. 43

3.50 Liquid temperature at the last node (Pressure sensitivity of the steam model). CFM off. 43

3.51 Pressure at the last node (Pressure sensitivity of the steam model). CFM on. 44

3.52 Pressure at the last node (Pressure sensitivity of the steam model). CFM off. 44

3.53 Mass flow at nozzle exit (Pressure sensitivity of the steam model). CFM on. 45

3.54 Mass flow at nozzle exit (Pressure sensitivity of the steam model). CFM off. 45

3.55 Mass flow at nozzle exit (Pressure sensitivity of the steam model). Comparison of CFM on and CFM off. 46

3.56 Pressure at the last node. SDC sensitivity of the steam model. 47

3.57 Temperature at the last node. SDC sensitivity of the steam model. . 48

3.58 Mass flow at nozzle exit. SDC sensitivity of the steam model. 48

3.59 Mass flow at nozzle exit. Temperature sensitivity of the subcooled Henry-Fauske model, with increasing temperature. 50

3.60 Mass flow at nozzle exit. Temperature sensitivity of the subcooled Henry-Fauske model, with decreasing temperature. 51

3.61 Mass flow at nozzle exit. Pressure sensitivity of the subcooled Henry-Fauske model, with decreasing pressure. 51

3.62 Mass flow at nozzle exit. Disequilibrium parameter sensitivity of the subcooled Henry-Fauske model. 52

3.63 Mass flow at nozzle exit. Forward energy loss coefficient sensitivity of the subcooled Henry-Fauske model. 52

3.64 Mass flow at nozzle exit. Void-fraction sensitivity of the Henry-Fauske model. 53

3.65 Void fraction at nozzle exit. Void-fraction sensitivity of the Henry-Fauske model. 54

3.66 Critical mass flux. Henry-Fauske model. 54

3.67 Mass flow at nozzle exit. Disequilibrium parameter sensitivity of the Henry-Fauske model. 55

3.68 Void fraction at nozzle exit. Disequilibrium parameter sensitivity of the Henry-Fauske model. 55

4.1 Pressure vessel diagram. 59

4.2 Discharge pipe and test nozzle. 60

4.3 Test nozzle used from Test 15 onwards. 61

4.4 Locations of typical measurements in the pressure vessel. 63

4.5 MARVIKEN initial conditions models. 66

4.6 MARVIKEN boundary conditions models. 67

4.7 Evaporation during flashing. CATHARE, DRUFAN, RELAP5/MOD2 and THYDE-P2 codes. 68

4.8 Evaporation during flashing of TRAC-PF1 code and comparison of the models. 69

4.9 Pressure at bottom vessel. Test data. CFT-01. 82

4.10 Liquid temperature at bottom vessel. Test data. CFT-01. 82

4.11 Static quality at bottom vessel. Test data. CFT-01. 83

4.12 Pressure at bottom vessel. Test data. CFT-06. 83

4.13 Liquid temperature at bottom vessel. Test data. CFT-06. 84

4.14 Static quality at bottom vessel. Test data. CFT-06. 84

4.15 Pressure at bottom vessel. Test data. CFT-11. 85

4.16 Liquid temperature at bottom vessel. Test data. CFT-11. 85

4.17 Static quality at bottom vessel. Test data. CFT-11. 86

4.18 Pressure at bottom vessel. Test data. CFT-15. 86

4.19 Liquid temperature at bottom vessel. Test data. CFT-15. 87

4.20 Static quality at bottom vessel. Test data. CFT-15. 87

4.21 Pressure at bottom vessel. Test data. CFT-17. 88

4.22 Liquid temperature at bottom vessel. Test data. CFT-17. 88

4.23 Pressure at bottom vessel. Test data. CFT-21. 89

4.24 Liquid temperature at bottom vessel. Test data. CFT-21. 90

4.25 Static quality at bottom vessel. Test data. CFT-21. 90

4.26 Pressure at bottom vessel. Test data. CFT-24. 91

4.27 Liquid temperature at bottom vessel. Test data. CFT-24. 91

4.28 Static quality at bottom vessel. Test data. CFT-24. 92

4.29 Mass flow at nozzle exit. Comparison between CFM and non-CFM (BCM). CFT-01. 94

4.30 Mass flow at nozzle exit. Comparison between CFM and non-CFM (BCM). CFT-06. 95

4.31 Mass flow at nozzle exit. Comparison between CFM and non-CFM (BCM). CFT-11. 96

4.32 Mass flow at nozzle exit. Comparison between CFM and non-CFM (BCM). CFT-15. 96

4.33 Mass flow at nozzle exit. Comparison between CFM and non-CFM (BCM). CFT-17. 97

4.34 Mass flow at nozzle exit. Comparison between CFM and non-CFM (BCM). CFT-21. 97

4.35 Mass flow at nozzle exit. Comparison between CFM and non-CFM (BCM). CFT-24. 98

4.36 Void fraction. Comparison between CFM and non-CFM (BCM). CFT-01. 99

4.37 Void fraction. Comparison between CFM and non-CFM (BCM). CFT-06. 100

4.38 Void fraction. Comparison between CFM and non-CFM (BCM). CFT-11. 100

4.39 Void fraction. Comparison between CFM and non-CFM (BCM). CFT-15. 101

4.40 Void fraction. Comparison between CFM and non-CFM (BCM). CFT-17. 101

4.41 Void fraction. Comparison between CFM and non-CFM (BCM). CFT-21. 102

4.42 Void fraction. Comparison between CFM and non-CFM (BCM). CFT-24. 102

4.43 Mass flow at nozzle exit. Comparison between Homogeneous and Non-homogeneous options. BCM-J. CFT-15. 103

4.44 Mass flow at nozzle exit. Comparison between Homogeneous and Non-homogeneous options. BCM-J. CFT-24. 103

4.45 Mass flow at nozzle exit. Comparison between Homogeneous and Non-homogeneous options. BCM-P. CFT-15. 104

4.46 Mass flow at nozzle exit. Comparison between Homogeneous and Non-homogeneous options. Nozzle modeled as PIPE (BCM). CFT-24. 104

4.47 Comparison of Single junction, Trip-Valve and Motor-Valve Models. Subcooled CFM. MDC=1.0, 0.85 (BCM). CFT-21. 105

4.48 Comparison of Single junction, Trip-Valve and Motor-Valve Models. Subcooled and two-phase CFM (BCM). CFT-21. 105

4.49 Mass flow at nozzle exit. Discharge coefficient adjustment, BCM-J. CFT-01. 107

4.50 Void fraction at nozzle exit. Discharge coefficient adjustment, BCM-J. CFT-01. 107

4.51 Liquid and saturation temperatures at nozzle exit. Discharge coefficient adjustment, BCM-J. CFT-01. 108

4.52 Mass flow at nozzle exit. Discharge coefficient adjustment, BCM-J. CFT-06. 108

4.53 Void fraction at nozzle exit. Discharge coefficient adjustment, BCM-J. CFT-06. 109

4.54 Liquid and saturation temperatures at nozzle exit. Discharge coefficient adjustment, BCM-J. CFT-06. 110

4.55 Mass flow at nozzle exit. Discharge coefficient adjustment, BCM-J. CFT-11. 111

4.56 Void fraction at nozzle exit. Discharge coefficient adjustment, BCM-J. CFT-11. 111

4.57 Liquid and saturation temperatures at nozzle exit. Discharge coefficient adjustment, BCM-J. CFT-11. 112

4.58 Mass flow at nozzle exit. Discharge coefficient adjustment, BCM-J. CFT-15. 112

4.59 Void fraction at nozzle exit. Discharge coefficient adjustment, BCM-J. CFT-15. 113

4.60 Liquid and saturation temperatures at nozzle exit. Discharge coefficient adjustment, BCM-J. CFT-15. 113

4.61 Mass flow at nozzle exit. Discharge coefficient adjustment, BCM-J. CFT-17. 114

4.62 Liquid and saturation temperatures at nozzle exit. Discharge coefficient adjustment, BCM-J. CFT-17. 114

4.63 Mass flow at nozzle exit. Discharge coefficient adjustment, BCM-J. CFT-21. 115

4.64 Void fraction at nozzle exit. Discharge coefficient adjustment, BCM-J. CFT-21. 115

4.65 Liquid and saturation temperatures at nozzle exit. Discharge coefficient adjustment, BCM-J. CFT-21. 116

4.66 Mass flow at nozzle exit. Discharge coefficient adjustment, BCM-J. CFT-24. 116

4.67 Void fraction at nozzle exit. Discharge coefficient adjustment, BCM-J. CFT-24. 117

4.68 Liquid and saturation temperatures at nozzle exit. Discharge coefficient adjustment, BCM-J. CFT-24. 117

4.69 Void fraction at nozzle exit, BCM-J. 118

4.70 Mass flow at nozzle exit. Discharge coefficient adjustment, BCM-P. CFT-01. 119

4.71 Void fraction at nozzle exit. Discharge coefficient adjustment, BCM-P. CFT-01. 119

4.72 Mass flow at nozzle exit. Discharge coefficient adjustment, BCM-P. CFT-11. 120

4.73 Void fraction at nozzle exit. Discharge coefficient adjustment, BCM-P. CFT-11. 120

4.74 Mass flow at nozzle exit. Discharge coefficient adjustment, BCM-P. CFT-15. 121

4.75 Void fraction at nozzle exit. Discharge coefficient adjustment, BCM-P. CFT-15. 121

4.76 Mass flow at nozzle exit. Discharge coefficient adjustment, BCM-P. CFT-17. 122

4.77 Void fraction at nozzle exit. Discharge coefficient adjustment, BCM-P. CFT-17. 122

4.78 Mass flow at nozzle exit. Discharge coefficient adjustment, BCM-P. CFT-21. 123

4.79 Void fraction at nozzle exit. Discharge coefficient adjustment, BCM-P. CFT-21. 123

4.80 Comparison of MDC and TDC adjustment for BCM-J and BCM-P. . 124

4.81 MDC and TDC adjustment. Nozzle modeled as SINGLE JUNCTION (ICM). CFT-06. 127

4.82 MDC and TDC adjustment. Nozzle modeled as SINGLE JUNCTION (ICM). CFT-15. 127

4.83 MDC and TDC adjustment. Nozzle modeled as SINGLE JUNCTION (ICM). CFT-21. 128

4.84 TDC adjustment. Nozzle modeled as SINGLE JUNCTION (ICM). CFT-24. 128

4.85 MDC and TDC adjustment. Mass flow at nozzle exit. Nozzle modeled as PIPE (ICM). CFT-06. 129

4.86 MDC adjustment. Mass flow at nozzle exit. Nozzle modeled as PIPE (ICM). CFT-15. 129

4.87 TDC adjustment. Mass flow at nozzle exit. Nozzle modeled as PIPE (ICM). CFT-15. 130

4.88 MDC and TDC adjustment. Mass flow at nozzle exit. Nozzle modeled as PIPE (ICM). CFT-21. 130

4.89 MDC and TDC adjustment. Mass flow at nozzle exit. Nozzle modeled as PIPE (ICM). CFT-24. 131

4.90 Mass flow at nozzle exit. Comparison between TRAC-BF1 and RELAP5/MOD3.2 results. Nozzle modeled as PIPE. CFT-24. 132

4.91 Mass flow at nozzle exit. Comparison between BCM-J and BCM-P with $dp = 0.14$ and 0.01. CFT-15. 135

4.92 Mass flow at nozzle exit. Comparison between BCM-J and BCM-P with $dp = 0.14$ and 0.01. CFT-21. 135

4.93 Mass flow at nozzle exit. Comparison between BCM-J and BCM-P with $dp = 0.14$ and 0.01. CFT-24. 136

4.94 Void-fraction at nozzle exit. Comparison between BCM-J and BCM-P with $dp = 0.14$ and 0.01. CFT-15. 136

4.95 Void-fraction at nozzle exit. Comparison between BCM-J and BCM-P with $dp = 0.14$ and 0.01. CFT-21. 137

4.96 Void-fraction at nozzle exit. Comparison between BCM-J and BCM-P with $dp = 0.14$ and 0.01. CFT-24. 137

1 Subroutine JCHOKE flow logic. 151

2 Subroutine JCHOKE flow logic (continued). 152

3 Subroutine JCHOKE flow logic (continued). 153

4 Subroutine JCHOKE flow logic (continued). 154

5 Subroutine JCHOKE flow logic (continued). 155

6 Subroutine JCHOKE flow logic (continued). 156

7 Subroutine JCHOKE flow logic (continued). 157

8 Subroutine JCHOKE flow logic (continued). 158

9 Subroutine JCHOKE flow logic (continued). 159

10 Subroutine JCHOKE flow logic (continued). 160

11 Subroutine JCHOKE flow logic (continued). 161

12 Subroutine JCHOKE flow logic (continued). 162

List of Tables

4.1 Main characteristics of the Marviken Tests 65

4.2 Discharge coefficient adjustment. Comparison between BCM-J and BCM-P 124

4.3 Discharge coefficient adjustment. Comparison between ICM-J and ICM-P 126

4.4 Discharge coefficient adjustment. Comparison between ICM and BCM results (The values marked with * do not adjust with test data) . . 131

Executive Summary

The analysis and assessment of the critical flow models of RELAP5/MOD3.2.2beta (Ransom-Trapp and Henry-Fauske) has been performed in three stages:

Firstly, the implementation of the RELAP5/MOD3.2.2beta models has been checked. It was concluded that the transition from the critical to the non-critical flow model is not always adecuate in the Ransom-Trapp model because one of the conditions checked in the subroutine in order to determine whether the flow is critical or non-critical (flow critical in the previous time step and pressures strictly decreasing in the flow direction) is only a neccesary but no sufficient condition to assure if the flow will unchoke.

Secondly, a sensitivity analysis of both models in subcooled, two-phase and vapor conditions has been taken with respect to temperature, pressure, void-fraction, discharge coefficients, energy loss coefficient and disequilibrium parameter. In these analysis several anomalous behaviours of the Ransom-Trapp model are shown. In the other hand the Henry-Fauske model shows a good behaviour.

Finally, RELAP5/MOD3.2.2beta simulations have been conducted to assess the critical flow models of the code. As a part of this assessment an adjustment of the discharge coefficients for the Ransom-Trapp model with different nodalizations has been done and also it has been checked which are the better values of the disequilibrium parameter for the Henry-Fauske model in subcooled and two-phase conditions. The main conclusions of this assessment are:

From the simulation of the Marviken tests with the Ransom-Trapp model it is observed that the comparison between the Initial Condition Model (ICM) and the Boundary Condition Model (BCM) results and their discharge coefficients shows that the values used to adjust the mass flow for ICM are always greater than for BCM. This problem may be caused by experimental errors or some constitutive relations or correlations not compatibles with the critical flow model (e.g. the $\Gamma_{flashing}$ model and the interfacial friction model).

From the simulation of the Marviken tests with the Henry-Fauske model it is concluded that,

1. The best values of dp for adjusting the model are,
   - $dp = 0.14$ for subcooled blowdown and $L/D < 1.5$.
   - $dp = 0.01$ for $L/D > 1.5$.
   - $dp = 0.01$ for saturated blowdown.

2. The best models for the different nozzles are,

   - Short nozzles $L/D \leq 0.3$ should be modeled as a junction.
   - Long nozzles $L/D \geq 1.5$ should be modeled as a pipe.
   - This assessment does not give enough information about the which is the best model for intermediate nozzles $1.5 > L/D > 0.3$.

3. At present, only one *dp* value can be used for subcooled and two-phase periods. So, two disequilibrium parameters should be implemented in order to include the values mentioned above (one of them for the subcooled period and another for the two-phase one), and also the transition between them. This solution generates a problem because it implies a new degree of freedom, and therefore a negative consequence for the user effect.

Chapter 1

Introduction

In a Loss of Coolant Accident (LOCA) analysis, the accurate prediction of the mass flow through a break during the blowdown phase is very important in evaluating the remaining coolant inventory and system pressure. In the RELAP5/MOD3.2 code, the break flow is calculated primarily by a critical flow model, consisting of the Lienard-Alamgir-Jones (LAJ) model for subcooled critical flow, and the Ransom-Trapp model for two-phase flow.

As part of the Code Assessment and Maintenance Program (CAMP), the sensitivity analysis and assessment of the RELAP5/MOD3.2 for the critical flow model has been carried out. The purpose of the sensitivity analysis is performing a qualitative and quantitative analysis of the model in comparison with data from the available bibliography, and its application to the uncertainty analysis of the plant models. The goal of this assessment is also to complete the previous Marviken critical flow tests analysis performed by other work teams (STUDSVIK, KAERI, INEL, ...). With this in mind, seven tests have been simulated using all the different models found in the bibliography, and compared with the test data. The discharge coefficients for all the models have also been obtained.

It is important to remark that new versions of the code (RELAP5/MOD3.2.2beta and RELAP5/MOD3.2.2gamma) have been developed during the realization of this report. These new versions include the Henry-Fauske model, which was not in RELAP5/MOD3.2. Therefore, a sensitivity analysis of this new model and also an assessment with Marviken tests has been performed.

Chapter 2

Analysis of RELAP5/MOD3.2 Critical Flow Model

In order to deeply understand the Critical Flow Model (CFM) used by RELAP5/MOD3.2 and its implementation into the JCHOKE subroutine, the following tasks have been achieved:

- Analysis of the implementation of the model, relating the equations and the subroutine block diagram in volume 4 of the RELAP5/MOD3 manuals.
- Numbering of the subroutine block diagram, shown in Appendix I.
- Modification of the subroutine, including the comments and the previous numbering of the block diagram. The commented subroutine with the numbering of the block diagram is shown in Appendix II.
- From the last two items, a simplified block diagram have been obtained, shown in Figure 2.1.

In the simplified block diagram of the subroutine (Figure 2.1), the following points can be remarked:

- Sound velocity selection (among subcooled, two-phase and steam) depending on the thermal-hydraulic conditions of the junction analyzed. The variable which represents the sound velocity is SONIC.
- Interpolation and under relaxation of SONIC and JCAT variables. We performed a comparison between TRAC-BF1 and RELAP5/MOD3 critical flow models and its interpolations and under relaxations, to be found in [CQS-97].

- Logic of transition from critical flow to non-critical flow (TEST1 and TEST2 blocks).

In order to understand the transition from critical to non-critical flow, a more detailed analysis has been performed in the next section.

2.1 Problems with the transition from CFM to Non-CFM. Logic of JCHOKE subroutine

In JCHOKE subroutine, a test is performed in order to check if the flow is critical or not, as is shown in Figure 2.2. So, in the subroutine, the flow is critical if one of the following conditions is verified:

1. The mass flow calculated from the momentum solution is greater than the critical mass flow.
2. The logical variable CHOKE is equal to TRUE. This condition is verified if the flow was critical in the previous time step and the pressures are strictly decreasing in the flow direction (two-fold pressure comparison).

We must remark that the pressure condition is a poor test for determining if a junction will unchoke (it is only a necessary but not sufficient condition), and so the logic of the subroutine could fail. Several examples of this problem are shown in the next chapter.

In RELAP5/MOD3.2.2beta, the Henry-Fauske model has been also included. This new model has not been analyzed with the same level of detail in this work, but it has been checked that only the first condition is used. Therefore, the logic problem is not present in the new Henry-Fauske model.

The solution of the problem is very easy, only it is necesary to remove the second condition (CHOKE=.TRUE.) from the second test. The problem has been reported to Scientech and they agreed with the previous statements.

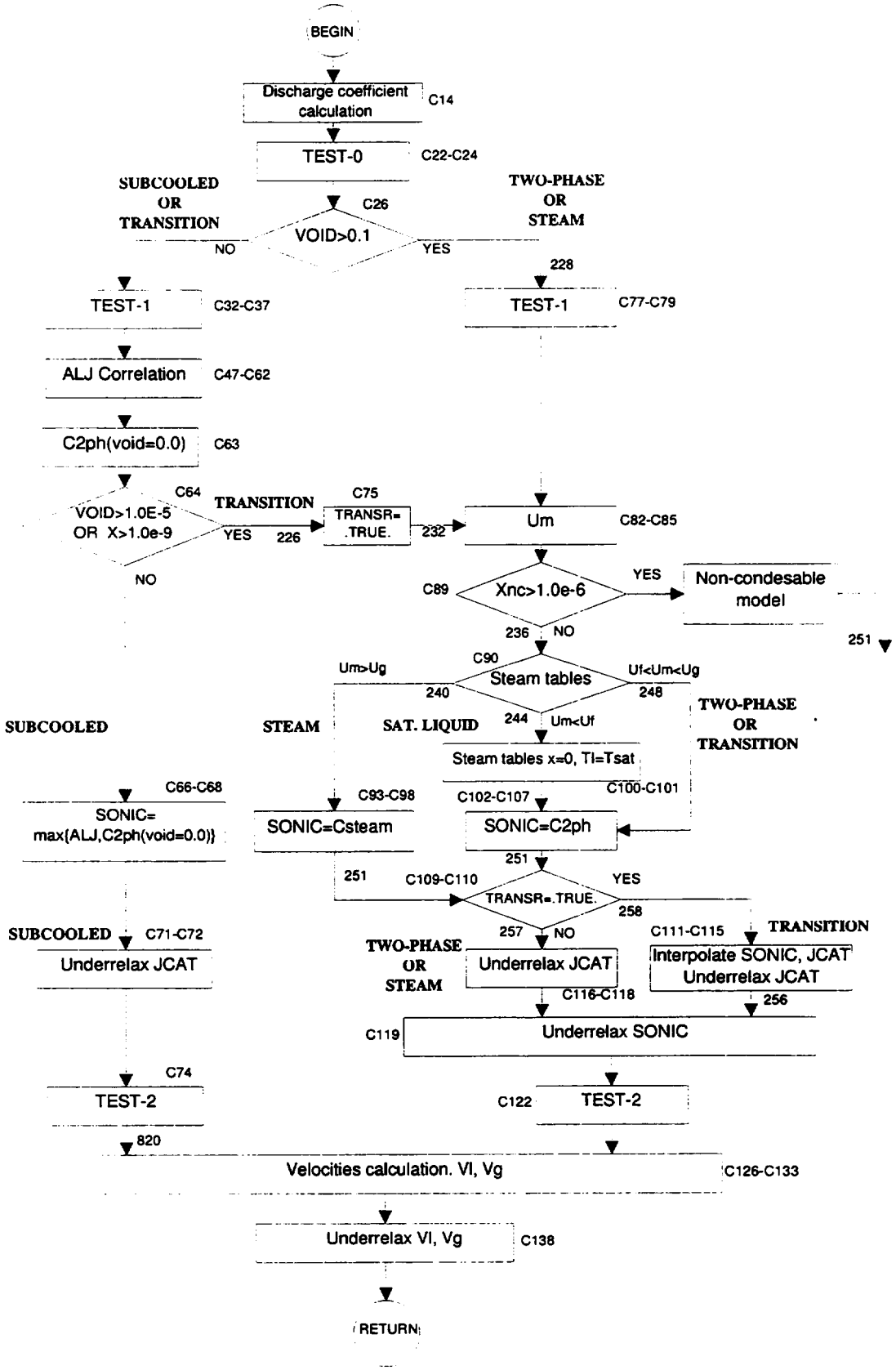

Figure 2.1: Selection model block diagram. JCHOKE Subroutine.

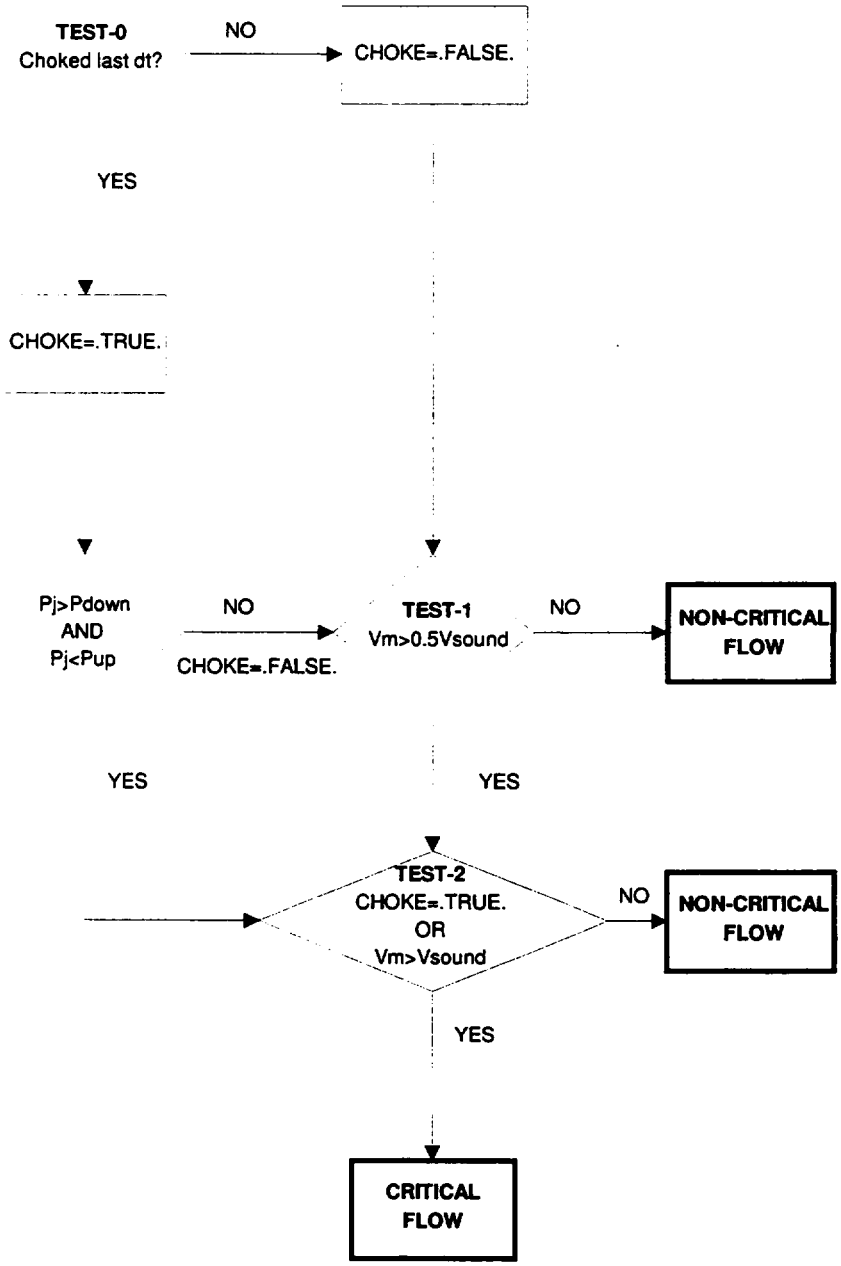

Figure 2.2: Transition from CFM to Non-CFM block diagram. JCHOKE subroutine.

Chapter 3

Sensitivity Analysis of RELAP5/MOD3 CFM

In RELAP5/MOD3.2.2beta, there are two critical flow models available: Ransom-Trapp and Henry-Fauske. A sensitivity analysis has been done for each model and a comparison of the results is presented at the end of the chapter.

The model used for the sensitivity analysis is a vertical straight pipe, 0.441 m^2 of area, with an outlet single junction (abrupt area change option), 0.0707 m^2 of area, and two time dependent volumes limiting the pipe, Figure 3.1. This model corresponds to the discharge pipe of Marviken critical flow test 06. The conditions for the analysis are given in the upper volume, while the atmospheric conditions are fixed in the lower one.

The main applications of these results are:

- Performing qualitative and quantitative analysis in comparison with the bibliography data.
- Uncertainty analysis for plant models or experimental tests: If the uncertainty in the thermal hydraulic variables is known, one can estimate its impact in the associated critical mass flow uncertainty.

3.1 Sensitivity Analysis of Ransom-Trapp Model

A sensitivity analysis of the subcooled, two-phase and steam CFMs is presented in this section. The objective of this analysis is to obtain the dependence of the CFM with respect to the following variables:

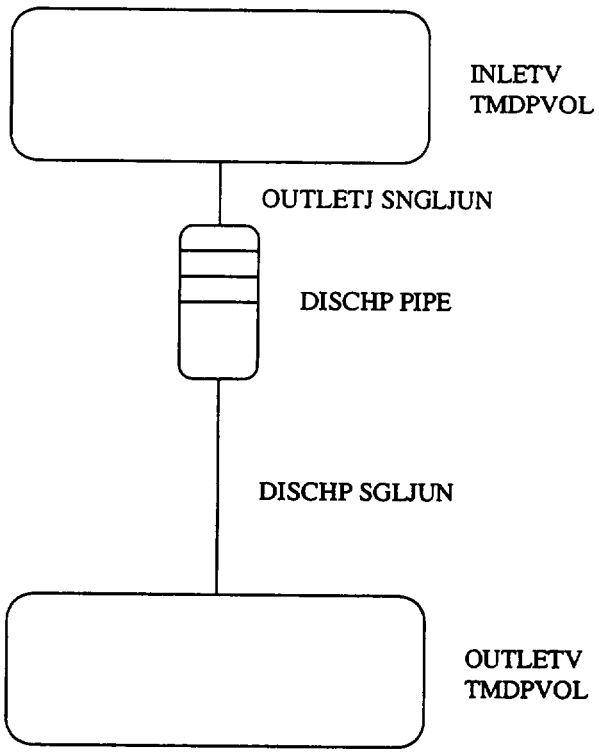

Figure 3.1: Sensitivity nodalization model.

- Temperature.

- Pressure.

- Void Fraction.

- Discharge Coefficient.

- Forward Energy Loss Coefficient

In the same way, critical mass flow is compared with the non-critical mass flow in the same conditions in order to observe the differences between them. On the course of the analysis of the subcooled CFM, several problems associated with the logic of transition from critical to non-critical flow have appeared.

3.1.1 Sensitivity Analysis of Subcooled CFM to Temperature, Pressure, MDC and Forward Energy Loss Coefficient

For the subcooled model, sensitivity analysis has been done with respect to the following variables:

- Temperature.
- Pressure.
- Monophasic Discharge Coefficient (MDC).
- Forward Energy Loss Coefficient

The temperature sensitivity analysis was performed in the following way: The pipe inlet pressure (upper TMDPVOL) was fixed for each case and the temperature was ramped from 373 K to T_{sat} (increasing temperatures, 1 K/s). These calculations have been done for different pressures (from 10 bar to 150 bar).

The same analysis have also been performed with temperatures decreasing from T_{sat} to 373 K, due to the non-expected results related to the transition from Non-CFM to CFM.

The pressure sensitivity was performed in a similar way to the temperature sensitivity:

The pipe inlet temperature (upper TMDPVOL) was fixed for each case and the pressure was varied from 10 bar to P_{sat} (increasing pressures). These calculations have been done for different temperatures (from 373 K to 613 K). For the same reason than in temperature analysis, a decreasing pressure analysis was also performed.

For the MDC sensitivity analysis, a case from pressure sensitivity analysis was used as the base case, varying MDC from 0.6 to 1.4. In order to compare the CFM with the Non-CFM, temperature and pressure were checked values at the last node for assuring that they were similar.

In the Forward Energy Loss Coefficient sensitivity analysis, the pipe inlet pressure was fixed to 40 bar and the temperature was varied from 373 K to 523 K. The mass flow is also compared for five different values of the forward energy loss coefficient (0, 25, 50, 75 and 100).

The results obtained for the different sensitivity analysis are described below:

Temperature Sensitivity. First, an increasing temperature sensitivity analysis was made for CFM and Non-CFM. In the results, it can observed that pressure, Figures 3.2 and 3.3, and temperature at the last node, Figures 3.4 and 3.5, are quite similar, so that the critical mass flow, Figure 3.6, and non-critical mass flow, Figure 3.7, results can be compared.

Two different behaviours are observed in Figure 3.6. These differences can be explained by comparison of CFM and Non-CFM, Figure 3.8, where a transition point is observed for each pressure. Also it is observed that critical mass flow is greater than non critical mass flow in a wide range of values. This is clearly a non-physical behaviour and also means that the transition from CFM to Non-CFM is not well implemented in the JCHOKE subroutine, as it was described in Section 2.1.

Second, a decreasing temperature sensitivity analysis was made for CFM and Non-CFM, Figures 3.9 and 3.10. Results of CFM-on and CFM-off are shown in Figures 3.11 and 3.12, and a comparison between them in Figure 3.13. Results of CFM-on, Figure 3.11, show a different behaviour than in the increasing temperature analysis, Figure 3.6, with no transition for any pressure.

This is in accordance with the explanation given in Section 2.1, because if a decreasing temperature transient begins with critical flow, the model selection logic could fail and then it could stay critical during all the transient. Moreover, if at beginning of the transient the JCHOKE subroutine selects the non-critical flow model, for increasing temperature transients with $P < 50$ bar, the model becomes non-critical while non-critical flow is smaller than critical one. The latter means that the selection of CFM or Non-CFM will depend on the history of the transient, and not only on the instantaneous physical conditions.

Finally, for achieving a complete analysis of the problem, the transitions points for each pressure are obtained from Figure 3.8, and with these values the transition temperature and subcooling as a function of pressure are obtained, Figures 3.14 and 3.15. The values of the transition subcoling point out that this transition problem is only important for large subcolings.

Pressure Sensitivity. First, an increasing pressure sensitivity analysis was made for CFM and Non-CFM. In the results it can be observed that pressure, Figures 3.18 and 3.19, and temperature, Figures 3.16 and 3.17, at the last node are quite similar, so that the critical mass flow, Figure 3.20, and non-critical mass flow, Figure 3.21, results can be compared, Figure 3.22. As in the temperature sensitivity analysis

a non-physical behaviour is observed: the critical flow is sometimes greater than non-critical mass flow for a wide range of values.

Second, a decreasing pressure sensitivity analysis was made for CFM and Non-CFM, Figures 3.23 and 3.24. The comparison between CFM-on and CFM-off, Figure 3.25 shows a similar behaviour than in the increasing pressure analysis, Figure 3.22.

MDC Sensitivity. For this analysis, a case from pressure sensitivity analysis was taken as a base case. Temperature is fixed at the pipe inlet, T= 553 K, and the pressure is varied from 160 to 65 bar. The results show that pressure, Figure 3.28, and temperature, Figure 3.29, are quite similar for all the discharge coefficients values. It is easy to check in Figure 3.30 that the variation of the mass flow with the discharge coefficient has the same value than the discharge coefficient, as expected.

Forward Energy Loss Coefficient Sensitivity. The base case used here was taken from the temperature sensitivity analysis. Pressure is fixed to 40 bar and temperature is varied from 373 to 523 K at the pipe inlet.

This case was chosen because in the first part of the transient the Non-CFM is selected by JCHOKE while in the second part the CFM is selected. The variation of both models with respect to the loss coefficient can thus be observed. In Figure 3.31 it can be seen that Non-CFM varies with the loss coefficient, as expected, while the CFM does not. Thus, the CFM is independent of the loss coefficient. This shows that the energy loss coefficient must be used with care in junctions where critical mass flow is expected, because the CFM does not depend on it but non-CFM decreases with it.

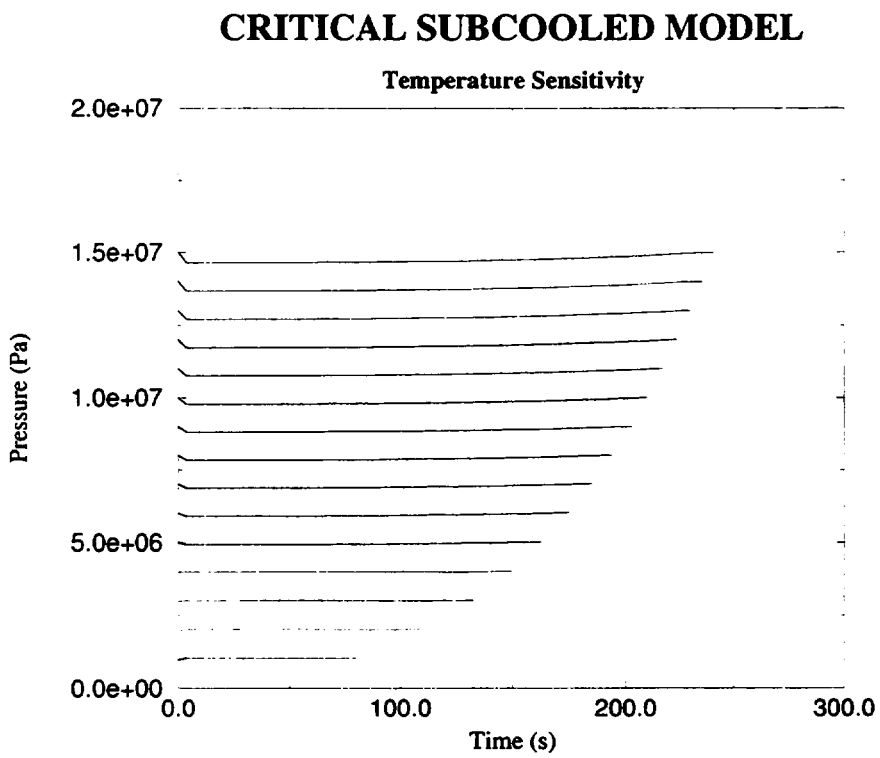

Figure 3.2: Pressure at the last node (Temperature sensitivity of the subcooled model, with increasing temperature). CFM on.

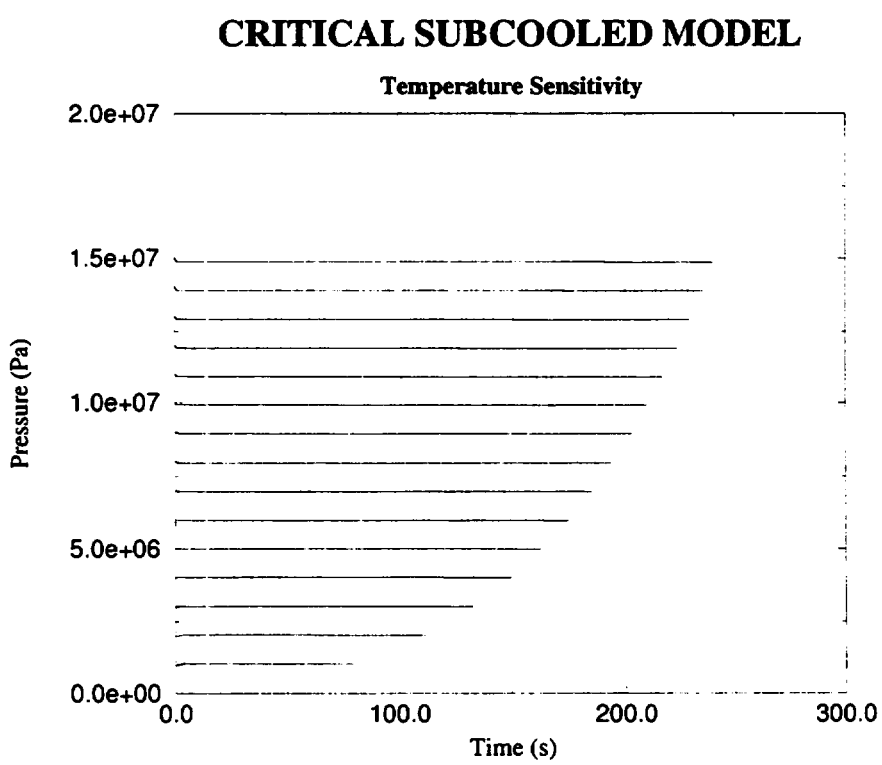

Figure 3.3: Pressure at the last node (Temperature sensitivity of the subcooled model, with increasing temperature). CFM off.

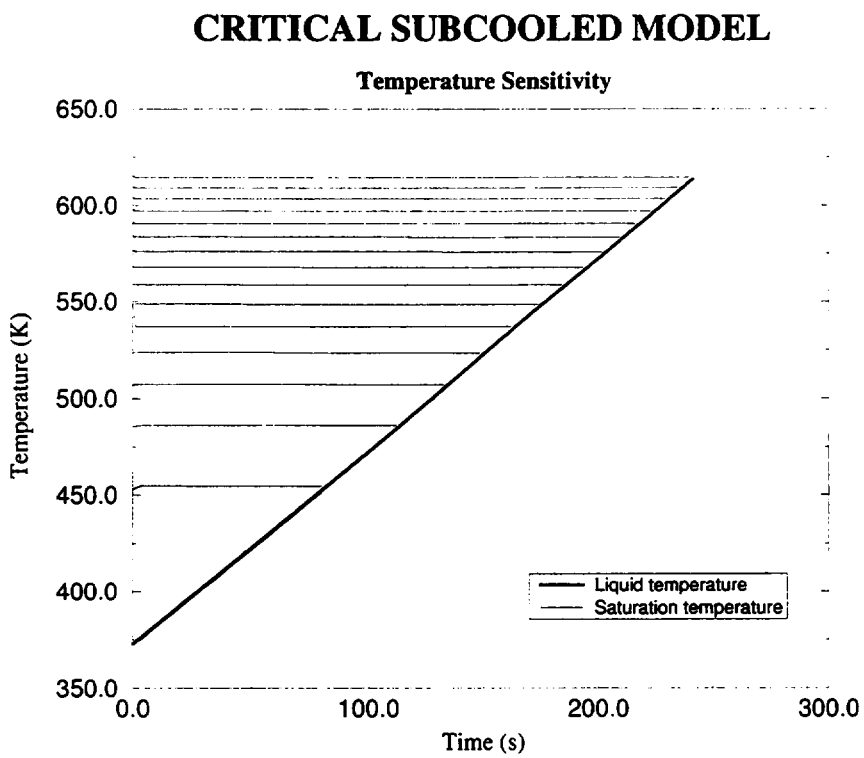

Figure 3.4: Temperature at the last node (Temperature sensitivity of the subcooled model, with increasing temperature). CFM on.

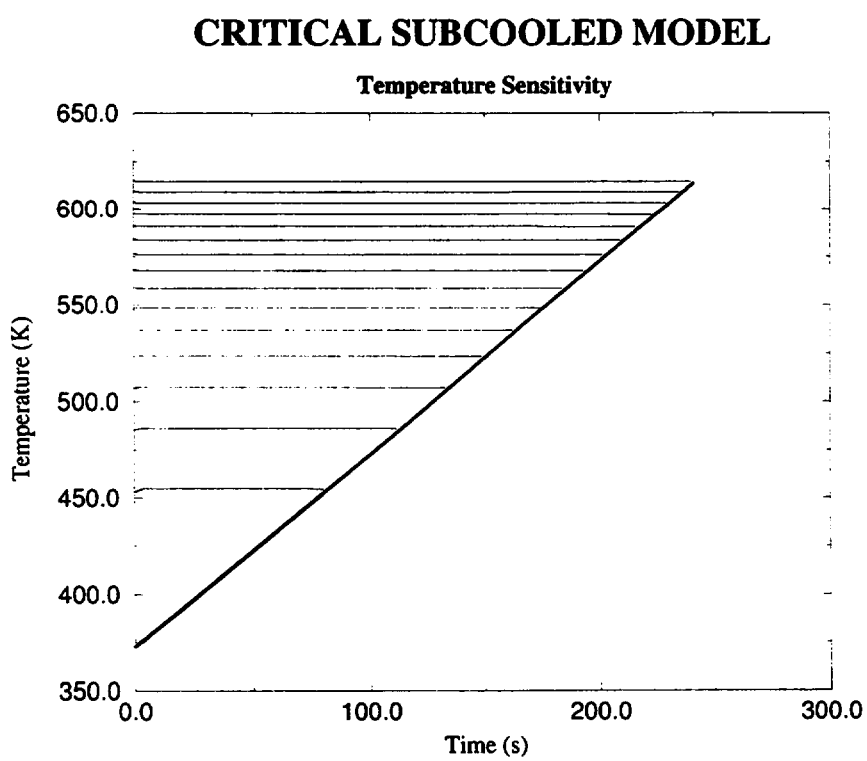

Figure 3.5: Temperature at the last node (Temperature sensitivity of the subcooled model, with increasing temperature). CFM off.

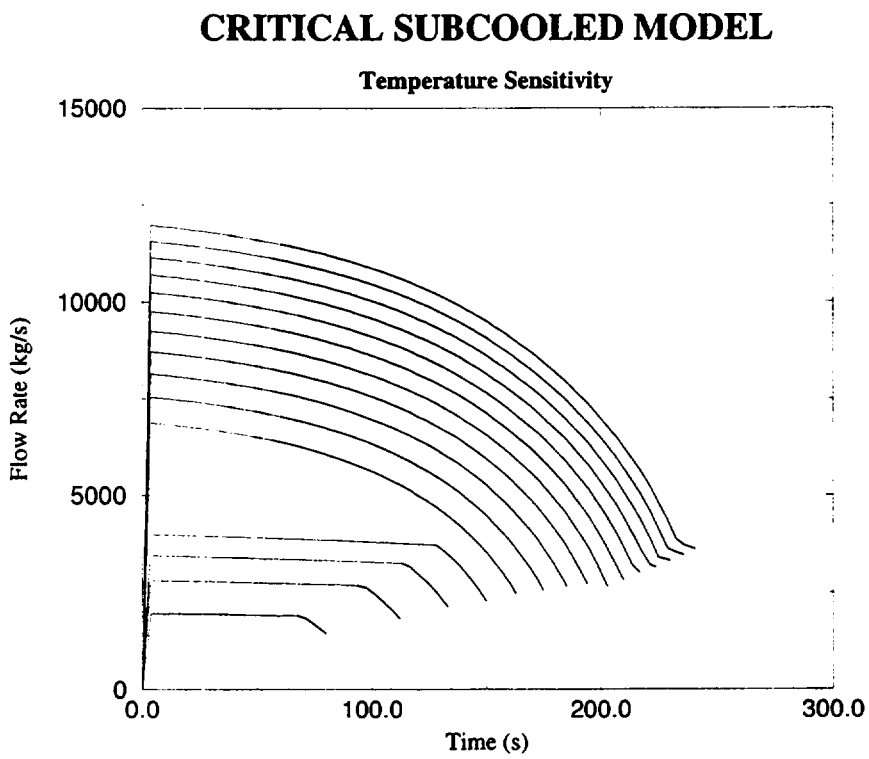

Figure 3.6: Mass flow at the last node (Temperature sensitivity of the subcooled model, with increasing temperature). CFM on.

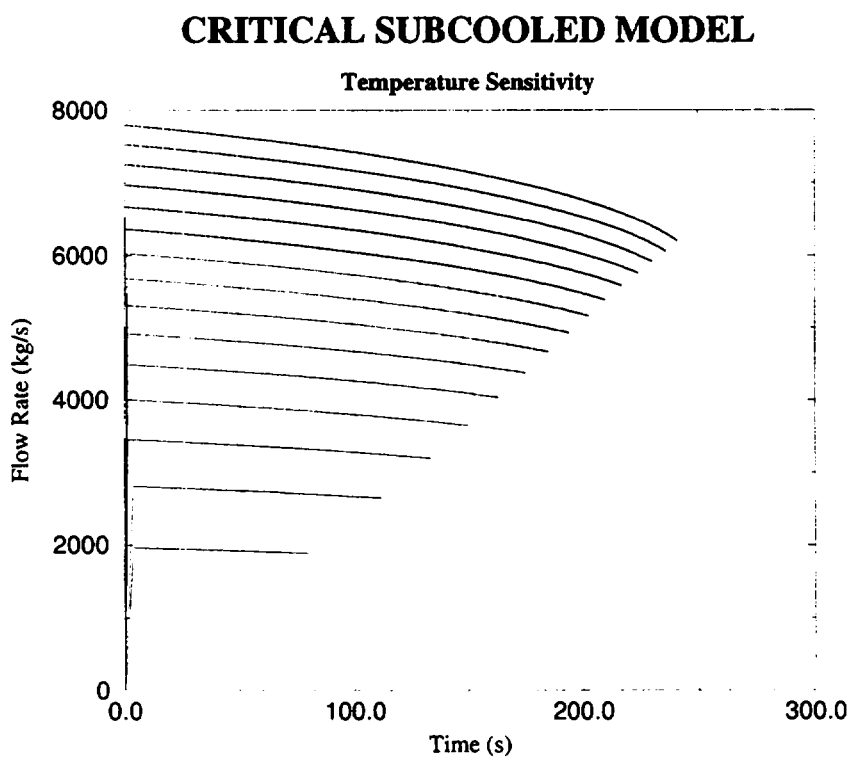

Figure 3.7: Mass flow at the last node (Temperature sensitivity of the subcooled model, with increasing temperature). CFM off.

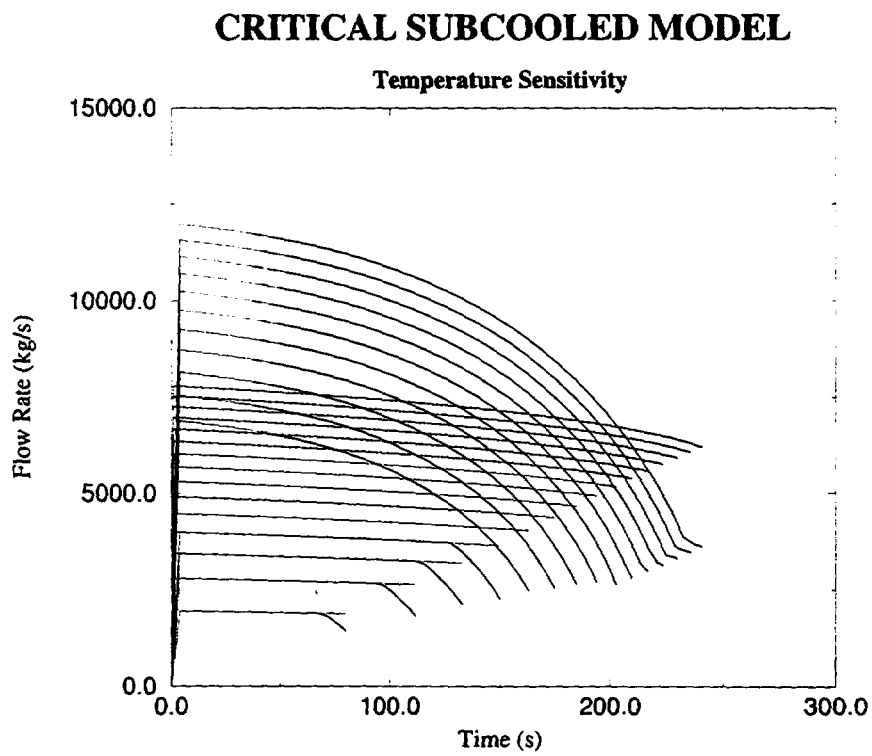

Figure 3.8: Mass flow at the last node (Temperature sensitivity of the subcooled model, with increasing temperature). Comparison of CFM on with CFM off.

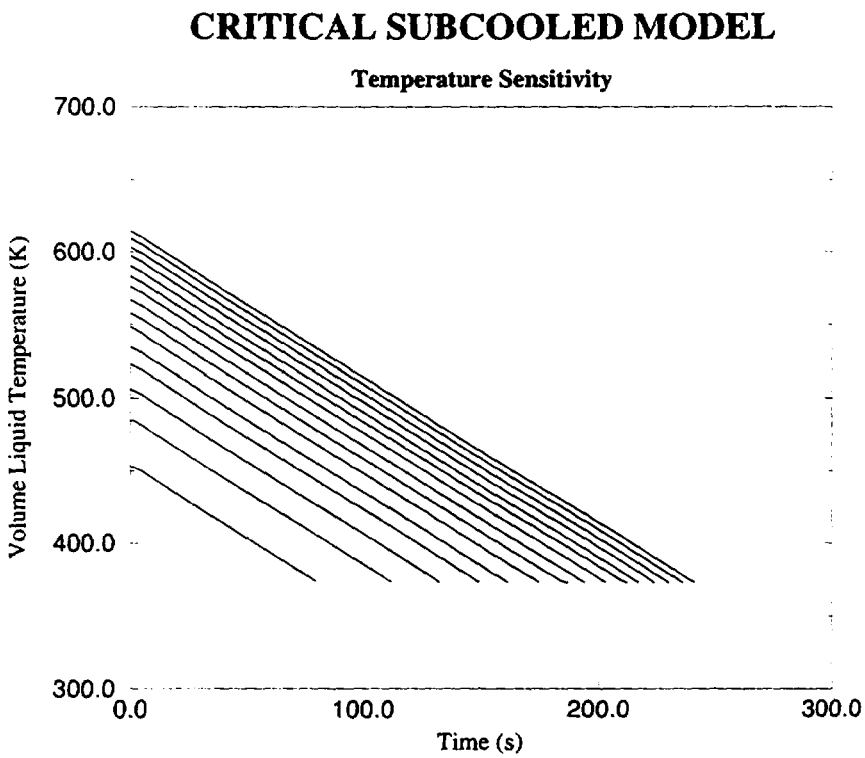

Figure 3.9: Temperature at the last node (Temperature sensitivity of the subcooled model, with decreasing temperature). CFM on.

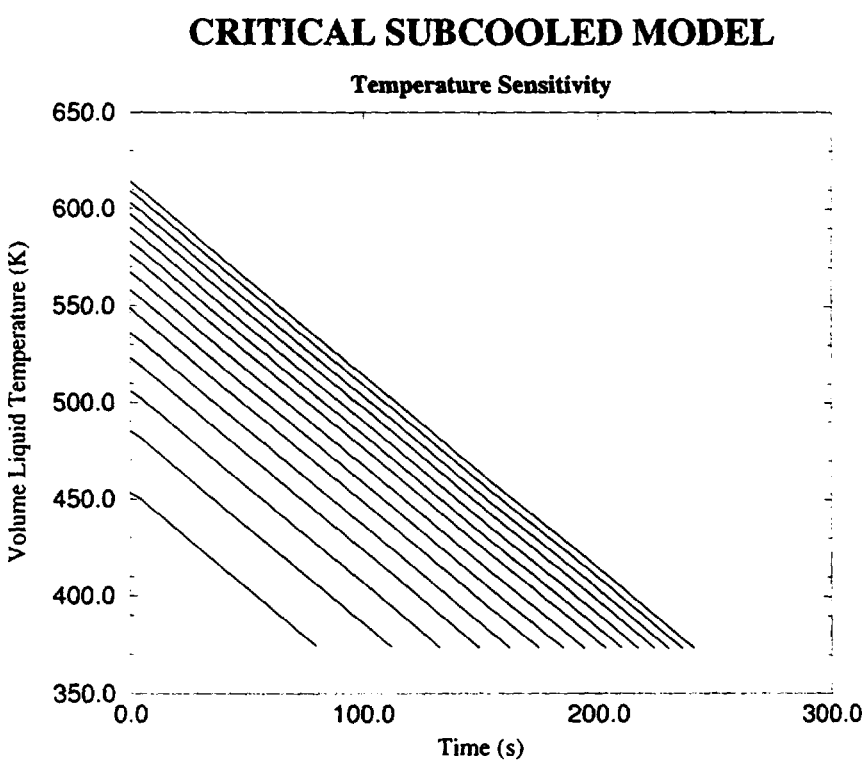

Figure 3.10: Temperature at the last node (Temperature sensitivity of the subcooled model, with decreasing temperature). CFM off.

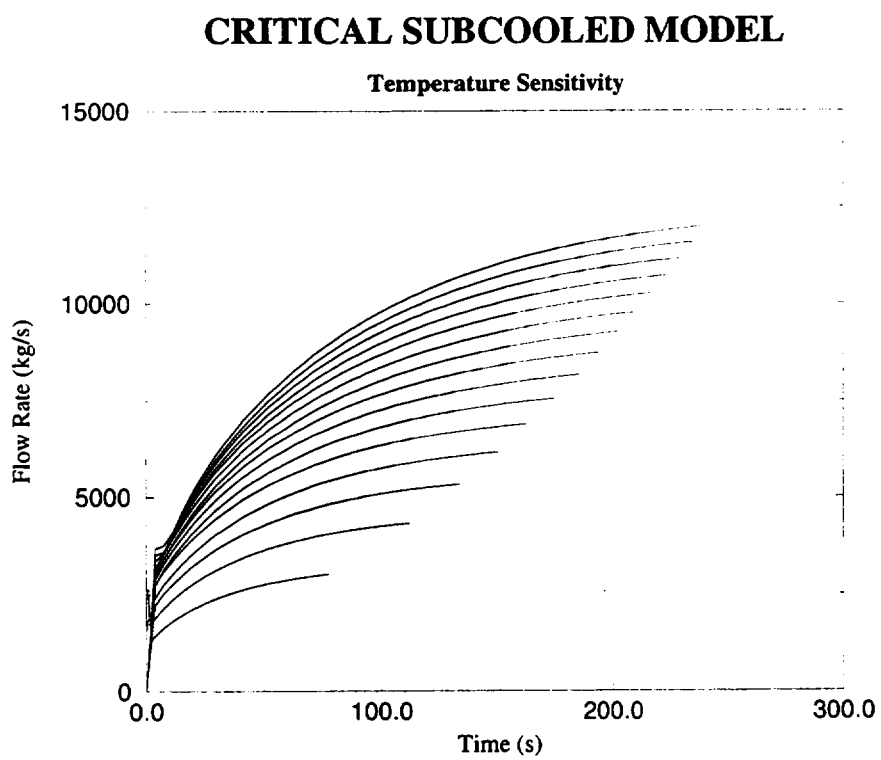

Figure 3.11: Mass flow at the last node (Temperature sensitivity of the subcooled model, with decreasing temperature). CFM on.

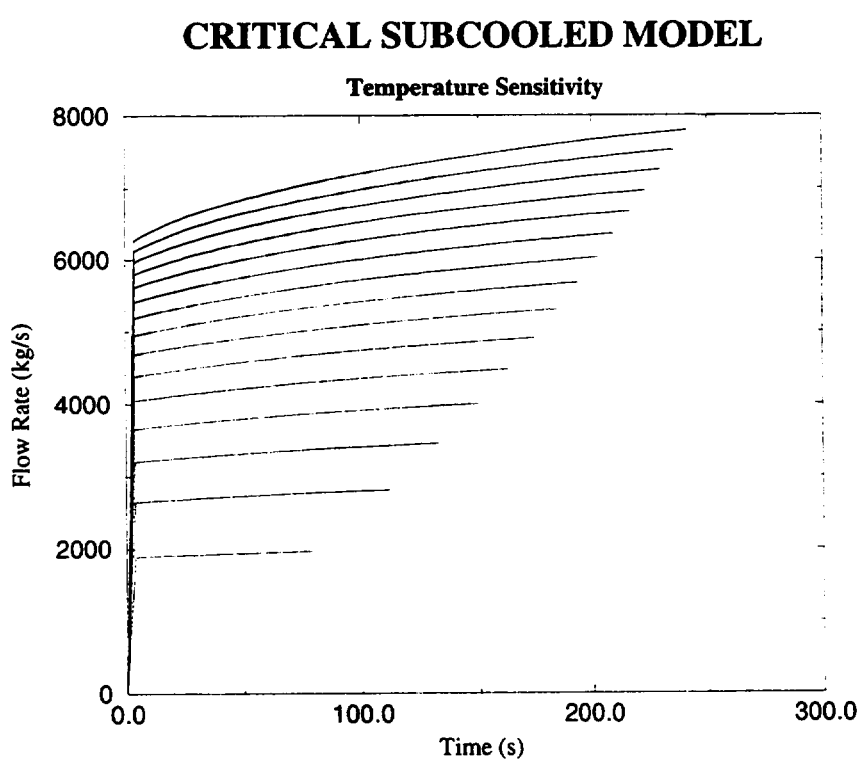

Figure 3.12: Mass flow at the last node (Temperature sensitivity of the subcooled model, with decreasing temperature). CFM off.

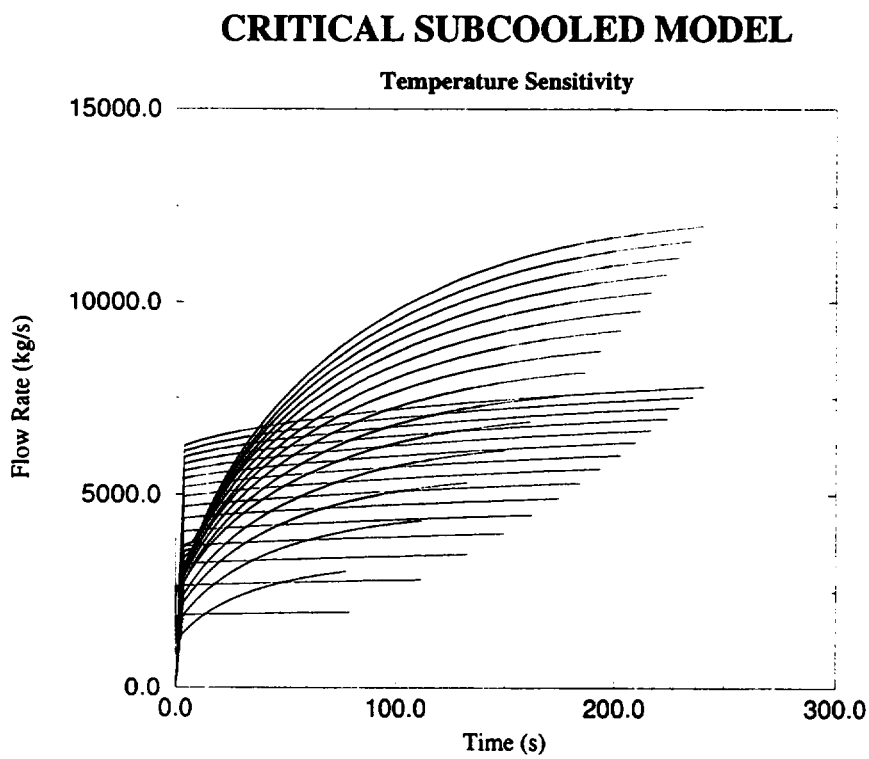

Figure 3.13: Mass flow at the last node (Temperature sensitivity of the subcooled model, with decreasing temperature). Comparison of CFM on with CFM off.

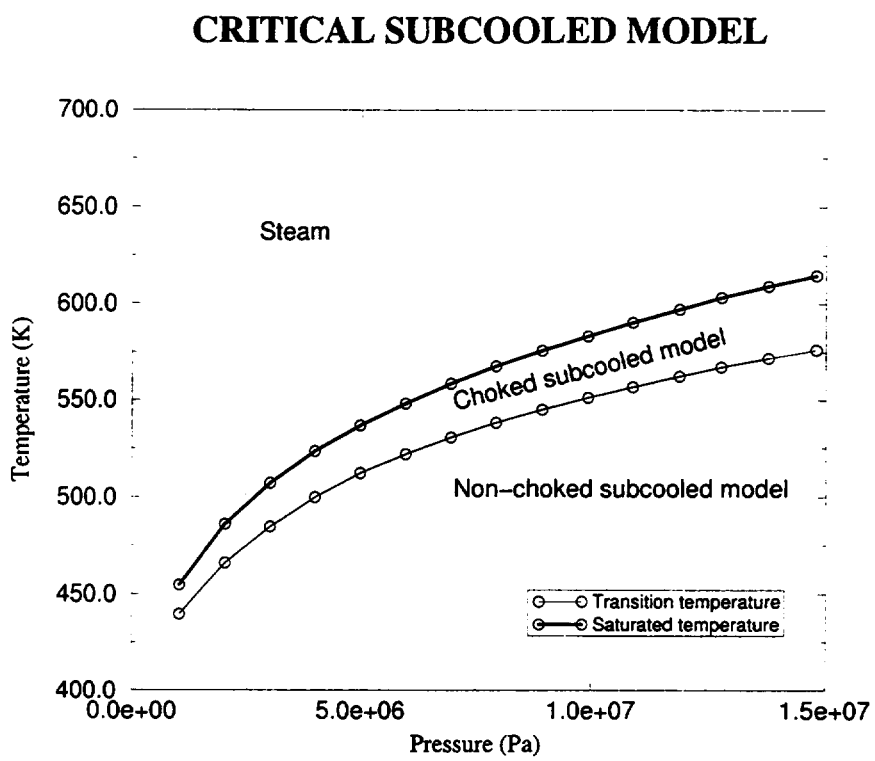

Figure 3.14: Transition at temperature from CFM to Non-CFM. Subcooled region.

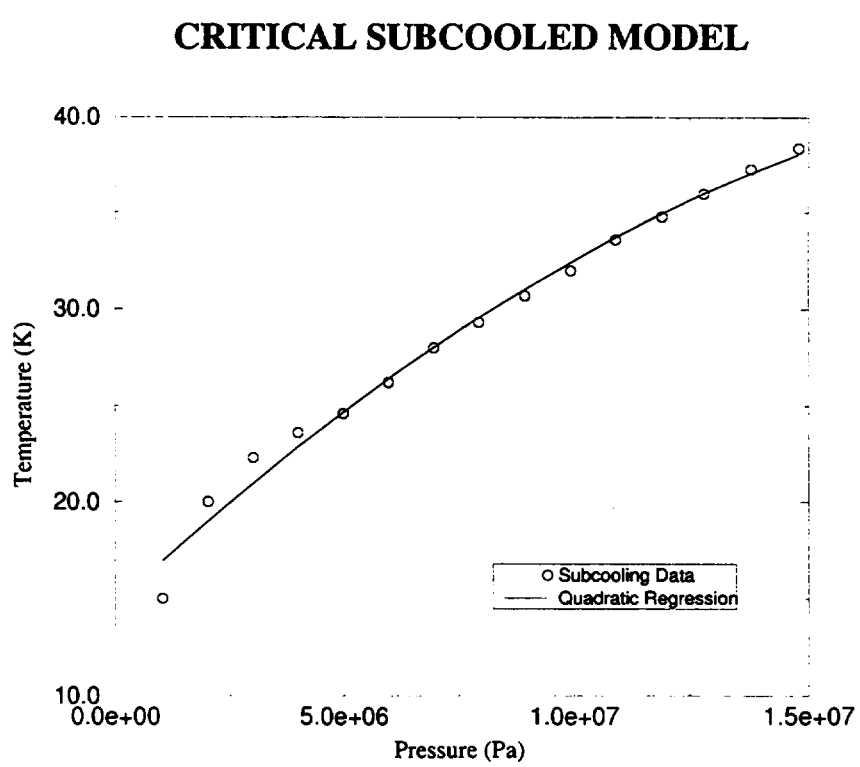

Figure 3.15: Subcooling. Transition from CFM to Non-CFM. Subcooled region.

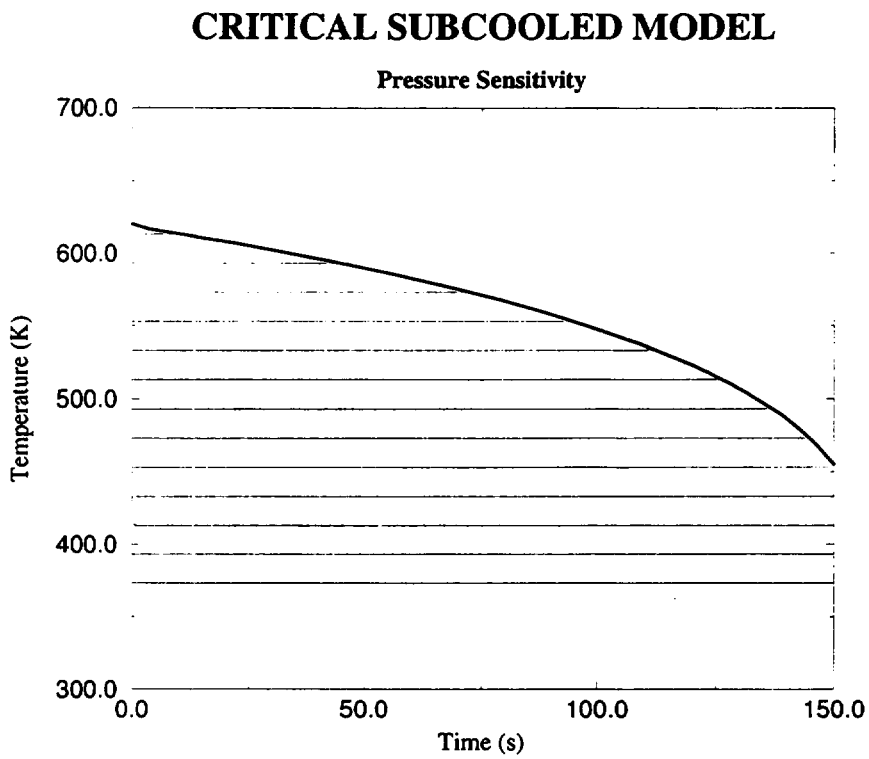

Figure 3.16: Liquid temperature at the last node (Pressure sensitivity of the subcooled model, with increasing pressure). CFM on.

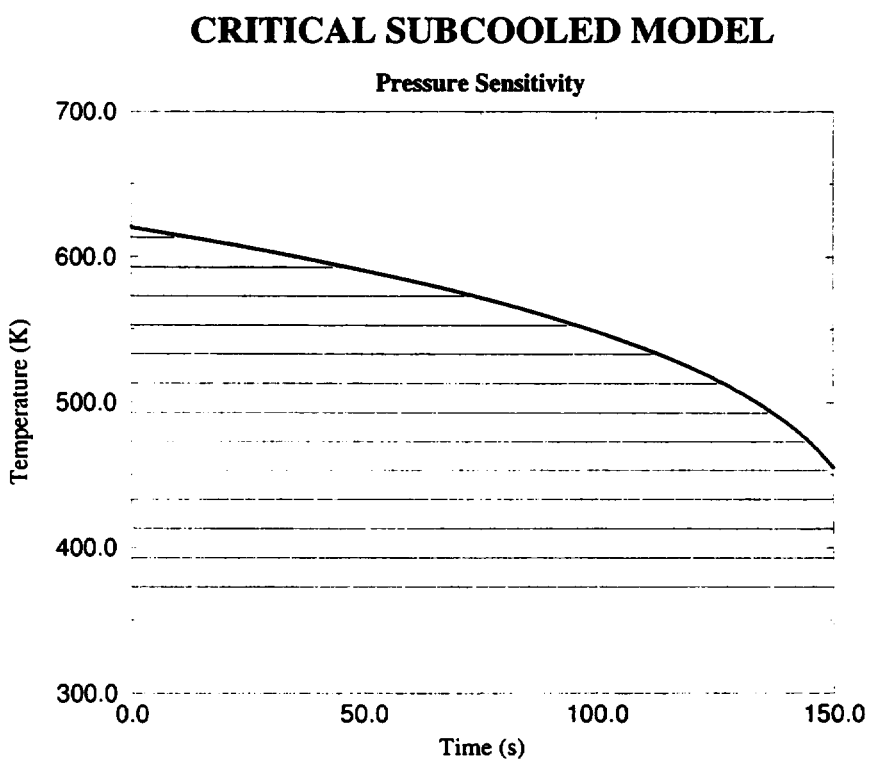

Figure 3.17: Liquid temperature at the last node (Pressure sensitivity of the subcooled model, with increasing pressure). CFM off.

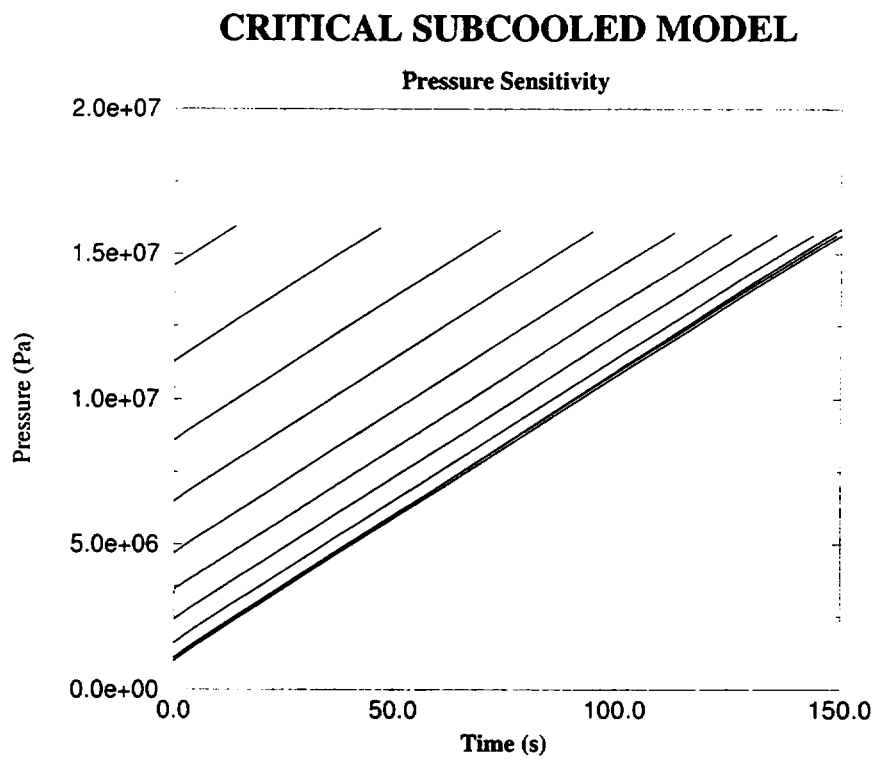

Figure 3.18: Pressure at the last node (Pressure sensitivity of the subcooled model, with increasing pressure). CFM on.

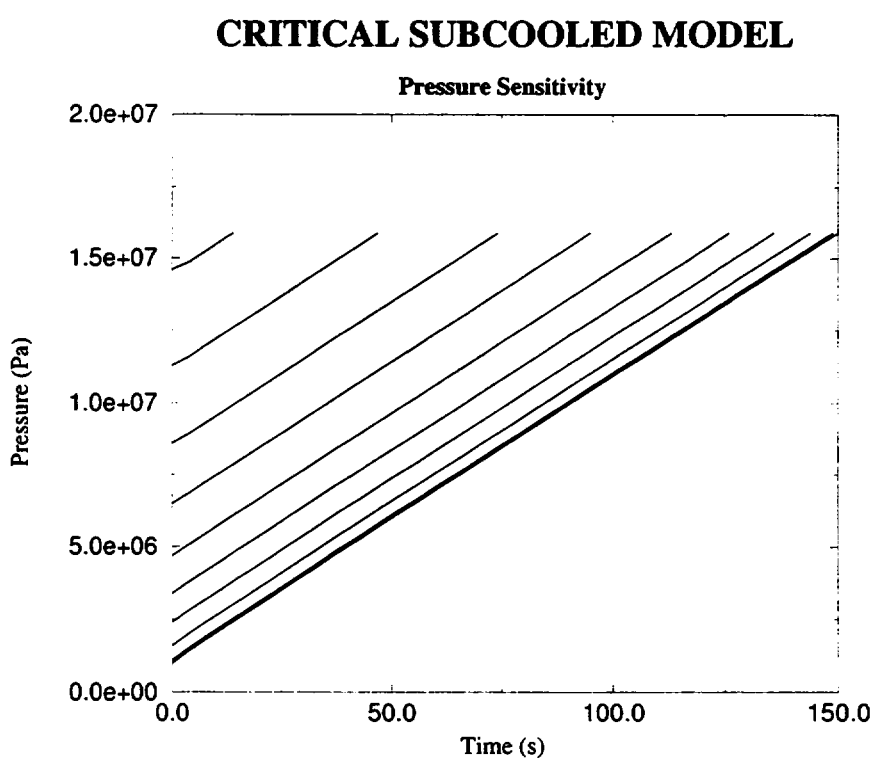

Figure 3.19: Pressure at the last node (Pressure sensitivity of the subcooled model, with increasing pressure). CFM off.

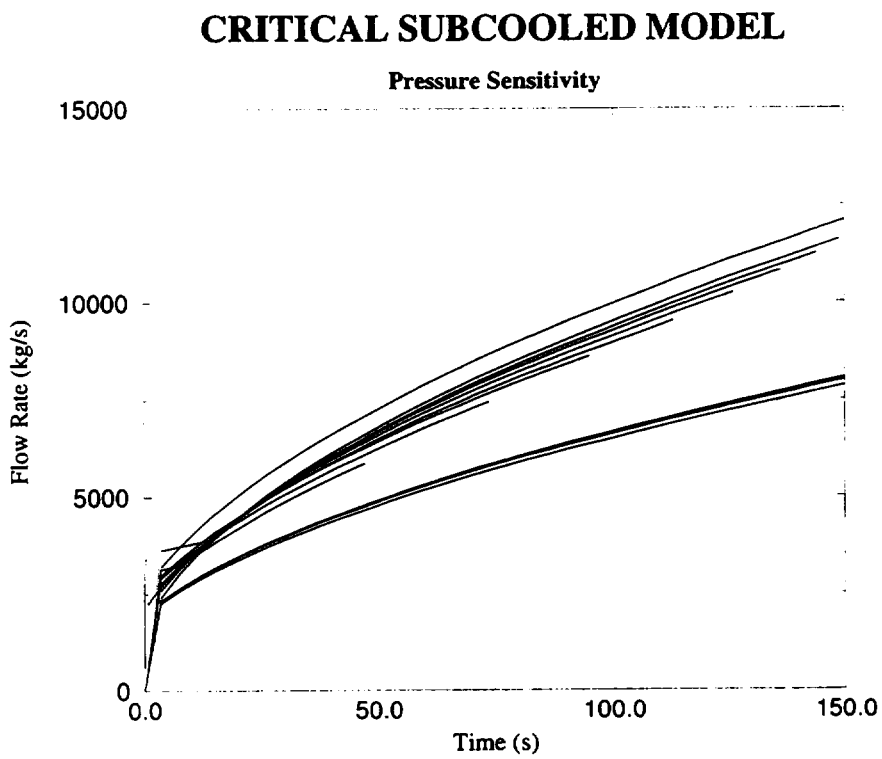

Figure 3.20: Mass flow at nozzle exit (Pressure sensitivity of the subcooled model, with increasing pressure). CFM on.

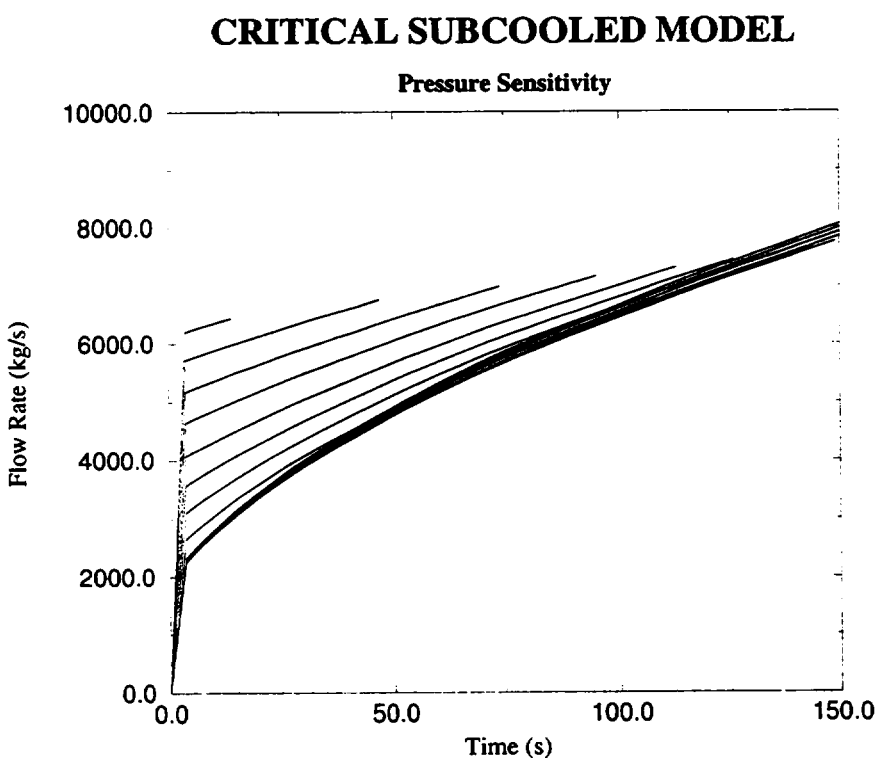

Figure 3.21: Mass flow at nozzle exit (Pressure sensitivity of the subcooled model, with increasing pressure). CFM off.

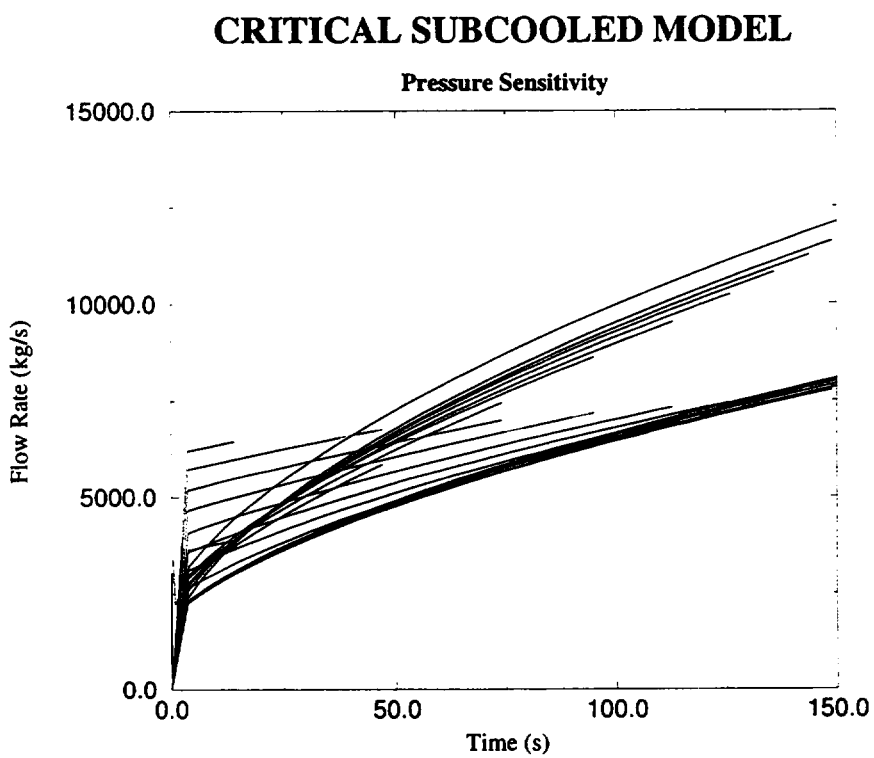

Figure 3.22: Mass flow at nozzle exit (Pressure sensitivity of the subcooled model, with increasing pressure). Comparison of CFM on with CFM off.

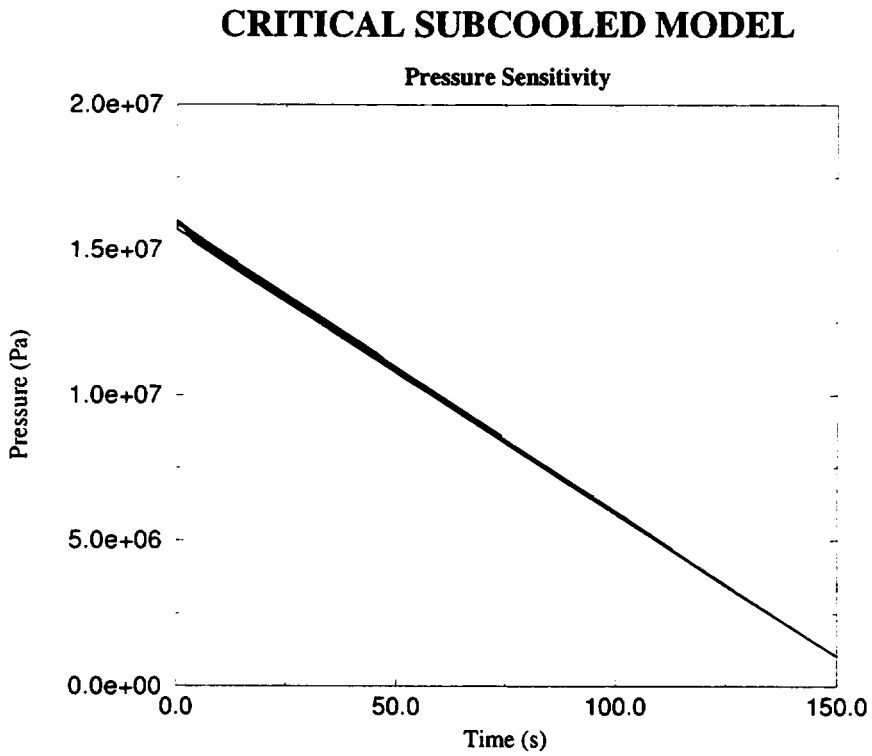

Figure 3.23: Pressure at the last node (Pressure sensitivity of the subcooled model, with decreasing pressure). CFM on.

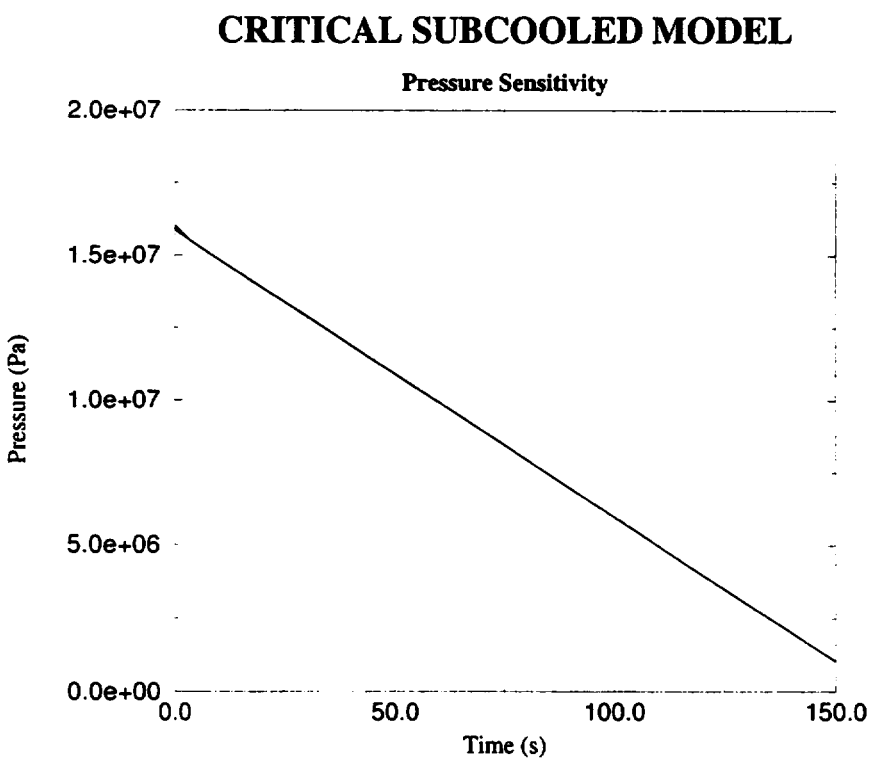

Figure 3.24: Pressure at the last node (Pressure sensitivity of the subcooled model, with decreasing pressure). CFM off.

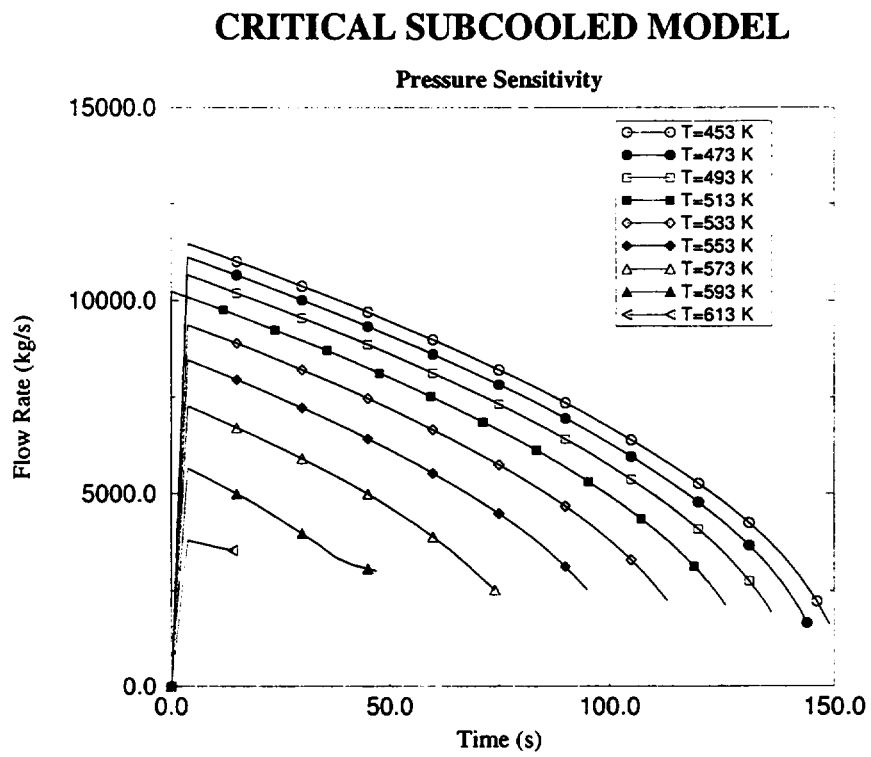

Figure 3.25: Mass flow at nozzle exit (Pressure sensitivity of the subcooled model, with decreasing pressure). CFM on.

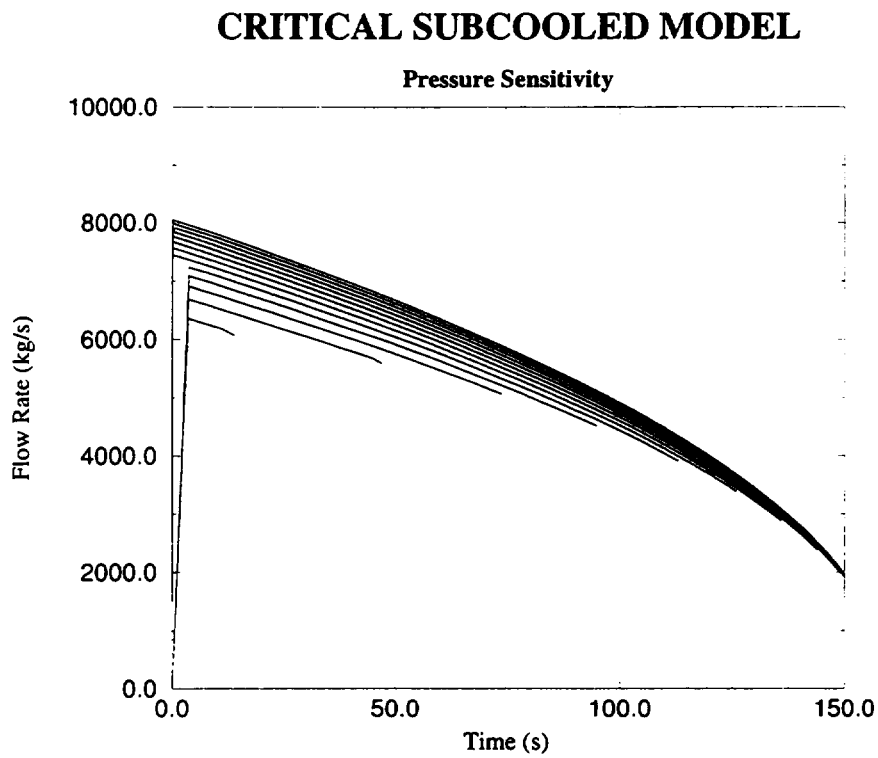

Figure 3.26: Mass flow at nozzle exit (Pressure sensitivity of the subcooled model, with decreasing pressure). CFM off.

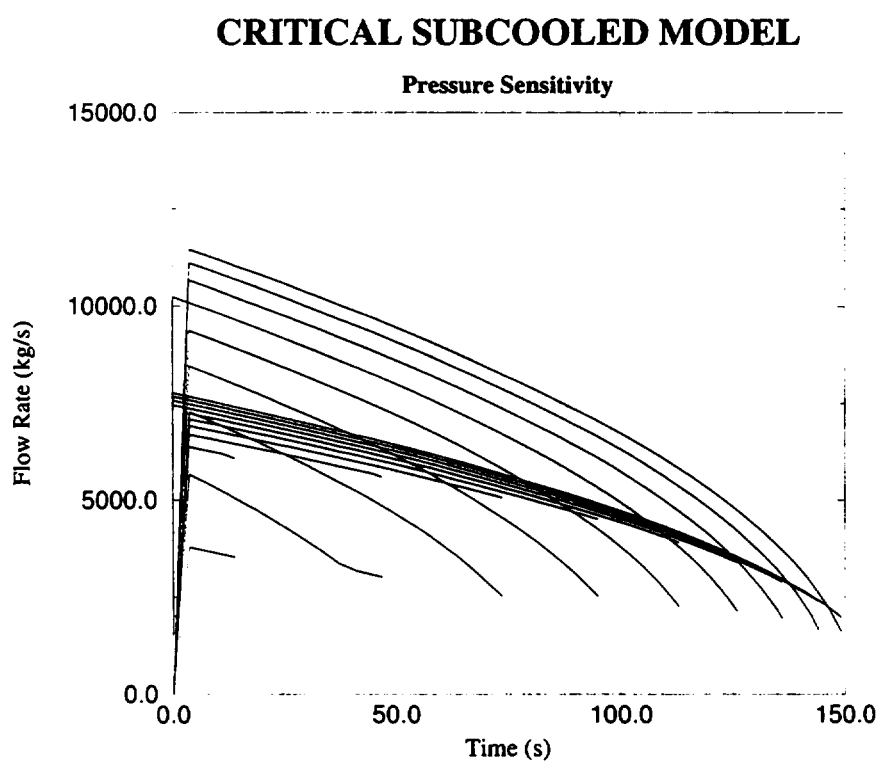

Figure 3.27: Mass flow at nozzle exit (Pressure sensitivity of the subcooled model, with decreasing pressure). Comparison of CFM on with CFM off.

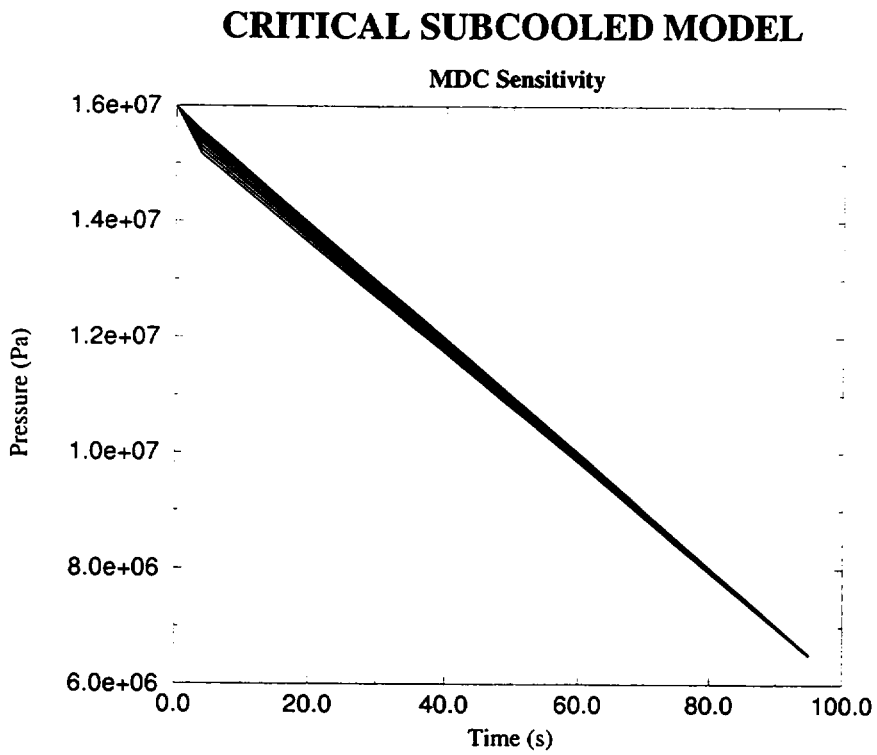

Figure 3.28: Pressure at the last node. MDC sensitivity of the subcooled model.

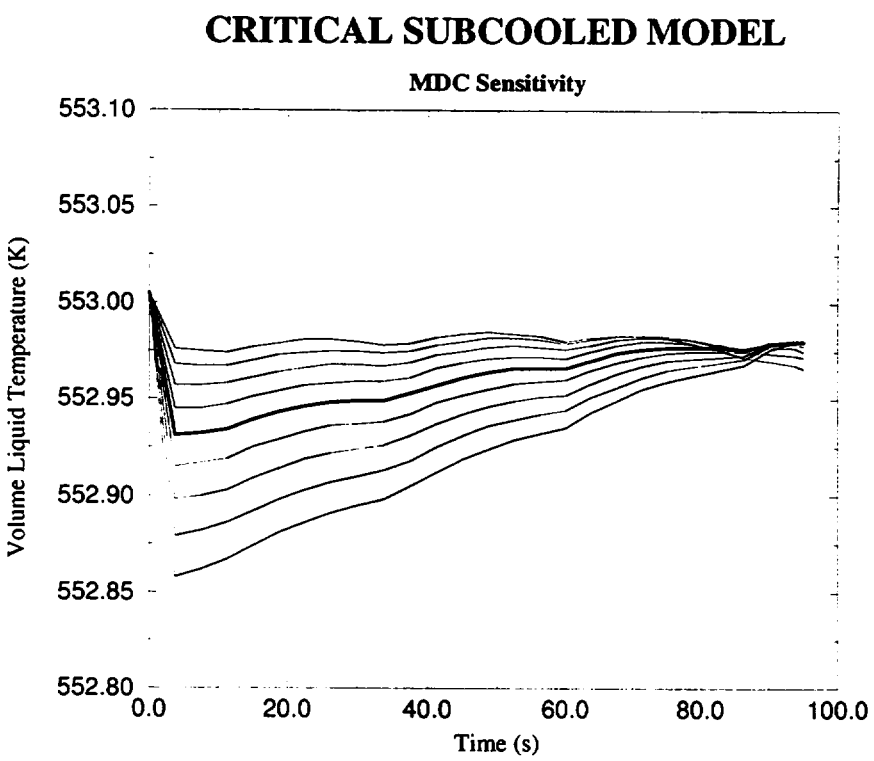

Figure 3.29: Temperature at the last node. MDC sensitivity of the subcooled model.

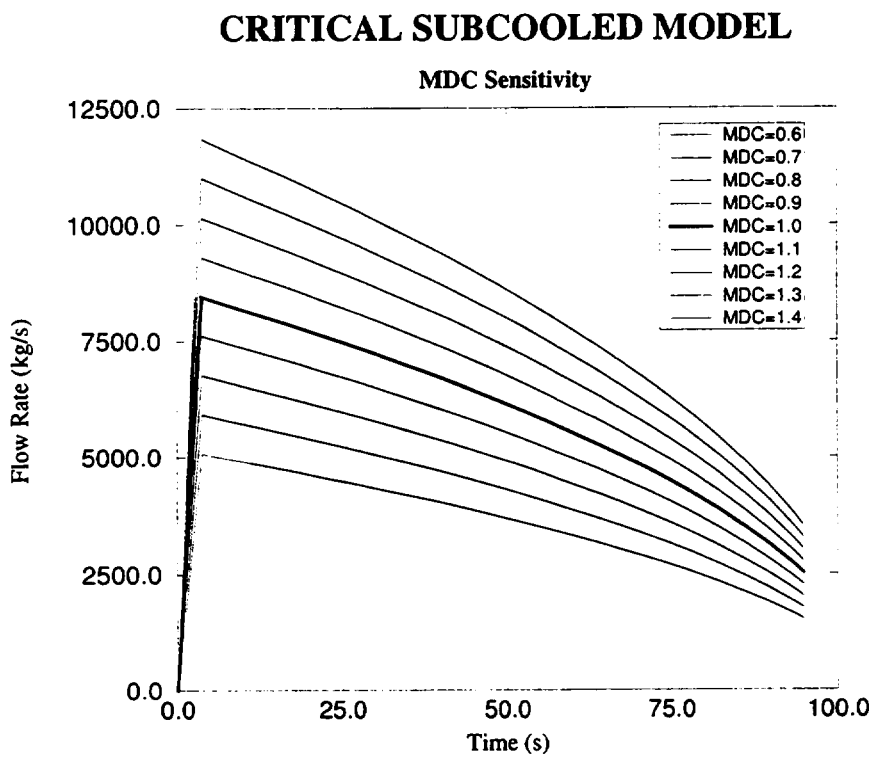

Figure 3.30: Mass flow at nozzle exit. MDC sensitivity of the subcooled model.

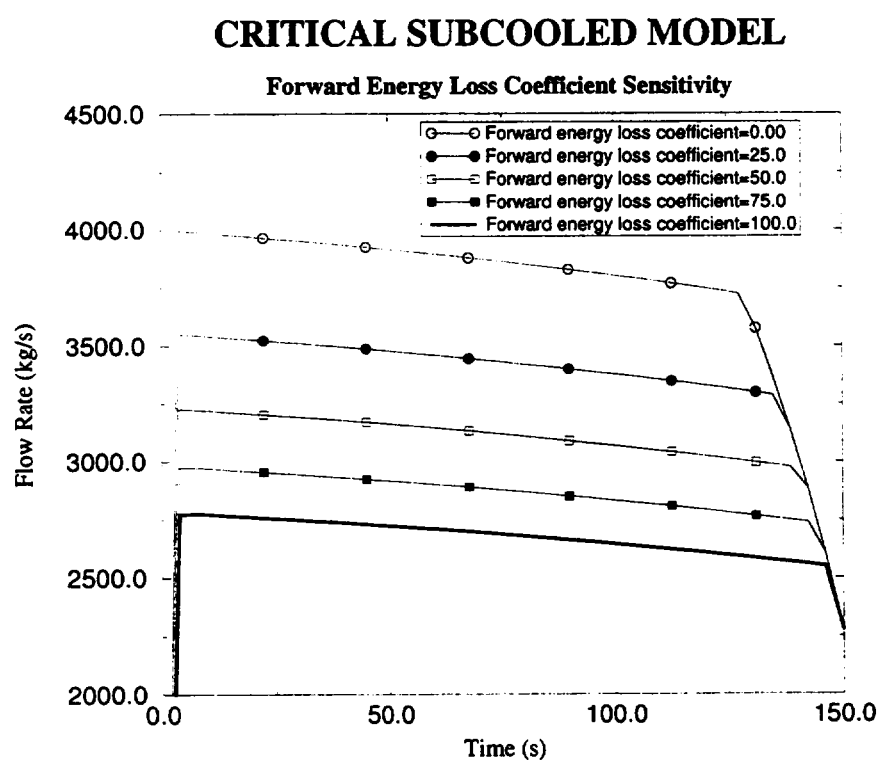

Figure 3.31: Mass flow at nozzle exit. Energy loss coefficient sensitivity of the subcooled model.

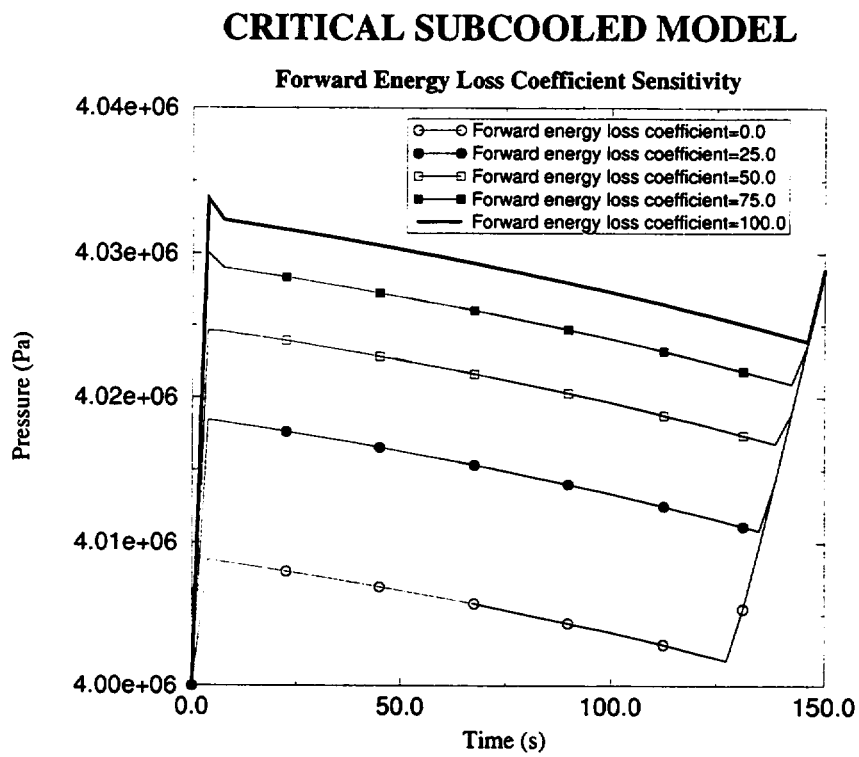

Figure 3.32: Pressure at the last node. Energy loss coefficient sensitivity of the subcooled model.

3.1.2 Sensitivity Analysis of Two-phase CFM to Void-fraction and TDC

For the two-phase model, a sensitivity analysis has been done with respect to the following variables:

- Void-fraction.
- Two-phase Discharge Coefficient (TDC).

A sensitivity analysis with respect to the pressure was not performed because if the quality is fixed and the pressure is varied at the pipe inlet, the void-fraction and quality are not fixed at the last node. So, it is not possible to make a pressure sensitivity analysis for the two-phase CFM.

The void-fraction sensitivity analysis was performed in the following way: the pipe inlet pressure (upper TMDPVOL) was fixed for each case and the quality was varied from 0.001 to 0.9999 (increasing void-fractions). These calculations have been done for different pressures (from 10 bar to 150 bar). In order to compare the homogeneous and non-homogeneous options the analysis has been made for both models.

In TDC sensitivity analysis, a case taken from the void-fraction sensitivity analysis was used, with $P = 80$ bar, varying TDC from 0.6 to 1.4.

Void Fraction Sensitivity. An increasing void-fraction sensitivity analysis was made for CFM with the homogeneous and non-homogeneous options. In the results it can be observed that the last node pressure, Figure 3.33, remains constant during the transient and the void-fraction, Figures 3.34 and 3.38, grows from 0 to 1. The mass flow shows an unexpected behaviour for homogeneous and non-homogeneous options:

- Homogeneous option, Figure 3.35. A maximum is observed for void-fractions near to 0.1 and pressures higher than 90 bar. In order to show the dependence of the critical mass flux upon the void fraction, the stationary states of the Figures 3.34 and 3.35, are represented in Figure 3.36.
- Non-homogeneous option, Figure 3.39. One or two maxima are observed depending on pressure.

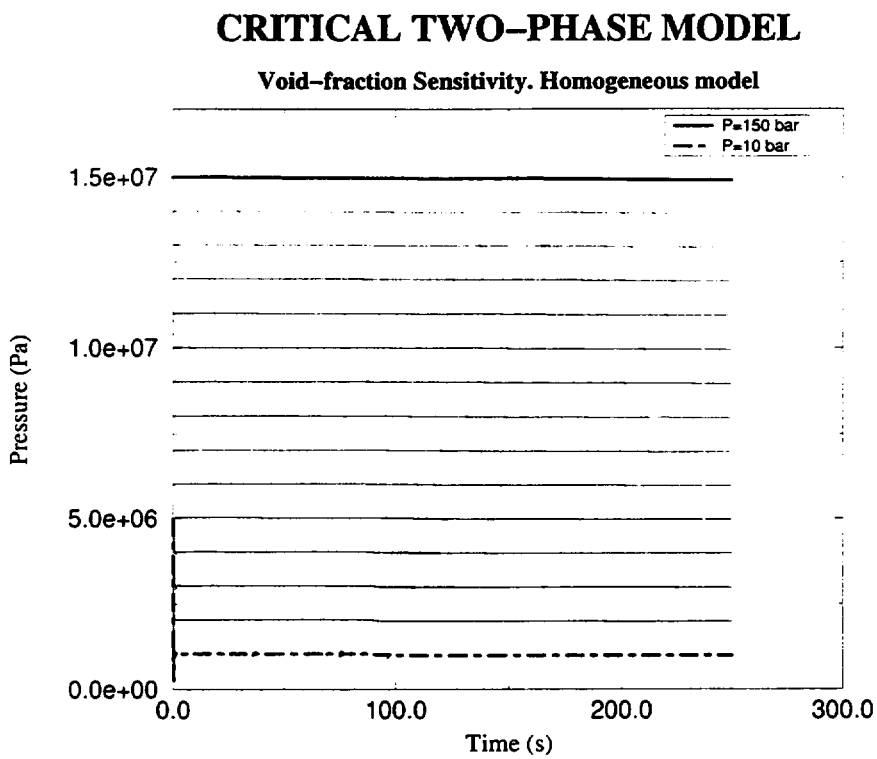

Figure 3.33: Pressure at the last node. Void-fraction sensitivity of the two-phase model. Homogeneous and non-homogeneous models.

Typical data of the homogeneous model, Figure 3.37, and experimental data do not show any maximum.

For pressures below 50 bar, an oscillatory behaviour is observed, Figures 3.35 and 3.39. This problem can not be removed with a smaller time step. Clearly, this is a numerical phenomenon, because for higher pressures a similar oscillatory behaviour was observed and removed diminishing the time step.

Two-phase Discharge Coefficient Sensitivity. In this analysis the base case was taken from the void fraction sensitivity analysis. With fixed pressure at the pipe inlet, $P = 80\ bar$, and quality varying from 0.001 to 0.999. The results show that pressure, Figure 3.40, and void-fraction, Figure 3.41, are quite similar for the different discharge coefficients. In Figure 3.42 is easy to check that for a void fraction between 0.1 and 0.9, the variation of the mass flow with the discharge coefficient has the same value than the discharge coefficient, as expected. For void fractions smaller than 0.1 the transition from MDC=1.0 to TDC can be observed. Also, for void fractions greater than 0.9 the transition from TDC to SDC=1.0 can be observed.

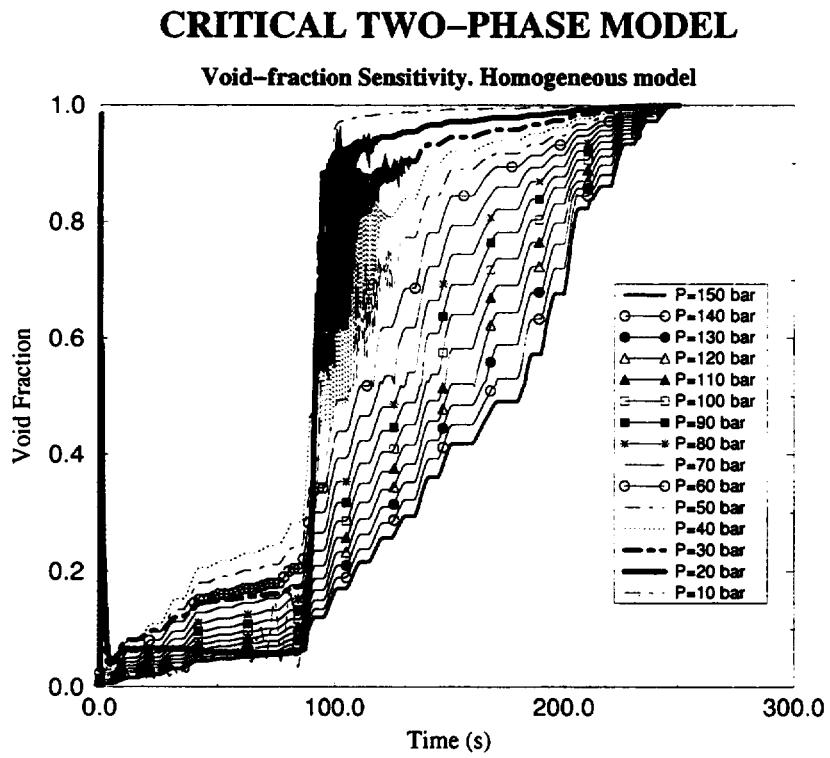

Figure 3.34: Void-fraction at nozzle exit. Void-fraction sensitivity of the two-phase model. Homogeneous model.

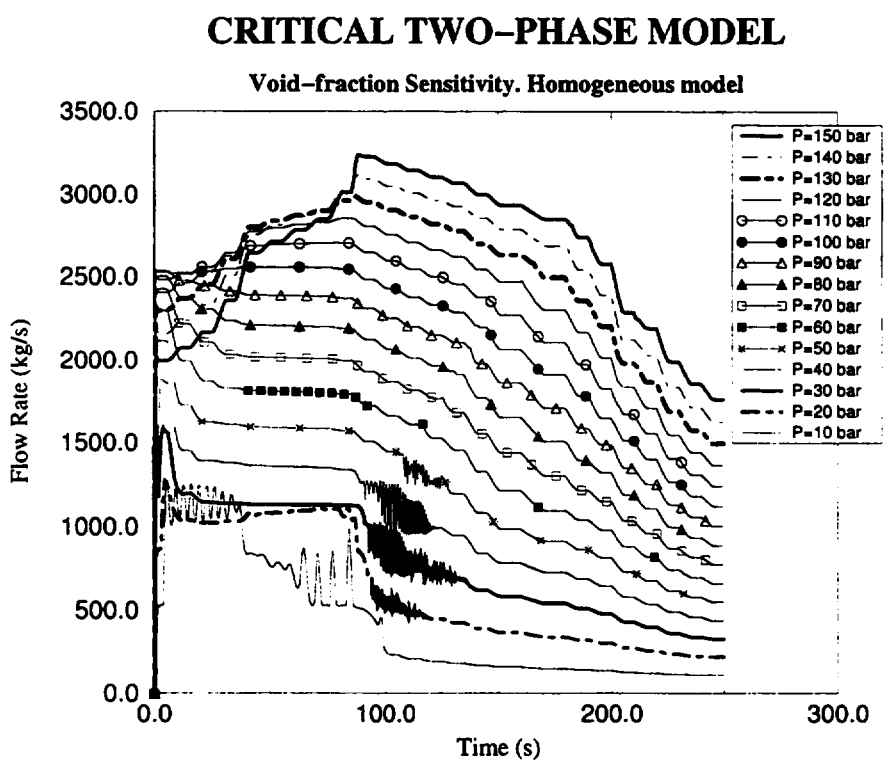

Figure 3.35: Mass flow at nozzle exit. Void-fraction sensitivity of the two-phase model. Homogeneous model.

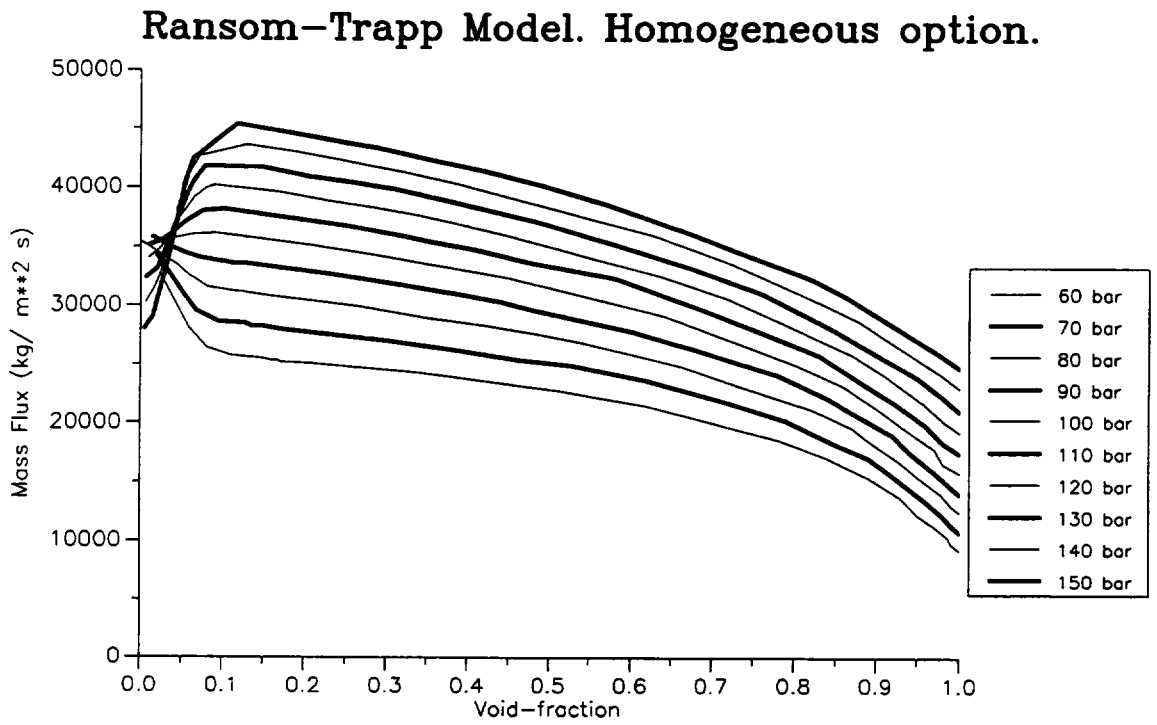

Figure 3.36: Critical mass flux. Ransom-Trapp model.

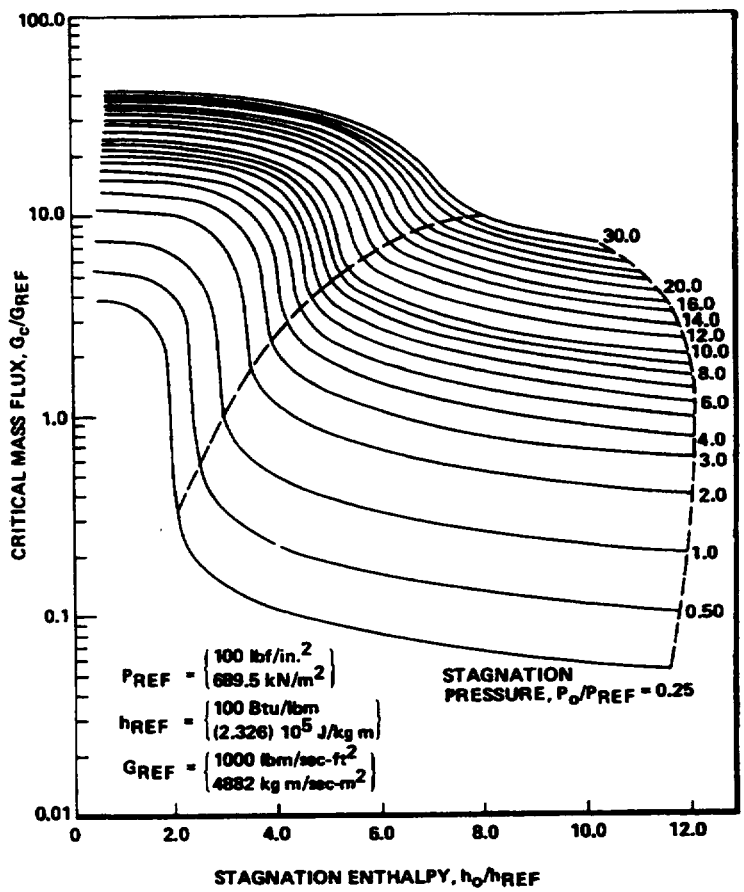

Figure 3.37: Critical mass flux. Homogeneous model (Taken from [LAH-93] pp 444).

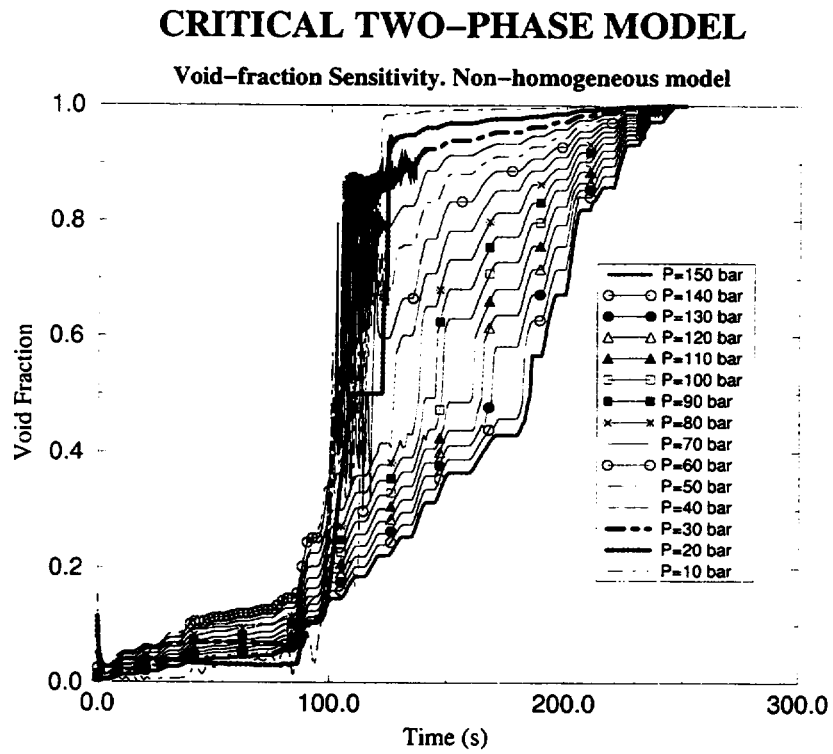

Figure 3.38: Void-fraction at nozzle exit. Void-fraction sensitivity of the two-phase model. Non-homogeneous model.

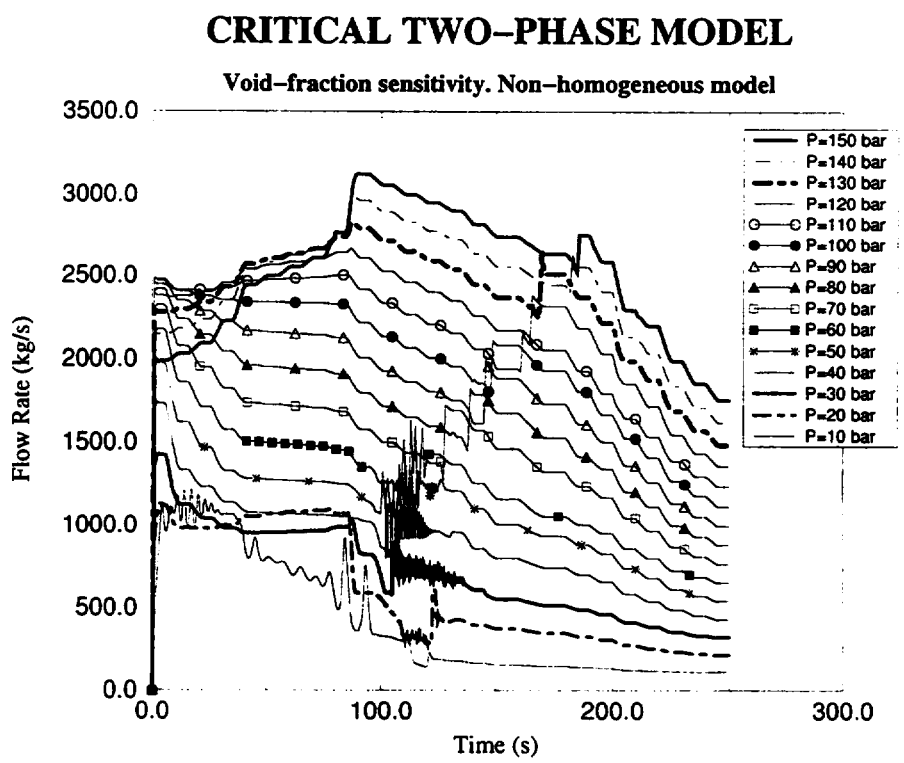

Figure 3.39: Mass flow at nozzle exit. Void-fraction sensitivity of the two-phase model. Non-homogeneous model.

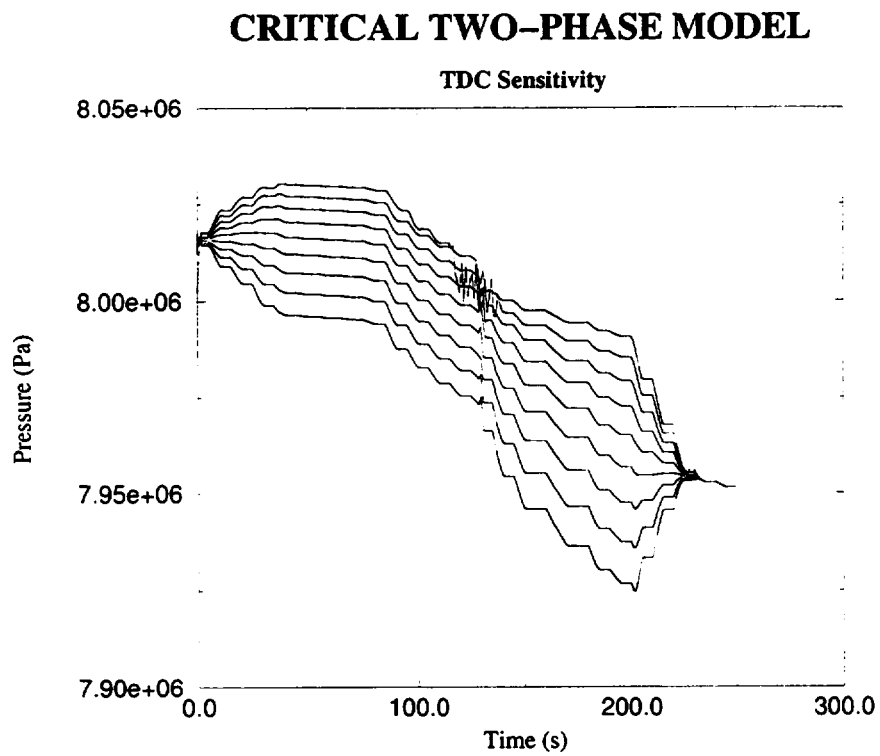

Figure 3.40: Pressure at the last node. TDC sensitivity of the two-phase model.

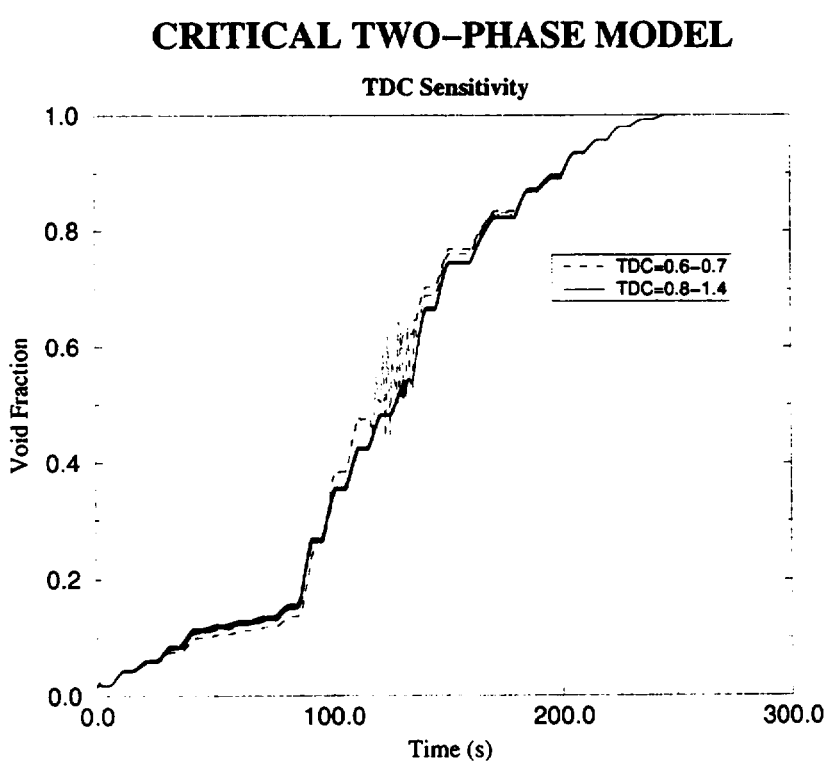

Figure 3.41: Void-fraction at nozzle exit. TDC sensitivity of the two-phase model.

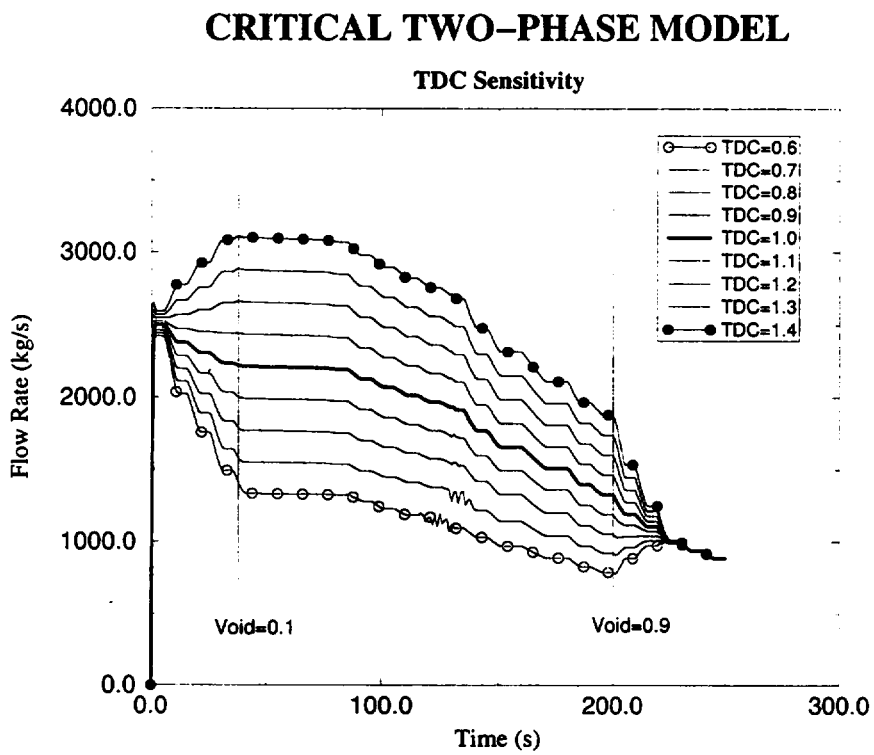

Figure 3.42: Mass flow at nozzle exit. TDC sensitivity of the two-phase model.

3.1.3 Sensitivity Analysis of Steam CFM to Temperature, Pressure and SDC

For the steam model, a similar study to the subcooled CFM (Section 3.1.1) has been performed. The sensitivity analysis has been done with respect to the following variables:

- Temperature.
- Pressure.
- Steam Discharge Coefficient (SDC).

The temperature sensitivity analysis was performed in the following way: fixed pipe inlet pressure (upper TMDPVOL) for each case and decreasing temperature from 673 K to T_{sat}. These calculations have been done for different pressures (from 10 bar to 150 bar).

The pressure sensitivity was performed in a similar way to temperature sensitivity: fixed pipe inlet temperature (TMDPVOL) each case and pressure varying from 10 bar to P_{sat} (increasing pressures). These calculations have been done for different temperatures (from 473 K to 673 K).

For the SDC sensitivity analysis, a case from the pressure sensitivity analysis was taken, varying SDC from 0.6 to 1.4. In order to compare the CFM with the Non-CFM, both temperature and pressure were checked at the last node to make sure that they were similar.

The results obtained for the different sensitivity analysis are described below:

Temperature Sensitivity. An increasing temperature sensitivity analysis was made for CFM and Non-CFM. In the results the similarity between the pressure, Figures 3.43 and 3.44, and the temperature at the last node, Figures 3.45 and 3.46, can be seen, so that the critical mass flow, Figure 3.47, and non-critical mass flow results, Figure 3.48, can be compared: the mass flow with CFM-on is always lower than CFM-off. This implies that the transition logic from CFM to Non-CFM is correct.

Pressure Sensitivity. An increasing pressure sensitivity analysis was made for CFM and Non-CFM. In the results it can be observed that pressure, Figures 3.51 and 3.52, and temperature at the last node, Figures 3.49 and 3.50, are quite similar,

so critical mass flow, Figure 3.53, and non-critical mass flow results, Figure 3.54, can be compared. Mass flow of CFM-on is always lower than CFM-off, as is shown in Figure 3.55. Anyway, the user must be careful because if an energy loss coefficient is used, the non-critical mass flow could decrease and become lower than the critical mass flow.

Steam Discharge Coefficient Sensitivity. In this analysis a case from pressure sensitivity analysis was used. The temperature is fixed at the pipe inlet, T= 673 K, and pressure is varied from 10 to 150 bar. The results show that pressure, Figure 3.56, and temperature, Figure 3.57, are quite similar for the different discharge coefficients. In Figure 3.58 it is easy to check that the variation of the mass flow with the discharge coefficient has the same value than the discharge coefficient, as expected.

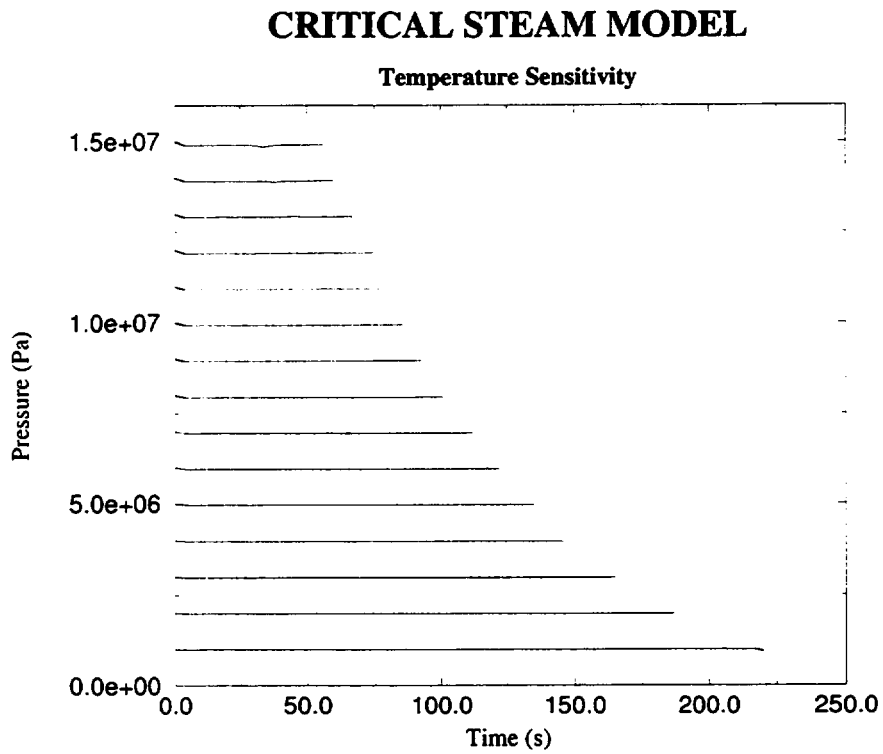

Figure 3.43: Pressure at the last node (Temperature sensitivity of the steam model). CFM on.

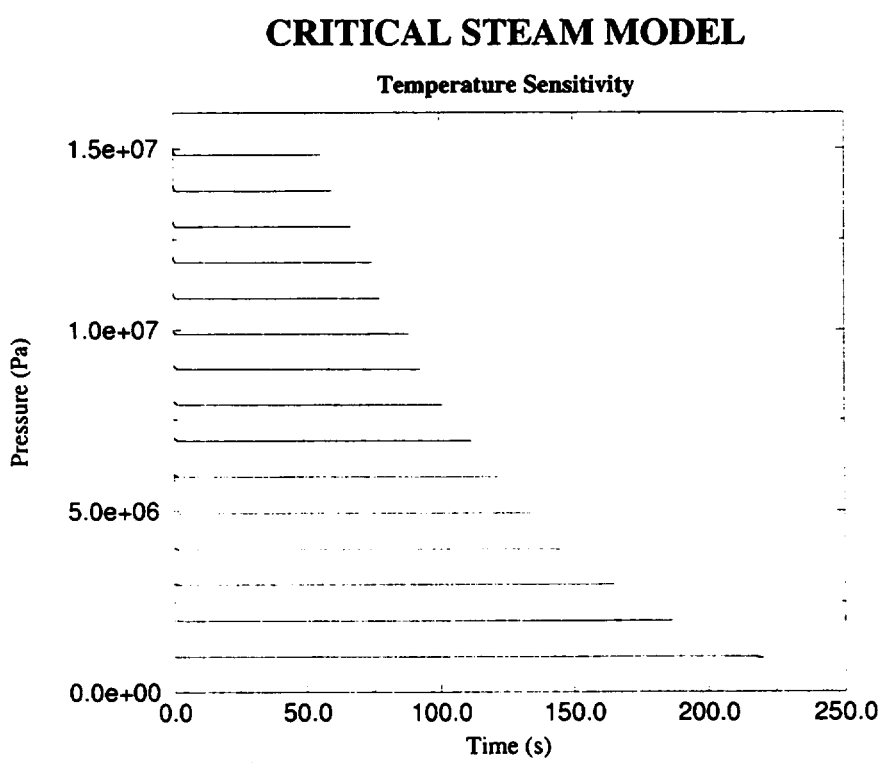

Figure 3.44: Pressure at the last node (Temperature sensitivity of the steam model). CFM off.

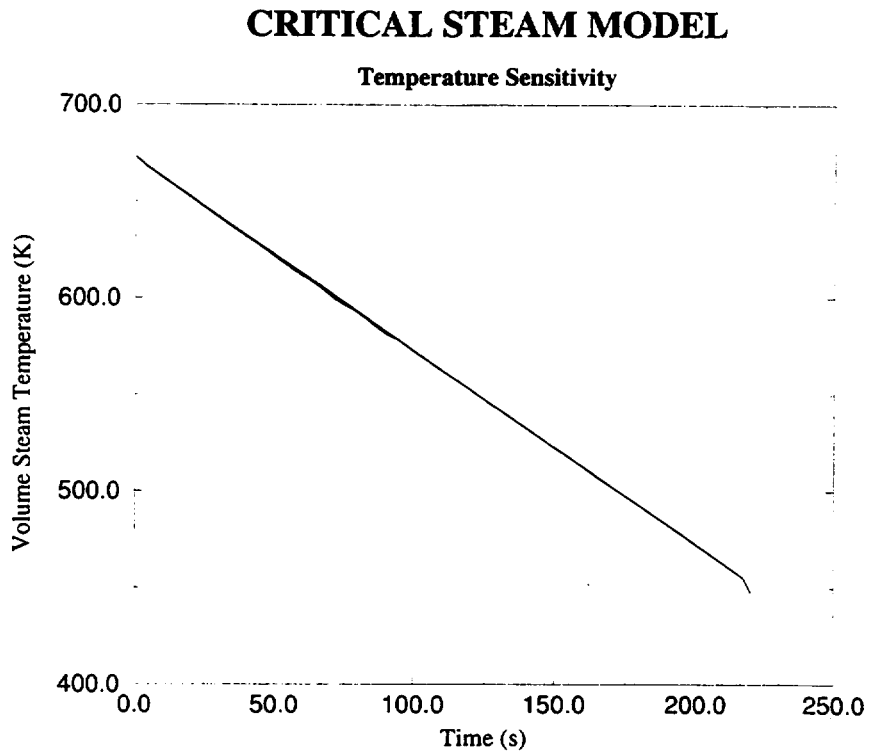

Figure 3.45: Temperature at the last node (Temperature sensitivity of the steam model). CFM on.

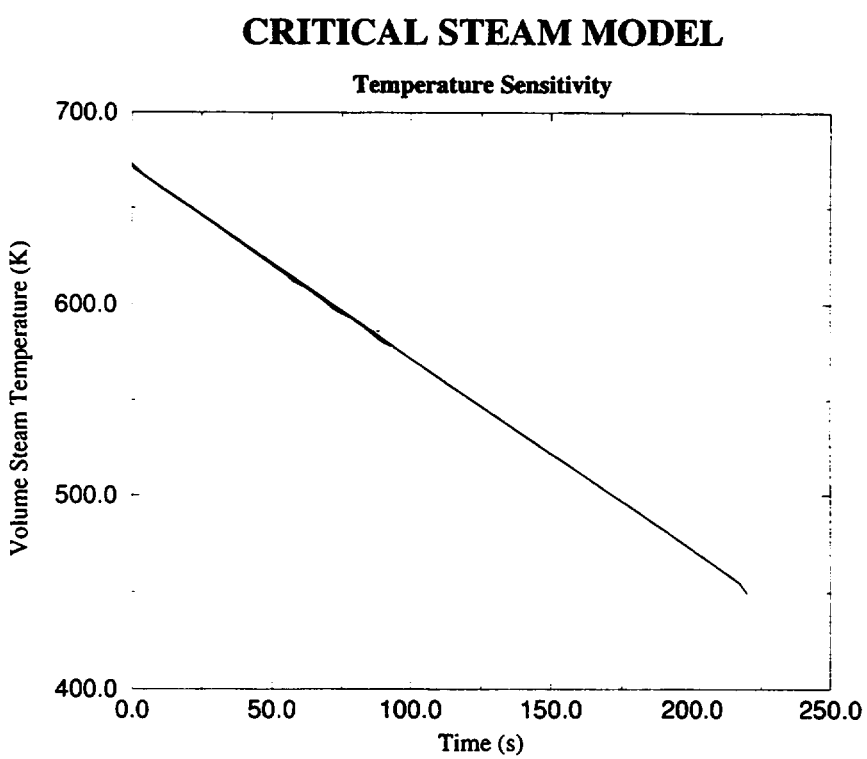

Figure 3.46: Temperature at the last node (Temperature sensitivity of the steam model). CFM off.

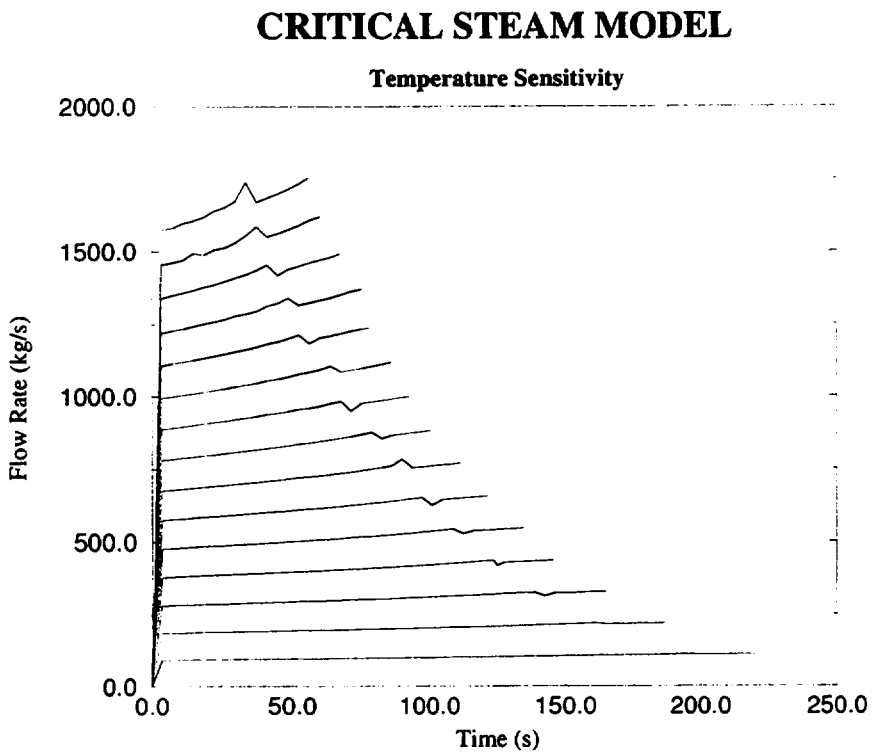

Figure 3.47: Mass flow at nozzle exit (Temperature sensitivity of the steam model). CFM on.

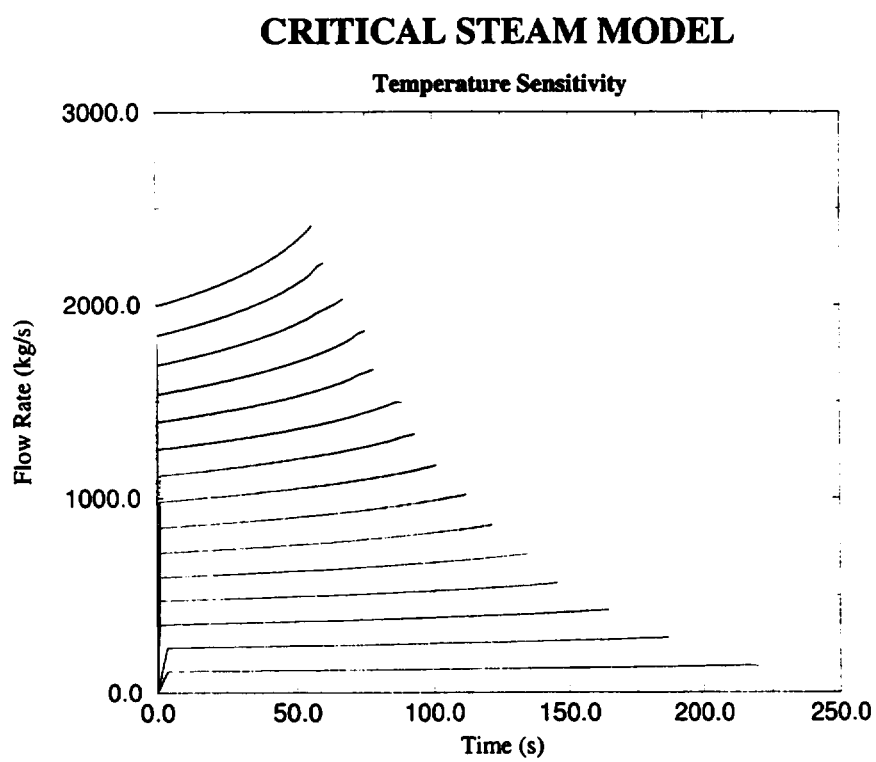

Figure 3.48: Mass flow at nozzle exit (Temperature sensitivity of the steam model). CFM off.

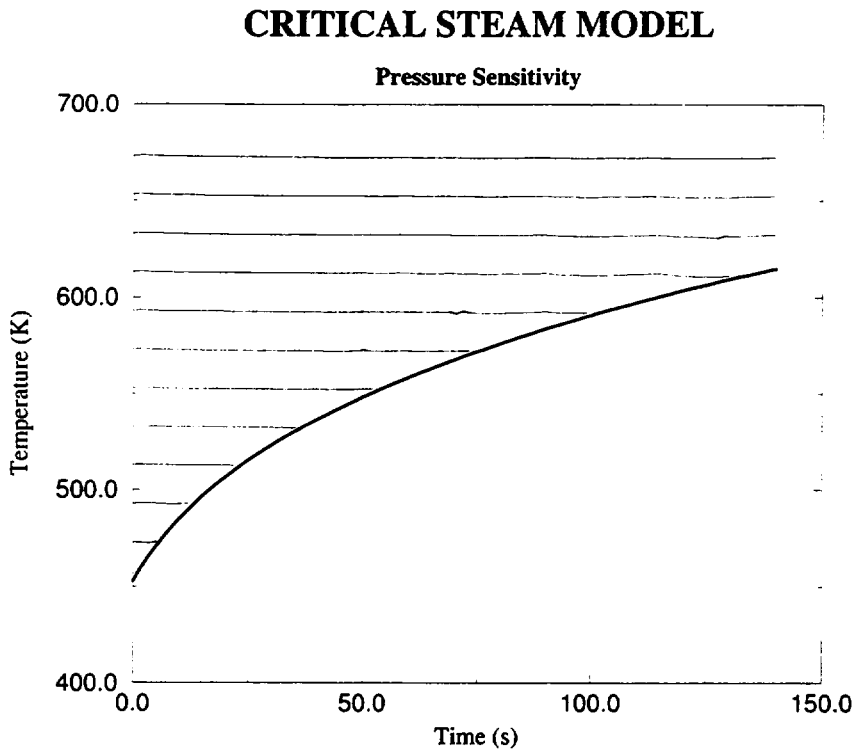

Figure 3.49: Liquid temperature at the last node (Pressure sensitivity of the steam model). CFM on.

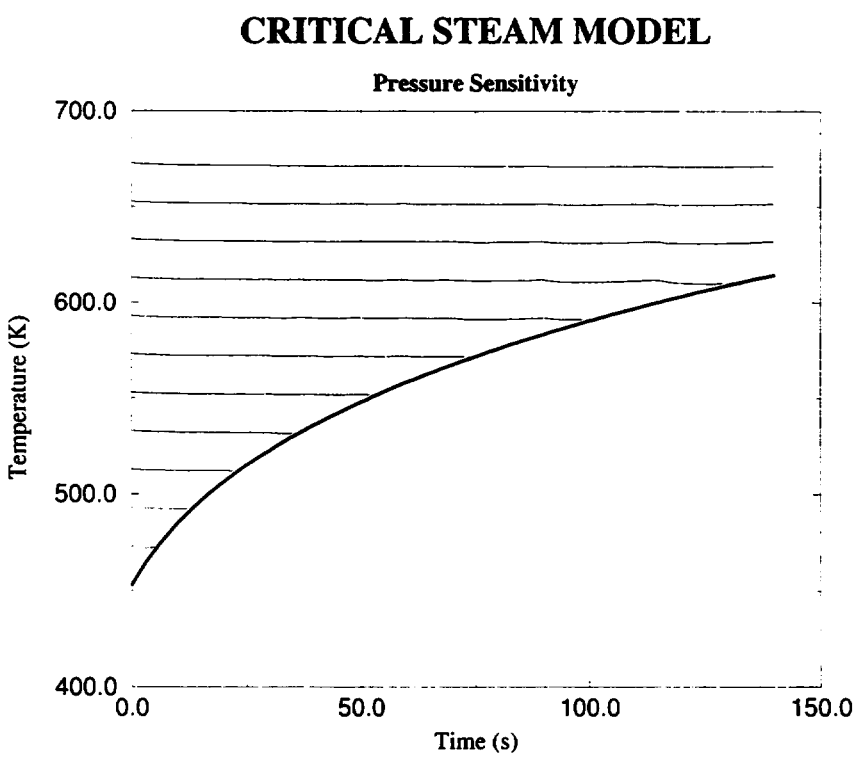

Figure 3.50: Liquid temperature at the last node (Pressure sensitivity of the steam model). CFM off.

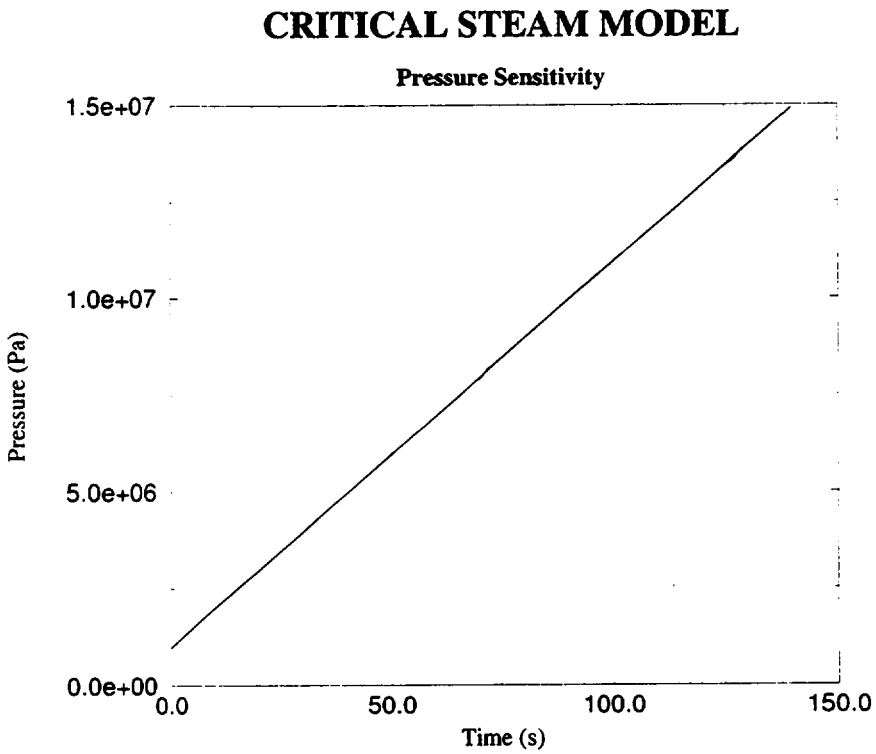

Figure 3.51: Pressure at the last node (Pressure sensitivity of the steam model). CFM on.

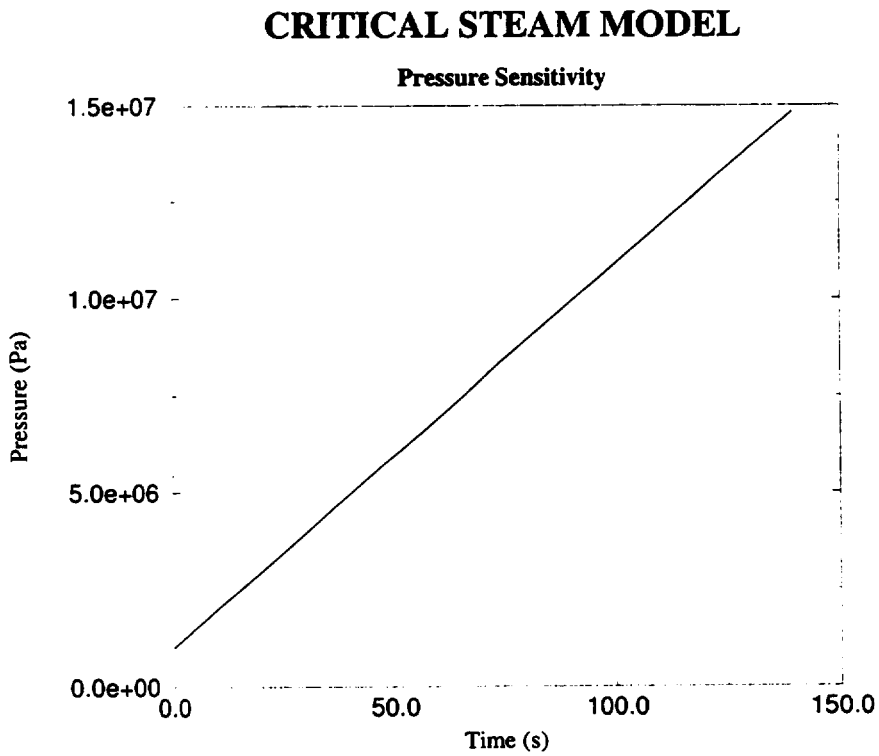

Figure 3.52: Pressure at the last node (Pressure sensitivity of the steam model). CFM off.

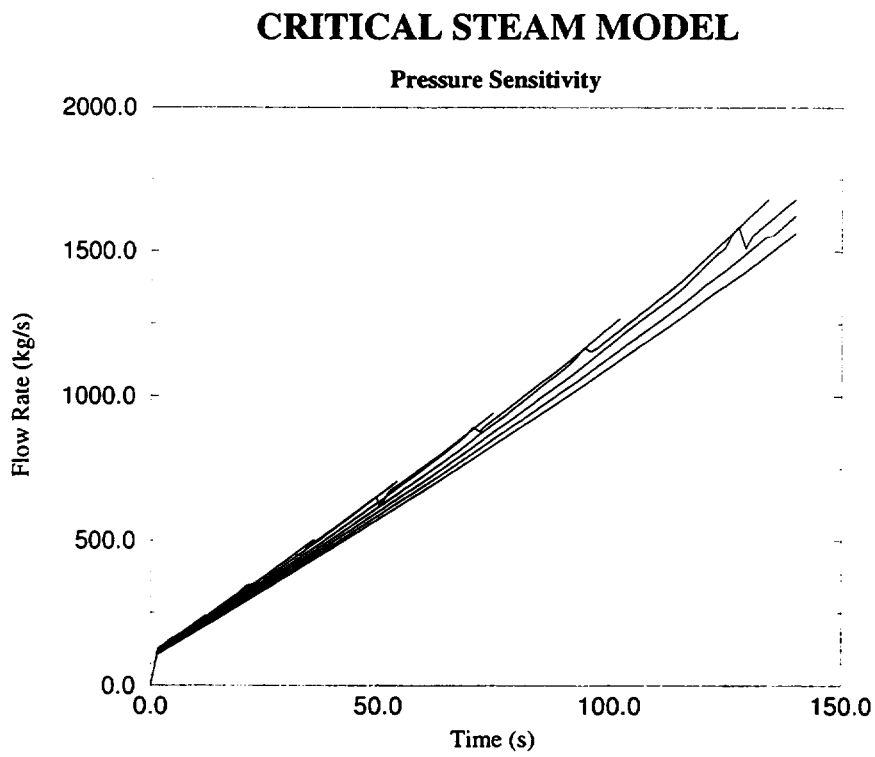

Figure 3.53: Mass flow at nozzle exit (Pressure sensitivity of the steam model). CFM on.

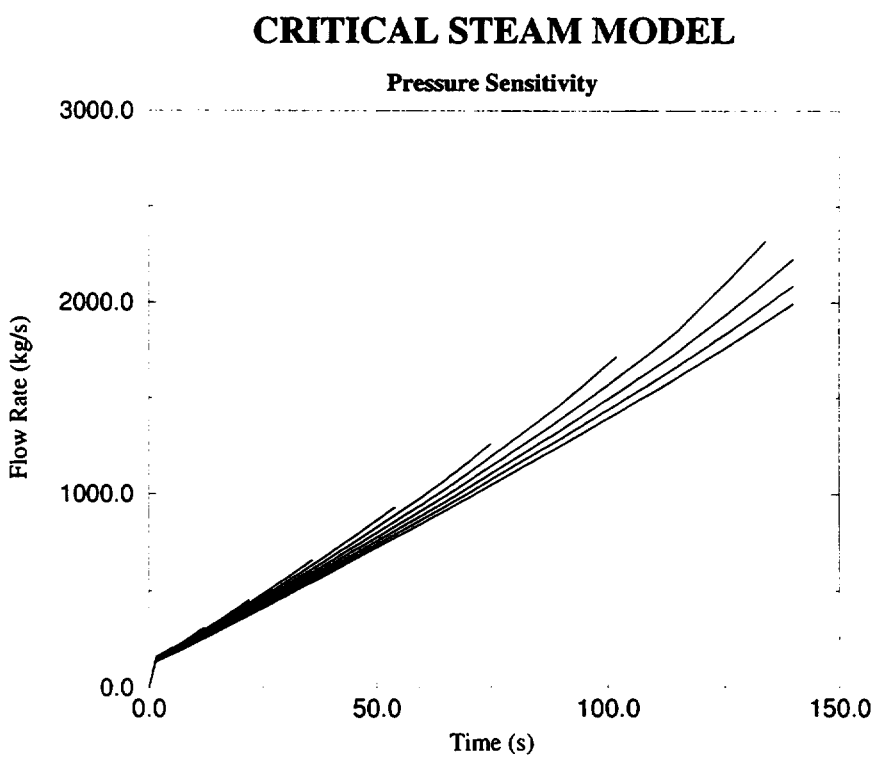

Figure 3.54: Mass flow at nozzle exit (Pressure sensitivity of the steam model). CFM off.

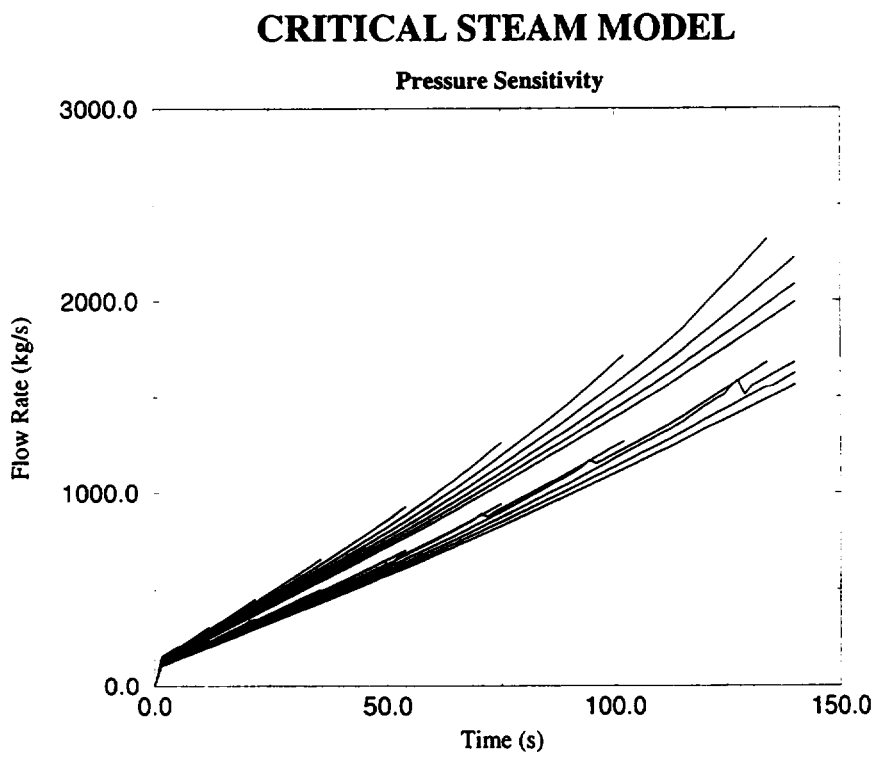

Figure 3.55: Mass flow at nozzle exit (Pressure sensitivity of the steam model). Comparison of CFM on and CFM off.

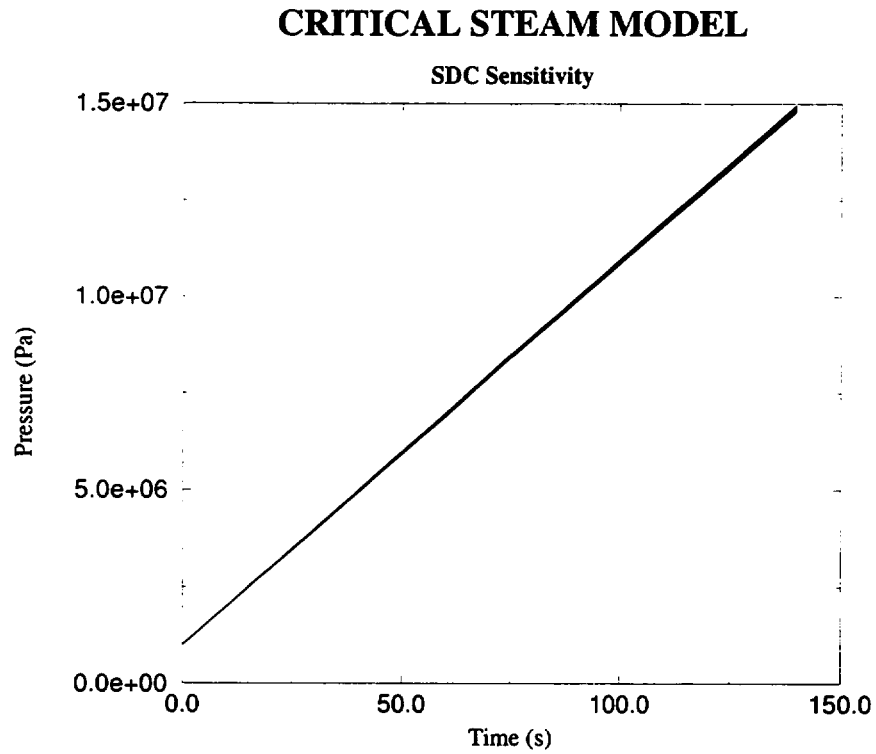

Figure 3.56: Pressure at the last node. SDC sensitivity of the steam model.

3.2 Sensitivity Analysis of Henry-Fauske Model

In this section, the sensitivity analysis of the subcooled and two-phase CFMs is analyzed in a way similar to that done for the Ransom-Trapp model. The objective of this analysis is to obtain the dependence of the CFM with respect to the following variables:

- Temperature.
- Pressure.
- Void Fraction.
- Disequilibrium Parameter.
- Forward Energy Loss Coefficient.

The range of variation of the variables and the models used for the sensitivity analysis is the same than for the Ransom-Trapp model, see Section 3.1.

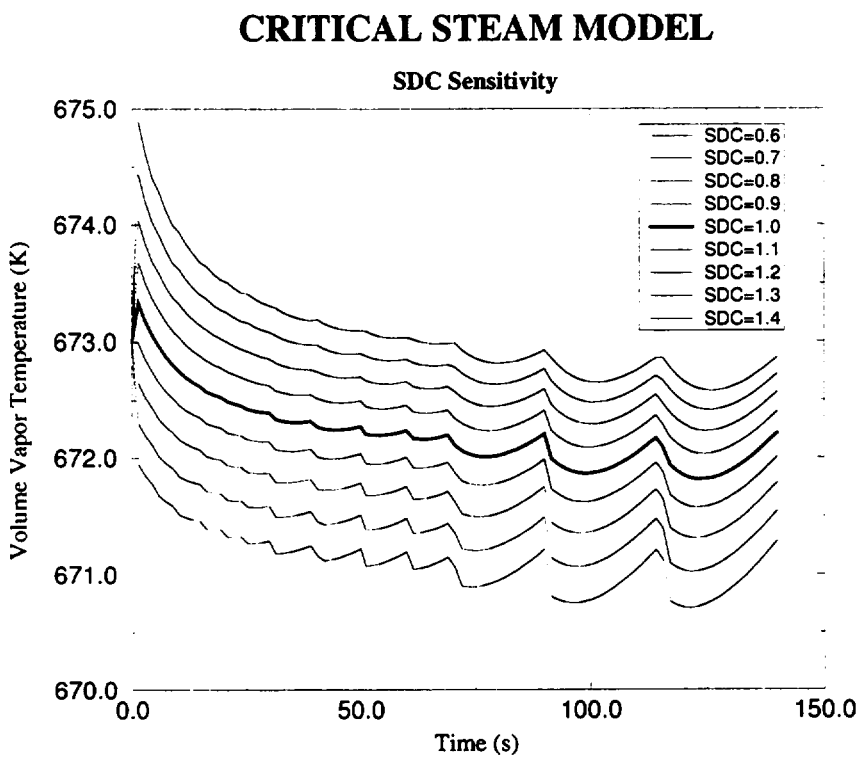

Figure 3.57: Temperature at the last node. SDC sensitivity of the steam model.

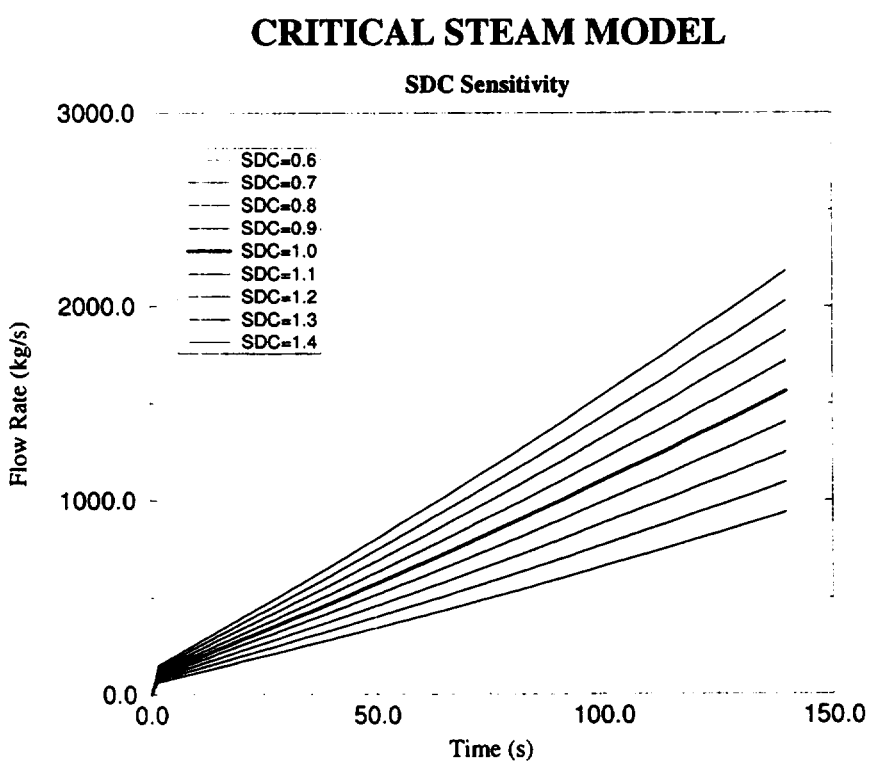

Figure 3.58: Mass flow at nozzle exit. SDC sensitivity of the steam model.

3.2.1 Sensitivity Analysis of Subcooled CFM to Temperature, Pressure, Disequilibrium Parameter and Forward Energy Loss Coefficient

For the subcooled model, sensitivity analyses have been done with respect to the following variables:

- Temperature.
- Pressure.
- Disequilibrium Parameter.
- Forward Energy Loss Coefficient.

The temperature sensitivity analysis was performed in the following way: pipe inlet pressure (upper TMDPVOL) was fixed for each case and temperature was varied from 373 K to T_{sat} (increasing temperatures). These calculations have been done for different pressures (from 10 bar to 150 bar).

The same analyses have also been performed for temperatures decreasing from T_{sat} to 373 K, in order to compare with the results of the Ransom-Trapp model.

The pressure sensitivity analysis was performed in the same way than for Ransom-Trapp model: pipe inlet temperature (upper TMDPVOL) was fixed for each case and pressure was varied from P_{sat} to 10 bar (decreasing pressures). These calculations have been done for different temperatures (from 373 K to 613 K).

For the disequilium parameter sensitivity analysis, the pipe inlet pressure was fixed to 80 bar and the temperature varied from 373 K to 523 K. The mass flow was calculated for several values of the disequilibrium parameter (0, 0.01, 0.05, 0.1, 0.14, 0.3, 0.5, 1, 1000), using the abrupt area change option of the code.

The results obtained for the different sensitivity analysis are described below:

Temperature Sensitivity. In both cases (decreasing and increasing temperatures), Figures 3.60 and 3.59, the behaviour is the same, with no transition logic problems. This is in accordance with the analysis performed in Section 2.1.

Pressure Sensitivity. The results in this case, Figure 3.61, do not show any transition problems. This is also in accordance with the analysis performed in Section 2.1.

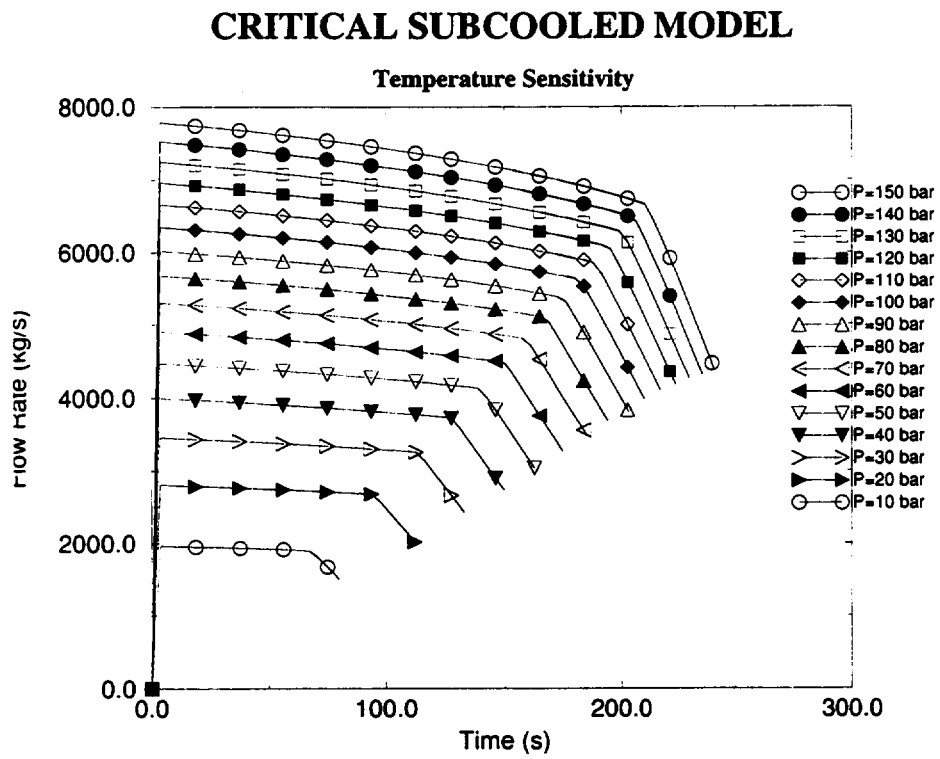

Figure 3.59: Mass flow at nozzle exit. Temperature sensitivity of the subcooled Henry-Fauske model, with increasing temperature.

Disequilibrium Parameter Sensitivity. As is shown in Figure 3.62, the critical flow is strongly dependent on the disequilibrium parameter. This dependence is more important when the temperature approaches the saturation temperature.

Forward Energy Loss Coefficient Sensitivity. The results and conclusions of this analysis, Figure 3.63, show the same behaviour than in the Ransom-Trapp model, Figure 3.31.

3.2.2 Sensitivity Analysis of Two-phase CFM to Void-fraction and Disequilibrium Parameter

For the two-phase model, a sensitivity analysis has been done with respect to the following variables:

- Void-fraction.
- Disequilibrium Parameter.

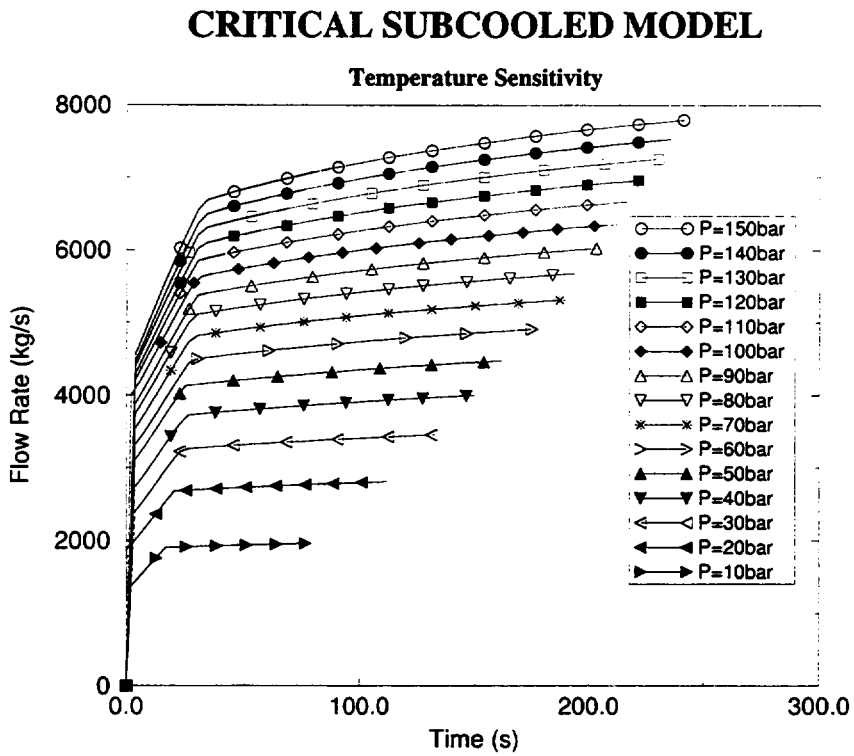

Figure 3.60: Mass flow at nozzle exit. Temperature sensitivity of the subcooled Henry-Fauske model, with decreasing temperature.

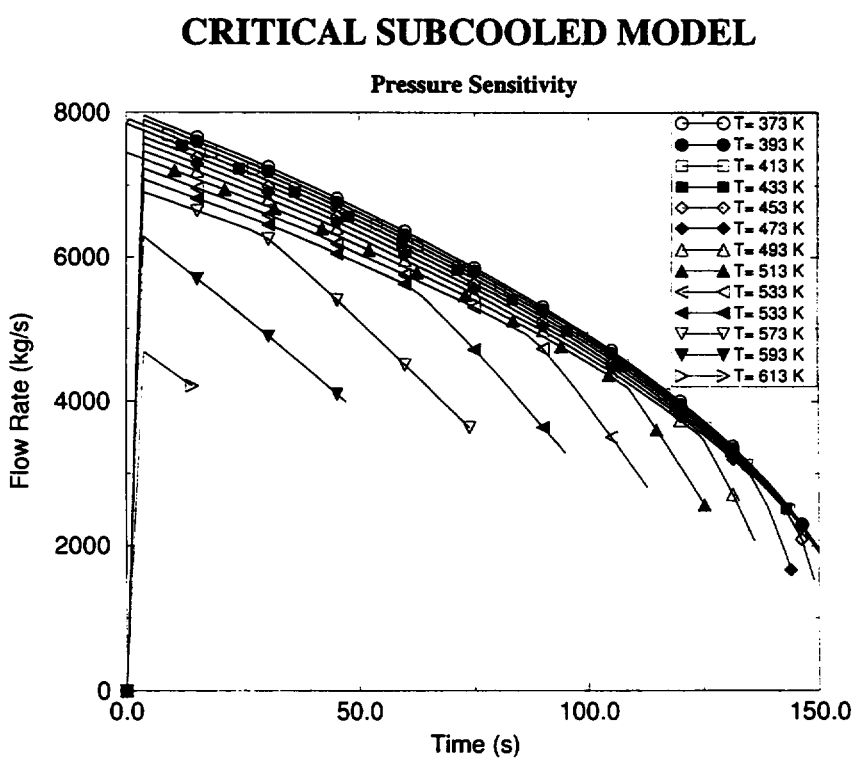

Figure 3.61: Mass flow at nozzle exit. Pressure sensitivity of the subcooled Henry-Fauske model, with decreasing pressure.

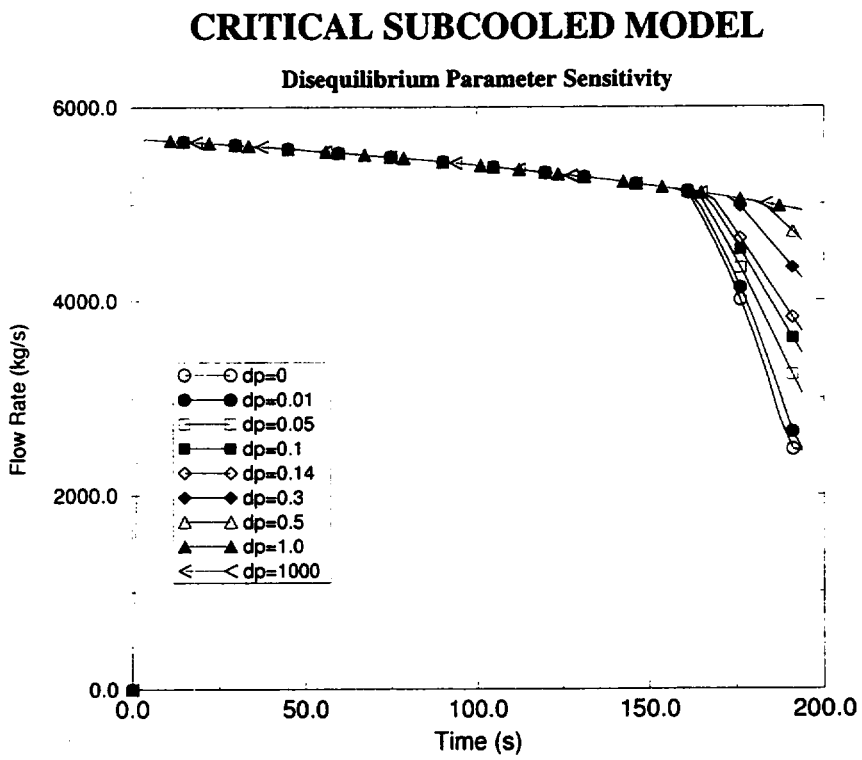

Figure 3.62: Mass flow at nozzle exit. Disequilibrium parameter sensitivity of the subcooled Henry-Fauske model.

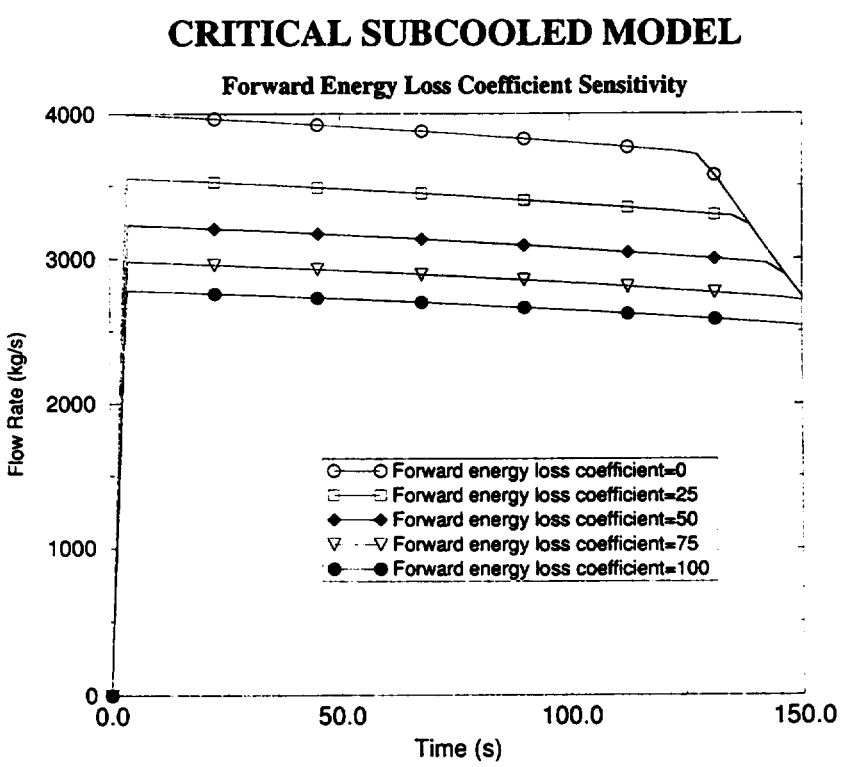

Figure 3.63: Mass flow at nozzle exit. Forward energy loss coefficient sensitivity of the subcooled Henry-Fauske model.

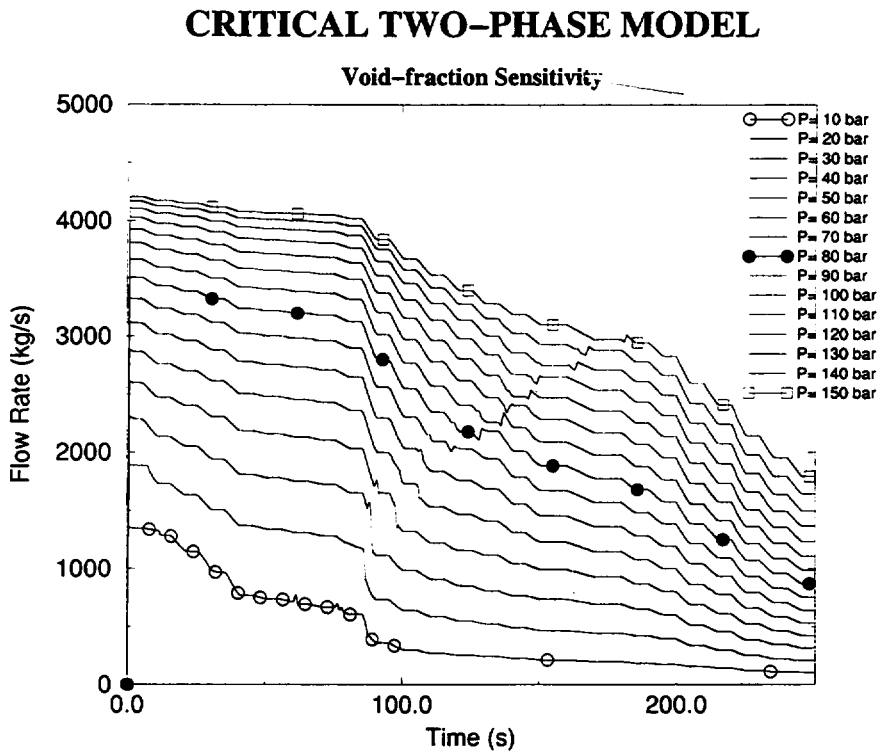

Figure 3.64: Mass flow at nozzle exit. Void-fraction sensitivity of the Henry-Fauske model.

The void-fraction sensitivity analysis was performed in the following way: the pipe inlet pressure (upper TMDPVOL) was fixed for each case and the quality varied from 0.001 to 0.9999 (increasing void-fraction). These calculations have been done for different pressures (from 10 bar to 150 bar).

For the sensitivity analysis of the disequilium parameter, the pipe inlet pressure was fixed to 80 bar and the void fraction was varied from 0 to 1. The mass flow was calculated for the same values of the disequilibrium parameter than for the subcooled analysis, using the abrupt area change option of the code.

Void Fraction Sensitivity. The results of this analysis, Figure 3.64, do not show any maximum, nor oscillatory behaviours unlike in the Ransom-Trapp model. In order to show the dependence of critical mass flux with void fraction, the stationary states of the Figures 3.64 and 3.65, are represented in Figure 3.66.

Disequilibrium Parameter Sensitivity. As is shown in Figure 3.67, critical flow is also strongly dependent on the disequilibrium parameter. This dependence is more important when the void fraction approaches zero, Figure 3.68.

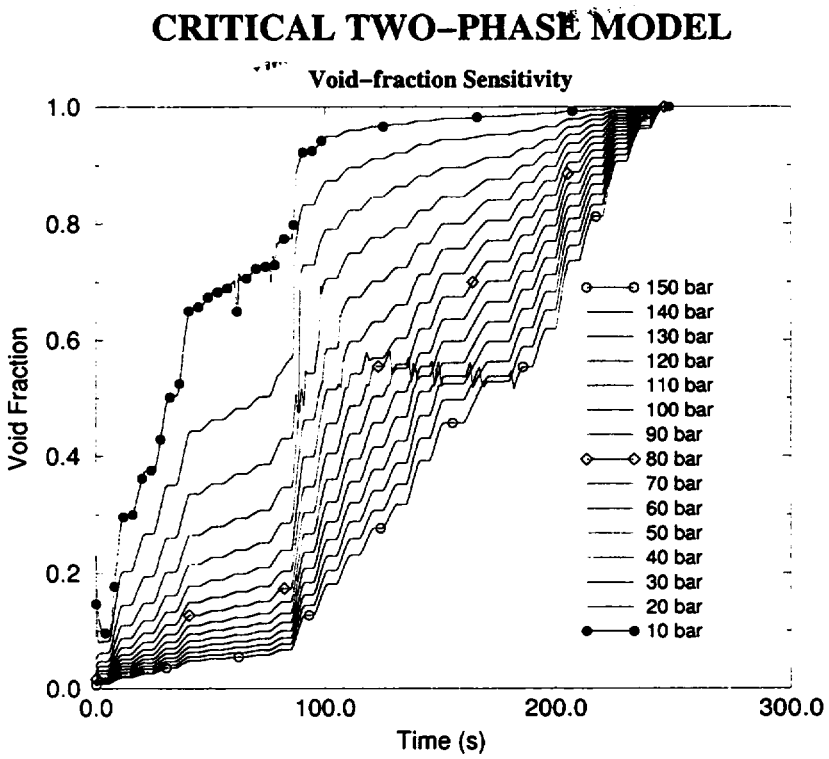

Figure 3.65: Void fraction at nozzle exit. Void-fraction sensitivity of the Henry-Fauske model.

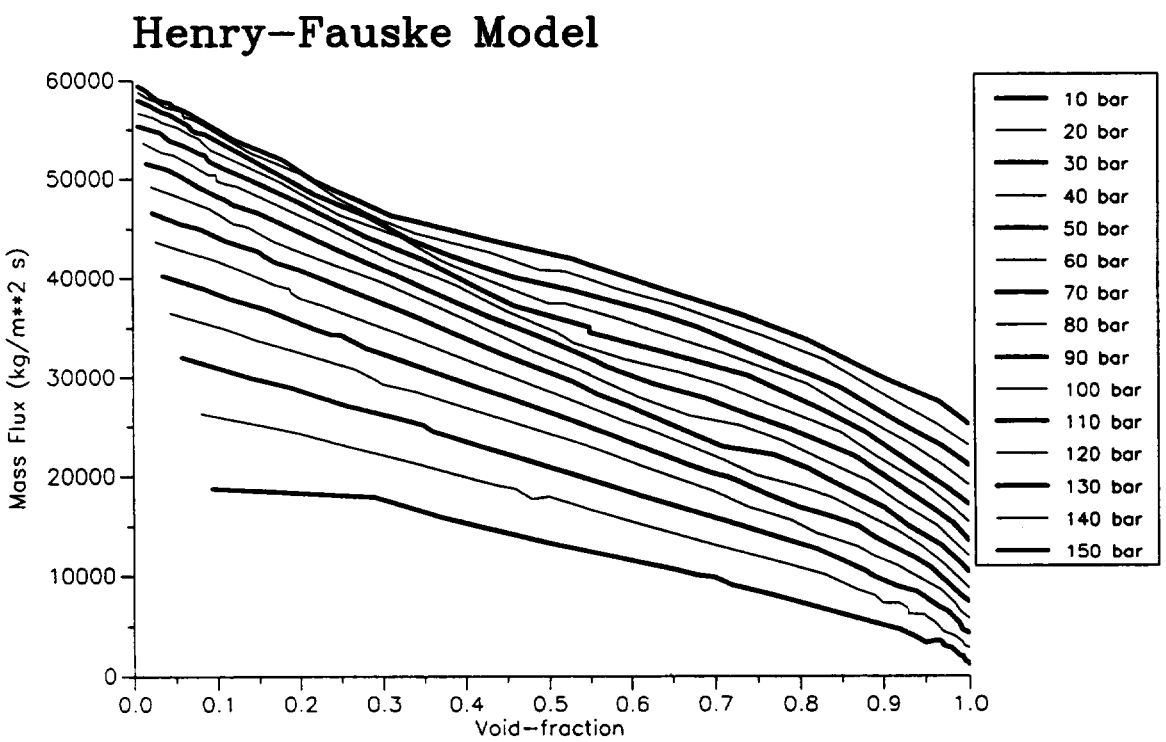

Figure 3.66: Critical mass flux. Henry-Fauske model.

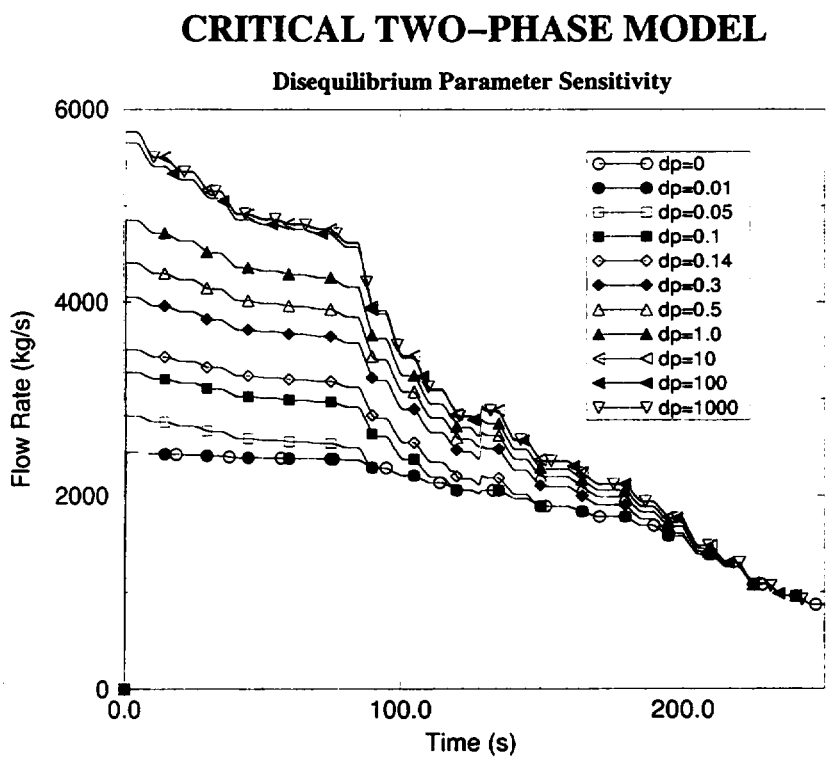

Figure 3.67: Mass flow at nozzle exit. Disequilibrium parameter sensitivity of the Henry-Fauske model.

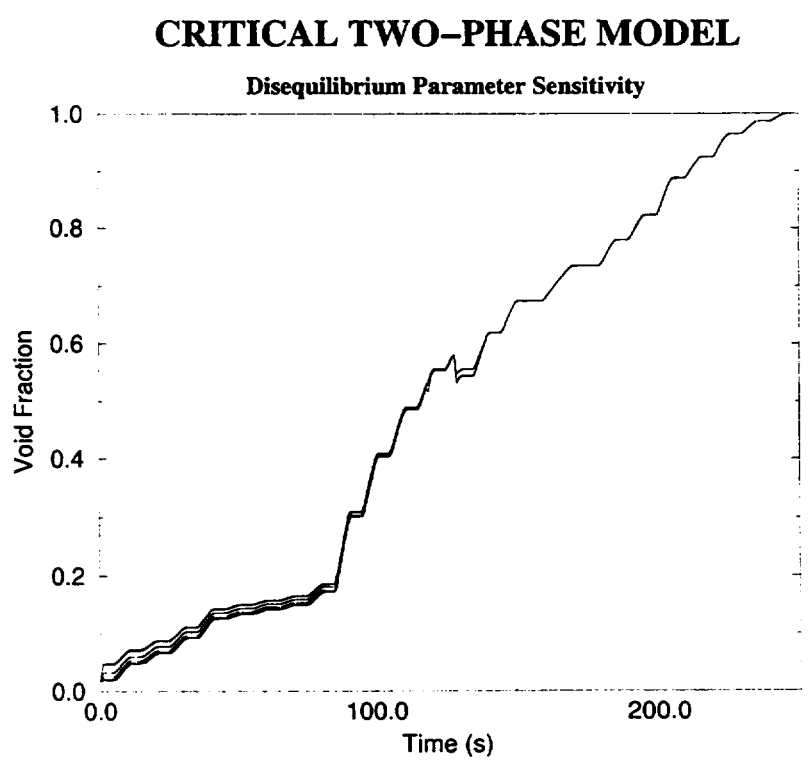

Figure 3.68: Void fraction at nozzle exit. Disequilibrium parameter sensitivity of the Henry-Fauske model.

3.3 Discussion and Conclusions of the Sensitivity Results

The main conclusions for the Ransom-Trapp model are:

- Subcooled. The behaviour is anomalous due to the transition logic from critical flow to non-critical flow.
- Two-phase. The results show one or two maxima for the mass flow. This is not an expected behaviour and is not found in the literature. Oscillatory results below 60 bar are observed.
- Energy loss coefficient. It must be used with care in junctions where critical mass flow is expected, because the CFM does not depend on it but non-CFM decreases with it.
- Discharge coefficients. From the results it can be concluded that the variation of the mass flow with the discharge coefficient has the same value than the discharge coefficient.
- There are several other known problems with this model, that makes it necessary changing the model or avoiding its use.

The main conclusions for the Henry-Fauske model are:

- Subcooled. There are no problems with the transition logic from critical flow to non-critical flow.
- Two-phase. There is not any maxima for the mass flow, nor is here oscillatory behaviour unlike in the Ransom-Trapp model.
- Energy loss coefficient. It must be used with care in junctions where critical mass flow is expected, because the CFM does not depend on it, but non-CFM decreases with it.
- Disequilibrium parameter. Mass flow is strongly dependent on this parameter. In order to avoid the user effect, this value should be internally fixed or at least detailed user guidelines should be supplied.
- In general the model shows good behaviour, but user guidelines should be supplied for the discharge coefficient and the disequilibrium parameter.

Chapter 4

Assessment of RELAP5/MOD3 CFM against Marviken Tests

One of the main objetives of the Marviken tests was the assessment of critical-flow calculations at a scale and in a geometry important for large-break LOCAs. The Marviken full-scale critical-flow tests provide data to assess the ability of the CFM implemented in the computer codes to calculate large pressure-vessel blowdowns and critical flow in large-size pipes, in a critical-flow geometry that is reasonably typical of that assumed in the licensing design-basis, large-break LOCA. The tests cover both subcooled and two-phase critical flow.

In this chapter, data from Marviken Tests CFT-01, 06, 11, 15, 17, 21 and 24 are used to assess the default critical flow model of RELAP5/MOD3.2, Ransom-Trapp model, and the new Henry-Fauske option.

To achieve this goal, the following steps have been included:

- Description of the facility and of the test.
- Description of the RELAP5/MOD3.2 facility models used for the simulation.
- Review of the bibliography of the Marviken tests simulation.
- Comparison of critical and non-critical flow models with test data.
- Comparison and selection of the options for the different models.
- Discharge coefficient adjustment for subcooled and two-phase conditions with different nozzle models.
- Analysis of the results.

4.1 Facility and Test Description

Marviken Power Station was originally built as a boiling heavy water direct cycle reactor with natural circulation and provisions for nuclear super-heating of the steam, but nuclear fuel was never charged. The reason was that the plant could not verify General Design Criterion 12 about stability. An oil fired boiler was built instead to provide steam for the turbine, leaving the nuclear steam supply system intact: reactor vessel and most of the auxiliary systems, pressure containment, reactor hall and fuel handling area. After testing the containment pressure-suppression systems, the nuclear island was modified to accommodate the Marviken series large scale critical flow experiments.

Two full scale critical flow series of experiments were developed at the site:

- Critical Flow Test (CFT) project. The test phase was conducted between January 1978 and July 1979. The objective of this test program was to obtain full scale critical flow data for test nozzles as a function of pressure, subcooling, low inlet quality, length and nozzle diameter from two-phase mixtures from 27 experiments.
- Jet Impingement Test (JIT) program. This test program, developed after the CFT program, was focused on measuring loads due to a fluid jet impinging upon a flat plate, and also generated full scale critical flow data.

The aim at the CFT experiments was to collect critical flow data as a function of the nozzle geometries and the initial steam conditions at the upper plenum. The significance of this test program as a large scale experiment was to be the first one performed with nozzle diameters comparable to existing plant geometries - in order to avoid the use of estimations -, and also to provide a connection with the large amount of the small-scale critical flow data previously available.

The major components of the facility are the pressure vessel, the discharge pipe, the test nozzles and rupture disk assemblies, and the containment and exhaust tubes.

A complete description of the components and dimensions are amply described in [MAR-4-90].

Figure 4.1 shows the vessel, that includes part of the core superstructure and the moderator tank, plus three gratings installed to limit vortex formation. Figure 4.2 shows the discharge-pipe. All elevations in both figures are measured relative to the vessel bottom. Pressure and temperature transducers are located along the vessel and the discharge pipe (see Figures 4.4 and 4.2). The signals from

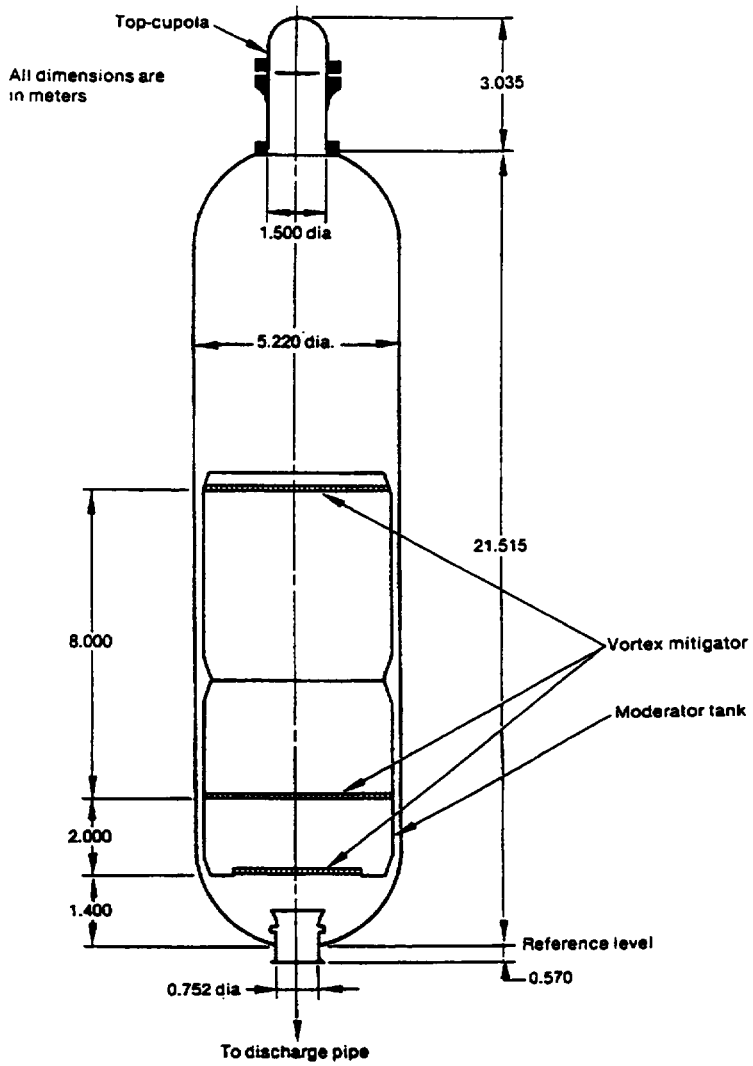

Figure 4.1: Pressure vessel diagram.

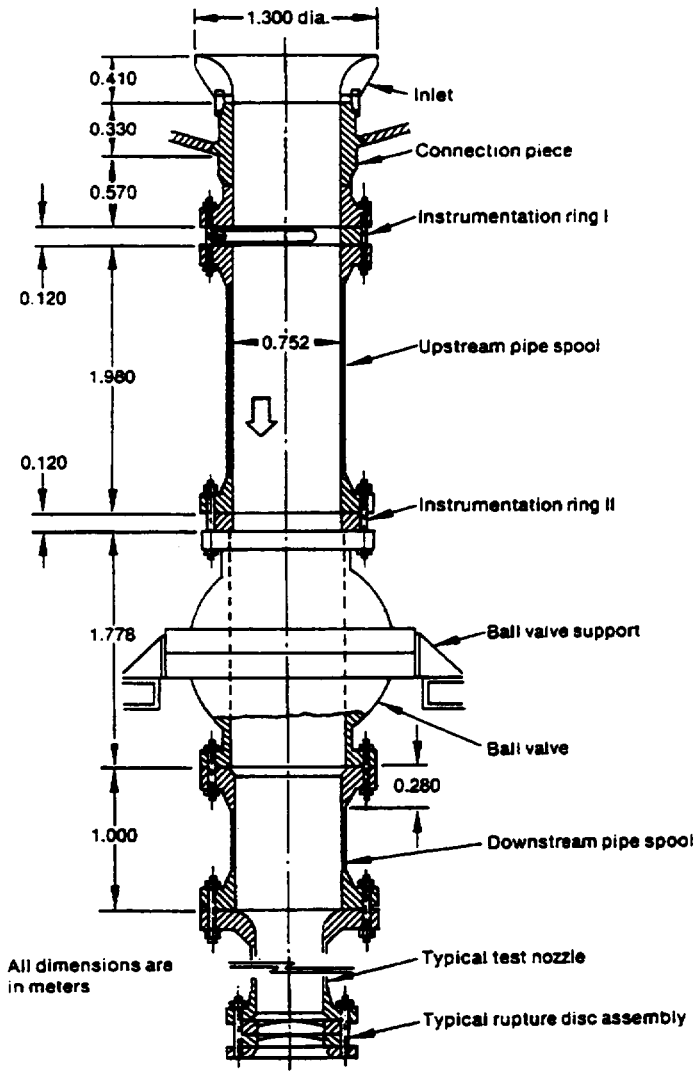

Figure 4.2: Discharge pipe and test nozzle.

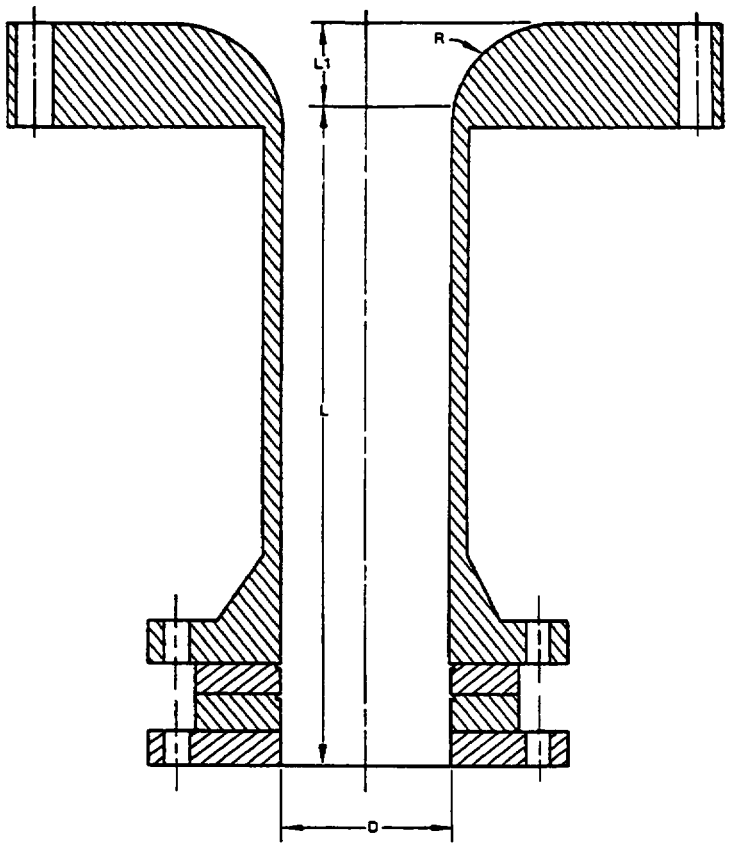

Figure 4.3: Test nozzle used from Test 15 onwards.

the various transducers are processed through a signal-conditioning unit with its channels connected to a pulse-code modulation system and with a process computer. Before a test is run, the vessel is partially filled with deionized water and heated by removing water from the vessel bottom, passing it through an electric heater, and returning it to the steam dome at the vessel top. This procedure produces a complicated initial temperature distribution in the vessel. A saturated steam dome fills the vessel region above the initial water level and the water at the nozzle inlet is substantially subcooled ($\Delta T_{sub} = -60$ K).

Most of the test fluid was contained in the pressure vessel. A test was initiated by breaking the disks contained in the rupture disk assembly and terminated by closing a ball valve in the discharge pipe when voiding is detected upstream of the test nozzle. Data obtained from the vessel, discharge pipe, and test nozzle provided measurements needed to meet the test objectives, whereas the vessel fluid, in the form of a steam-water mixture, was exhausted through the test nozzle into the containment. Most of the liquid discharge was retained in the containment, and the containment pressure was relieved by discharging a steam-water mixture through the ground level and upper exhaust tubes to the atmosphere. The main characteristics of the CFT program are resumed in Table 4.1.

The purpose of the experiments was to get enough data so that the critical flow problem could be deeply undertaken, and analyze the dependence on nozzle geometries, and initial pressure and temperature conditions. For this goal, different subcoolings, upper plenum pressures and temperature profiles were used.

Nozzles used had nominal diameters from 200 mm to 500 mm, and L/D ratios between 0.3 and 3.7. Nozzle diameters larger than 500 mm were not tested because of the restrictions of the equipment. L/D range was selected to provide information just for short pipes (with $L/D \leq 4$).

The behavior observed during each of the Marviken tests can be characterized as having three distinct periods:

1. Following the opening of the break, the system experiences a pressure undershoot, which is terminated by the incidence of flashing inside the vessel. As the vessel water begins to flash, the system pressure rapidly increases until a stable flashing rate is established, after which the vessel begins to depressurize again.

2. The second period during MARVIKEN experiments is marked by a steadily decreasing flow rate and pressure with an established vessel-water flashing rate.

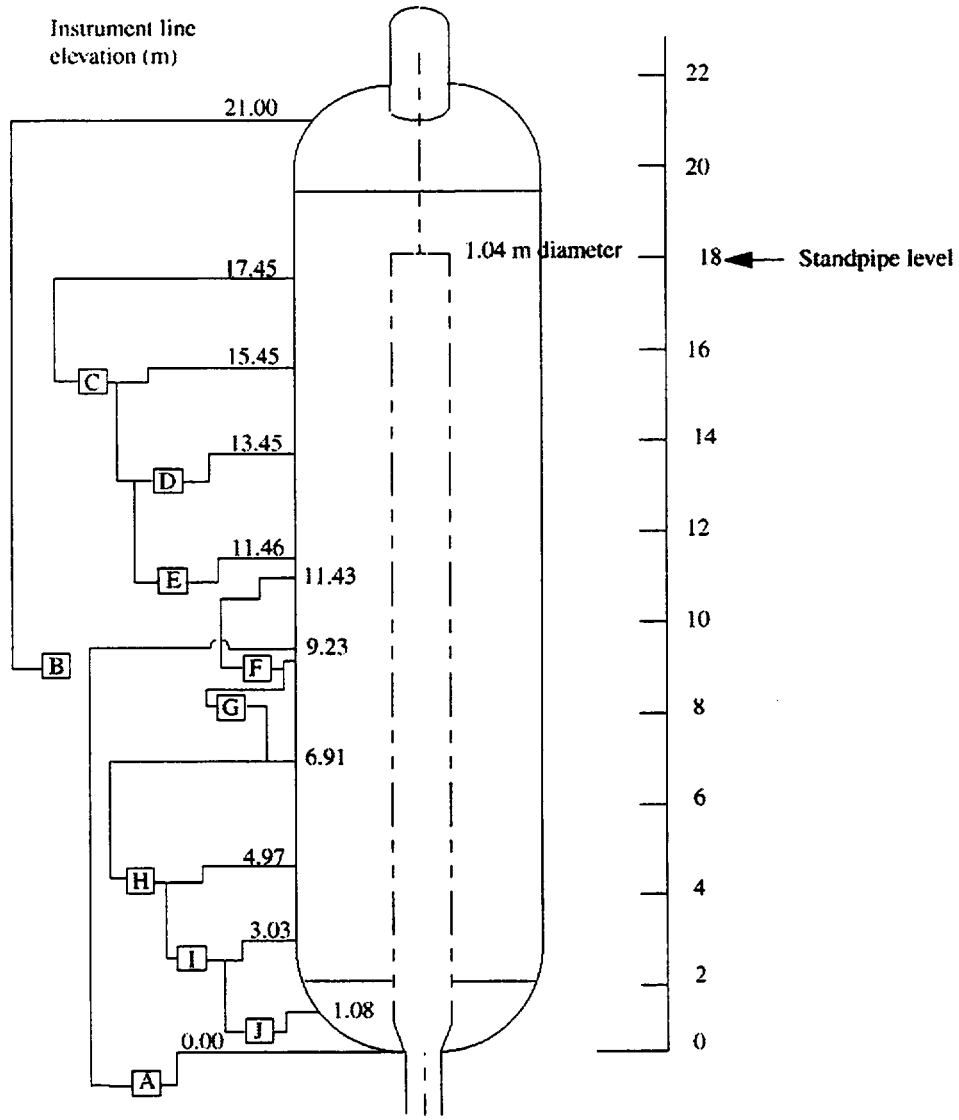

Figure 4.4: Locations of typical measurements in the pressure vessel.

The water entering the test nozzle during this period is subcooled, although a mixture of subcooled and saturated water was discharged from the nozzle near the end of the second and the beginning of the third period.

3. The third period is characterized by a reduction in the discharge flow rate as a result of two phase water entering the test nozzle.

4.2 Models Description

When the Marviken tests simulation amply bibliography is analyzed, see Section 4.3, it is observed that several models have been used for simulating the experiments. The Marviken facility has been modeled in two different ways:

- Only the discharge pipe and the nozzle are modeled, and the boundary conditions at the inlet of the discharge pipe are specified. This model is referred to here as Boundary Condition Model (BCM).
- All the facility is modeled, and the initial conditions are specified. This model is referred to here as Initial Conditions Model (ICM).

For both models, the nozzle has been modeled as a PIPE or as a SINGLE JUNCTION, in order to evaluate the importance of the nucleating time inside the nozzle. Therefore, there are four different models, shown in Figures, 4.5 and 4.6. The four models will be referred to as:

- BCM-P: Boundary Condition Model with the nozzle modeled as a PIPE.
- BCM-J: Boundary Condition Model with the nozzle modeled as a SINGLE JUNCTION.
- ICM-P: Initial Condition Model with the nozzle modeled as a PIPE.
- ICM-J: Initial Condition Model with the nozzle modeled as a SINGLE JUNCTION.

In this report, the simulation of the Marviken Test has been done with the four models. The BCM allows the analysis of critical mass flow in an independent way from other physical phenomena. Furthermore, this kind of model gives the instantaneous error between experimental and simulated mass flow, as the

Test No	Diameter (mm)	Length (mm)	L/D	Subcooling (C)	Steam Pressure (MPa)	Test Category	Test Duration (s)	Saturation Temp. (C)	Initial Water Level (m)
13	200	590	3.0	< 5	5.09	I	148	265	17.52
14				30	4.97	III	146	264	18.10
6	300	290	1.0	30	4.95	I	87	263	17.81
7				15	5.01	I	87	264	17.86
25		511	1.7	< 5	4.92	III	88	263	19.73
26				30	4.91	II	147	263	19.31
1		895	3.0	15	4.94	I	108	263	19.73
2				30	4.98	I	93	264	17.41
12				30	5.00	I	126	264	17.52
17		1116	3.7	30	4.94	II	90	265	19.85
18				30	5.02	I	87	264	17.30
19				< 5	5.06	III	87	265	16.99
23	500	166	0.3	< 5	4.96	III	69	263	19.85
24				30	4.96	II	54	263	19.88
20		730	1.5	< 5	4.99	III	58	264	16.65
21				30	4.94	II	60	263	19.95
22				50	4.93	II	48	263	19.64
27				30	4.91	II	59	263	19.82
15		1809	3.6	30	5.04	II	55	264	19.93
16				30	5.00	I	49	264	17.60
3	509	1589	3.1	15	5.02	I	42	264	17.06
4				30	4.94	I	49	264	17.59
5				30	4.06	I	52	251	17.44
8				30	4.95	I	49	263	17.51
9				< 5	5.02	III	66	264	18.15
10				< 5	4.97	III	64	263.5	17.66
11				30	4.97	I	48	264	17.63

Table 4.1: Main characteristics of the Marviken Tests

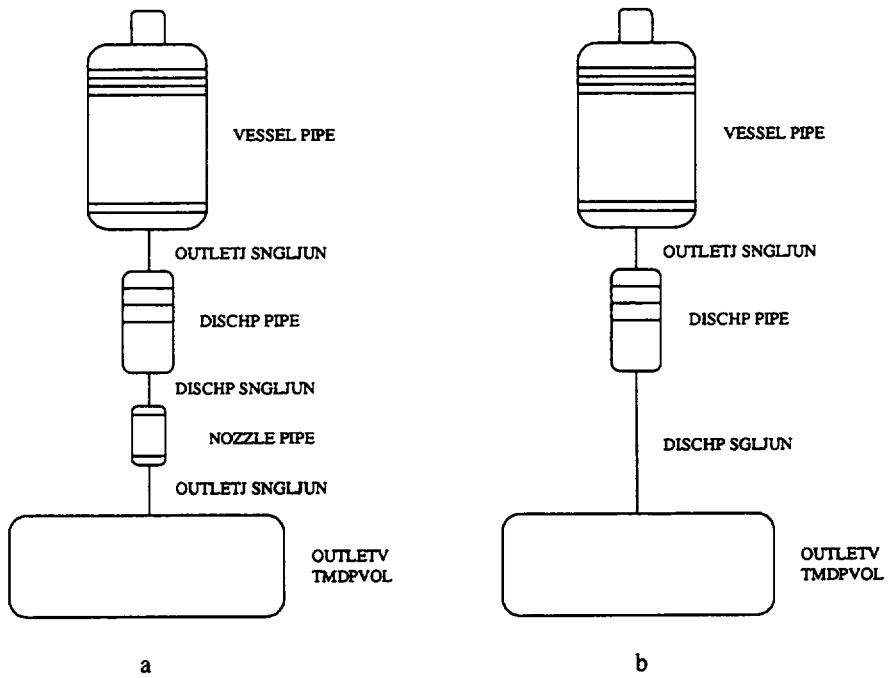

Figure 4.5: MARVIKEN initial conditions models.

experimental data are used as boundary conditions for the simulations. On the other side, the ICM mixes different physical phenomena: mass flow rate and steam generation rate due to flashing, $\Gamma_{flashing}$. Errors related to the steam generation rate have an effect on depressurization rate (system pressure), avoiding critical mass flow phenomena from being isolated. This model has also another problem: Since only initial conditions are imposed, the simulations give an error integrated on time.

The comparison of the different correlation for $\Gamma_{flashing}$ implemented in various thermal hydraulic codes shows great differences among them, [FOR-88] pp 360-364, Figures 4.7 and 4.8. With this in mind, it can not be ascertained it any of the flashing models (including RELAP5/MOD3 model) is right; so an error in the steam generation rate, that affects the system pressure, could be expected. This problem was detected in the assessment of the TRAC-PD2 code and several $\Gamma_{flashing}$ models were implemented in order to improve the critical flow calculation, [TRA-84], but none of the models gave good results.

Due to these differences, simulations with all the models have been performed and compared.

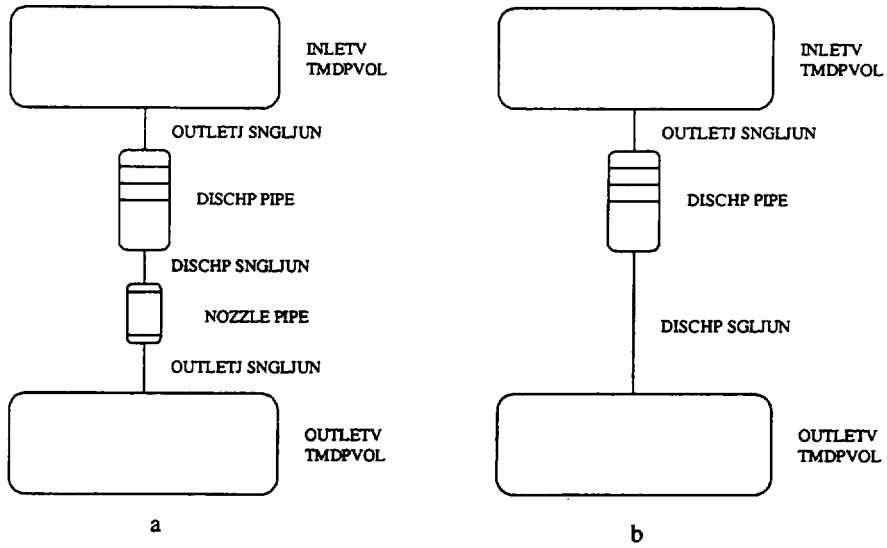

Figure 4.6: MARVIKEN boundary conditions models.

4.3 Review of the Marviken Tests Simulation Bibliography

This section is a review of all the bibliography that was found related to the Marviken experiments and their application in the assessment of several codes (CATHARE, TRAC-P1A, TRAC-PD2, TRAC-PF1/MOD1, TRAC-PF1/MOD2, TRAC-BD1/MOD1, TRAC-BF1, RELAP5/MOD2, RELAP5/MOD3 and RELAP5/MOD3.2.2) and also in the comparison of critical flow models. We have analyzed several aspects of the simulations in these reports and papers:

- Which are the CFT simulated?
- Which is the model used for the simulation?
- Which are the different critical flow models tested?
- Which are deficiencies of the code in these simulations?
- Which are the discharge coefficients used for adjusting the simulated to the test data?

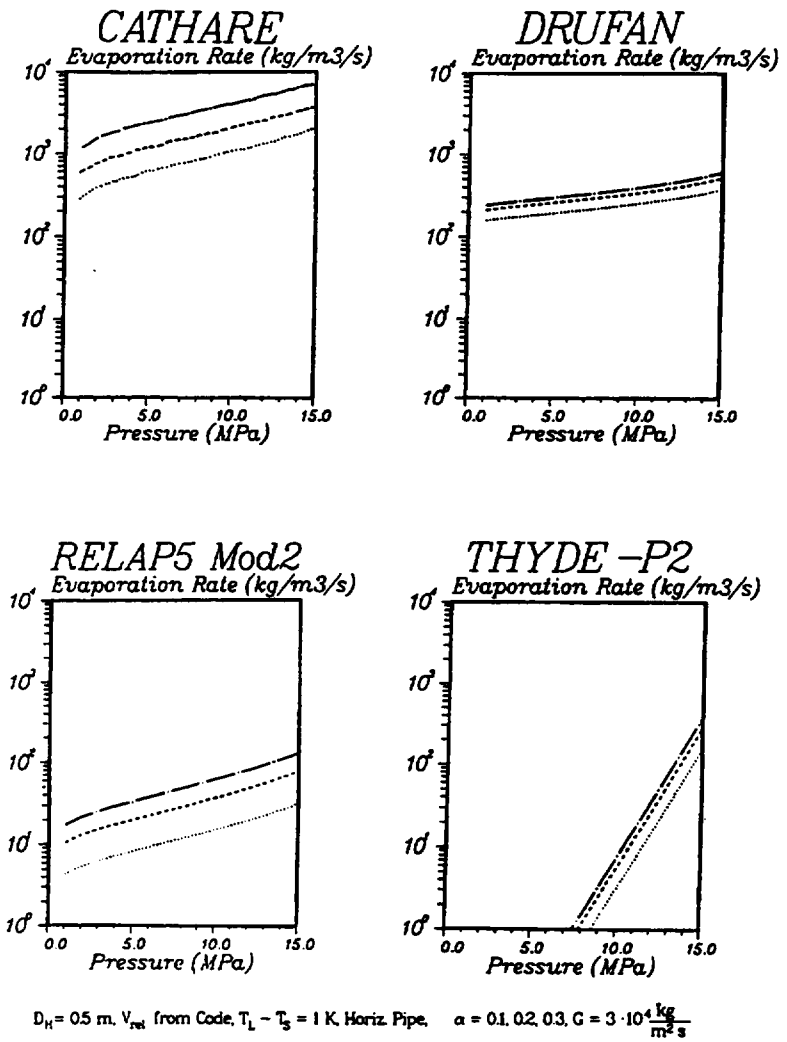

Figure 4.7: Evaporation during flashing. CATHARE, DRUFAN, RELAP5/MOD2 and THYDE-P2 codes.

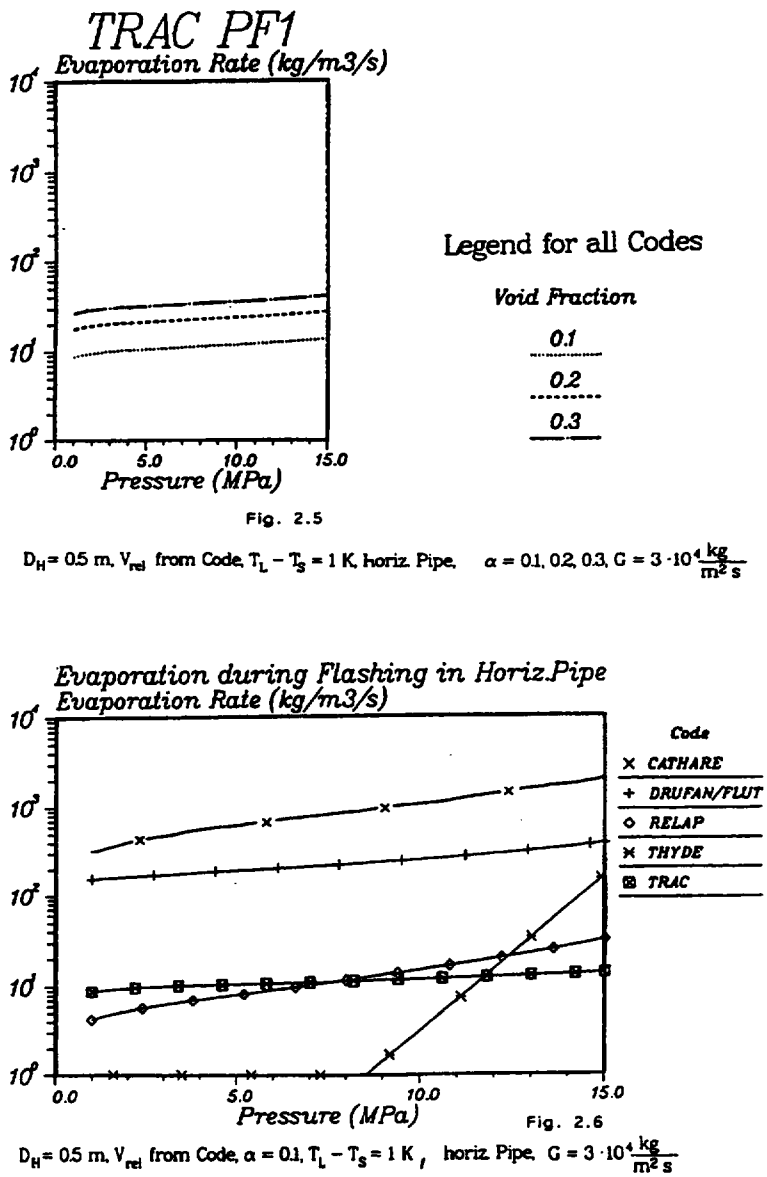

Figure 4.8: Evaporation during flashing of TRAC-PF1 code and comparison of the models.

- Which are the non-equilibrium constant values recommended for Henry-Fauske model?

- Which are the main conclusions of each report?

The comments and conclusions on the references founded are described below. They are divided in two groups: In the first, the thermal hydraulic codes references are commented; and in the second, the reviews on critical flow data and models are also commented.

- CATHARE.

  Two Marviken tests (CFT-17 and CFT-24) were selected for the validation matrix of CATHARE code. The main conclusions were, [BAR-90] and [BES-90]:

  - The initial pressure undershoot is not well predicted.
  - The mass flow rate is overestimated because the multidimensional phenomena which occur in a steep convergent nozzle and cause a flow area restriction cannot be taken into account by the CATHARE 1-dimensional model.

- TRAC-P1A.

  In the developmental assessment, the simulation of CFT-04 was performed, [TRA-79] and [TRA-80]. Later, several CFT (01, 02, 04, 07, 13, 22 and 24) were also simulated during the independent assessment, [TRA-81]. The model used was the ICM-P. The conclusions were similar in all reports:

  - The constitutive relations in TRAC-P1A did not permit delayed nucleation; this problem prevents the code from calculating the initial dip in the pressure at the beginning of the tests and forced the critical flow calculation toward equilibrium, resulting in an under prediction of the flow.
  - The simulation results under predict the subcooled part of the blowdown (10 %) and agree very well with the saturated part of the blowdown.
  - The quality of the comparisons, between simulated and test data, degraded with decreasing length to diameter ratio.

- TRAC-PD2.

  In the TRAC-PD2 independent assessment, five CFT were selected (04, 13, 20, 22 and 24), [TRA-84]. The model used was the same than TRAC-P1A model. In this assessment several steam generation rate models were implemented. The main conclusions were:

  - The unrealistically large steam generation rate causes the code to experience an early flow limitation caused by choking.
  - None of the steam generation rate models that were used in this analysis (Rivard and Travis, Jones, Hunt and RELAP5 models) adequately improve the critical flow calculation.
  - When the initial liquid temperature in the lower part of the vessel is artificially reduced, the flashing is avoided inside the nozzle during subcooled blowdown. In this case the comparison between simulated and experimental data is excellent. So, the flow through the nozzle seems to take place under highly non-equilibrium conditions. Such a high non-equilibrium is not calculated by any of the mass transfer models mentioned above.
  - An increase of the nozzle area does not increase the flow linearly because of the increased steam generation rate.
  - The constitutive relations in TRAC-PD2 did not permit delayed nucleation; this problem prevents the code from calculating the initial dip in the pressure at the beginning of the tests and forced the critical flow calculation toward equilibrium, resulting in an under prediction of the flow.
  - The simulation results under predict the subcooled part of the blowdown (10 %) and agree very well with the saturated part of the blowdown.

- TRAC-PF1/MOD1.

  In the TRAC-PF1/MOD1 description report, [TRA-83] and [TRA-86], the simulations of two tests used for the assessment of the code, CFT-04 and CFT-24, are described. ICM-P was selected to make the simulations. The main results were:

  - For the test with long nozzle (CFT-04), the calculations during the subcooled blowdown phase with CFM-on gave almost identical results than those with CFM-off and fine mesh (30 cells for CFT-04 and 12 cells

for CFT-24). During the two phase blowdown period the results with CFM-off and fine mesh are a 10% higher than the results with CFM-on. Both models calculations under predict the experimental mass flow by an average of 10% during the subcooled blowdown period. During the two phase blowdown phase the mass flow results with CFM-on are quite similar to test data.

- For the test with short nozzle (CFT-24), the agreement between both models is not as good as for CFT-04. This discrepancy is attributed to the predominance of non-equlibrium effects between the phases caused by the short nozzle length. These non-equilibrium effects are not modeled in the TRAC-PF1/MOD1 choking calculation. The comparison between choking model and test data shows that the simulation under predicts the experimental mass flow by 20% - 40% during the subcooled blowdown phase. During the two phase blowdown phase the mass flow results with CFM-on are quite similar to test data.
- To investigate non-equilibrium effects in CFT-24, short nozzle, a sensitivity run with the frozen assumption was performed. Using the frozen model the mass flow is over predicted and the pressure under predicted.
- The dip in the measured pressure during the first 3 seconds of the transient indicates a significantly more pronounced nucleation delay than predicted by the TRAC-PF1/MOD1 model.

In the independent assessment of TRAC-PF1/MOD1 performed by the CEA in the frame of the ICAP program, [SPI-90], several blowdown tests were selected: MOBY-DICK, SUPERMOBY-DICK, CANON, SUPER-CANON, VERTICAL CANON, OMEGA-TUBE, OMEGA-BUNDLE and MARVIKEN. Three Marviken test were simulated (CFT-06, CFT-17 and CFT-24). ICM-P (the one with the nozzle modeled with two or three cells is called "the reference model") was selected to make the simulations. The main conclusions were:

- The initial pressure undershoot is not predicted, due to the absence of a delayed boiling model.
- The mass flow rate obtained with the reference model is under predicted with discrepancies of 20% for the test with long nozzles (CFT-17) and of 25%-30% for the tests with short nozzles (CFT-24 and CFT-06).
- The results obtained with a fine mesh (six or more cells) at the nozzle give similar results than the reference model with a reduced time step.

- The simulation performed with the reference mesh at the nozzle and natural choking (CFM-off) gives different results than CFM-on.
- The results obtained with a fine mesh at the nozzle and natural choking give similar results for test with long nozzle (CFT-17) and a mass flow rate larger than the reference model (better agreement with test data) for test with short nozzle (CFT-24). The absence of thermal disequilibrium for CFT-17 leads to equivalent results, with and without the choked flow model. For CFT-24, a better agreement is found when the thermal disequilibrium is taken into account (CFM-off).
- Simulations of the first period (subcooled liquid at the discharge pipe) with the BCM-P were performed. The results of this model differ from the reference model results. Some of the results with BCM-P are in better agreement with test data, but others have higher discrepancies. There are not important conclusions respect these differences.
- The lack of virtual mass term in the natural choking model probably takes part in the poor agreement between simulation and test data in some of the tests simulations.
- An improvement of the choked flow model is needed in order to take into account the inter phase thermal disequilibrium.
- The inception of boiling is predicted too early, so a delayed boiling model is needed.

• TRAC-PF1/MOD2.

In the TRAC-PF1/MOD2 manual, [TRA-93] pp. 599 to 605, two tests used for the assessment of TRAC-PF1/MOD2, CFT-04 and CFT-24, are described (the input of CFT-04 is included in [TRA-96] appendix A-3, and a detailed description of the critical flow model can be found in [TRA-97]). The ICM-P was selected to make the simulations. The main conclusions of the report were identical to TRAC-PF1/MOD1 assessment, [TRA-86], however a few differences could be observed between the graphics of both reports. The main conclusions about TRAC-PF1/MOD2 were:

- For the test with long nozzle (CFT-04) the calculations during the subcooled blowdown phase with CFM-on give almost identical results to those for with CFM-off and fine mesh (30 cells for CFT-04 and 12 cells for CFT-24). During the two phase blowdown phase the results with

CFM-off and fine mesh are a 10% higher than the results with CFM-on. Both calculations under predict the experimental mass flow by an average of 5% (10% in the manual) during the subcooled blowdown phase. These results are better than those obtained in the TRAC-PF1/MOD1 assessment, [TRA-86]. During the two phase blowdown period the mass flow results with CFM-on are quite similar to test data.

- For the test with short nozzle (CFT-24) the agreement between both models is not as good as for CFT-04. This discrepancy is attributed to the predominance of non-equlibrium effects between the phases caused by the short nozzle length. These non-equilibrium effects are not modeled in the TRAC-PF1/MOD2 choking calculation. The comparison between choking model and test data shows that the simulation under predicts the experimental mass flow by 20%-40% during the subcooled blowdown period. During the two phase blowdown phase the mass flow results with CFM-on are quite similar to test data.
- The dip in the measured pressure during the first 3 seconds of the transient indicates a significantly more pronounced nucleation delay than predicted by the TRAC-PF1/MOD2 model.

During the update of the critical flow model subroutine of TRAC-P, FXCFM, several areas were corrected, [STE-98]. Knolls Atomic Power Laboratory, Marviken (CFT-04, CFT-13, CFT-20, CFT-22 and CFT-24), Edwards and Scientech critical flow tests were used for investigate the reported errors and further errors that were found and to verify their correction. The main conclusion about the Marviken tests was that better agreement with the experimental data probably requires making changes elsewhere in the choked flow model. Such changes may need to be made in the modeling assumptions rather than in searching for further corrections.

- TRAC-BD1/MOD1.

Three tests were simulated for the assessment of TRAC-BD1/MOD1, CFT-15, CFT-18 and CFT-24, [TBD-85a] pp 22-28 and [TBD-85b] pp 18-19, 41. ICM-P was selected to make the simulations. The main results were:

- The computed value is a 20-25% lower than test data during subcooled and low-quality period and 10-15% for high-quality period. The difference for high qualities may be due to some error in the extrapolated fluid properties used to calculate the sonic velocity or multidimensional effects not accounted for in the one-dimensional flow model.

- Independent calculations suggest that substantial improvement may be achieved by appropriated correcting the numerical treatment of the momentum equation to account for artificial pressure drop at flow restrictions due to the backward (donnor cell) differencing used in the TRAC numerical scheme.
- The subcooled CFM is very sensitive to the amount of fluid subcooling. A sensitivity study showed that a 5^oC change in break flow subcooling can cause a 15% decrease in break mass flow.
- An adjustment of the discharge coefficient, from 0.7 to 1.0, is required to correctly simulate the mass flow.

- TRAC-BF1/MOD1.

  Five tests (CFT-10, CFT-15, CFT-21, CFT-23 and CFT-24) were simulated to analyse de capacity of TRAC-BF1 to reproduce blowdowns under critical conditions, [GOM-98]. The ICM-P was selected to make the simulations. The main results were:

  - TRAC-BF1 numerical scheme is unable to reproduce critical solutions with natural choking, so an externally imposed critical condition is needed.
  - TRAC-BF1 fails to reproduce the thermal disequilibrium arising in the transition from liquid to boiling mixture. Therefore, the critical flow rates are underestimated in subcooled conditions through very short nozzles.

- RELAP5/MOD2.

  In the developmental assessment of RELAP5/MOD2 two CFT were simulated, [REL-87] pp 21-25. ICM-J was used for the test with short nozzle (CFT-24, $L/D = 0.33$) and ICM-P for the long one (CFT-22, $L/D = 1.5$). The subcooled period is well adjusted for both cases, but in the two-phase period the simulation underestimates the mass flow in 10%.

  In the independent assessment of RELAP5/MOD2 performed by the Swedish Nuclear Power Inspectorate, [ROS-86], in the framework of ICAP, two tests were analyzed (JIT-11 and CFT-21). The models used were BCM-J and BCM-P. The main conclusions were:

  - The subcooled critical mass flow rate for CFT-21 is over predicted with the BCM-J; a discharge coefficient of 0.85 is necessary to agree the calculated mass flow with the measured ones.

- When the nozzle geometry was explicitly modeled (BCM-P) mass flow rates for CFT-21 were under predicted. Application of discharge coefficients greater than unity did not improve the computed results; on the contrary, doing so gave rise to a very numerically noisy solution. It is concluded that short discharge nozzles or pipes ($L/D < 2$) should not be modeled explicitly in RELAP5.

- Other modeling deficiencies in the critical flow model were identified. These were the unrealistic spikes in the steam discharge choked flow of JIT-11, the unrealistic effects of discharge coefficients in the region of subcooled critical flow (non-linearity effect on the discharge coefficient), and the discontinuity of critical mass flow rate in the transition region. These deficiencies were modified in RELAP5/MOD3, and a new assessment was performed [WEA-89].

In the assessment of RELAP5/MOD2 and MOD3 performed by the Korea Institute of Nuclear Safety (KINS), two tests were analyzed (CFT-15 and CFT-24), [KIM-92]. In this report a sensitivity analysis of the nodalization of the discharge pipe and the nozzle are performed. The model used is the ICM. In the test with long nozzle (CFT-15, L/D=3.6), the nozzle is modeled as a PIPE (ICM-P). In the test with short nozzle (CFT-24), the nozzle is modeled as a PIPE (ICM-P) or SINGLE JUNCTION (ICM-J). The main conclusions are:

- For the CFT-15 simulation (long nozzle), it may be recommended that a nozzle is modeled as PIPE.

- For the CFT-24 simulation (short nozzle), ICM-J gives better results than ICM-P.

- In RELAP5 the pressure drop due to friction loss in a PIPE is over predicted relative to actual data.

- When the nozzle is modeled as a PIPE in CFT-24 the prediction with RELAP5/MOD2 of the inception of boiling at the nozzle inlet is somewhat faster and the calculated mass flow rate at the beginning of the two phase-region is very low due to the generation of high void-fraction. When the simulation is performed with RELAP5/MOD3 the inception of boiling appears at the beginning of the transient, which is not in accordance with experimental data.

- The critical flow model in RELAP5/MOD3 under predicts in about 5% the mass flow rate and shows oscillations during two-phase region, although it predicts a smoothly transition region.

- RELAP5/MOD3.

  In the developmental assessment of RELAP5/MOD3, [REL-90], the same analysis than RELAP5/MOD2, [REL-87] was performed. The conclusions were the same, but with one difference: The mass flow rate computed by RELAP5/MOD3 in the two-phase portion of the test lies slightly below the mass flow rate computed by RELAP5/MOD2. This is due to the change in the interfacial friction model for large-diameter pipes, which results in a higher slip ratio in RELAP5/MOD3 relative to MOD2 for the same set of fluid conditions. The slip ratio implied by the interfacial friction model is used to unfold the phasic velocities from the choking condition, and a higher slip ratio results in a lower liquid velocity and a higher vapor velocity. Since the void fraction at the choking plane remains relatively low (less than 0.3) throughout the test, the lower liquid velocity computed by RELAP5/MOD3 results in a slightly lower discharge flow rate. The results of this assessment demonstrate that changes to one code model (i.e. the interfacial friction model) can affect the performance of other, completely separate model (i.e. the critical flow model).

  The KAERI team has developed a new version of RELAP5/MOD3 called RELAP5/MOD3/KAERI. In this version the CFM is the same than in RELAP5/MOD3 (Ransom-Trapp model) and so, the conclusions are valid for both codes. They performed an uncertainty analysis of the CFM for its application in a best estimate methodology. Nine CFTs (03, 04, 08, 11, 15,16, 21, 22 and 27) with $L/D > 1.5$ were simulated with BCM-J and BCM-P, [KAE-94] and [KAE-95]. They only simulated tests with $L/D > 1.5$ for minimizing the effect of L/D ratio (it must be remembered that in MARVIKEN tests the critical mass flow under subcooled conditions diminishes with L/D ratio if $L/D < 1.5$, and also that further increase in L/D ratio does not reduce the mass flow appreciably). The main conclusions were:

  - The two-phase critical flow rates are nearly the same for all the discharge pipe nodalization (two to six cells), except the single cell case. So, the two-cell model was adopted.
  - The discharge coefficients and standard deviation (SD) for BCM-J are: 0.82115 (SD= $7.5E-2$) for subcooled flow and 1.1485 (SD= $8.8E-2$) for two-phase flow.

- The discharge coefficients for the BCM-P are: 0.89 (SD= $3.5E-2$) for subcooled flow and 1.07 (SD= $1.2E-1$) for the two-phase flow.

The evolution of RELAP5/MOD3.1 to MOD3.2 code version is described in [REL-98]. The changes performed in JCHOKE subroutine were:

- Improvement to the calculation of sonic velocity for critical flow of subcooled liquid: During critical flow of subcooled liquid, the mass flow rate may be unaffected by a change of upstream pressure. This problem occurs because the equilibrium sound speed at the junction is calculated assuming the junction contains saturated liquid at the upstream temperature. The change performed in JCHOKE subroutine was: Use momentum and mechanical energy balances to calculate the pressure and internal energy at the junction and use the water property tables to obtain the thermodynamic properties of a saturated liquid-vapor mixture at this pressure and internal energy.
- Improvement to the unchoking test used in the critical flow model: The unchoking test checked that the throat pressure was larger than the downstream pressure. Although this test was not plausible, it was left in the code because no problems were observed. Later, they saw that this test may cause oscillations in the flow rate. For this reason, an improved unchoking test was implemented.

- RELAP5/MOD3.2.2.

CFT-22 ($L/D = 1.5$) was simulated in order to compare the default CFM of RELAP5/MOD3.2 (Ransom-Trapp model) and the new option of the Henry-Fauske CFM, [JOH-96] and [MOR-98]. This new model sets a single discharge coefficient and the non-equilibrium constant dp based on geometry and test data. ICM-P was selected to make the simulations. The main results were:

- The comparison between test data, the Ransom-Trapp CFM and Henry-Fauske CFM show that the Henry-Fauske CFM gives better results than the Ransom-Trapp model.
- A discharge coefficient of 0.95 is necessary for adjusting to MARVIKEN data ($dp = 0.14$).
- The incorporation of the Henry-Fauske CFM overcomes the limitations of RELAP5/MOD3 CFM: multiple discharge coefficients, low two-phase critical flow at low pressures ($P < 0.2MPa$) or low quality (0.01 to 0.2).

- E. Elias and G.S. Lellouche.

  They made a detailed review in two phase critical flow problem, [ELI-94]. Several aspects of the problem are analyzed in this paper: Theoretical foundations, numerical considerations, critical flow models, experimental data sources and model evaluations. For the model evaluations, the inlet conditions at the start of the discharge pipe of several Marviken tests (CFT-04, CFT-06, CFT-09, CFT-13, CFT-14, CFT-18, CFT-19, CFT-23 and CFT-24) were used. Some of the conclusions of the report are:

  - Due to the errors in the initial period of the blowdown, the data of the first five seconds are no used.
  - The analytic and fitted models (Burnell, isenthalpic, Moody with slip, fit to the Moody model, Henry-Fauske, fit to Henry Fauske Model and HEM) do not provide good predictions, as required of a viable calculation tool.
  - Among the space-dependent models (Elias-Chambre model, complete drift flux model and Richter model), only the Richter model have been partly successful. It is surprising that these models fail in large diameter down flow situations if we take into account that all of them produce reasonable results for small diameter pipes. Perhaps it only shows that these correlations are based in data-based set for small diameter pipes and that the large extrapolation in diameter and mass flow rate that it is made when they are applied to Marviken tests is just too large. So, it is clear that much further work is needed at these conditions.
  - The TRAC-P code nearly always under predict the data.
  - In general, the calculated critical flow in a code (TRAC-P/B, RELAP5, RETRAN) may depend more on the constitutive relations and correlations than on the imposed critical flow model.
  - Best estimate calculations of large break situations are unreliable and can only be interpreted through an analysis which includes an uncertainty in the critical flow model.
  - The use of natural choking, the own critical flow condition of the system of equations (characteristic root null), presents several problems:
    * The existence of a spatial singularity in pressure cannot be resolved completely in discrete mesh. If we want to resolve the calculated critical flow rates to less than 1% of error, extremely fine meshes (3-10 mm) must be used.

* In the explicit and semi-implicit numerical methods (semi-implicit in RELAP5, SETS in TRAC-P) there is a stability limit near to the Courant limit that makes it necessary to use very little time steps when applying the natural choking criterion, for two reasons: extremely fine mesh and high speeds (sound speed). This has led to the introduction of separate choking models in codes as RELAP5 and TRAC-P.
* A separate choking model is not necessary if fully implicit schemes are used, like in the CATHARE code, because this kind of numerical methods allows the use of very fine meshes near the break without affecting the time step.

- Critical Flow Data Review and Analysis.

MARVIKEN data were analyzed in [LEV-82] to evaluate critical flow models against the large scale critical flow data. Some of the conclusions were:

- Comparison with more detailed models shows that non-equilibrium is important when the stagnation state is in the region of subcooled liquid or very low quality and $L/D < 1.5$. The duration of meta-stability is important.
- HEM results are in fair agreement for subcooled stagnation conditions and length-to-diameter ratios greater than 1.5. For two-phase conditions and long nozzles the predictions are close to experimental data, for short nozzles the mass flow is under predicted (20 %).
- The Henry-Fauske model, which was developed for orifices and short tubes, over predicts most of the data except the subcooled portions of tests with $L/D < 1.5$. If the non-equilibrium parameter of Henry-Fauske model is modified to be a function of stagnation conditions and nozzle geometry a good agreement with the experimental data is obtained. In the comparison of the test data of MARVIKEN CFT-04, 06, 10, 14, 18, 19, 23, 24, 25 with the Henry-Fauske CFM several values of the disequilibrium parameter, N, are compared. The best results are obtained with,
  * $N = 7.1X_e$ for subcooled blowdown and $\frac{L}{D} < 1.5$
  * $N = 100X_e$ for $\frac{L}{D} > 1.5$
  * $N = 100X_e$ for saturated blowdown

Where X_e is the equilibrium quality. The disequilibrium parameter used in RELAP5/MOD3.2.2beta (dp) is related with N through the expression, $N = \min(1, \frac{X_e}{dp})$. Therefore the recommended values for dp are,

* $dp = 0.14$ for subcooled blowdown and $\frac{L}{D} < 1.5$
* $dp = 0.01$ for $\frac{L}{D} > 1.5$
* $dp = 0.01$ for saturated blowdown

– The correlations included in best estimate codes that are used to represent phase interactions at conditions within the reactor primary system may not be appropriate to represent these phenomena at a choke plane.

No attempt is made to summarize these conclusions, because we believe it is better for everybody to take their own conclusions.

4.4 Results and Discussion of Boundary Condition Model (BCM). Ransom-Trapp Model

The analysis of Marviken experiments with this model has the following objectives,

- Comparison of critical and non-critical flow models with test data.
- Comparison and selection of model options:
  - Homogeneous versus non-homogeneous flow.
  - Comparison of SINGLE JUNCTION, trip valve and motor valve models.
  - Comparison of discharge coefficient and nozzle area variations.
- Discharge coefficient adjustment for subcooled and two-phase conditions with different nozzle models:
  - Nozzle modeled as SINGLE JUNCTION.
  - Nozzle modeled as PIPE.

For this analysis it is important to cover different thermo-hydraulic conditions at the nozzle, subcooled and two-phase, and also different L/D relations for the nozzles. For these reasons the experiments selected were: CFT-01, CFT-06, CFT-11, CFT-15, CFT-17, CFT-21 and CFT-24. In all these tests there are subcooled and two-phase periods, except in CFT-17, where only the subcooled period is observed. The boundary conditions used in this model are shown in Figures 4.9 to 4.28. The results and conclusions are described in next sections.

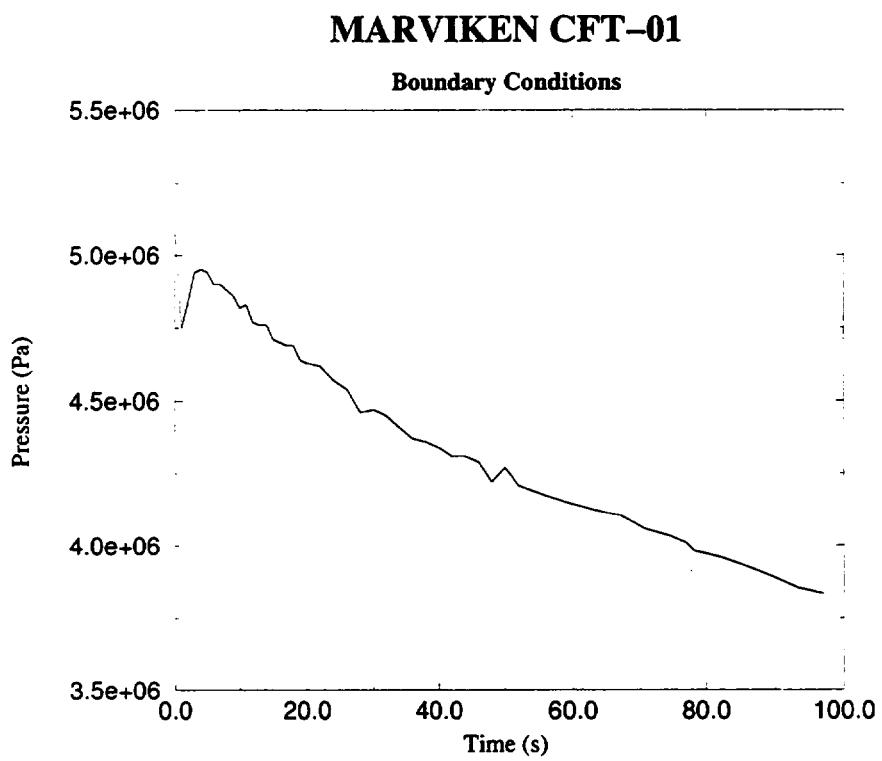

Figure 4.9: Pressure at bottom vessel. Test data. CFT-01.

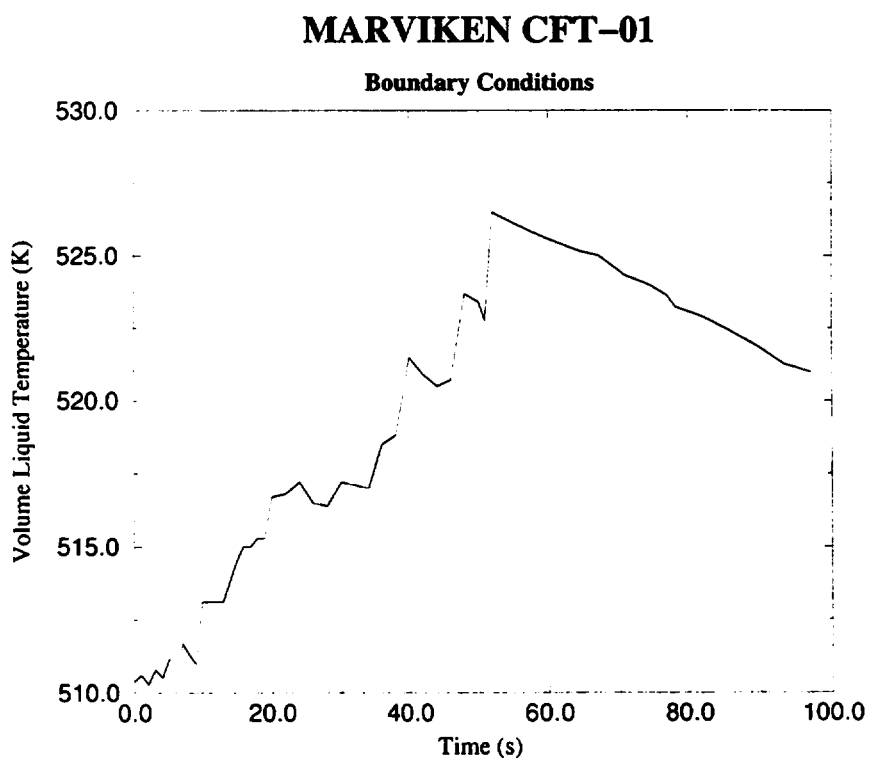

Figure 4.10: Liquid temperature at bottom vessel. Test data. CFT-01.

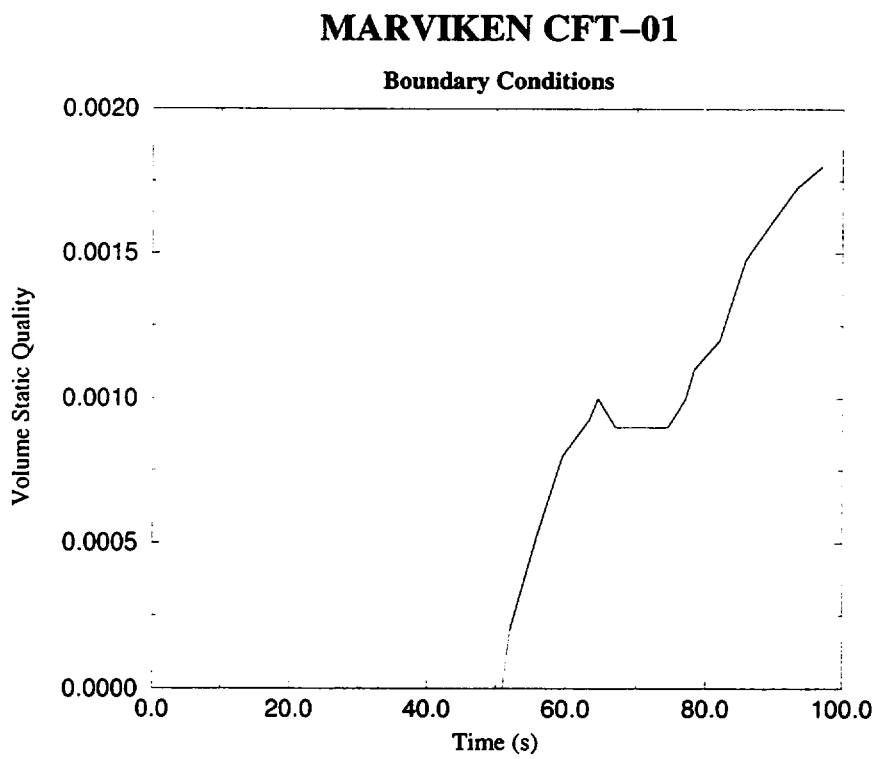

Figure 4.11: Static quality at bottom vessel. Test data. CFT-01.

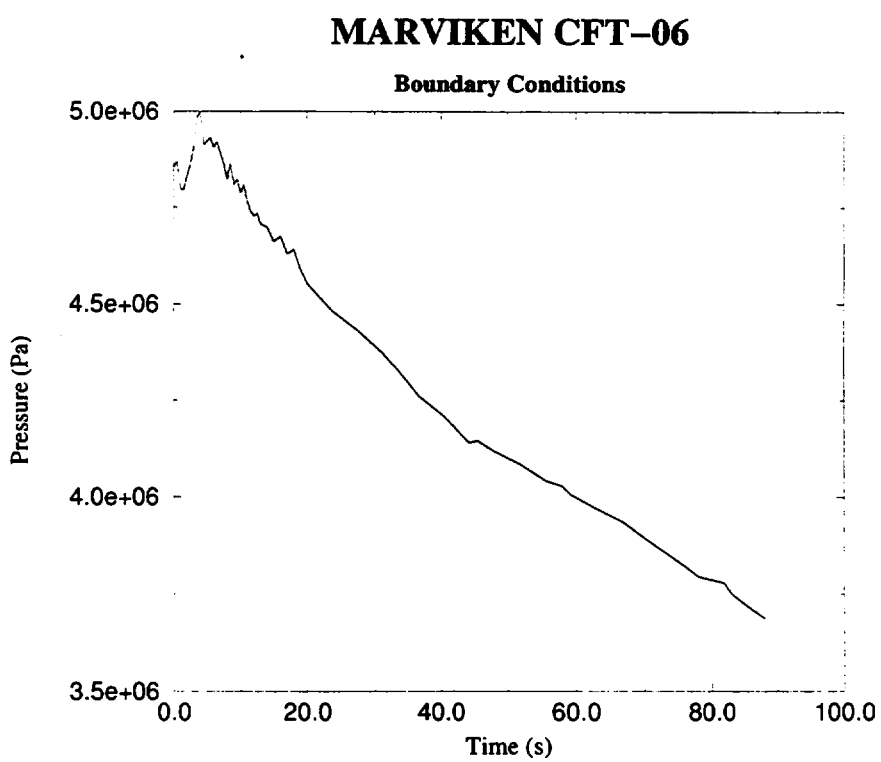

Figure 4.12: Pressure at bottom vessel. Test data. CFT-06.

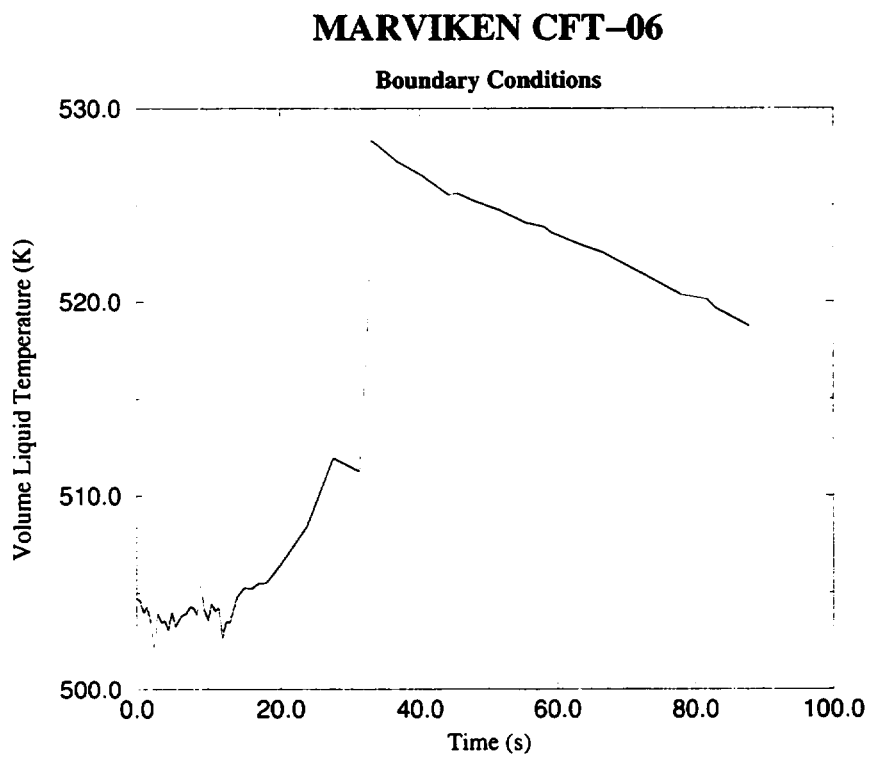

Figure 4.13: Liquid temperature at bottom vessel. Test data. CFT-06.

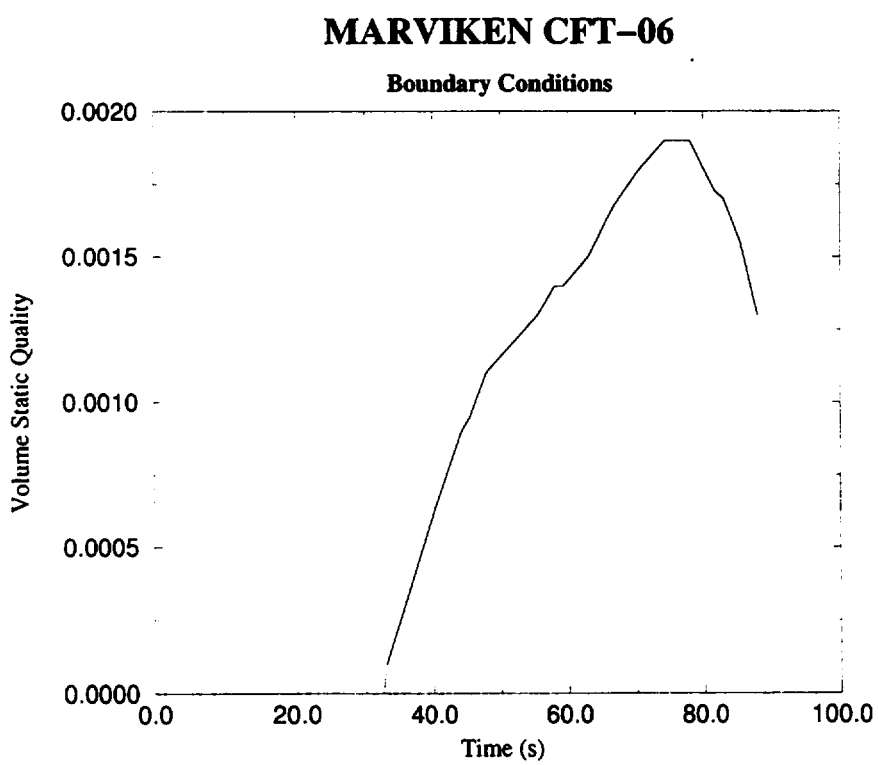

Figure 4.14: Static quality at bottom vessel. Test data. CFT-06.

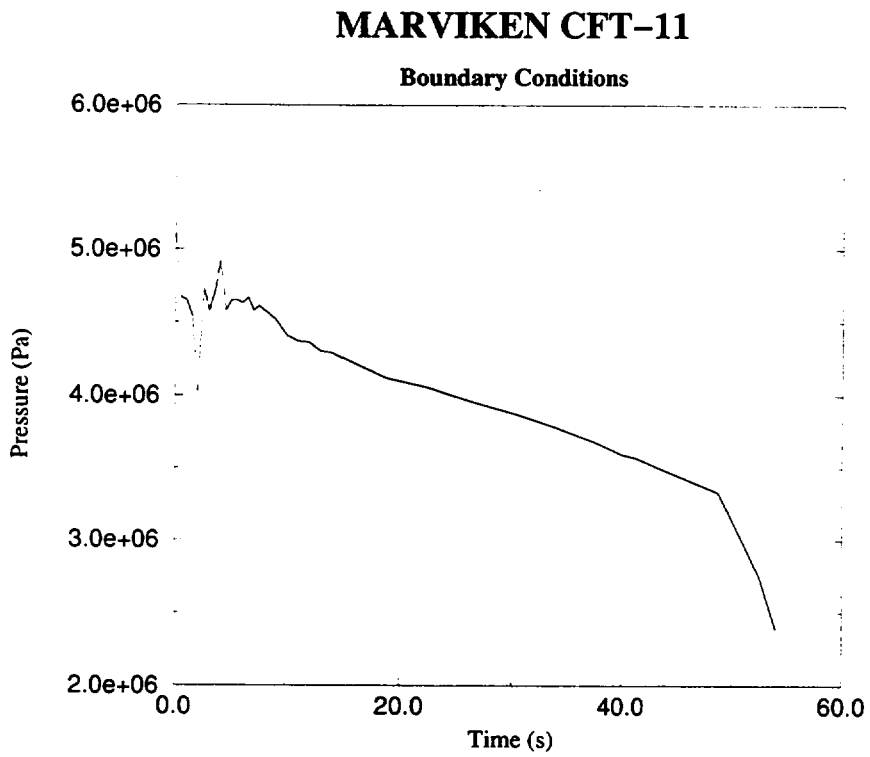

Figure 4.15: Pressure at bottom vessel. Test data. CFT-11.

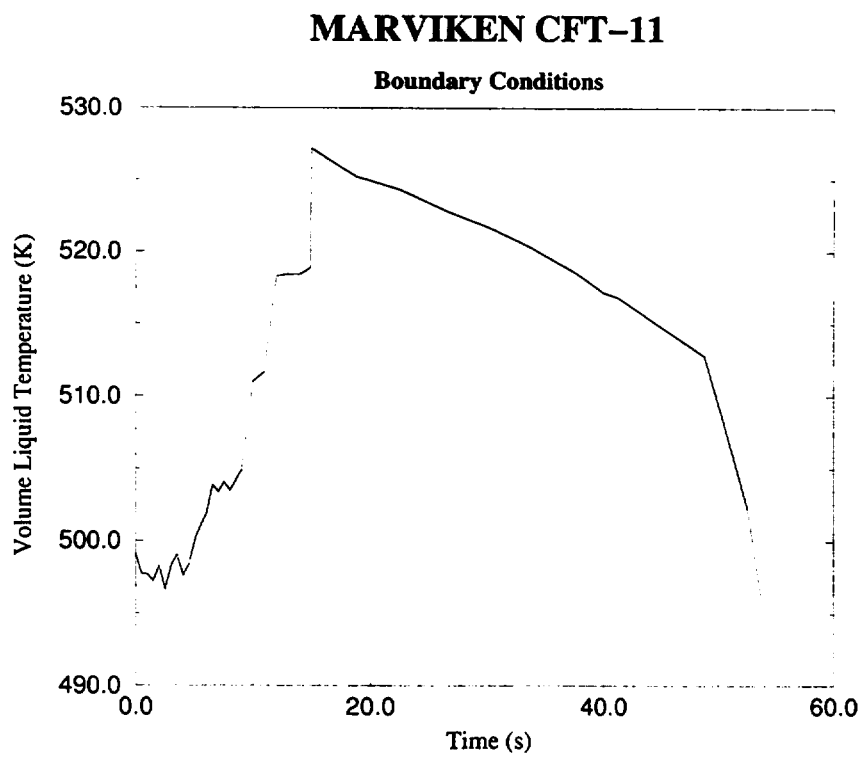

Figure 4.16: Liquid temperature at bottom vessel. Test data. CFT-11.

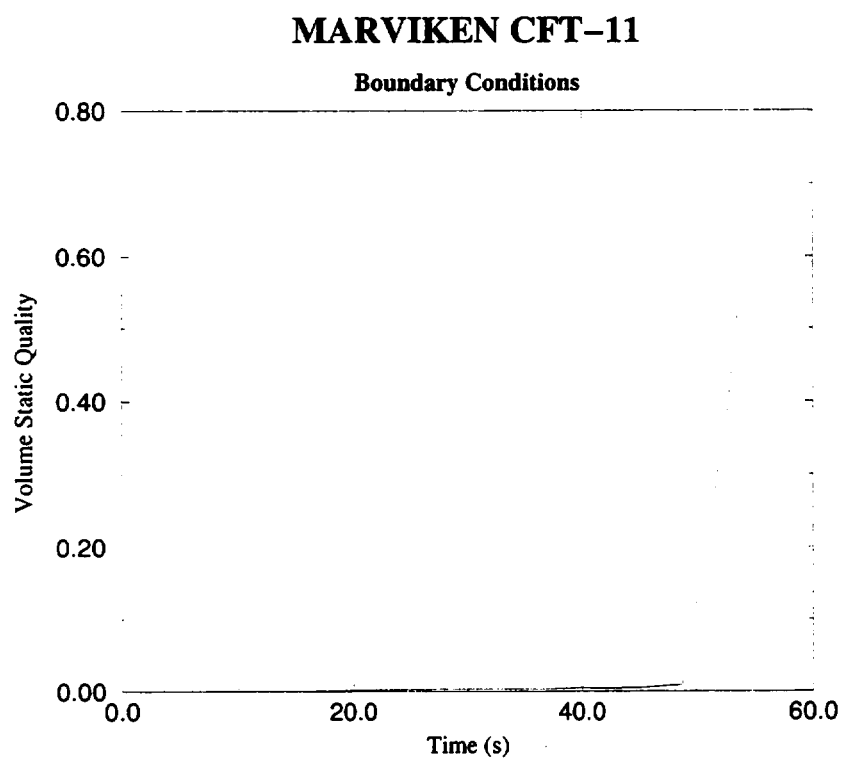

Figure 4.17: Static quality at bottom vessel. Test data. CFT-11.

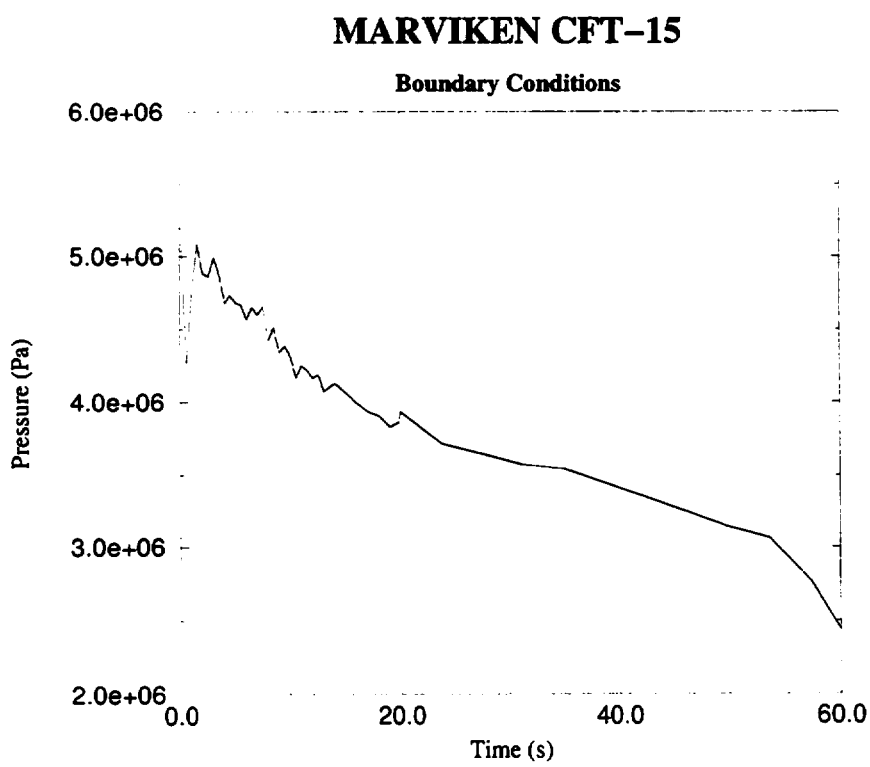

Figure 4.18: Pressure at bottom vessel. Test data. CFT-15.

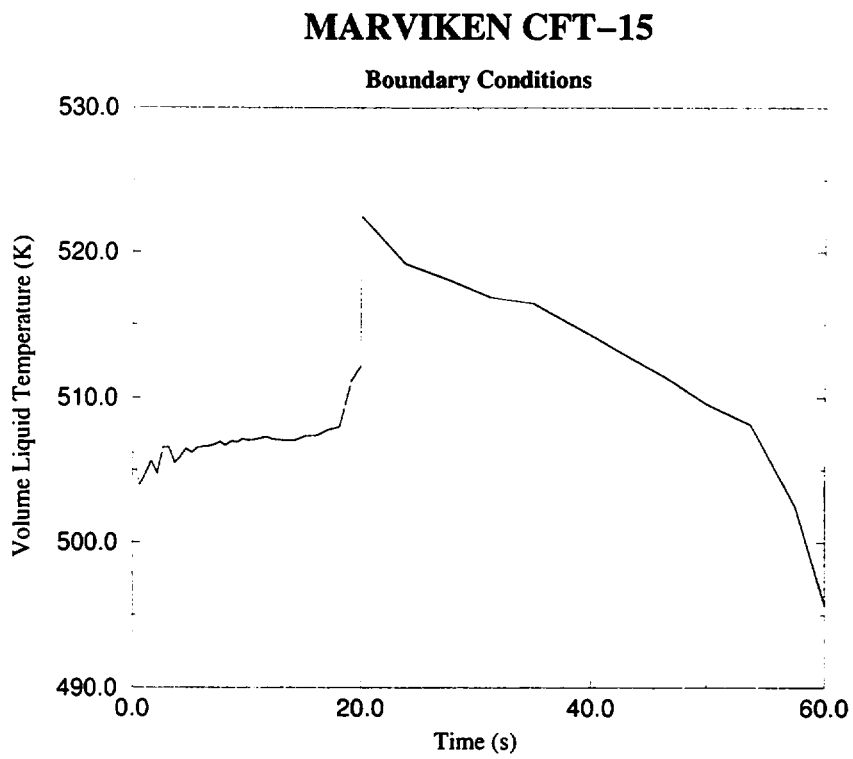

Figure 4.19: Liquid temperature at bottom vessel. Test data. CFT-15.

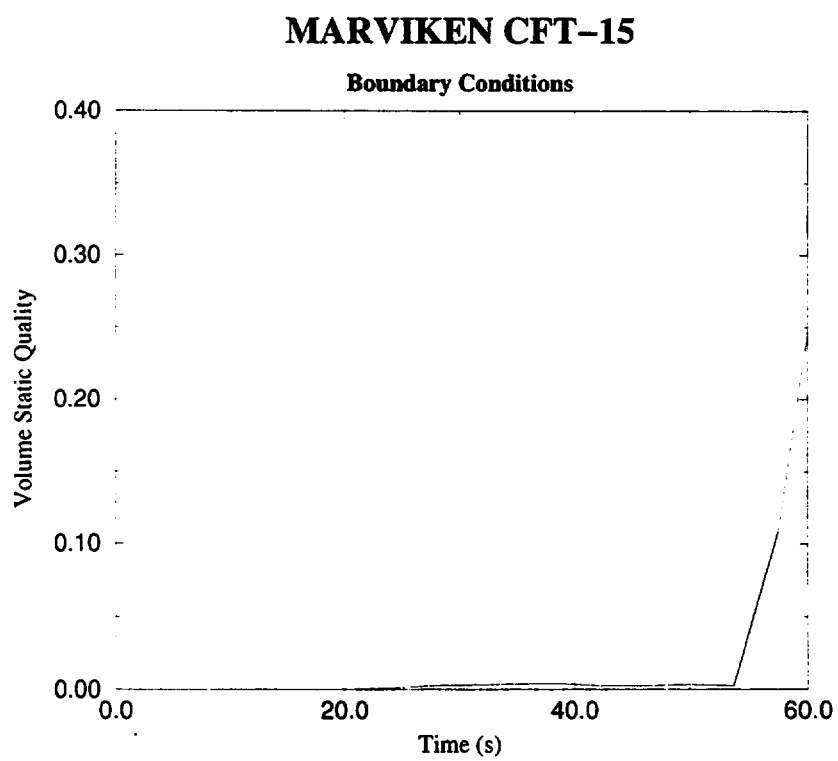

Figure 4.20: Static quality at bottom vessel. Test data. CFT-15.

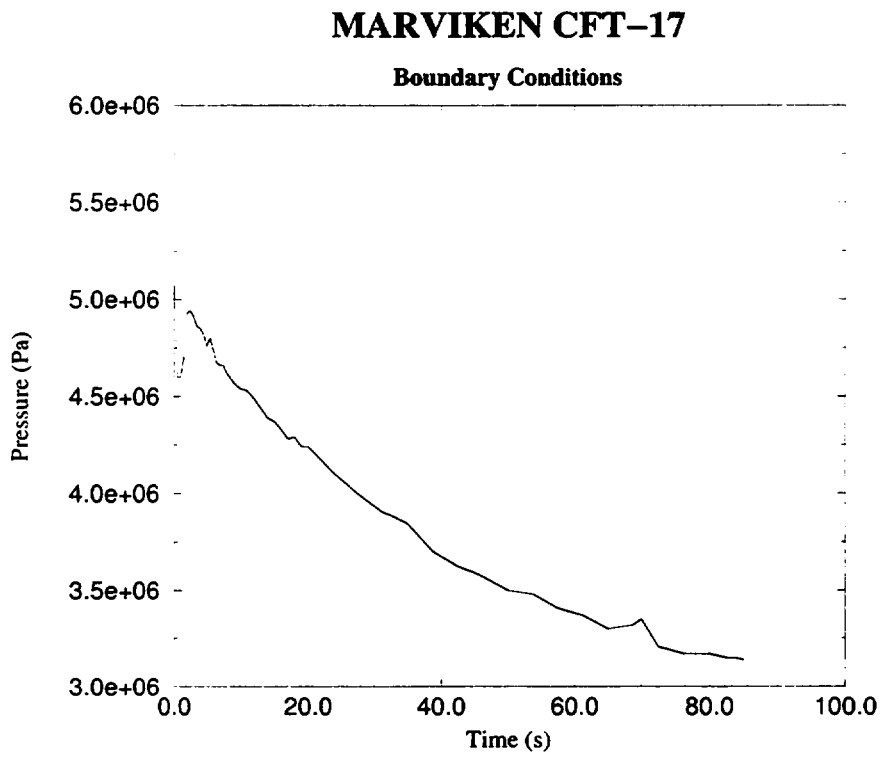

Figure 4.21: Pressure at bottom vessel. Test data. CFT-17.

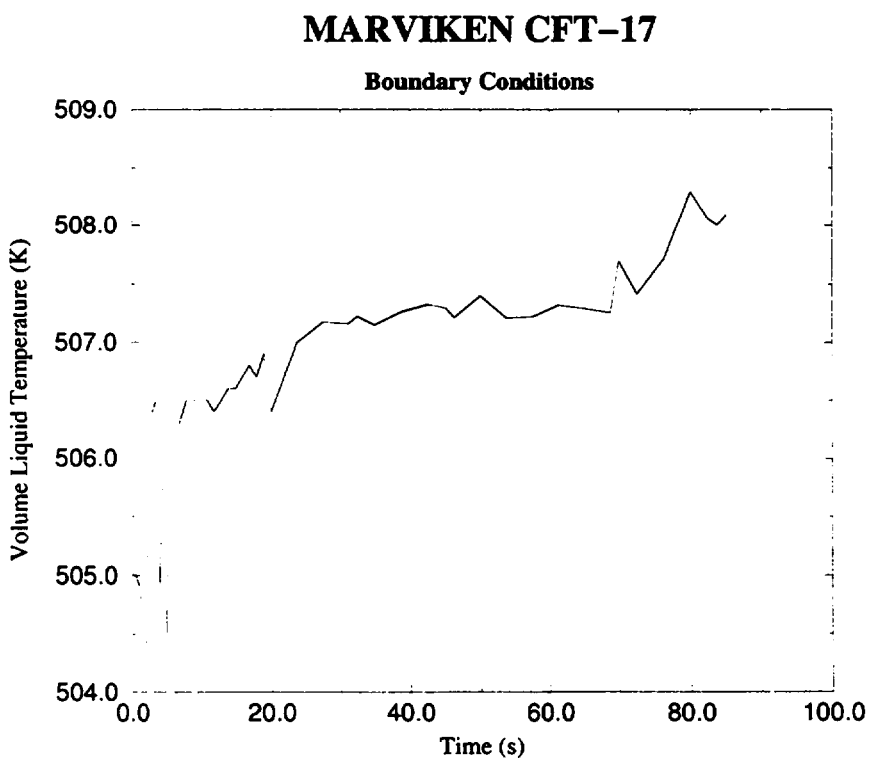

Figure 4.22: Liquid temperature at bottom vessel. Test data. CFT-17.

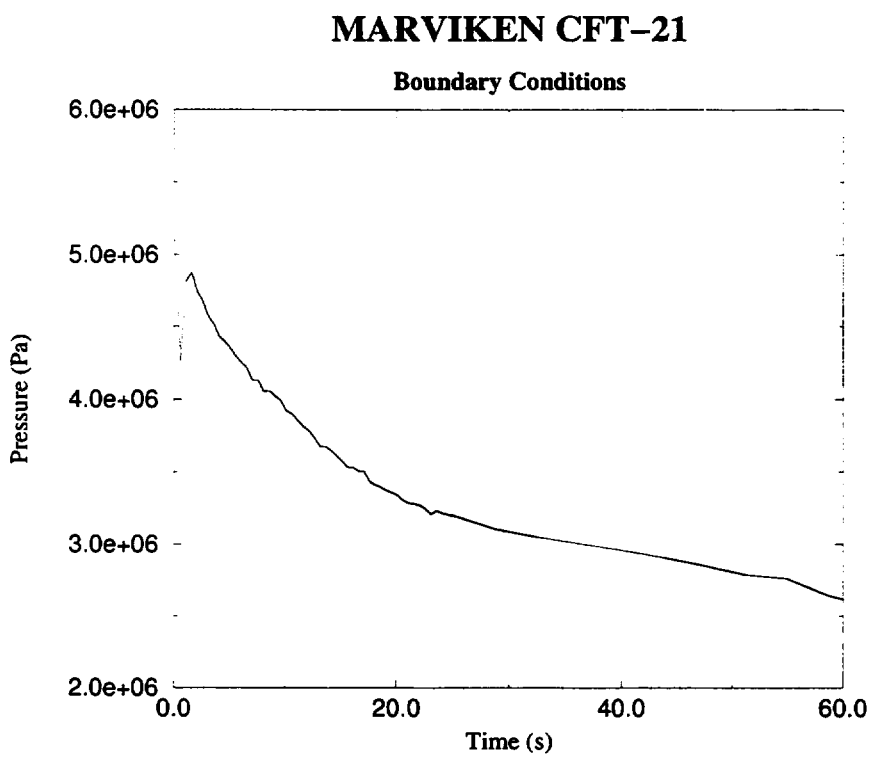

Figure 4.23: Pressure at bottom vessel. Test data. CFT-21.

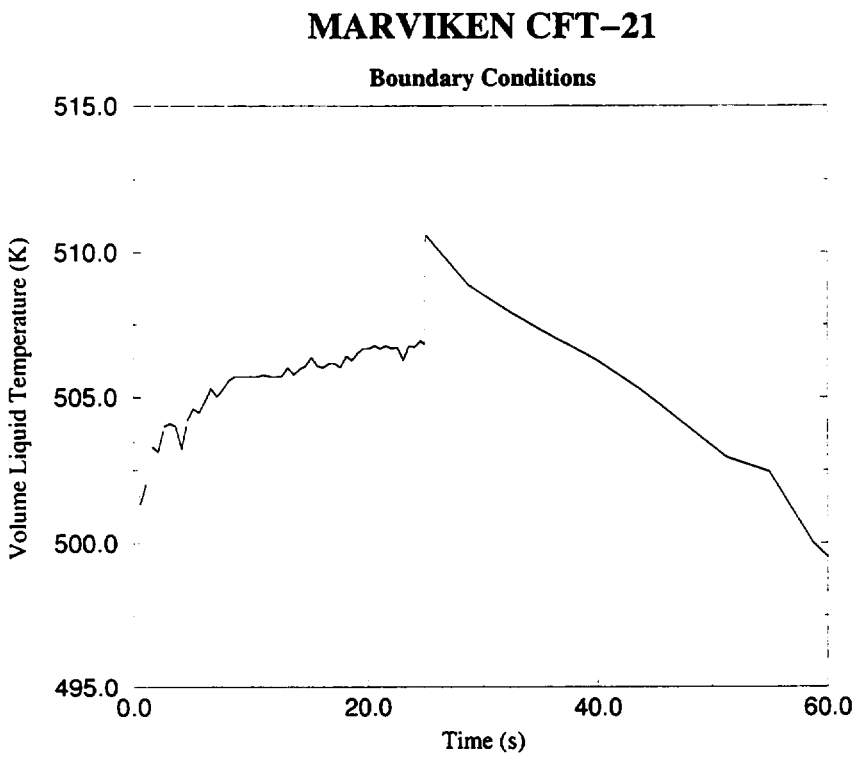

Figure 4.24: Liquid temperature at bottom vessel. Test data. CFT-21.

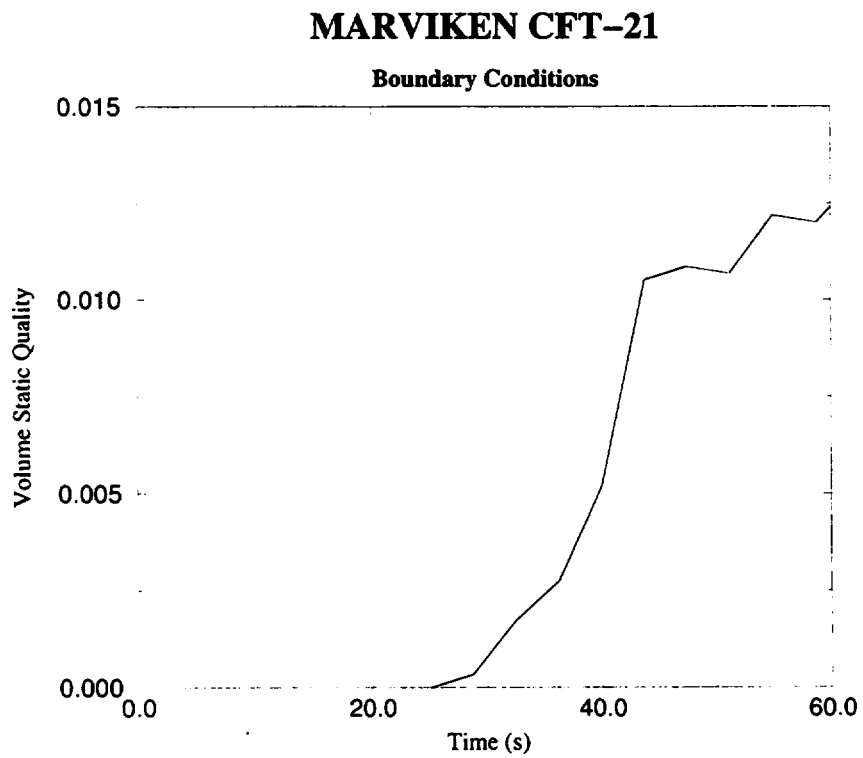

Figure 4.25: Static quality at bottom vessel. Test data. CFT-21.

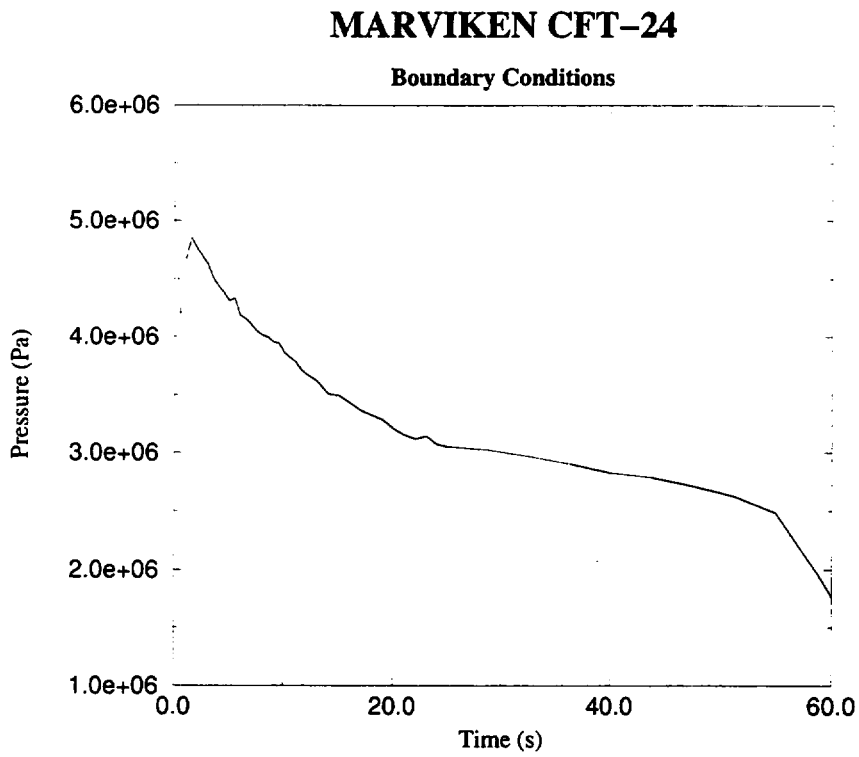

Figure 4.26: Pressure at bottom vessel. Test data. CFT-24.

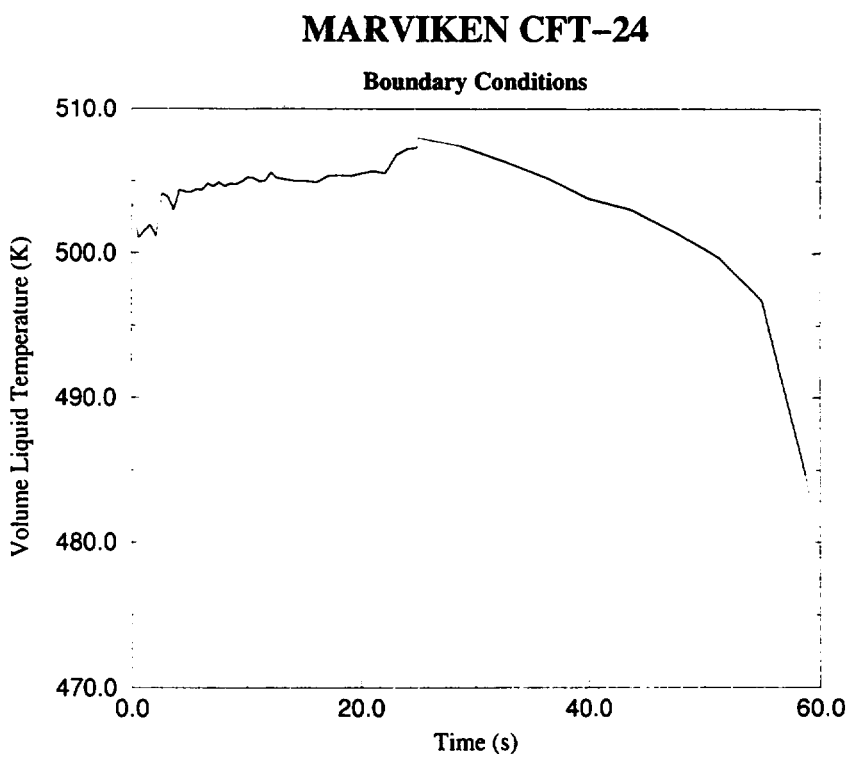

Figure 4.27: Liquid temperature at bottom vessel. Test data. CFT-24.

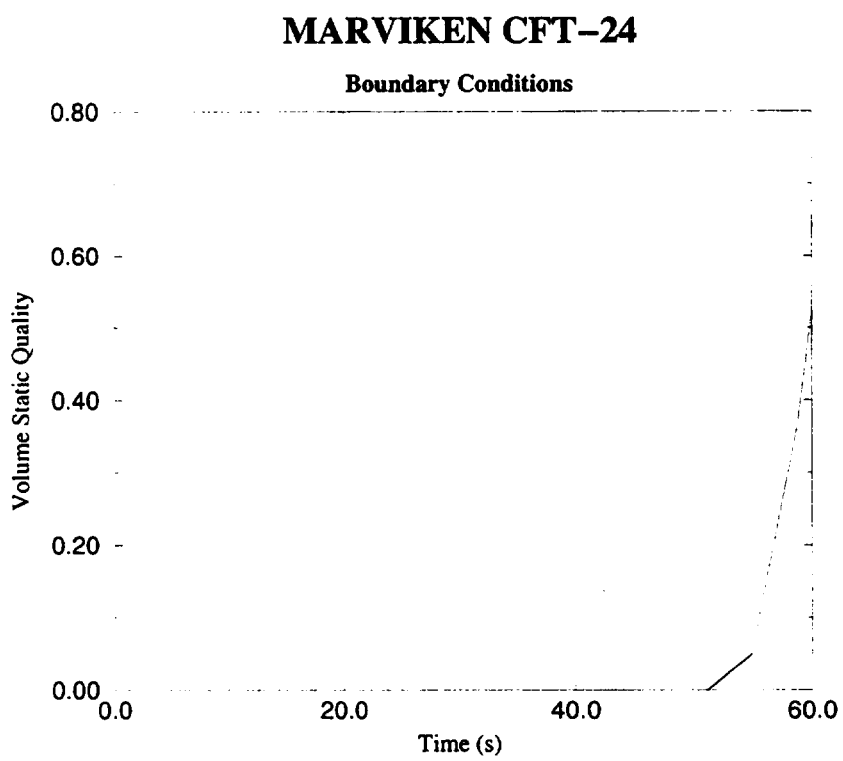

Figure 4.28: Static quality at bottom vessel. Test data. CFT-24.

4.4.1 Comparison of Critical and Non-critical Flow Models

The models and options being compared are:

- CFM-off and nozzle modeled as a SINGLE JUNCTION.
- CFM-on and nozzle modeled as a PIPE.
- CFM-on and nozzle modeled as a SINGLE JUNCTION, smooth area change.
- CFM-on and nozzle modeled as a SINGLE JUNCTION, abrupt area change.

The code options used for all the cases are:

- Homogeneous option, $v_g = v_l$.
- Discharge coefficients equal to one.
- Null friction coefficient at the nozzle outlet.

The following conclusions are obtained from Figures 4.29 to 4.42:

- In general, the mass flow simulated with CFM-off is always greater than with CFM-on, except at the beginning of CFT-01, CFT-06 and CFT-17 (see Section 2.1, problems with the transition from CFM-on to CFM-off). Also, the CFM-off results do not fit the experimental data and so the critical flow model is necessary.
- When nozzle is modeled as a single junction, the results obtained with the abrupt area change option are better than with the smooth area option. However, the differences between them are small.
- The subcooled period is apparently better reproduced with the nozzle modeled as a pipe than as a single junction (except in CFT-24), Figures 4.36 to 4.42, but it must be taken into account that the void fraction at nozzle outlet is not null from the beginning of the transient with the nozzle modeled as a pipe, which is not in accordance with experimental data. This problem is also reported in [KIM-92]. So, the subcooled period is modeled with a two-phase critical flow model with a non null void fraction, which is wrong. This problem is not present when the nozzle is modeled as a single junction because it is equivalent to freezing the model.

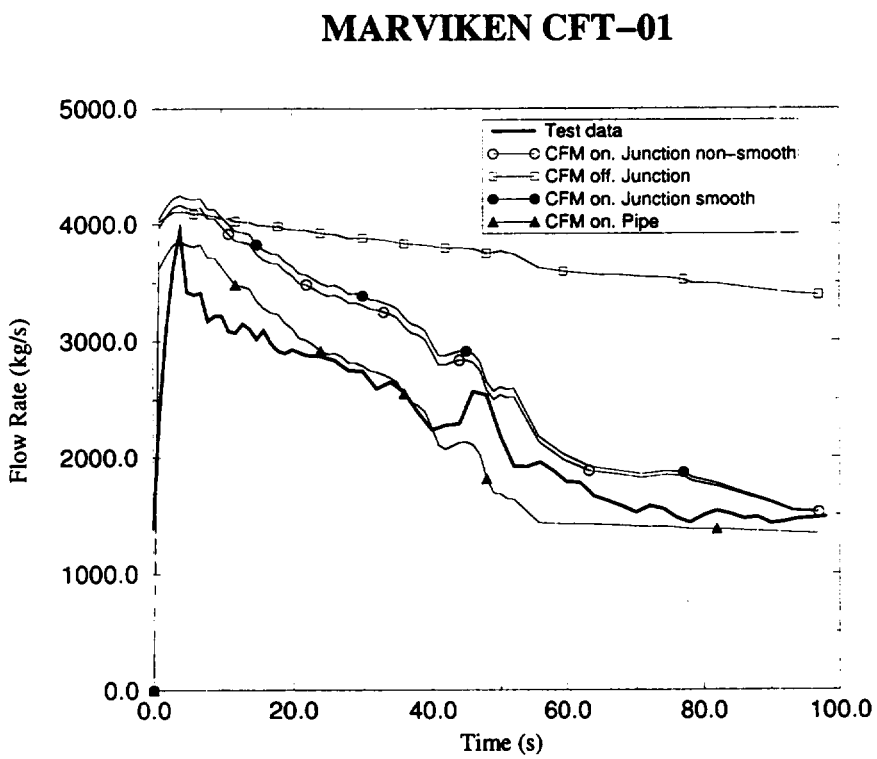

Figure 4.29: Mass flow at nozzle exit. Comparison between CFM and non-CFM (BCM). CFT-01.

- The results obtained with both models during the two-phase period are quite similar to experimental data, Figures 4.29 to 4.35. CFT-06 and CFT-24 are better reproduced with the nozzle modeled as a junction.
- As the subcooled period is better reproduced with the nozzle modeled as a junction and for the two phase period both models seem to give similar results, it should be better to choose the junction model for the nozzle.

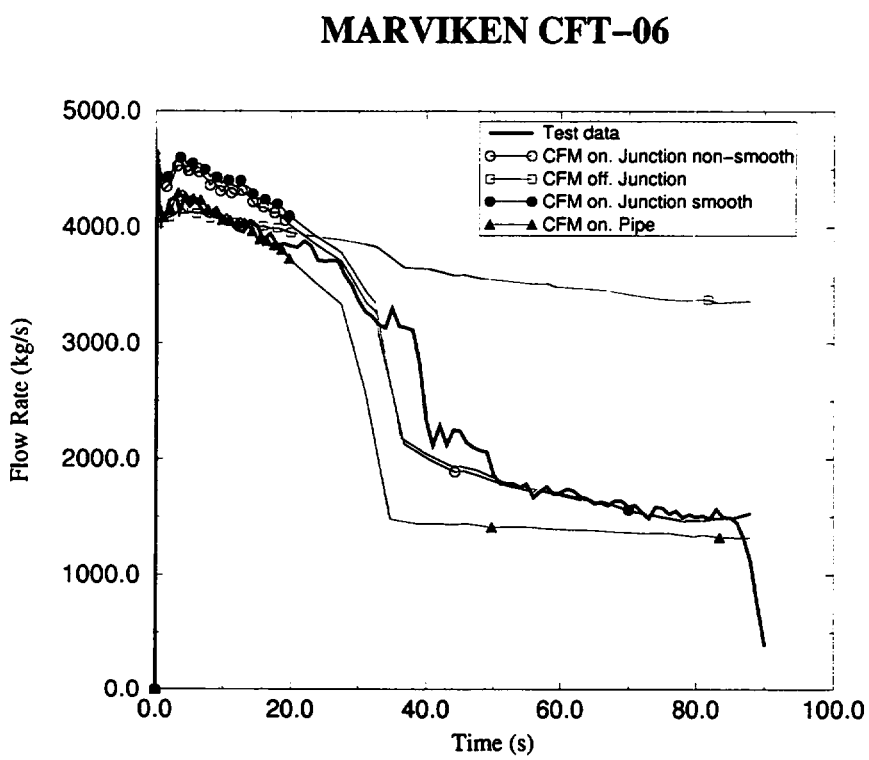

Figure 4.30: Mass flow at nozzle exit. Comparison between CFM and non-CFM (BCM). CFT-06.

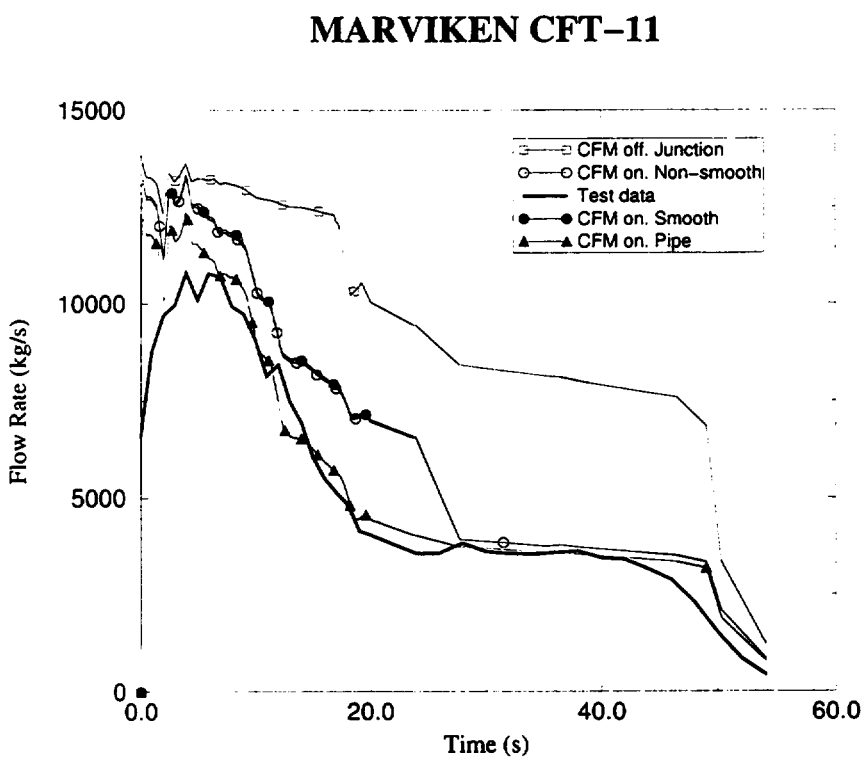

Figure 4.31: Mass flow at nozzle exit. Comparison between CFM and non-CFM (BCM). CFT-11.

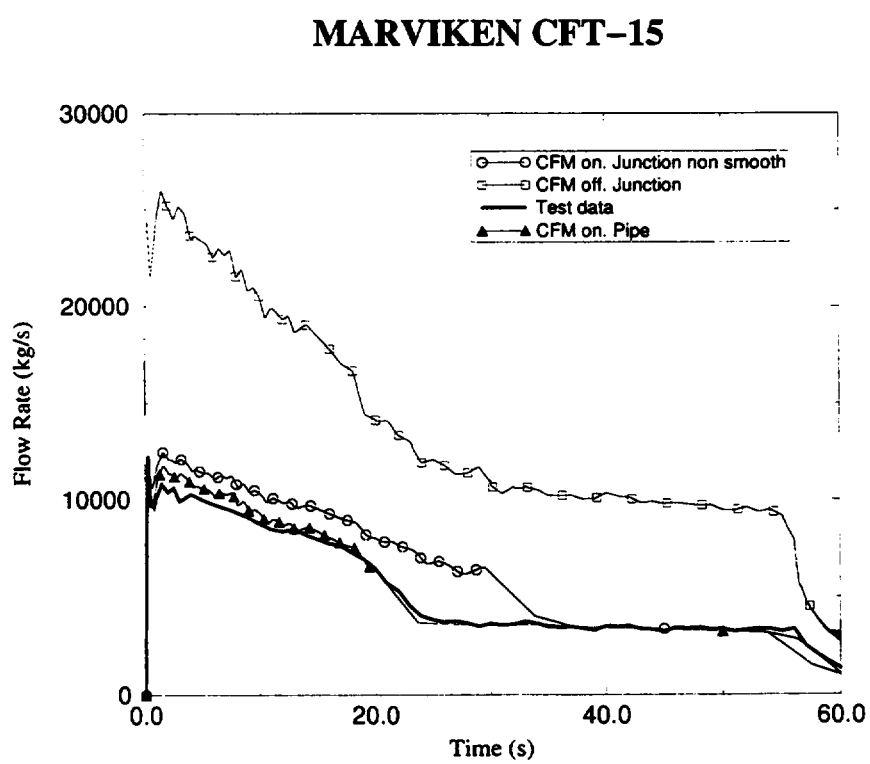

Figure 4.32: Mass flow at nozzle exit. Comparison between CFM and non-CFM (BCM). CFT-15.

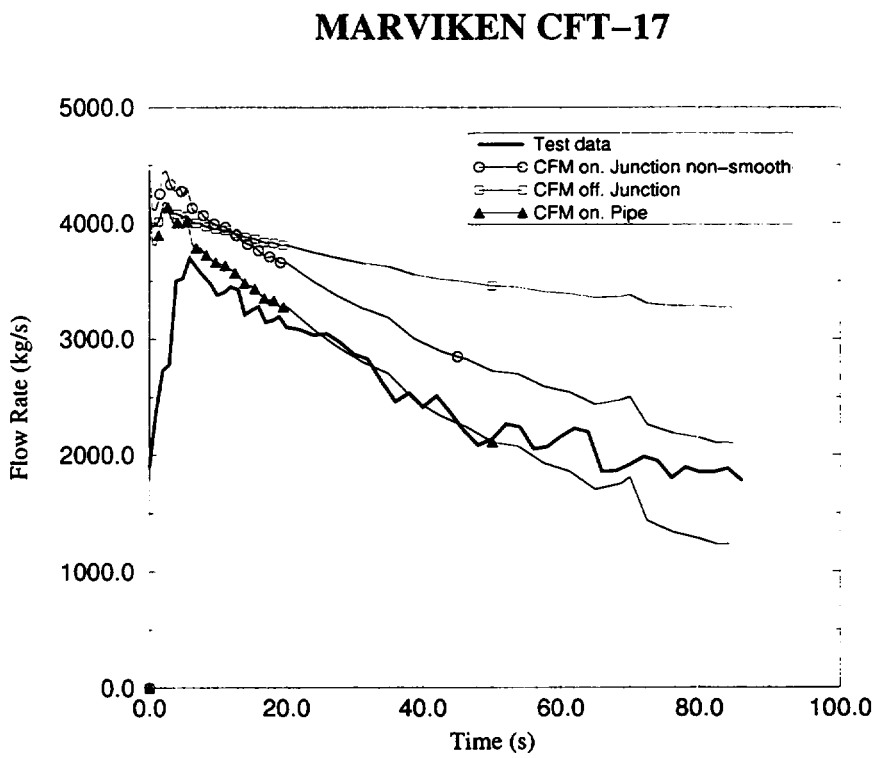

Figure 4.33: Mass flow at nozzle exit. Comparison between CFM and non-CFM (BCM). CFT-17.

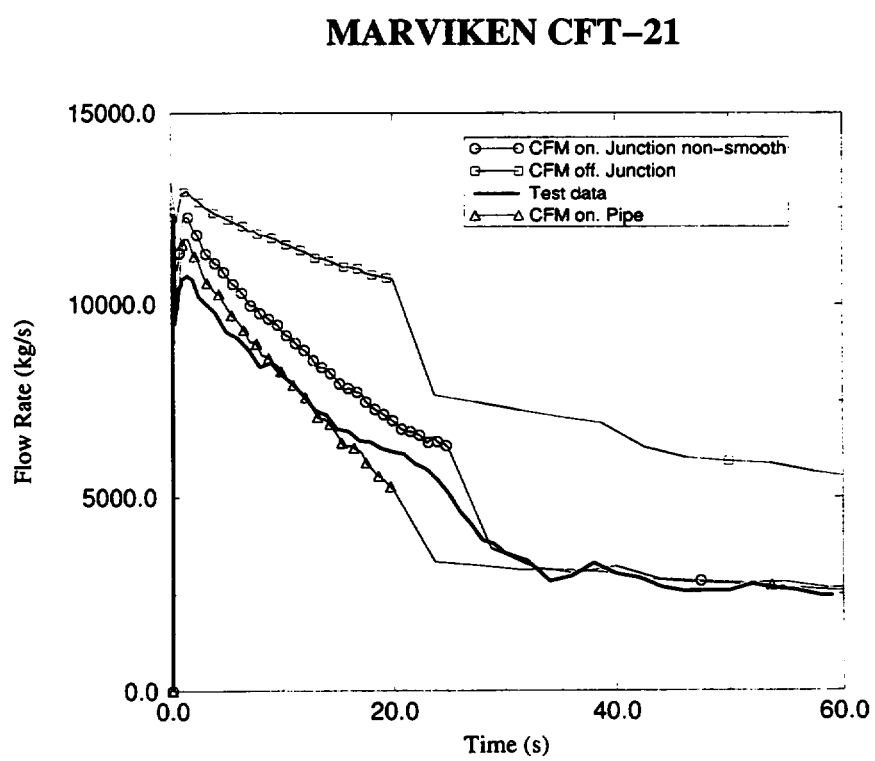

Figure 4.34: Mass flow at nozzle exit. Comparison between CFM and non-CFM (BCM). CFT-21.

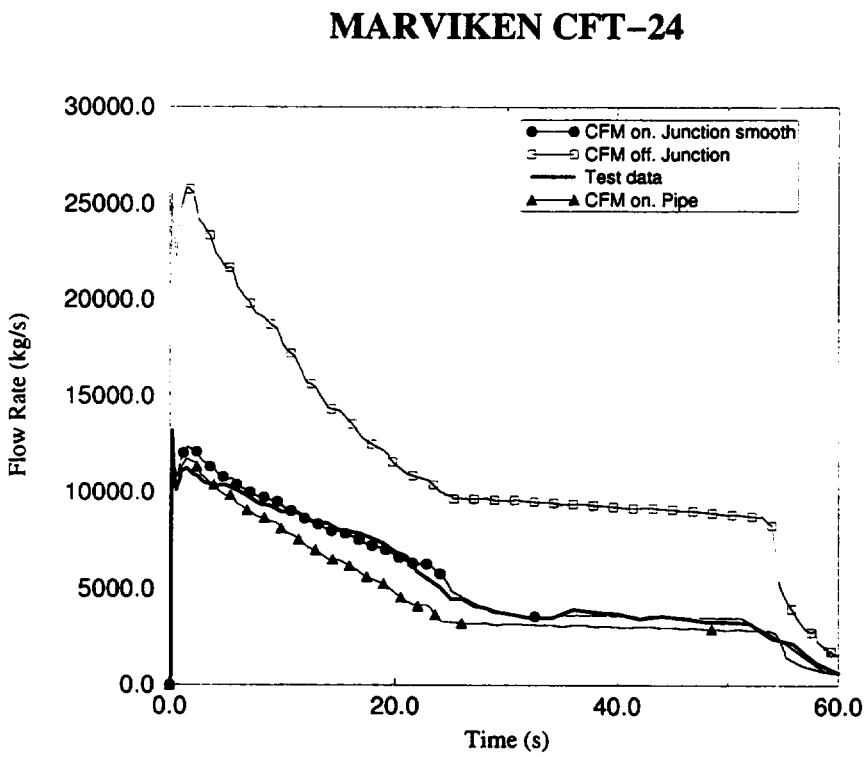

Figure 4.35: Mass flow at nozzle exit. Comparison between CFM and non-CFM (BCM). CFT-24.

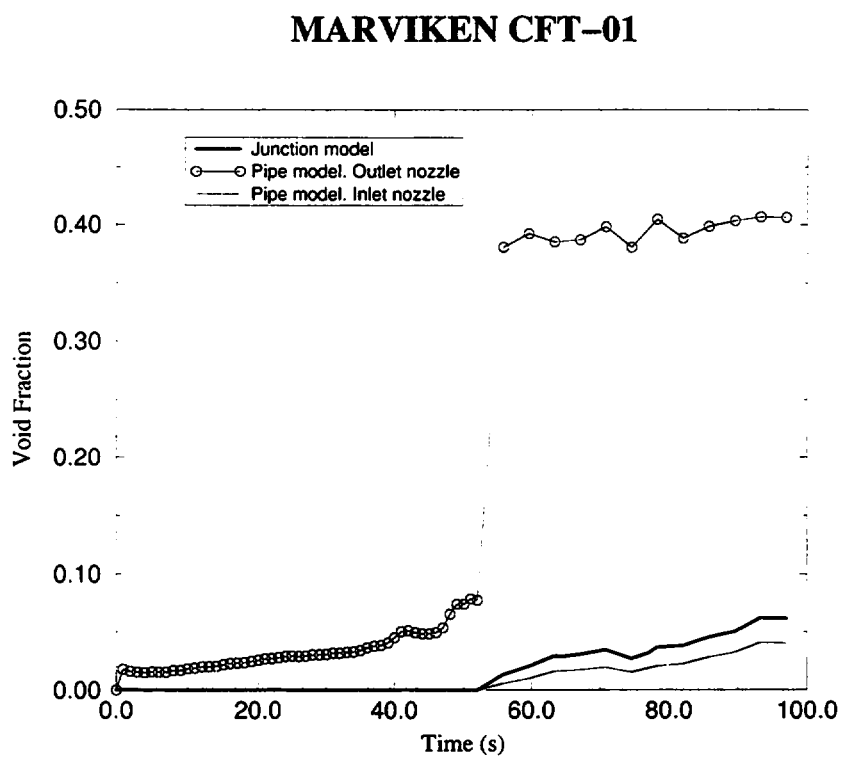

Figure 4.36: Void fraction. Comparison between CFM and non-CFM (BCM). CFT-01.

4.4.2 Selection of Model Options

The following comparisons have been made in order to analyze the influence of the different code options and available models:

- Comparison between Homogeneous and Non-homogeneous options. This option has only an effect on the two-phase period. CFT-15 and CFT-24 have been used for this analysis. The results obtained with the homogeneous option are closer to test data than those obtained with the non-homogeneous option, independently of the model used for the nozzle (pipe or junction), Figures 4.43 to 4.46.

- Comparison of SINGLE JUNCTION, trip-valve and motor-valve models. All the models give the same results for the CFT-21 simulation, Figures 4.47 and 4.48, for subcooled and two-phase periods, and also for discharge coefficients different from one.

From the previous analysis, the homogeneous option should be used with any of the three models above mentioned.

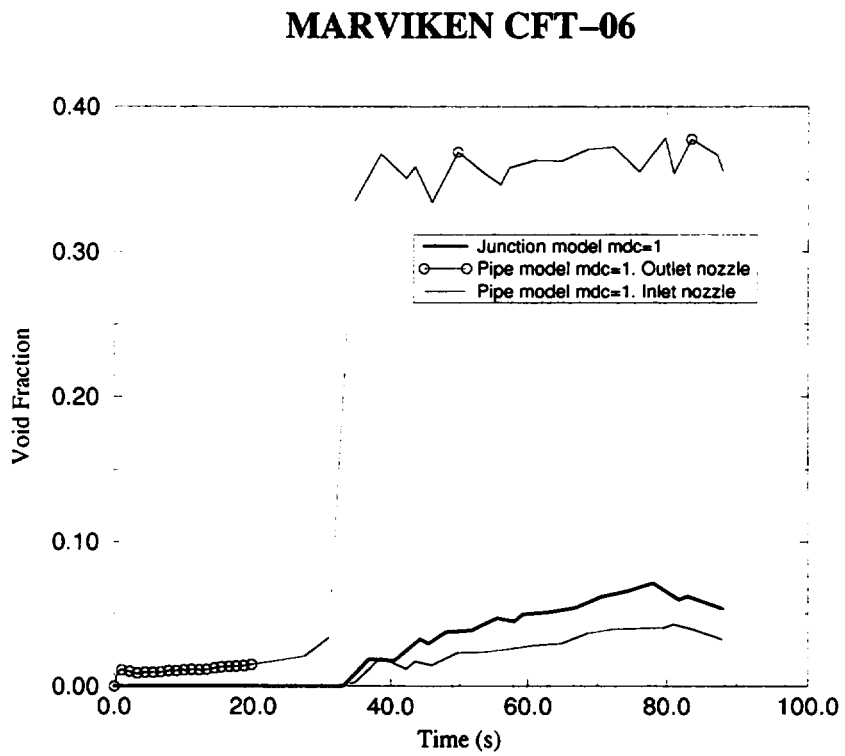

Figure 4.37: Void fraction. Comparison between CFM and non-CFM (BCM). CFT-06.

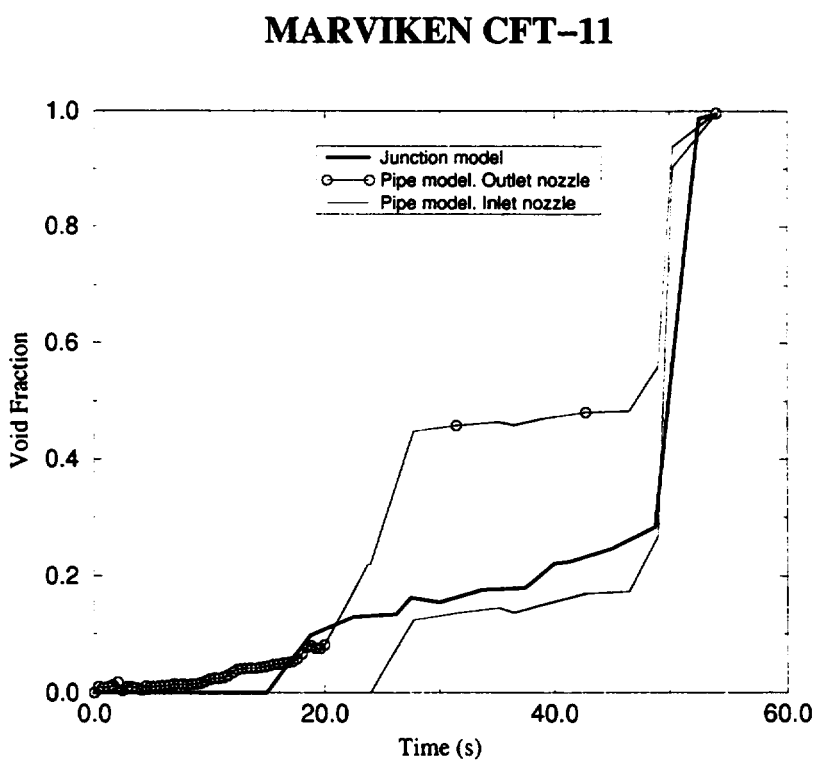

Figure 4.38: Void fraction. Comparison between CFM and non-CFM (BCM). CFT-11.

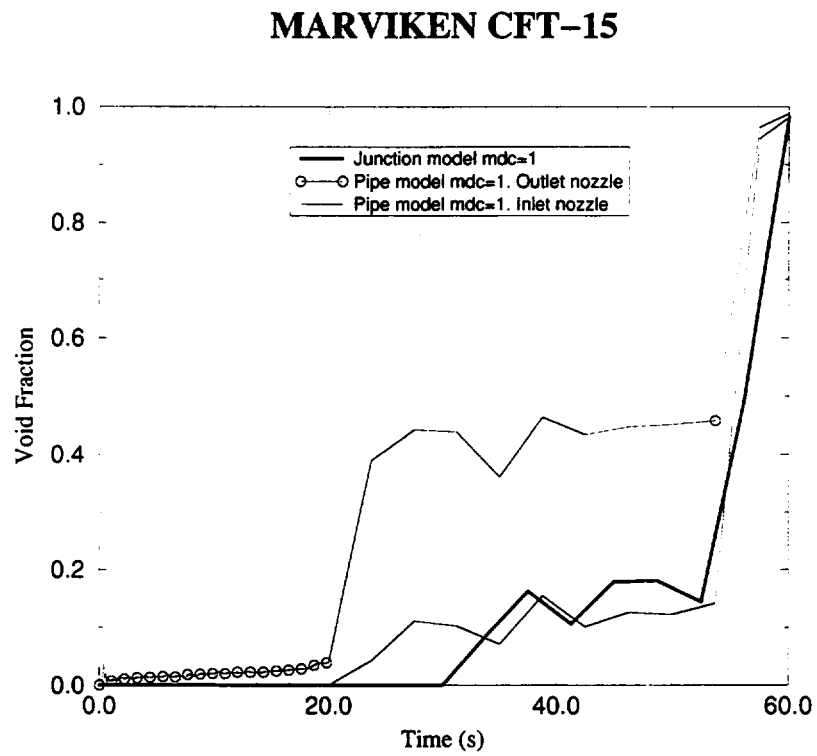

Figure 4.39: Void fraction. Comparison between CFM and non-CFM (BCM). CFT-15.

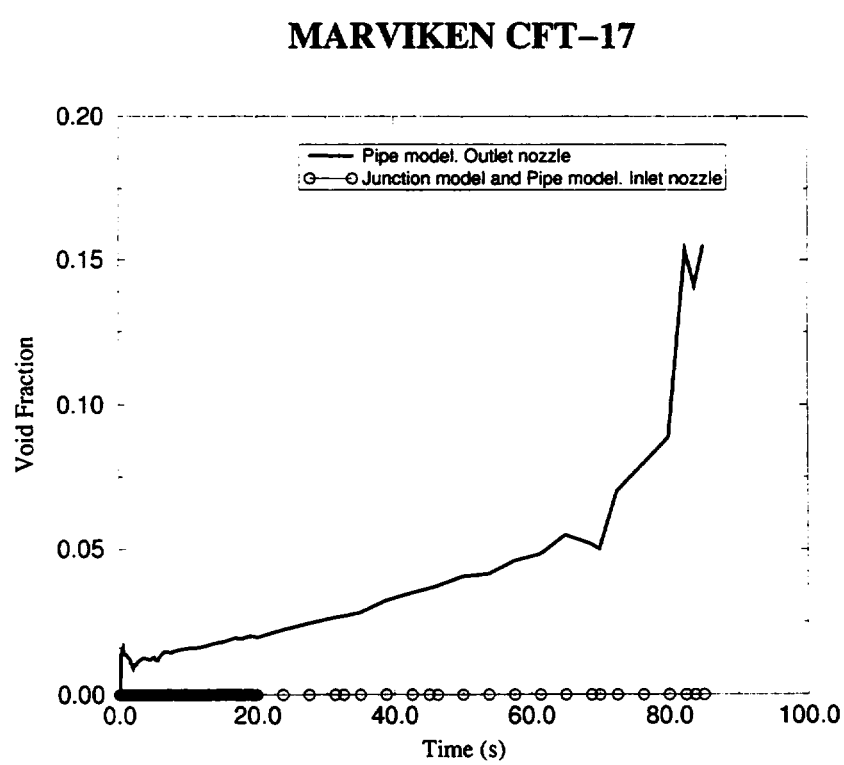

Figure 4.40: Void fraction. Comparison between CFM and non-CFM (BCM). CFT-17.

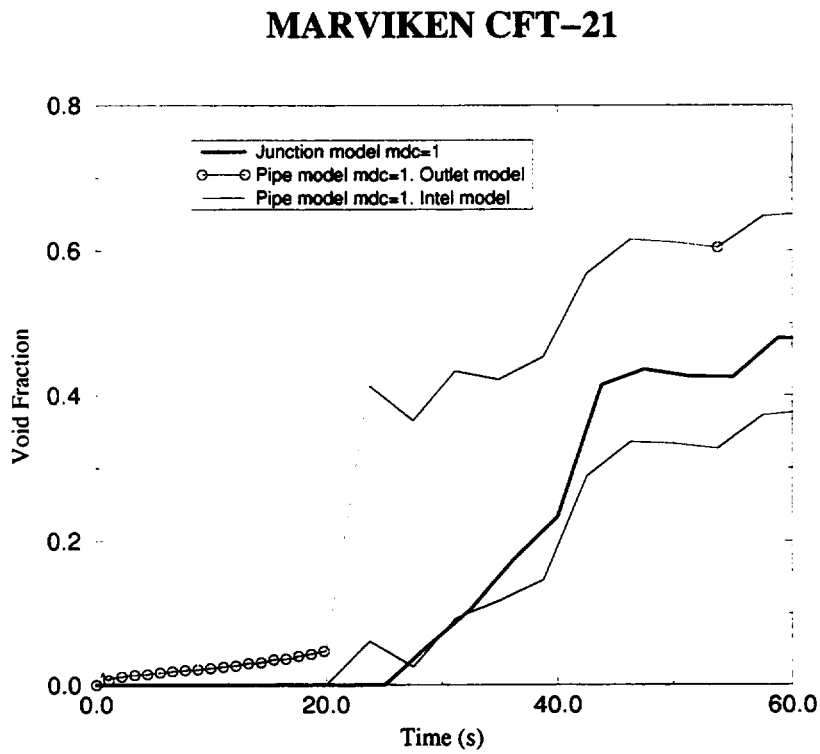

Figure 4.41: Void fraction. Comparison between CFM and non-CFM (BCM). CFT-21.

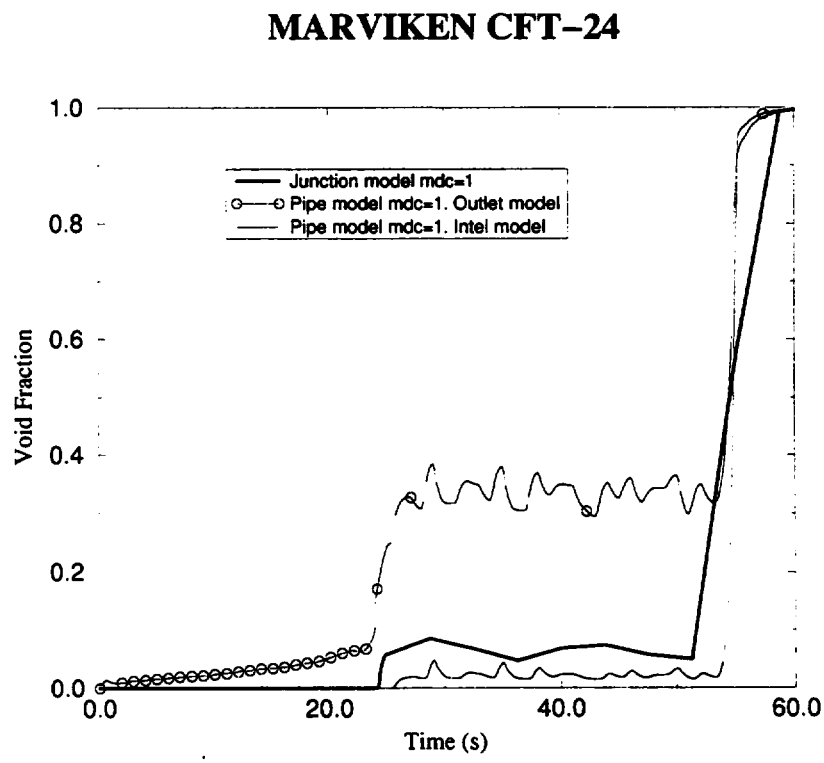

Figure 4.42: Void fraction. Comparison between CFM and non-CFM (BCM). CFT-24.

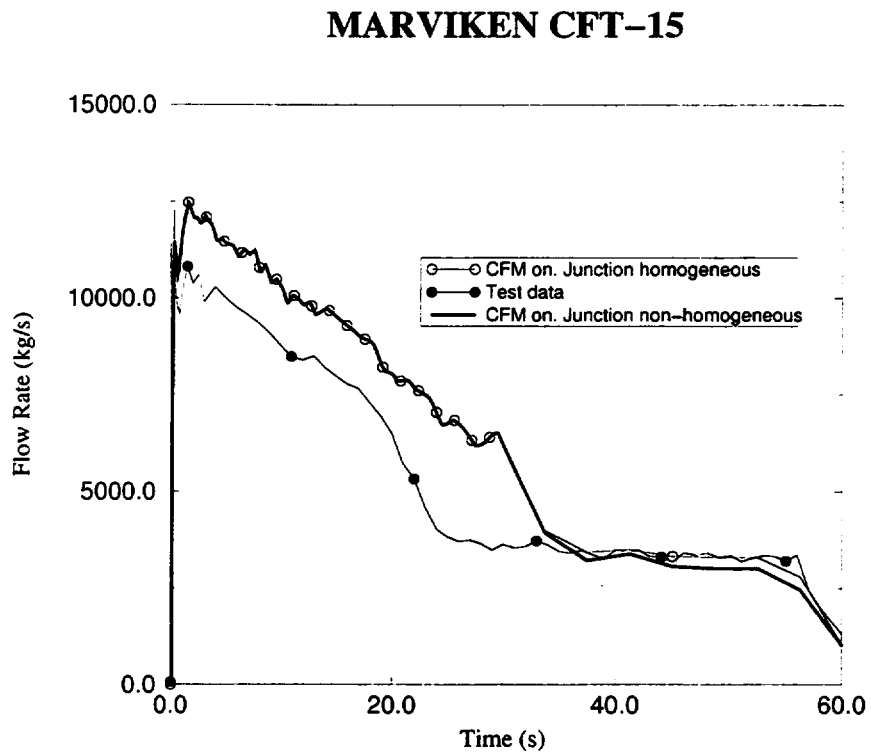

Figure 4.43: Mass flow at nozzle exit. Comparison between Homogeneous and Non-homogeneous options. BCM-J. CFT-15.

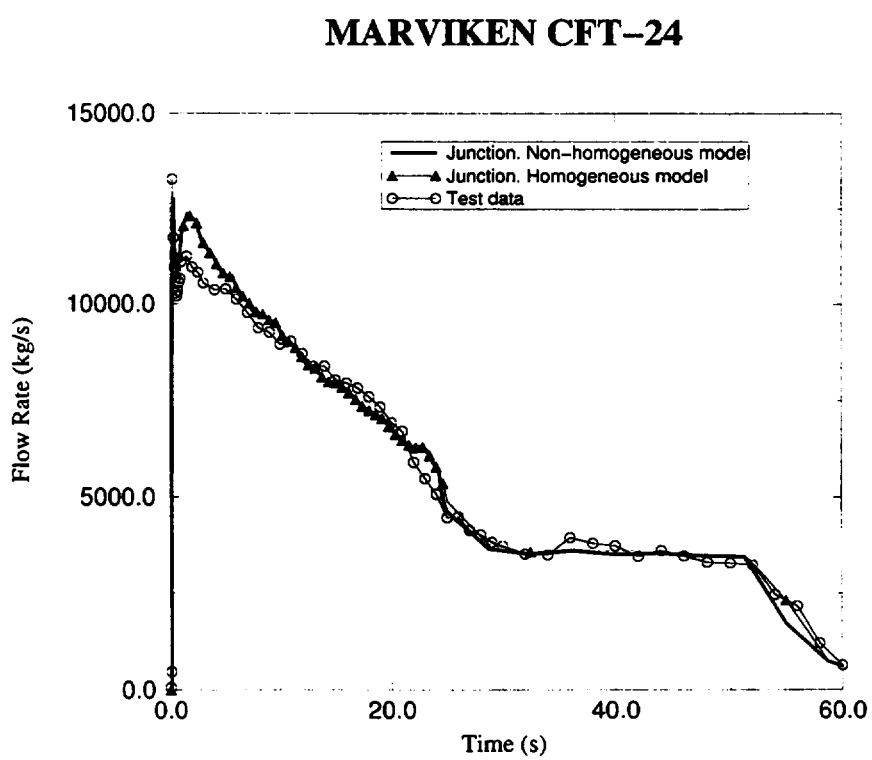

Figure 4.44: Mass flow at nozzle exit. Comparison between Homogeneous and Non-homogeneous options. BCM-J. CFT-24.

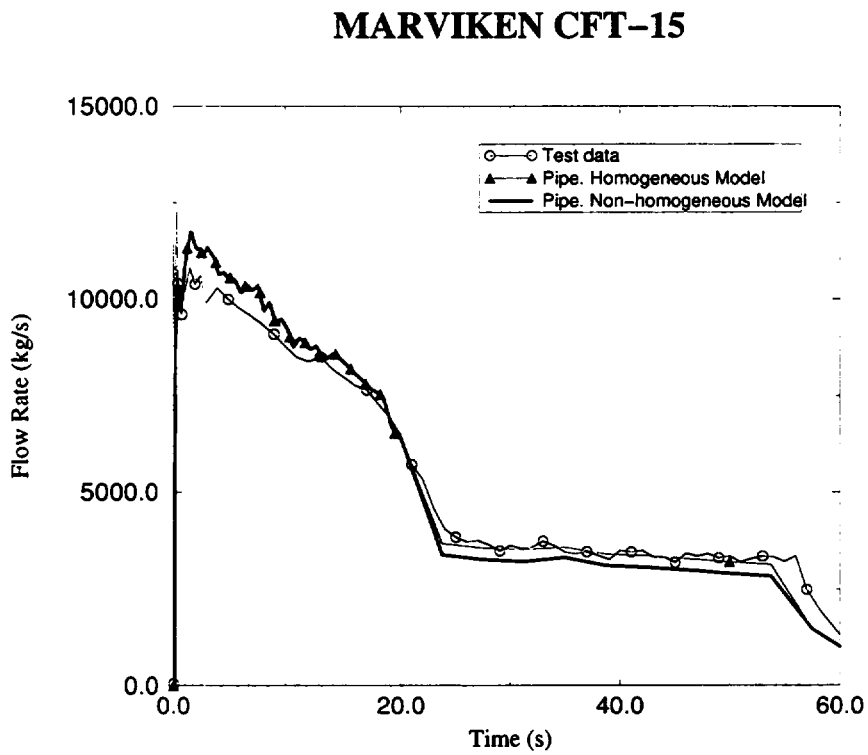

Figure 4.45: Mass flow at nozzle exit. Comparison between Homogeneous and Non-homogeneous options. BCM-P. CFT-15.

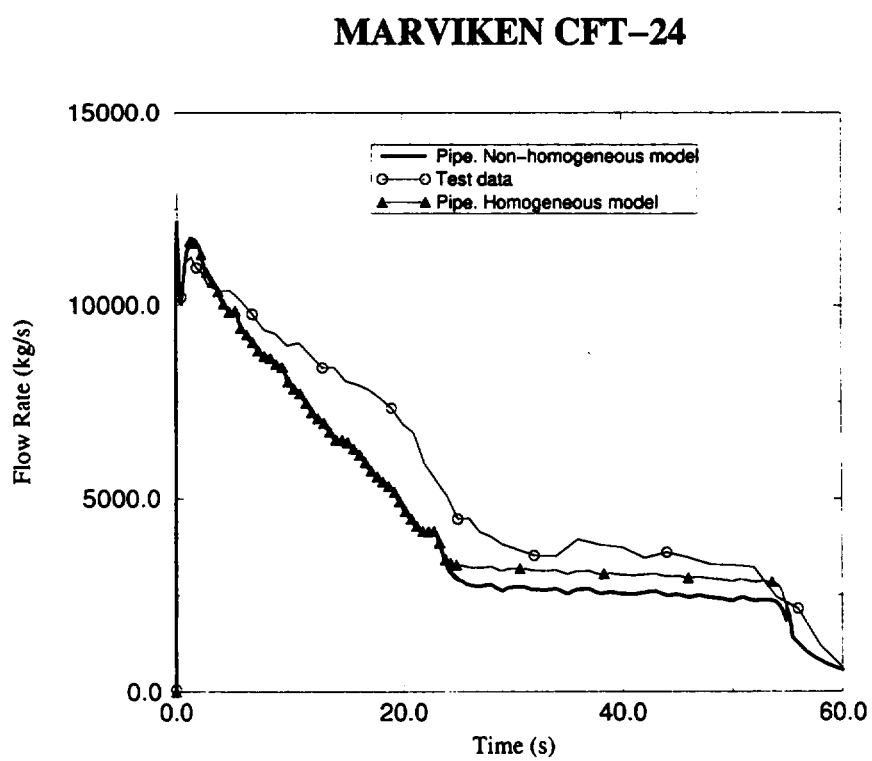

Figure 4.46: Mass flow at nozzle exit. Comparison between Homogeneous and Non-homogeneous options. Nozzle modeled as PIPE (BCM). CFT-24.

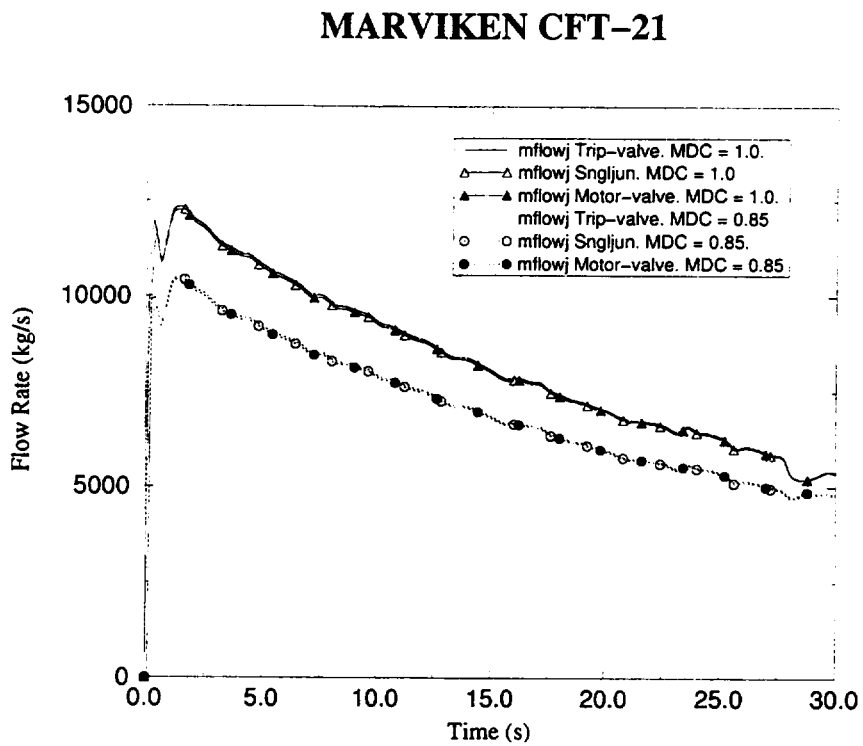

Figure 4.47: Comparison of Single junction, Trip-Valve and Motor-Valve Models. Subcooled CFM. MDC=1.0, 0.85 (BCM). CFT-21.

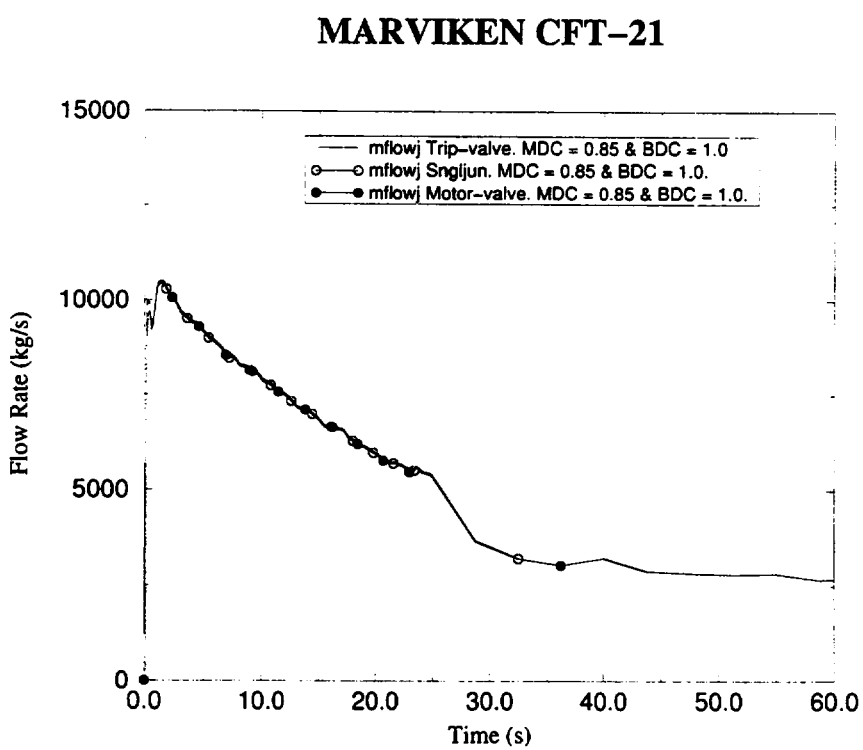

Figure 4.48: Comparison of Single junction, Trip-Valve and Motor-Valve Models. Subcooled and two-phase CFM (BCM). CFT-21.

4.4.3 Discharge Coefficient Adjustment

For the adjustment of the discharge coefficients (subcooled and two-phase), modelling the nozzle as a PIPE and a SINGLE JUNCTION, data from CFT-01, 11, 15, 17, 21 and 24 have been used.

- Nozzle modeled as SINGLE JUNCTION. The comparison between test data and the results for the mass flow with the adjustment of the discharge coefficients are shown in Figures 4.49, 4.52, 4.55, 4.58, 4.61, 4.63 and 4.66. A very good adjustment is achieved with the coefficients shown in table 4.2 The transitions present in the critical flow model (for void fractions $\alpha = 10^{-5}$, $\alpha = 0.1$, $\alpha = 0.9$, and $\alpha = 0.99$) are shown on the figures by means of vertical lines.

  Void fraction results, Figures 4.50, 4.53, 4.56, 4.59, 4.64 and 4.67, and liquid temperature with saturation temperature at the nozzle exit, Figures 4.51, 4.54, 4.57, 4.60, 4.62, 4.65 and 4.68, allow observing the range of variation of the void fraction and the subcooling in the simulations. It is important to remark that the range of variation of the void fraction is approximately below 0.4 in all the cases analyzed, Figure 4.69, and so, other experiments should be necessary in order to validate the model in all its range.

- Nozzle modeled as PIPE. The comparison between test data and the results for the mass flow with the adjustment of the discharge coefficients, table 4.2, Figures 4.70, 4.72, 4.74, 4.76 and 4.78, shows that the adjustment in the subcooled period is not so good as in the previous case. The reason is that when the subcooled discharge coefficients are fitted, the beginning of the boiling process is delayed, Figures 4.71, 4.73, 4.75, 4.77 and 4.79. However, it can be observed that boiling is still beginning too early respect to the test data.

  In the other hand, a good adjustment for the mass flow is achieved for the two-phase period, but the void fraction values are higher than with the nozzle modeled as a SINGLE JUNCTION.

- The comparison of the discharge coefficient adjustment for both models, Table 4.2 and Figure 4.80, shows that the discharge coefficients used with the BCM-P are higher than for BCM-J.

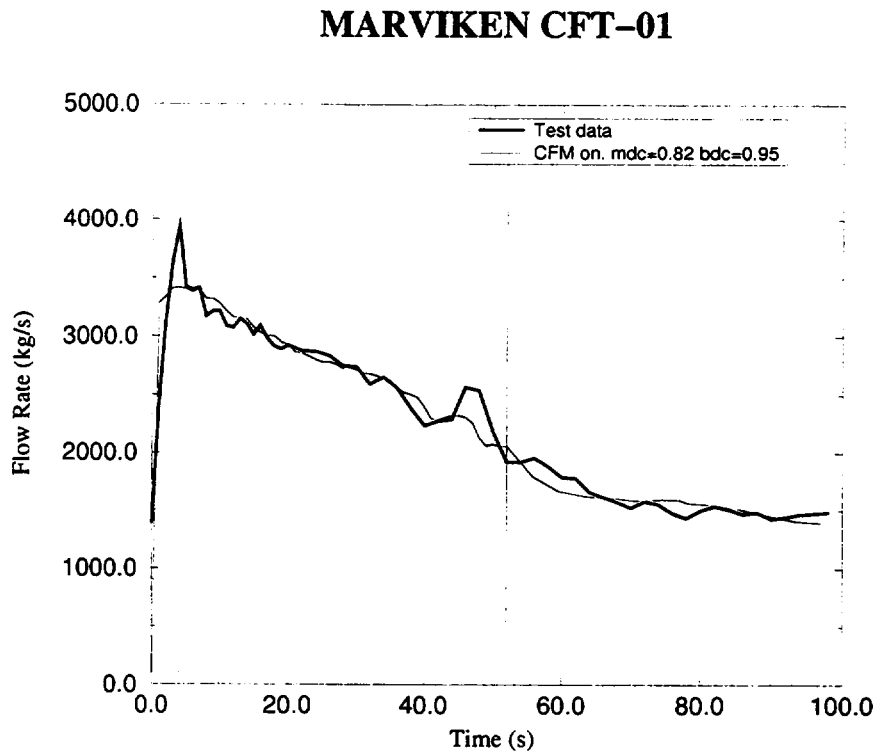

Figure 4.49: Mass flow at nozzle exit. Discharge coefficient adjustment, BCM-J. CFT-01.

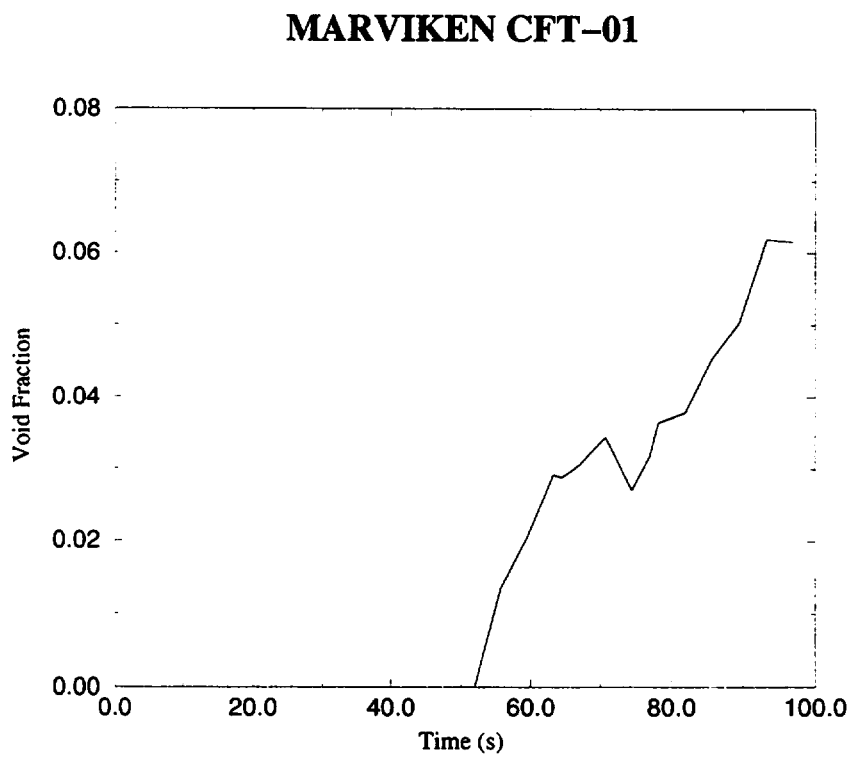

Figure 4.50: Void fraction at nozzle exit. Discharge coefficient adjustment, BCM-J. CFT-01.

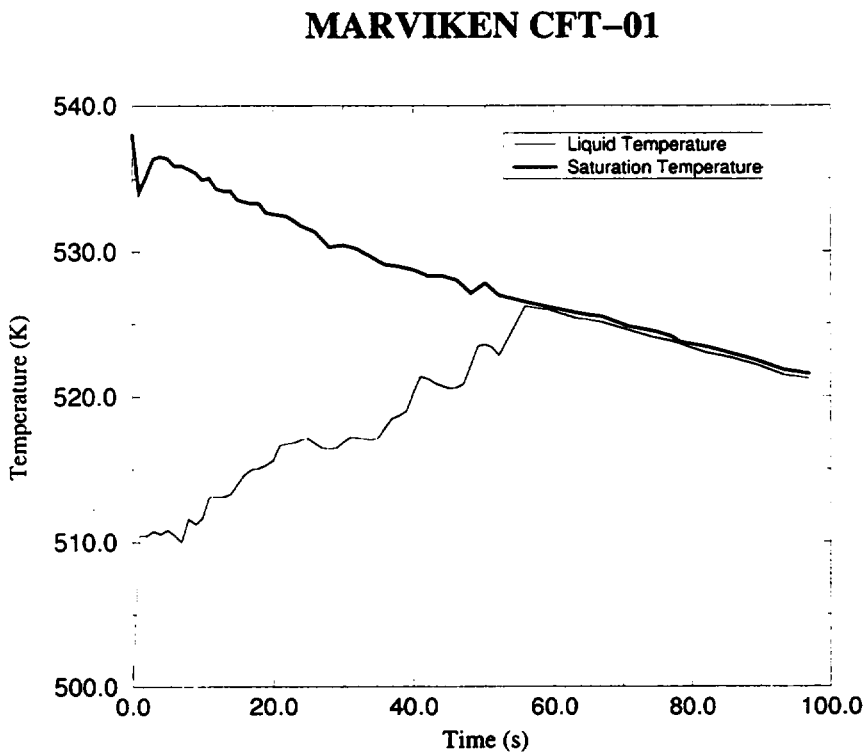

Figure 4.51: Liquid and saturation temperatures at nozzle exit. Discharge coefficient adjustment, BCM-J. CFT-01.

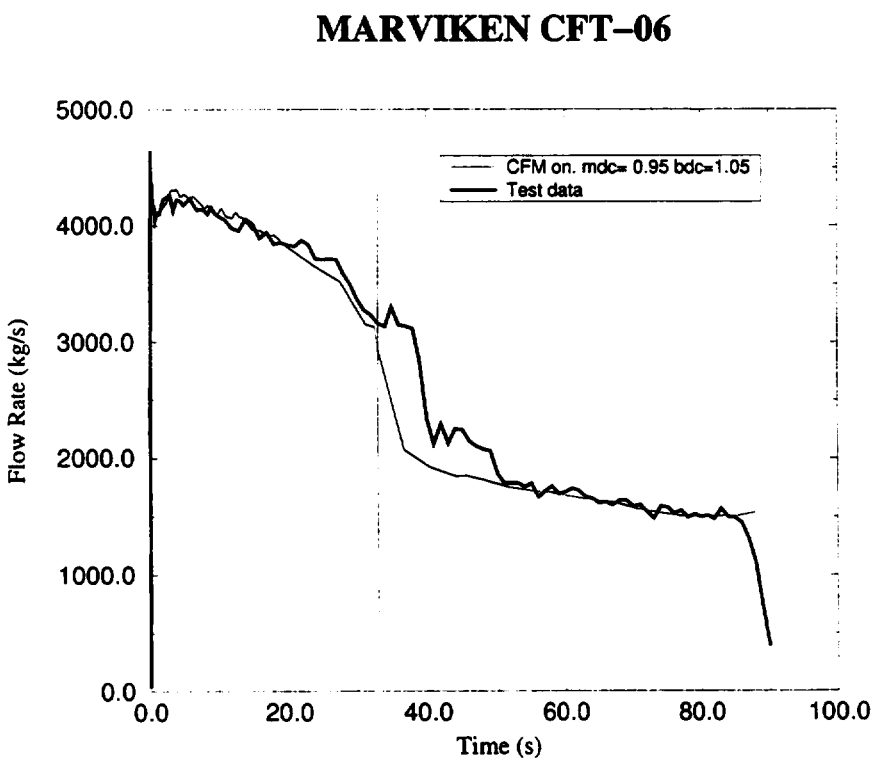

Figure 4.52: Mass flow at nozzle exit. Discharge coefficient adjustment, BCM-J. CFT-06.

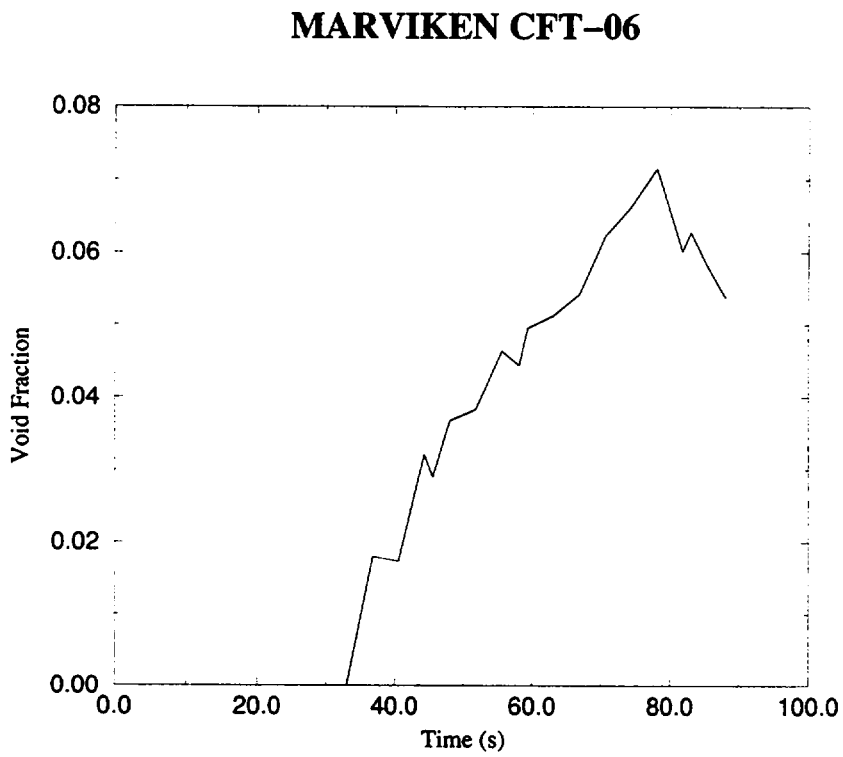

Figure 4.53: Void fraction at nozzle exit. Discharge coefficient adjustment, BCM-J. CFT-06.

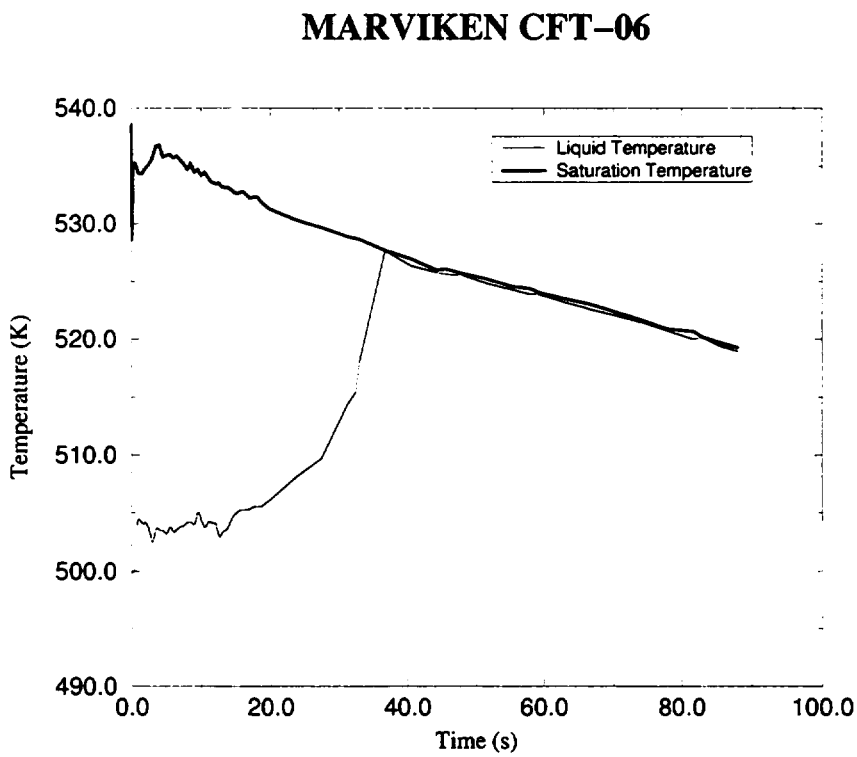

Figure 4.54: Liquid and saturation temperatures at nozzle exit. Discharge coefficient adjustment, BCM-J. CFT-06.

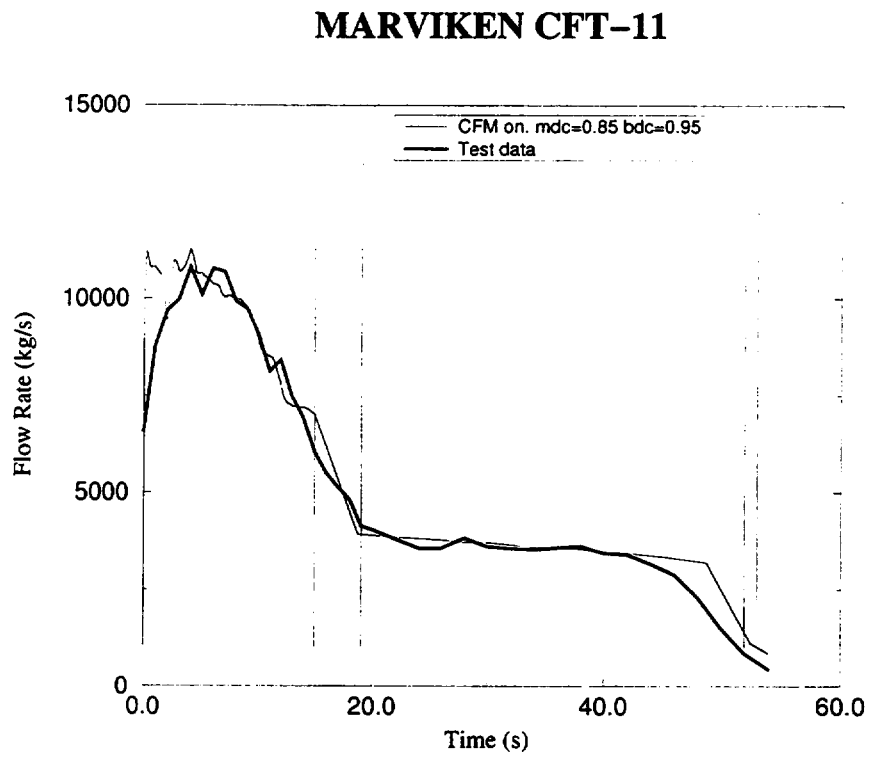

Figure 4.55: Mass flow at nozzle exit. Discharge coefficient adjustment, BCM-J. CFT-11.

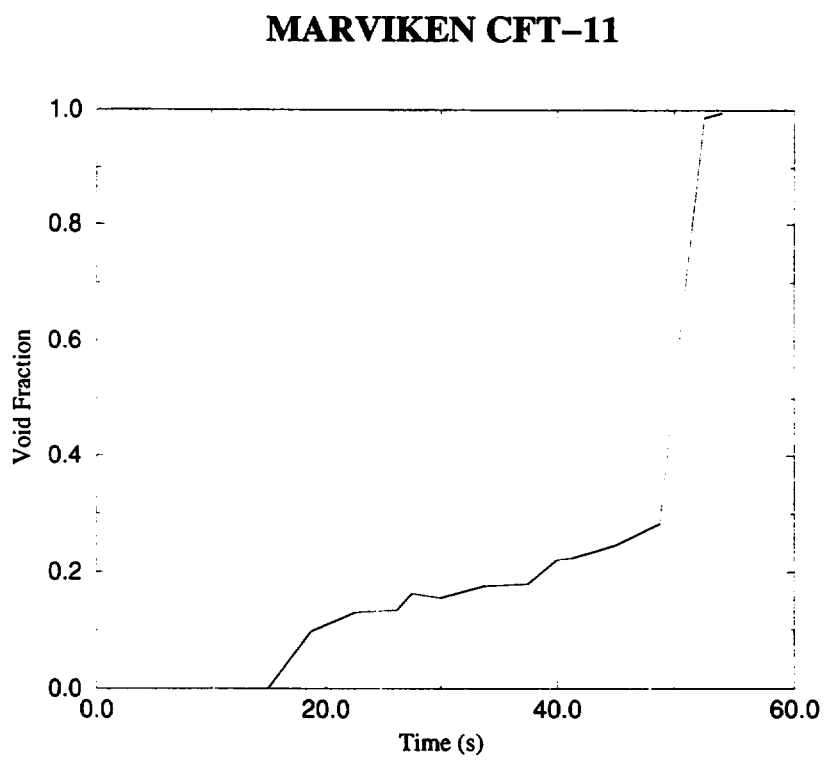

Figure 4.56: Void fraction at nozzle exit. Discharge coefficient adjustment, BCM-J. CFT-11.

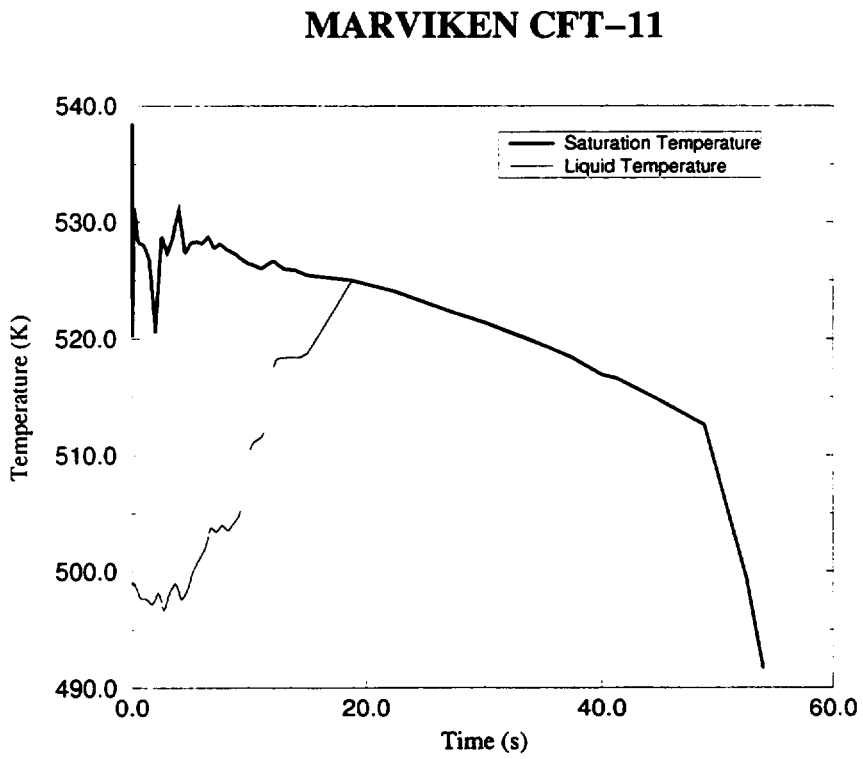

Figure 4.57: Liquid and saturation temperatures at nozzle exit. Discharge coefficient adjustment, BCM-J. CFT-11.

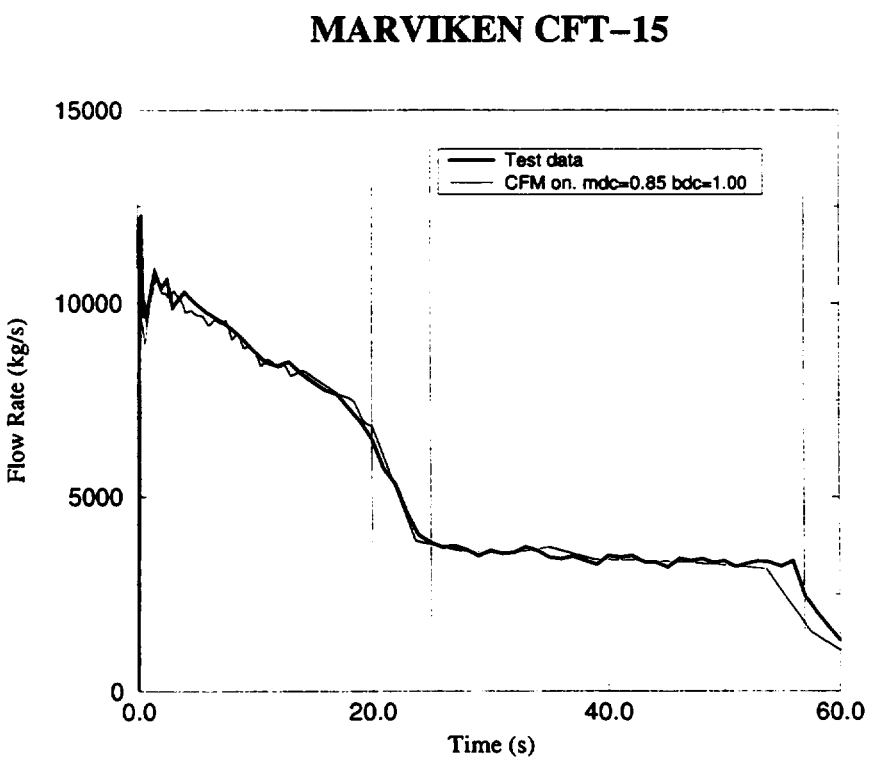

Figure 4.58: Mass flow at nozzle exit. Discharge coefficient adjustment, BCM-J. CFT-15.

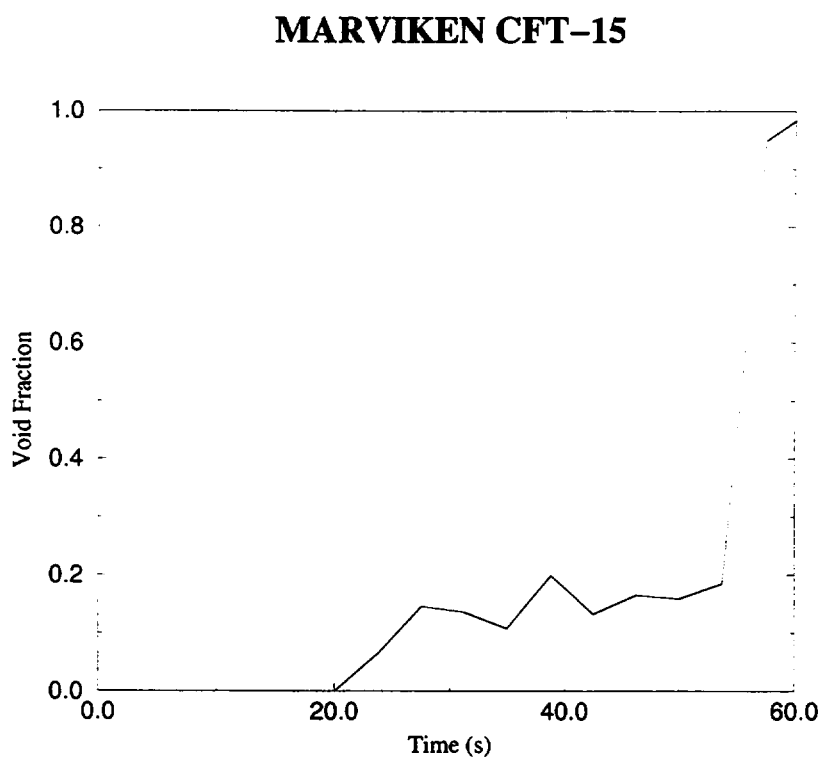

Figure 4.59: Void fraction at nozzle exit. Discharge coefficient adjustment, BCM-J. CFT-15.

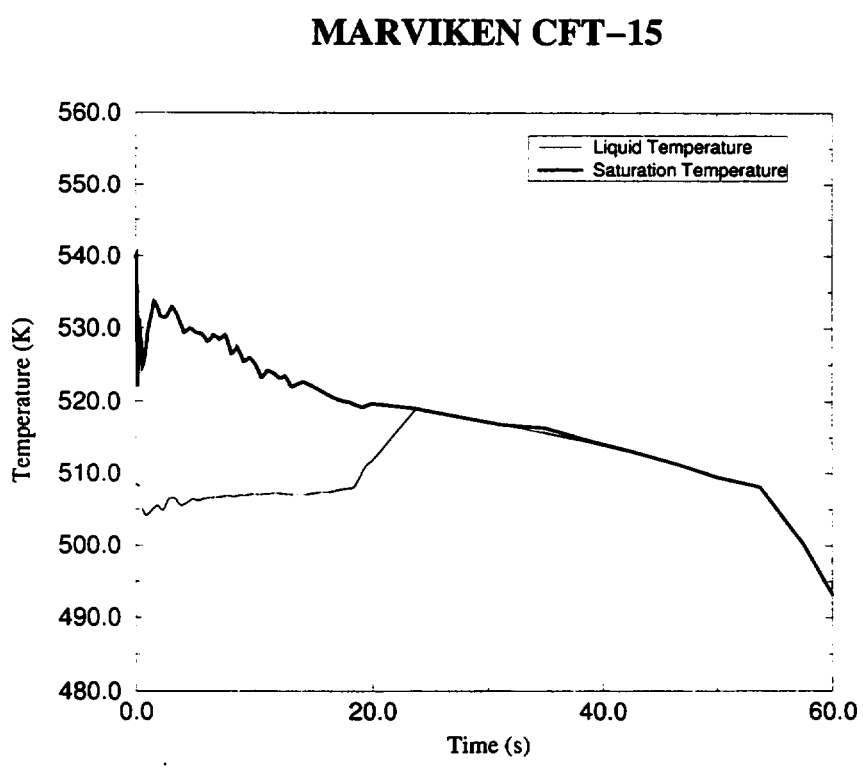

Figure 4.60: Liquid and saturation temperatures at nozzle exit. Discharge coefficient adjustment, BCM-J. CFT-15.

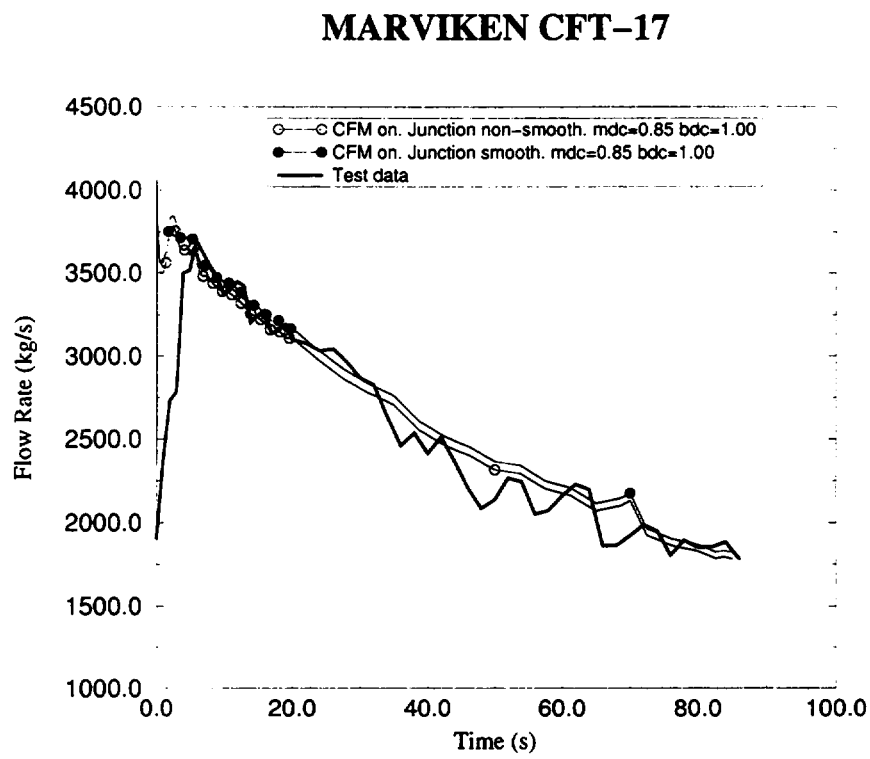

Figure 4.61: Mass flow at nozzle exit. Discharge coefficient adjustment, BCM-J. CFT-17.

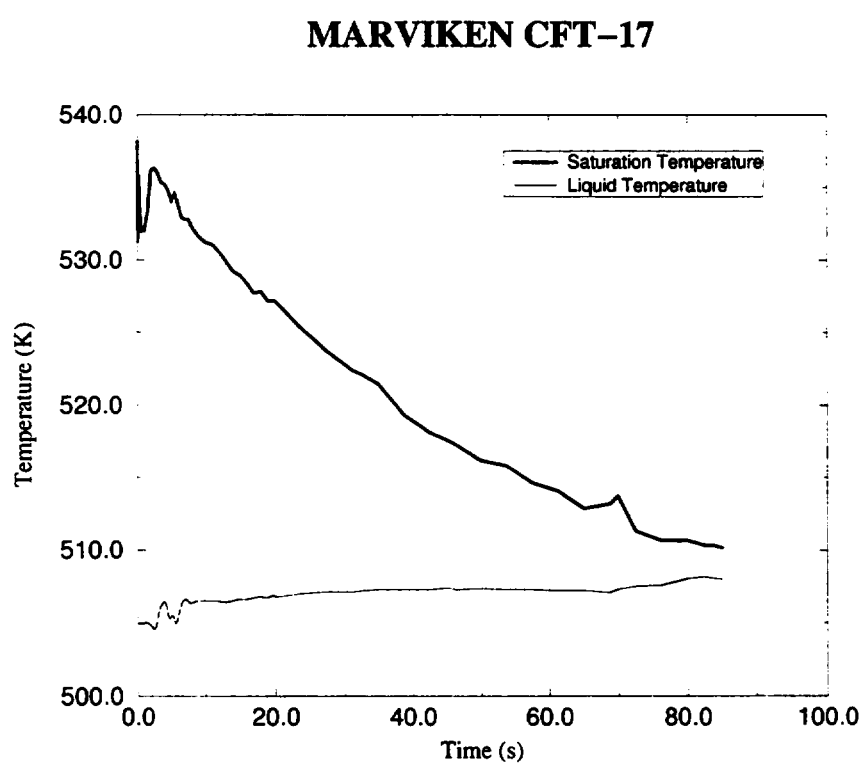

Figure 4.62: Liquid and saturation temperatures at nozzle exit. Discharge coefficient adjustment, BCM-J. CFT-17.

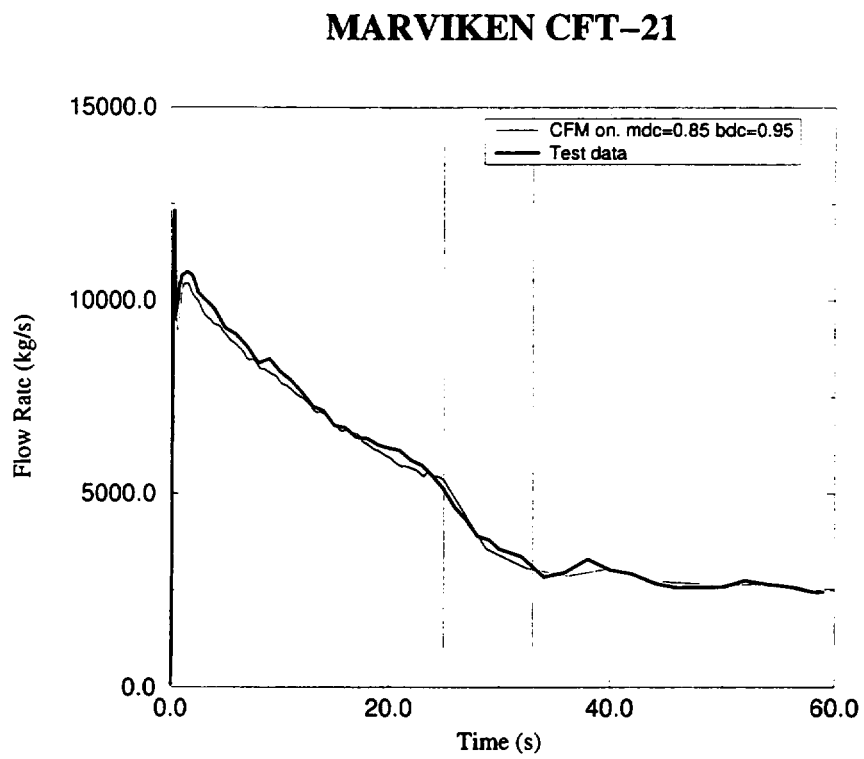

Figure 4.63: Mass flow at nozzle exit. Discharge coefficient adjustment, BCM-J. CFT-21.

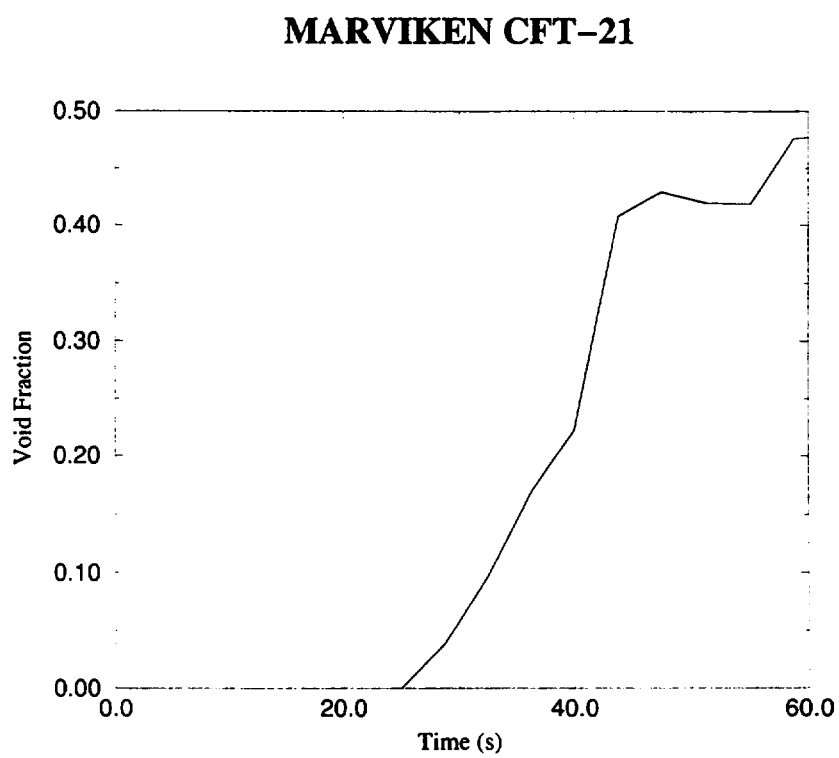

Figure 4.64: Void fraction at nozzle exit. Discharge coefficient adjustment, BCM-J. CFT-21.

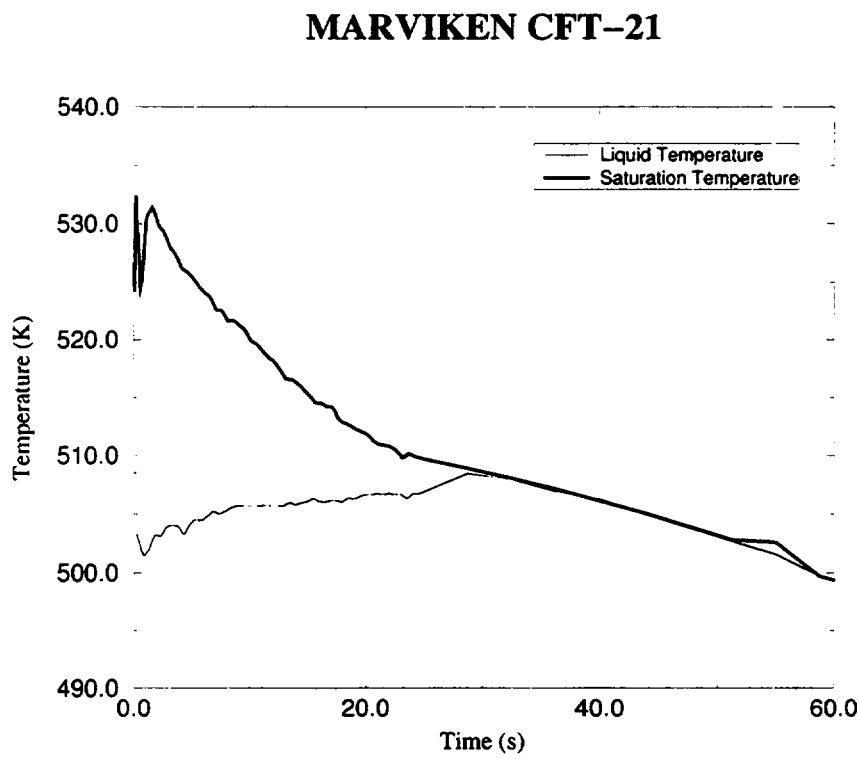

Figure 4.65: Liquid and saturation temperatures at nozzle exit. Discharge coefficient adjustment, BCM-J. CFT-21.

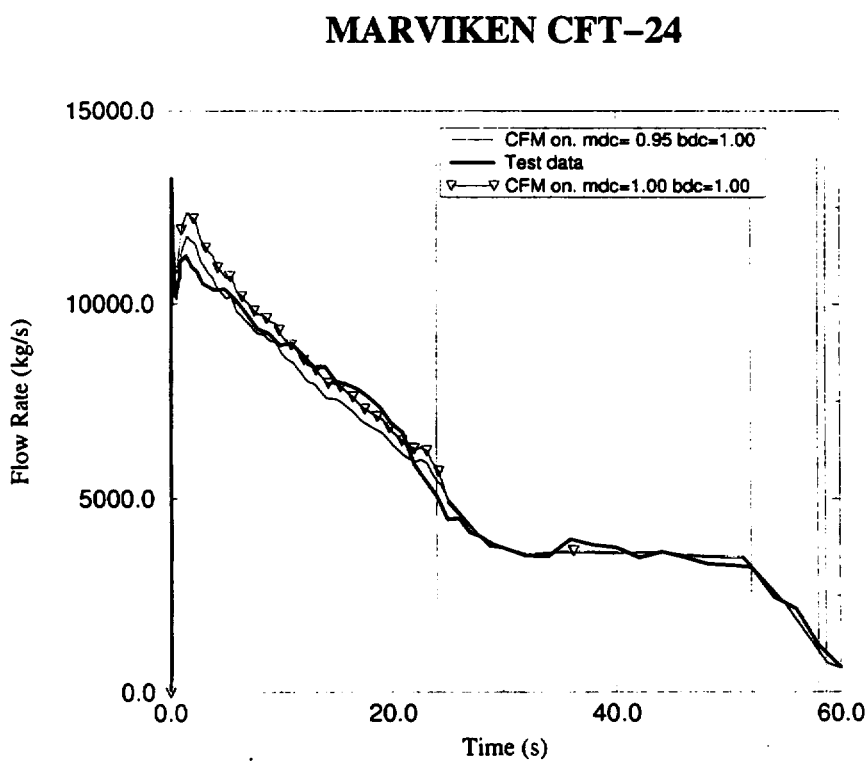

Figure 4.66: Mass flow at nozzle exit. Discharge coefficient adjustment, BCM-J. CFT-24.

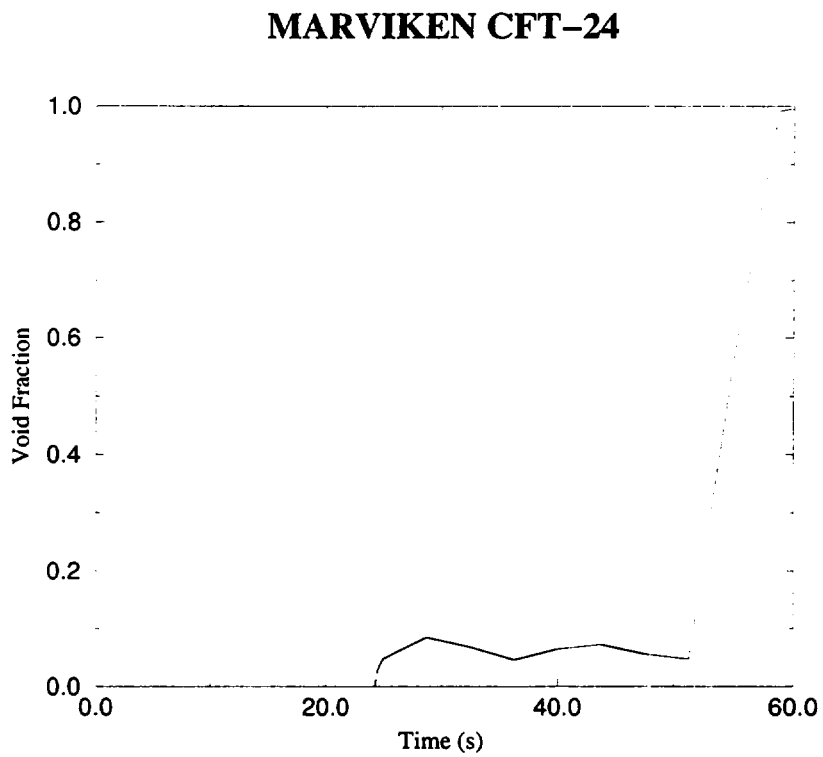

Figure 4.67: Void fraction at nozzle exit. Discharge coefficient adjustment, BCM-J. CFT-24.

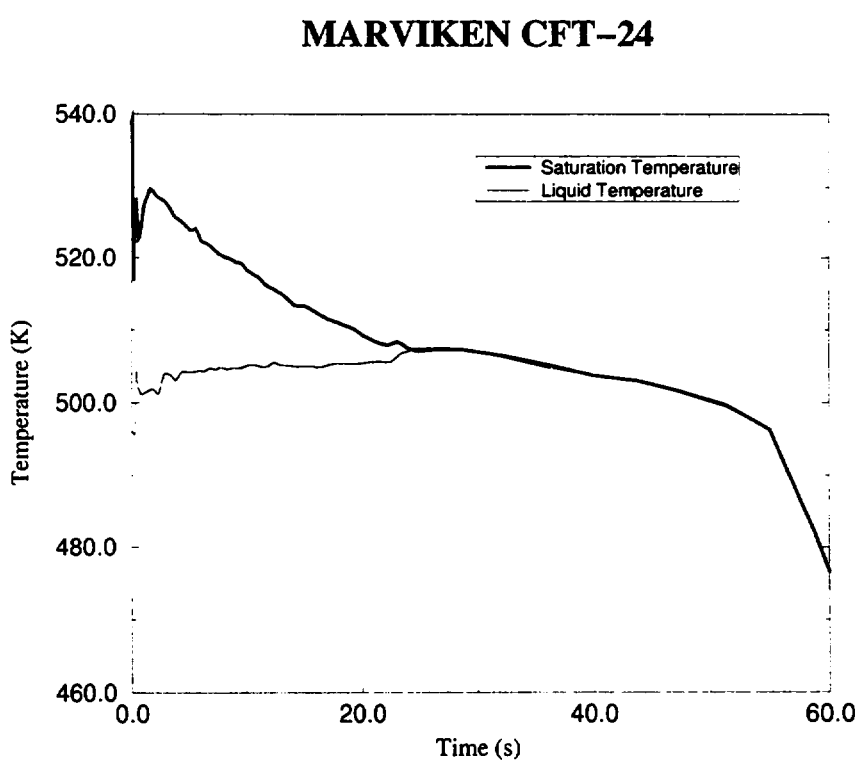

Figure 4.68: Liquid and saturation temperatures at nozzle exit. Discharge coefficient adjustment, BCM-J. CFT-24.

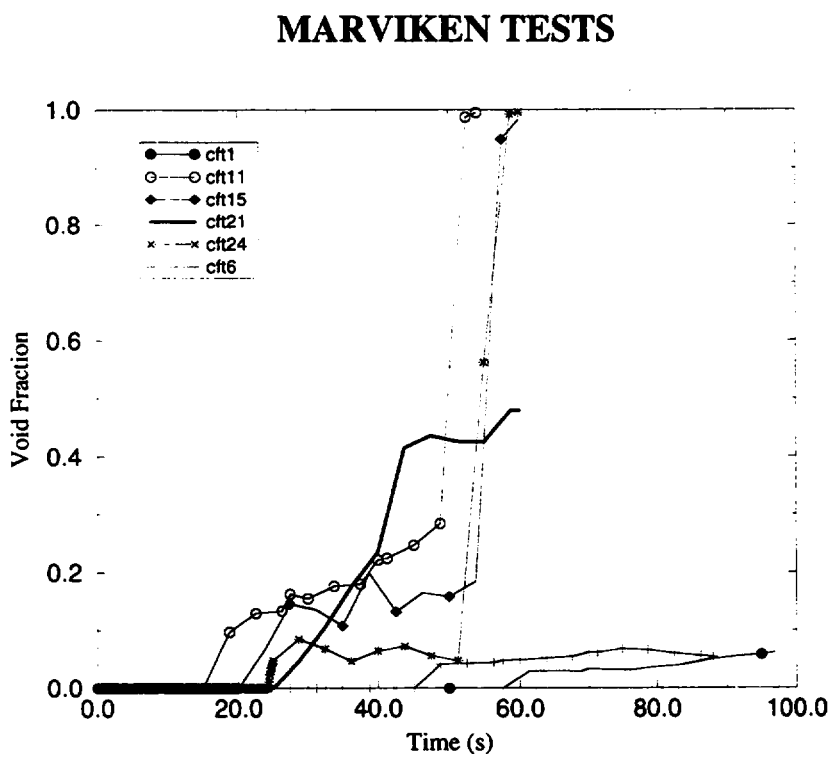

Figure 4.69: Void fraction at nozzle exit, BCM-J.

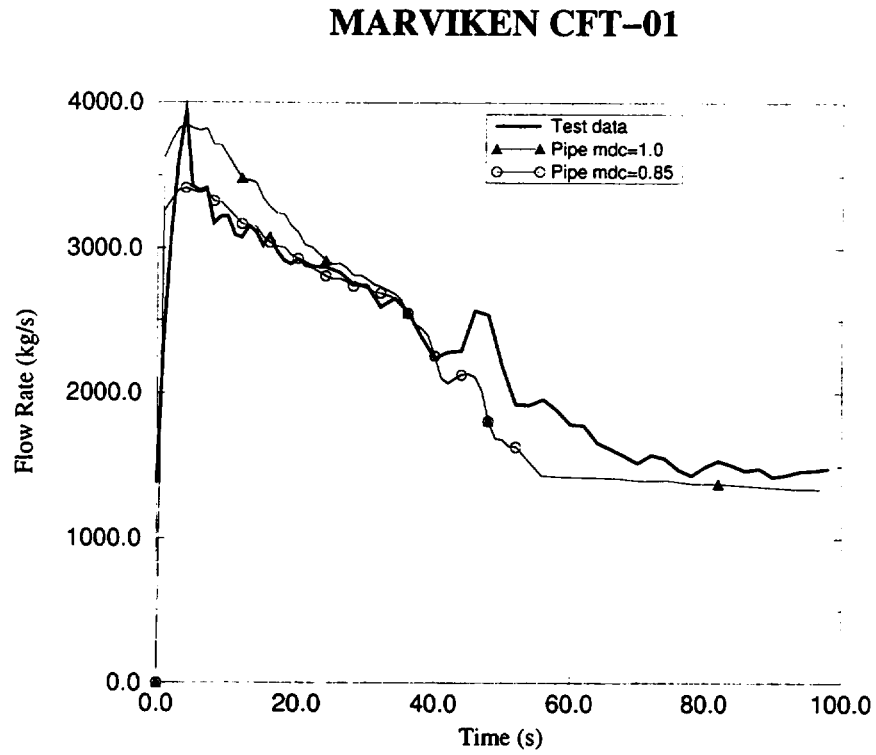

Figure 4.70: Mass flow at nozzle exit. Discharge coefficient adjustment, BCM-P. CFT-01.

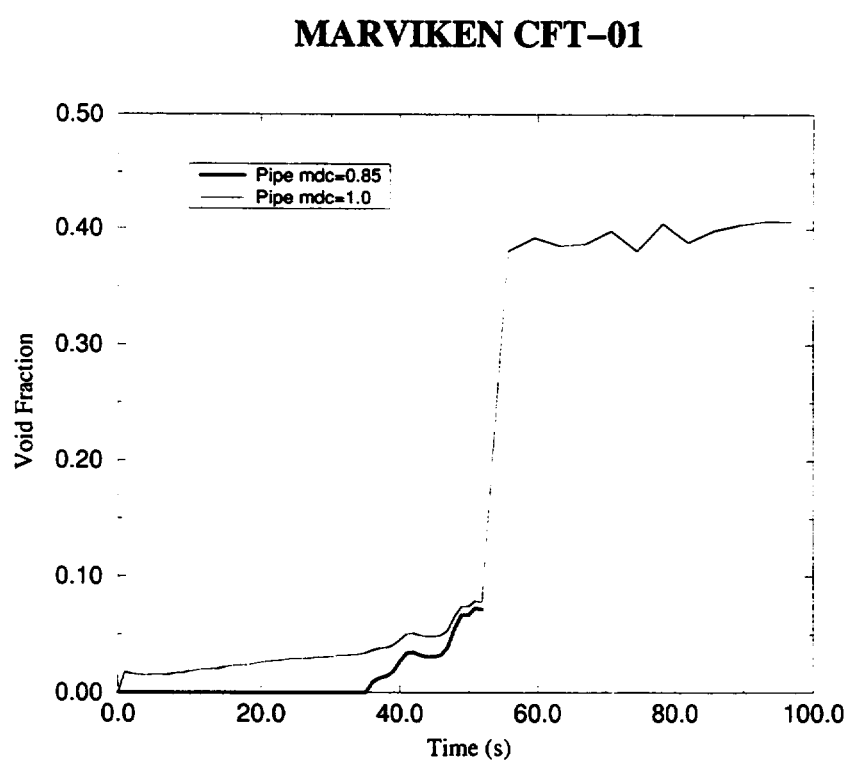

Figure 4.71: Void fraction at nozzle exit. Discharge coefficient adjustment, BCM-P. CFT-01.

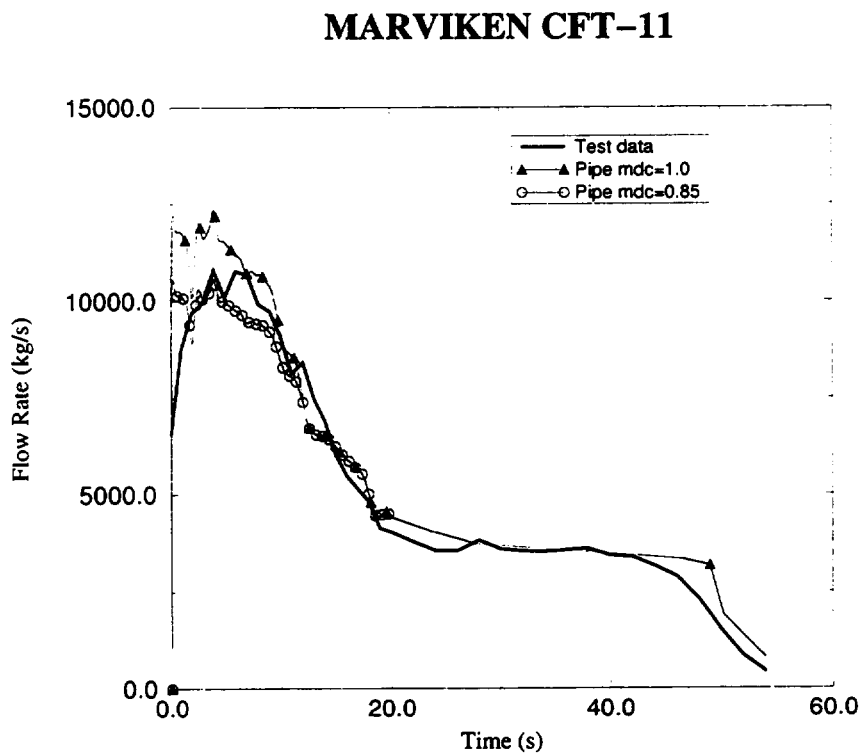

Figure 4.72: Mass flow at nozzle exit. Discharge coefficient adjustment, BCM-P. CFT-11.

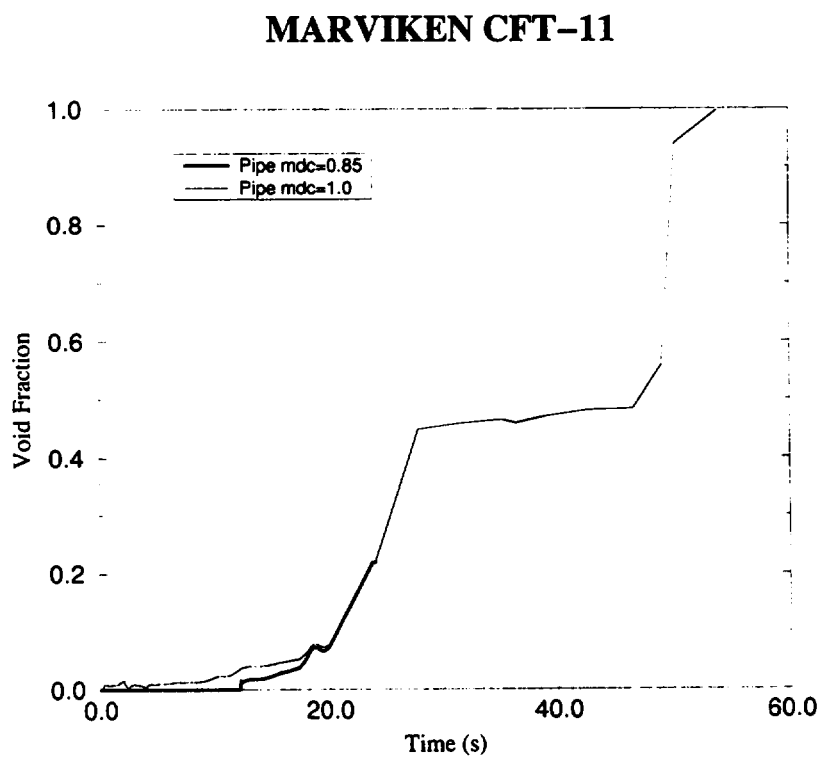

Figure 4.73: Void fraction at nozzle exit. Discharge coefficient adjustment, BCM-P. CFT-11.

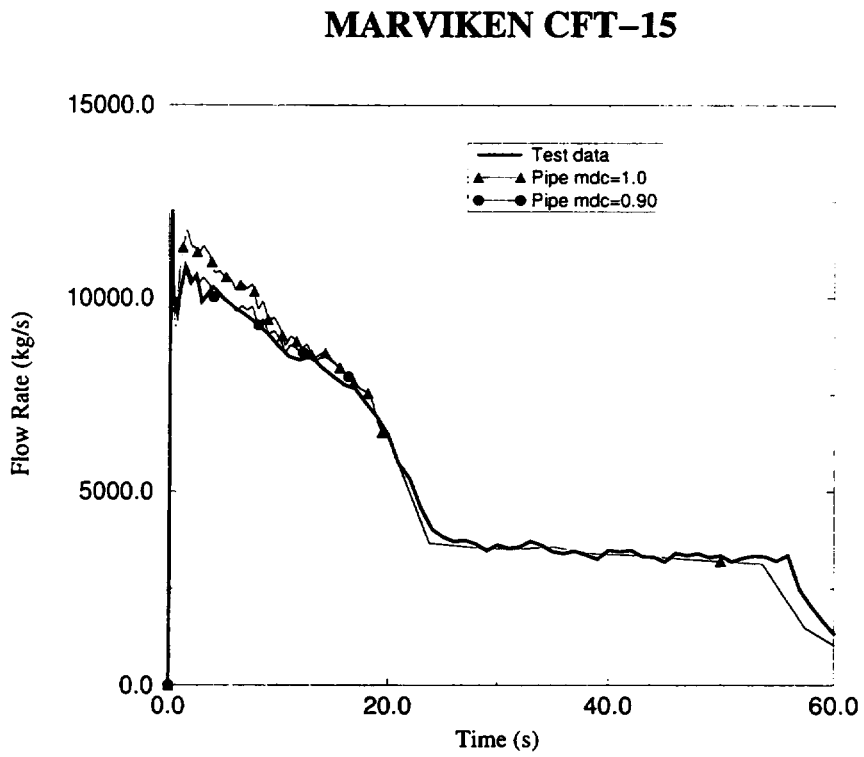

Figure 4.74: Mass flow at nozzle exit. Discharge coefficient adjustment, BCM-P. CFT-15.

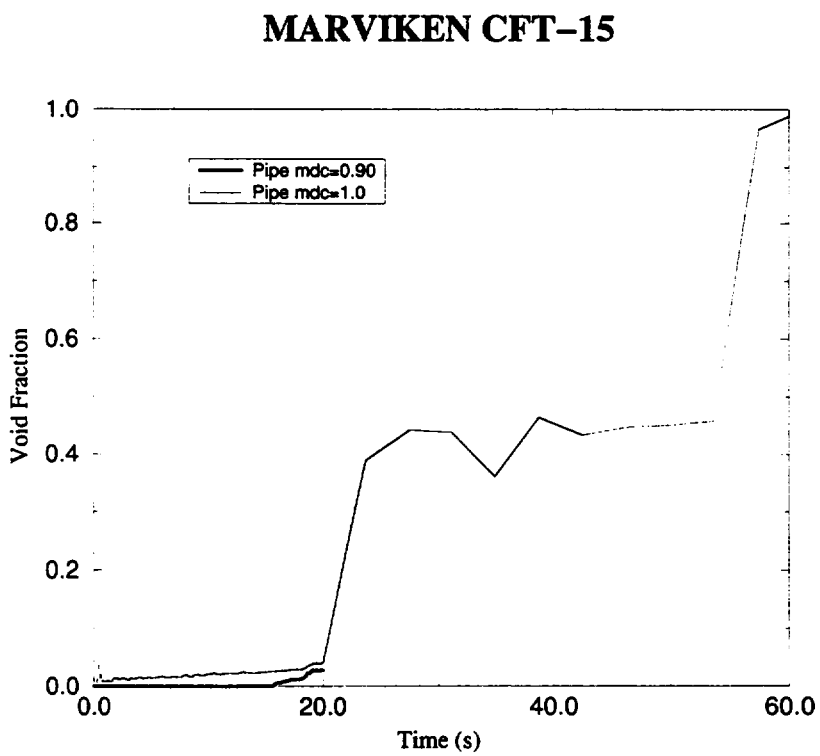

Figure 4.75: Void fraction at nozzle exit. Discharge coefficient adjustment, BCM-P. CFT-15.

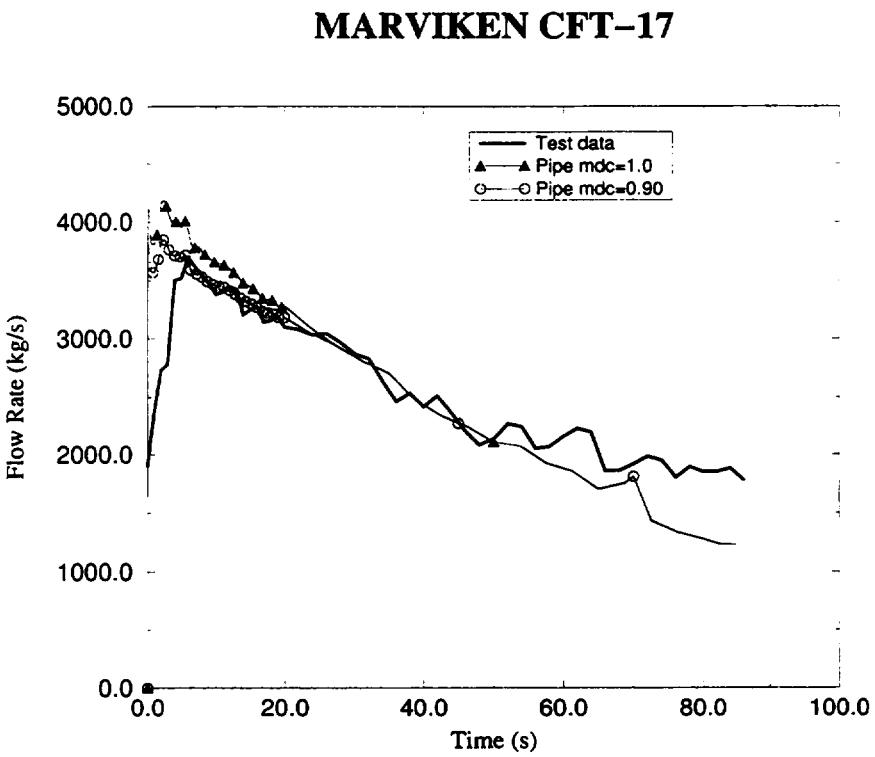

Figure 4.76: Mass flow at nozzle exit. Discharge coefficient adjustment, BCM-P. CFT-17.

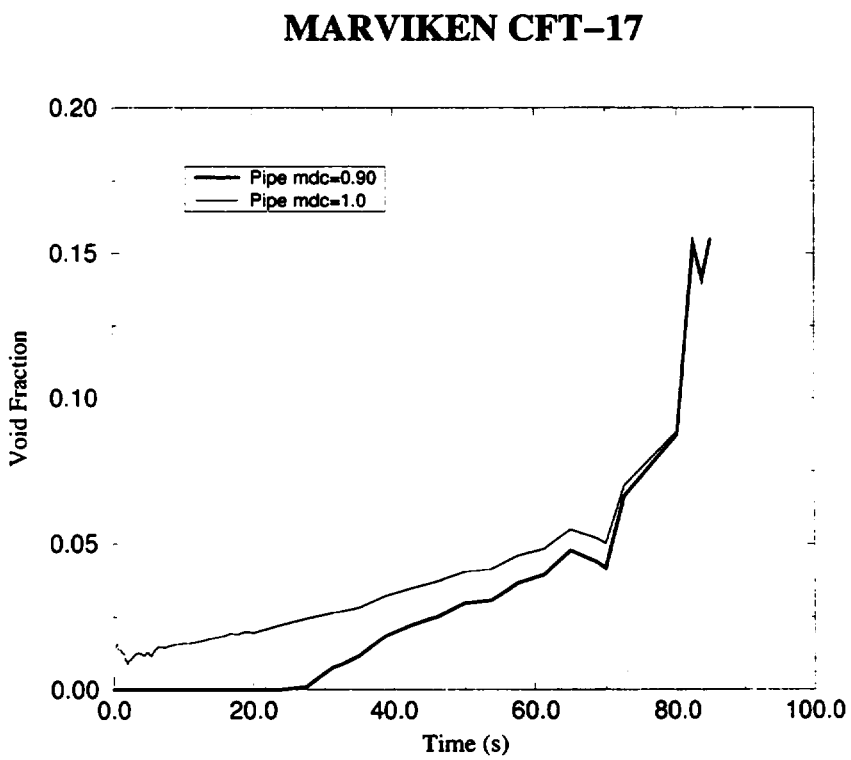

Figure 4.77: Void fraction at nozzle exit. Discharge coefficient adjustment, BCM-P. CFT-17.

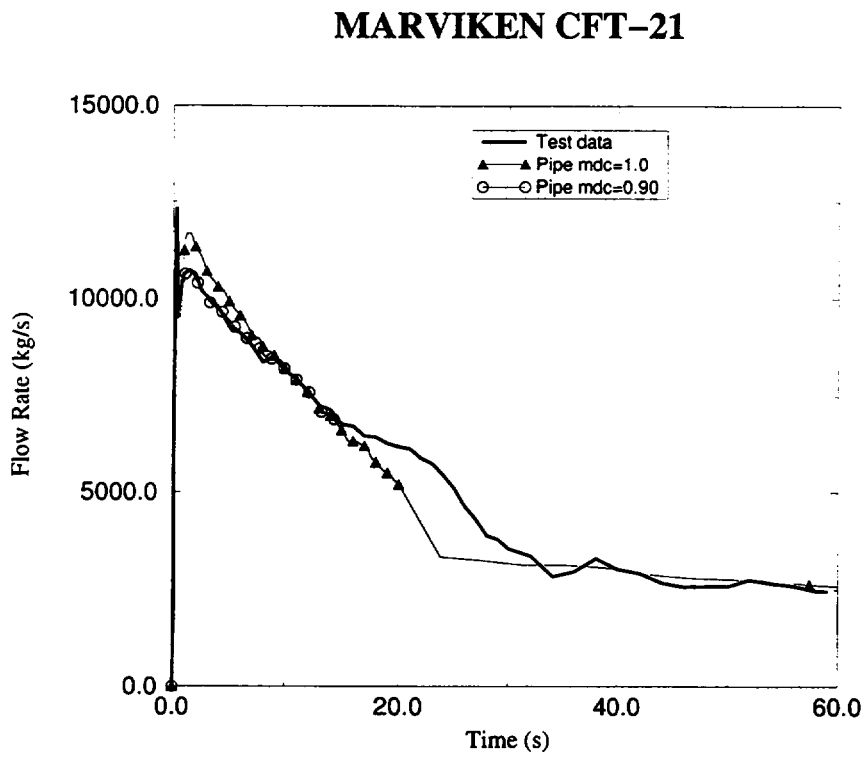

Figure 4.78: Mass flow at nozzle exit. Discharge coefficient adjustment, BCM-P. CFT-21.

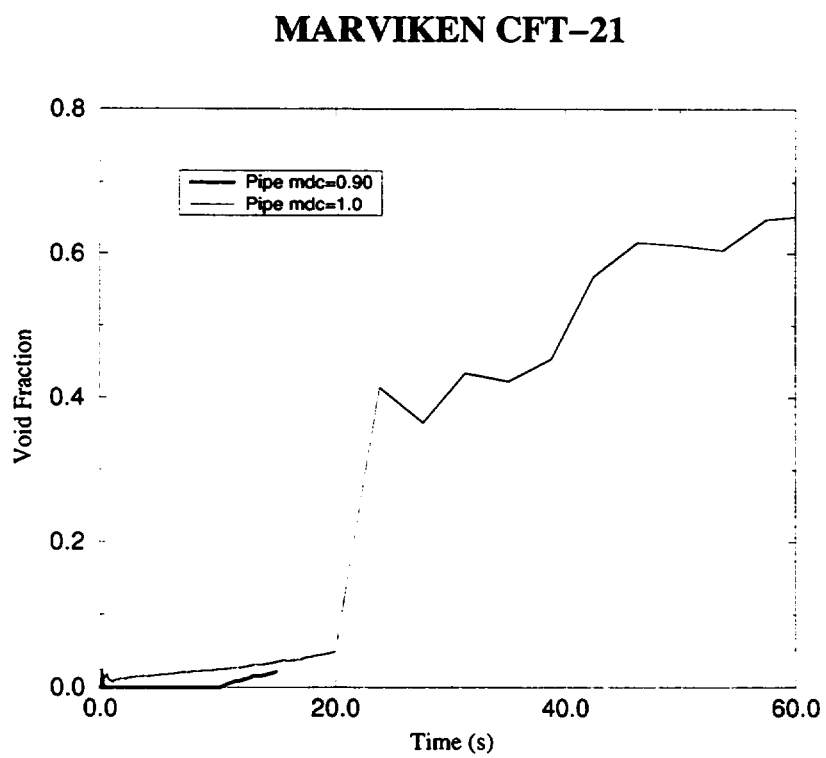

Figure 4.79: Void fraction at nozzle exit. Discharge coefficient adjustment, BCM-P. CFT-21.

		SINGLE JUNCTION		PIPE	
Test	L/D	MDC	TDC	MDC	TDC
24	0.3	0.95	1.00	-	$\leq$ 1.05
06	1.0	0.95	1.05	-	$\leq$ 1.05
21	1.5	0.85	0.95	0.90	1.00
01	3.0	0.82	0.95	0.85	$\leq$ 1.05
11	3.1	0.85	0.95	0.85	1.00
15	3.6	0.85	1.00	0.90	1.00
17	3.7	0.85	-	0.90	-
KAERI	>1.5	0.82	1.14	0.89	1.07

Table 4.2: Discharge coefficient adjustment. Comparison between BCM-J and BCM-P

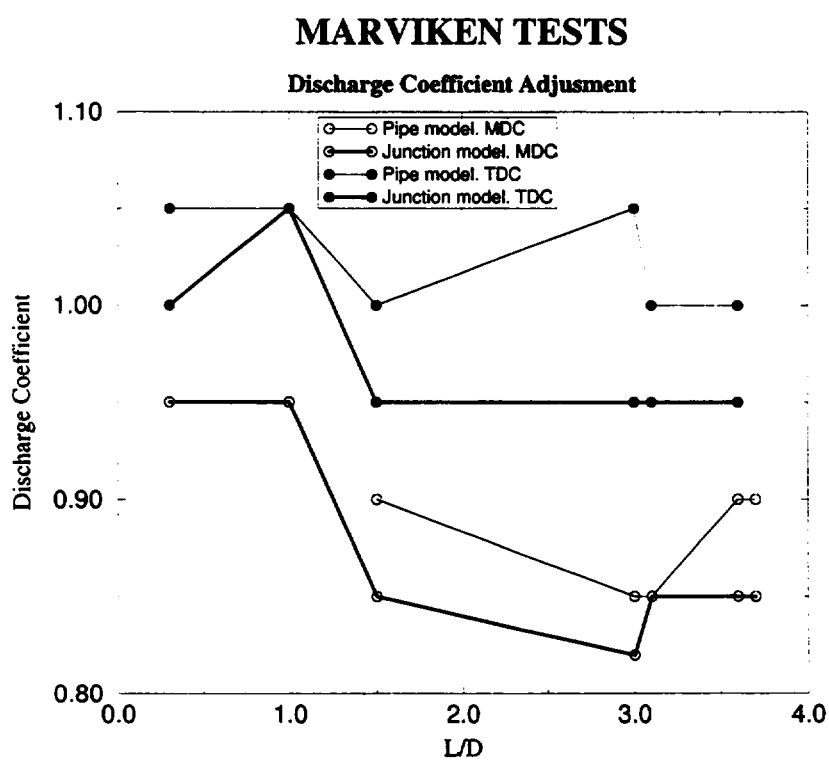

Figure 4.80: Comparison of MDC and TDC adjustment for BCM-J and BCM-P.

4.5 Results and Discussion of the Initial Condition Model (ICM). Ransom-Trapp Model

As it was pointed out in Section 4.2, ICM mixes different physical phenomena while BCM allows the analysis of critical mass flow in an independent way from other physical phenomena. In ICM the error related to steam generation rate has an effect on the depressurization rate (system pressure), avoiding critical mass flow phenomena to be isolated.

With this in mind, four cases have been simulated with the ICM, CFT-06, 15, 21 and 24, and the discharge coefficients have been adjusted for them. Then, comparing the results and the adjusted discharge coefficients of ICM and BCM, it is possible to analyze if the model of the steam generation rate due to flashing is the appropriate.

At the end of this section a comparison between the simulations of CFT-24 with TRAC-BF1, RELAP5/MOD3.2 and the experimental data is presented.

4.5.1 Discharge Coefficient Adjustment

For the adjustment of the discharge coefficients (subcooled and two-phase), modelling the nozzle as a PIPE and a SINGLE JUNCTION, data from CFT-06, 15, 21 and 24 have been used.

- Nozzle modeled as SINGLE JUNCTION. The comparison between the test data and the results for the mass flow with the adjustment of the discharge coefficients are shown in Figures 4.81, 4.82, 4.83 and 4.84, In general, a good adjustment is achieved with the coefficients shown in table 4.3, except in the subcooled period of CFT-21.

- Nozzle modeled as PIPE. The comparison between test data and the results for the mass flow with the adjustment of the discharge coefficients are shown in Figures 4.85, 4.86, 4.87, 4.88 and 4.89. The adjustment of the coefficients is shown in table 4.3. The fitting for the subcooled period for all cases is very poor, but on the other hand for the two-phase period the adjustment is good.

- The comparison of the adjusted discharge coefficients for both models is shown in table 4.3. The values are similar but taking in account that with the nozzle modeled as a PIPE the adjustment in the subcooled period is very poor, it seems to be better to model the nozzle as a SINGLE JUNCTION.

		SINGLE JUNCTION		PIPE	
Test	L/D	MDC	TDC	MDC	TDC
24	0.3	1.00	1.30	1.00*	1.15
06	1.0	1.00	1.15	1.00*	1.15
21	1.5	1.00*	1.00	1.00*	0.90
15	3.6	0.90	1.10	0.92	1.10

Table 4.3: Discharge coefficient adjustment. Comparison between ICM-J and ICM-P

- The comparison between the ICM and BCM results and their discharge coefficients, table 4.4, show that the values used to adjust the mass flow for ICM are always greater than for BCM. This problem may be caused by experimental errors or some constitutive relations or correlations not compatibles with the critical flow model, [ELI-94]. For example, one of the critical flow models and the $\Gamma_{flashing}$ model of CATHARE code, were simultaneously obtained from Moby Dyck experiments, [FOR-88].

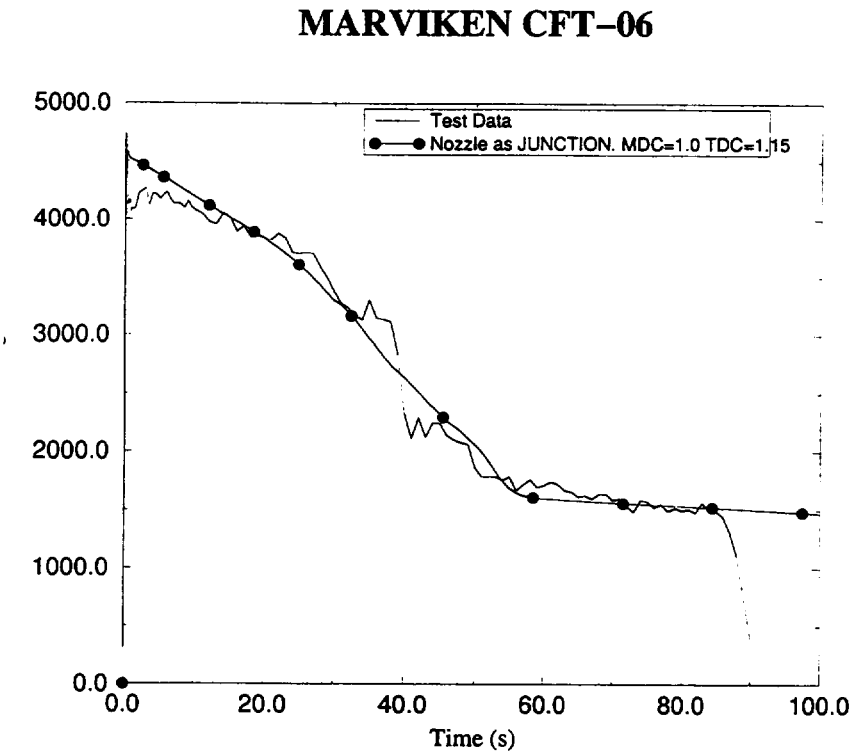

Figure 4.81: MDC and TDC adjustment. Nozzle modeled as SINGLE JUNCTION (ICM). CFT-06.

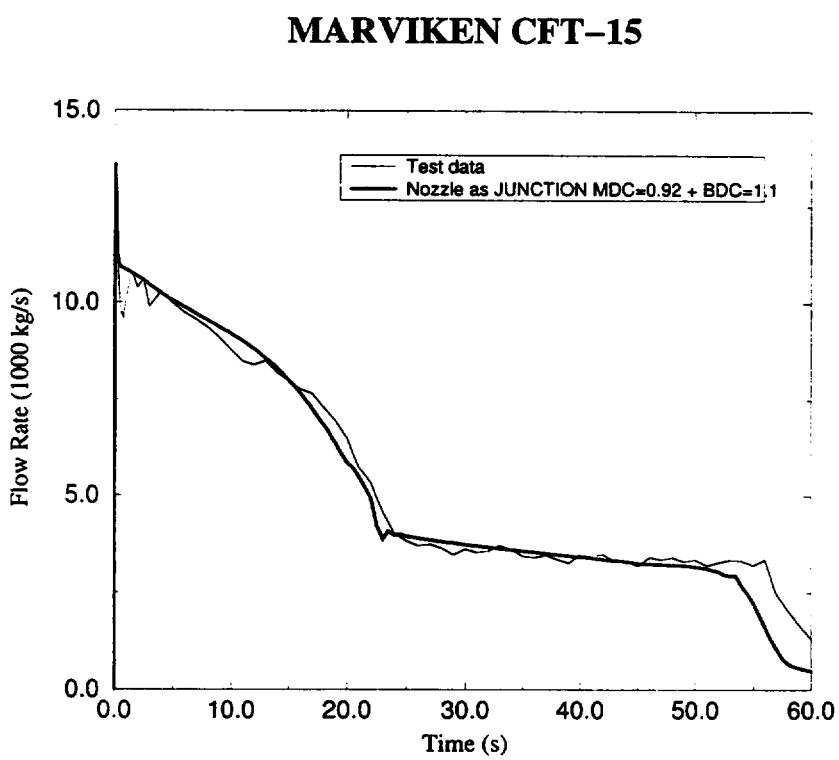

Figure 4.82: MDC and TDC adjustment. Nozzle modeled as SINGLE JUNCTION (ICM). CFT-15.

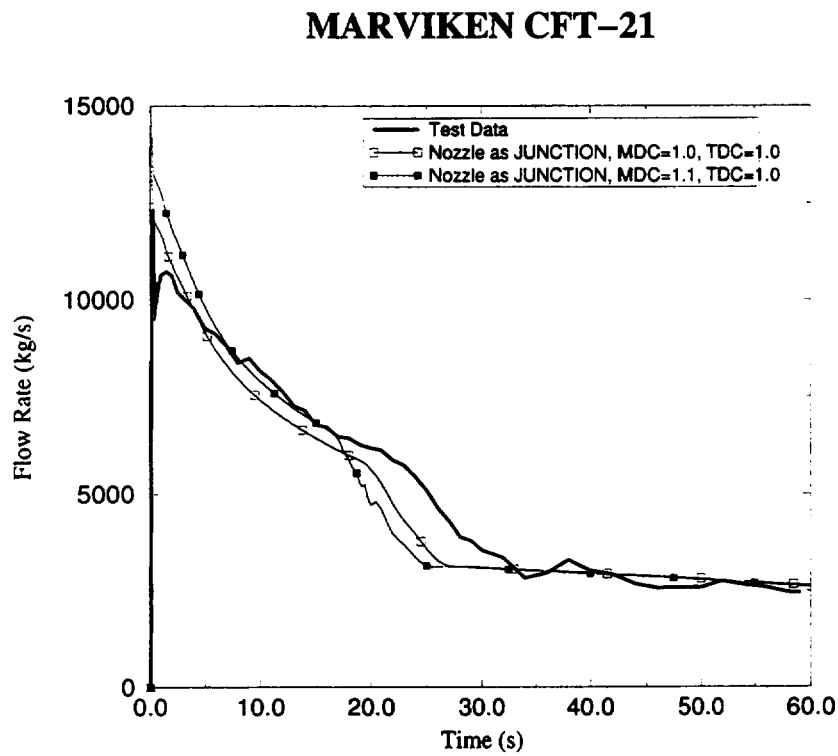

Figure 4.83: MDC and TDC adjustment. Nozzle modeled as SINGLE JUNCTION (ICM). CFT-21.

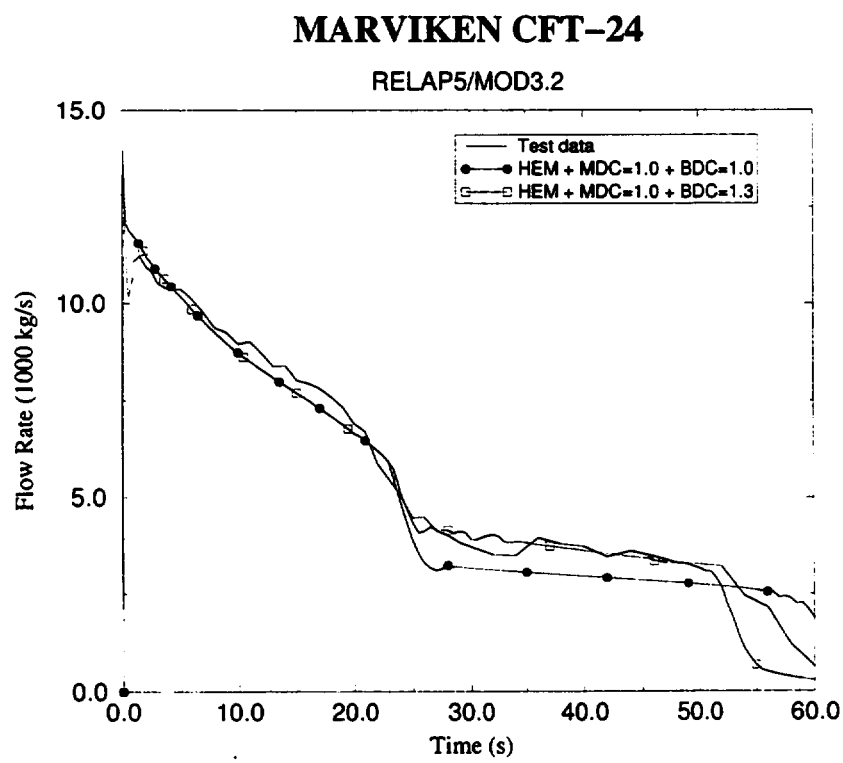

Figure 4.84: TDC adjustment. Nozzle modeled as SINGLE JUNCTION (ICM CFT-24.

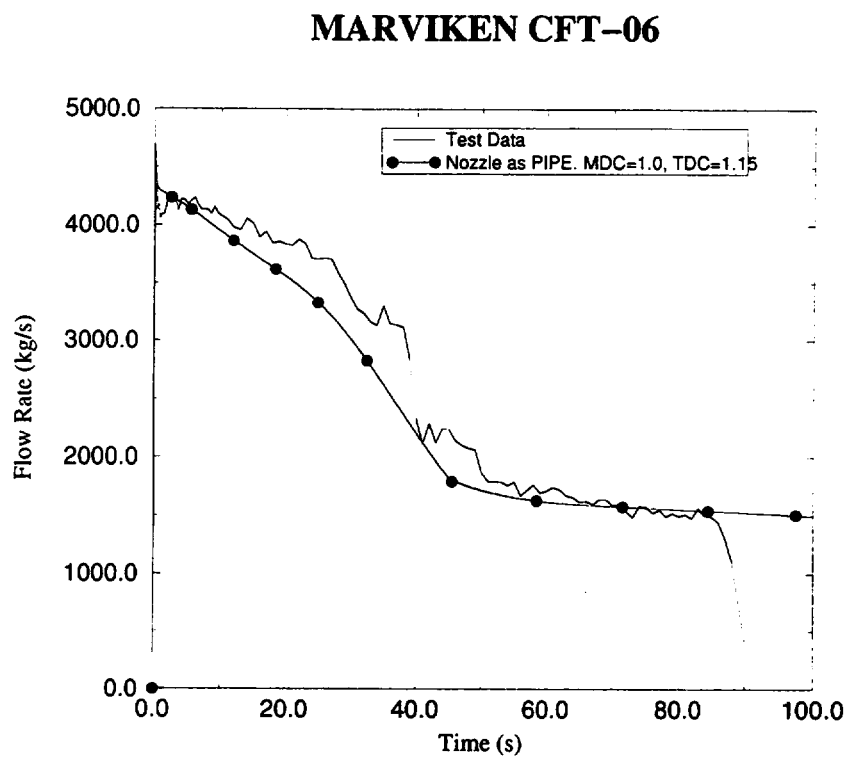

Figure 4.85: MDC and TDC adjustment. Mass flow at nozzle exit. Nozzle modeled as PIPE (ICM). CFT-06.

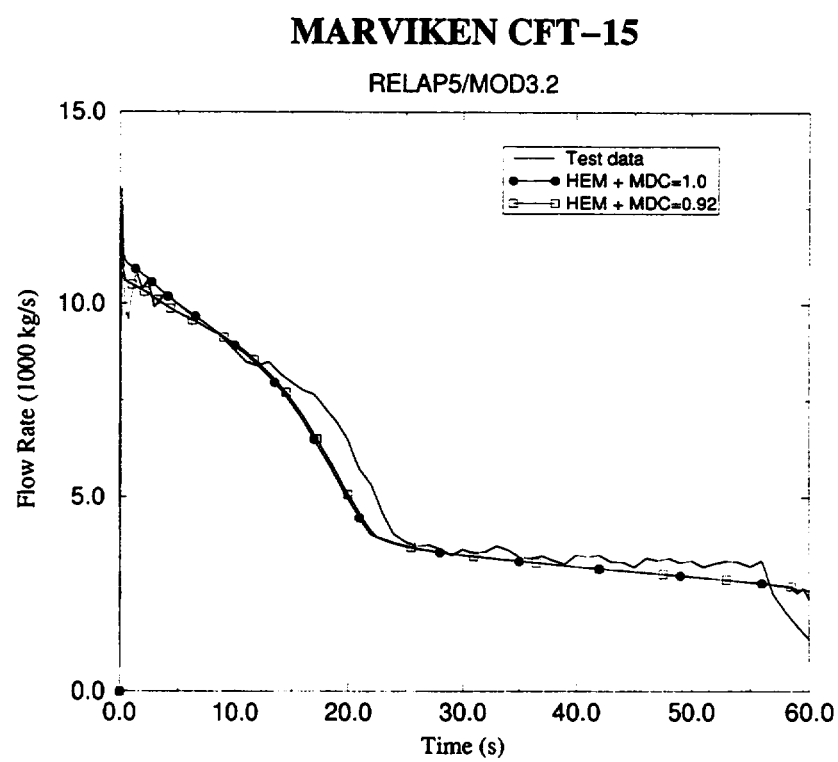

Figure 4.86: MDC adjustment. Mass flow at nozzle exit. Nozzle modeled as PIPE (ICM). CFT-15.

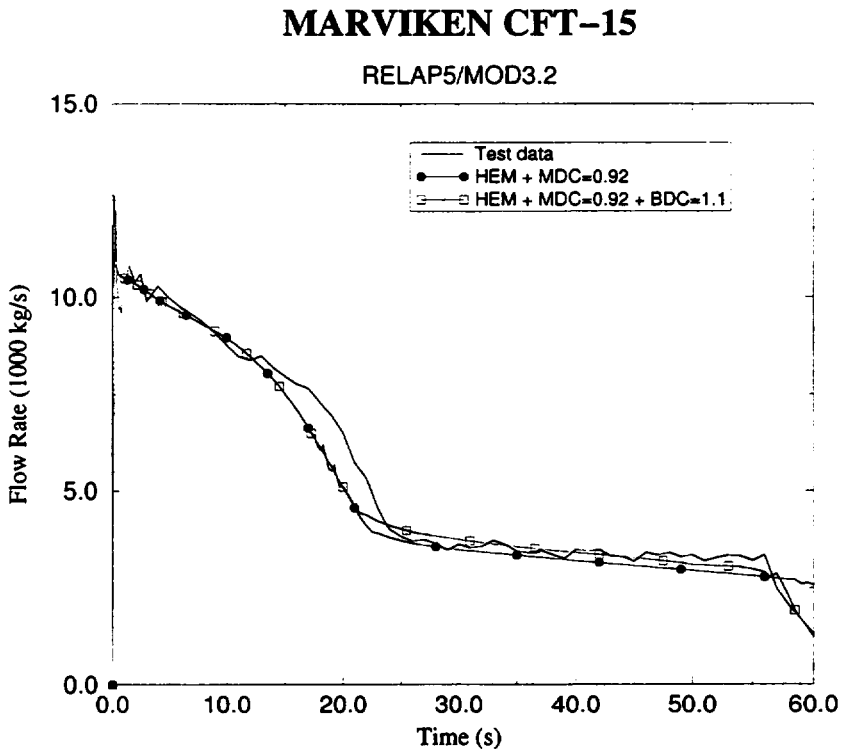

Figure 4.87: TDC adjustment. Mass flow at nozzle exit. Nozzle modeled as PIPE (ICM). CFT-15.

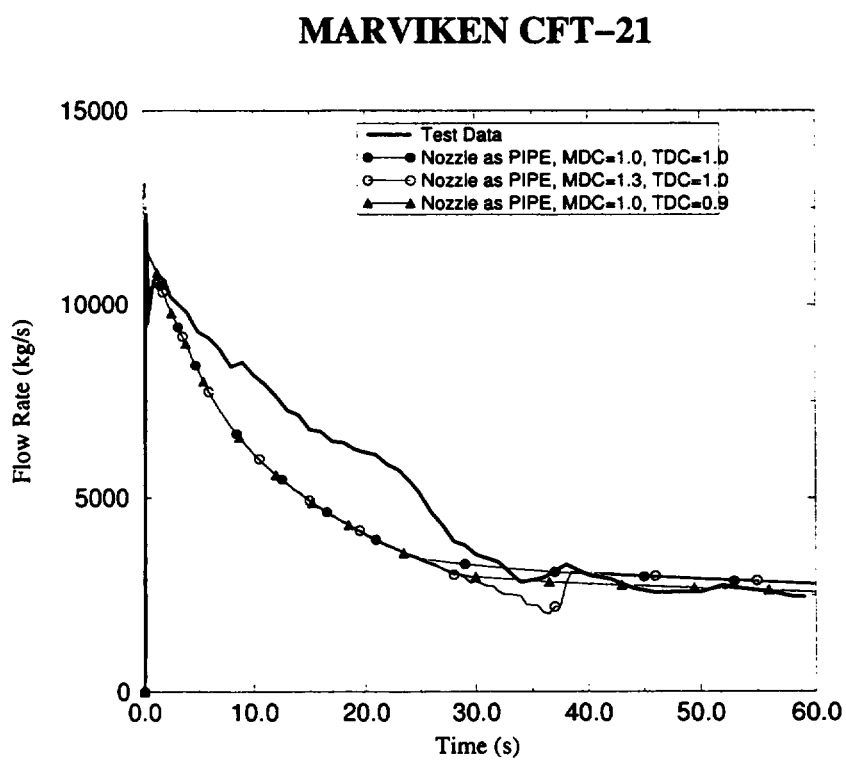

Figure 4.88: MDC and TDC adjustment. Mass flow at nozzle exit. Nozzle modeled as PIPE (ICM). CFT-21.

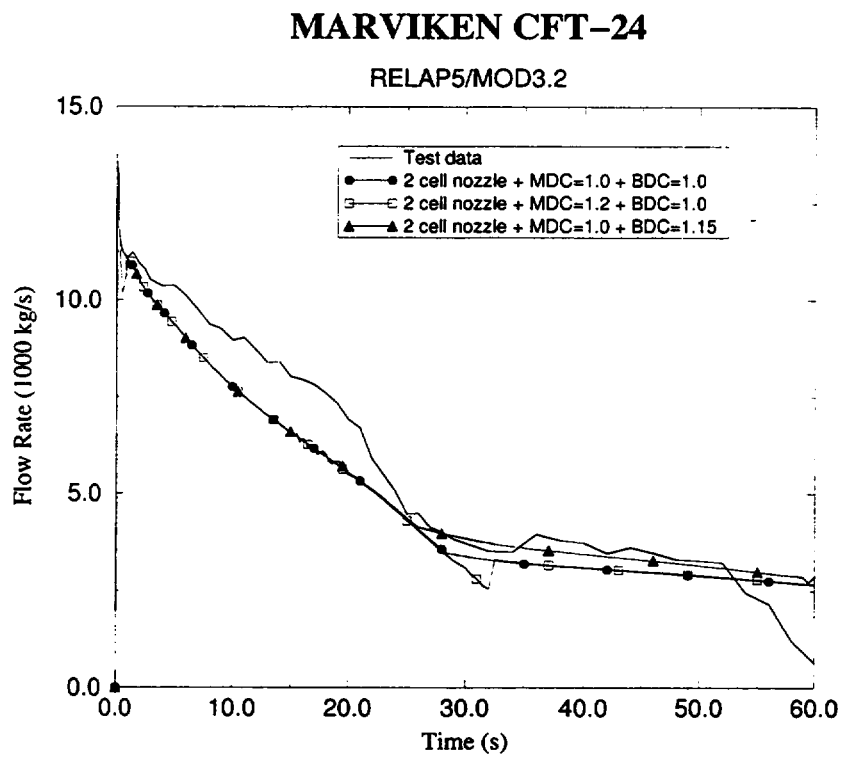

Figure 4.89: MDC and TDC adjustment. Mass flow at nozzle exit. Nozzle modeled as PIPE (ICM). CFT-24.

		ICM				BCM			
		JUNCTION		PIPE		JUNCTION		PIPE	
Test	L/D	MDC	TDC	MDC	TDC	MDC	TDC	MDC	TDC
24	0.3	1.00	1.30	1.00*	1.15	0.95	1.00	1.3*	$\simeq$ 1.05
06	1.0	1.00	1.15	1.00*	1.15	0.95	1.05	1.0*	$\simeq$ 1.05
21	1.5	1.00*	1.00	1.00*	0.90	0.85	0.95	0.90	1.00
01	3.0	-	-	-	-	0.82	0.95	0.85	$\simeq$ 1.05
11	3.1	-	-	-	-	0.85	0.95	0.85	1.00
15	3.6	0.90	1.10	0.92	1.10	0.85	1.00	0.90	1.00
17	3.7	-	-	-	-	0.85	-	0.90	-
KAERI	>1.5	-	-	-	-	0.82	1.14	0.89	1.07

Table 4.4: Discharge coefficient adjustment. Comparison between ICM and BCM results (The values marked with * do not adjust with test data)

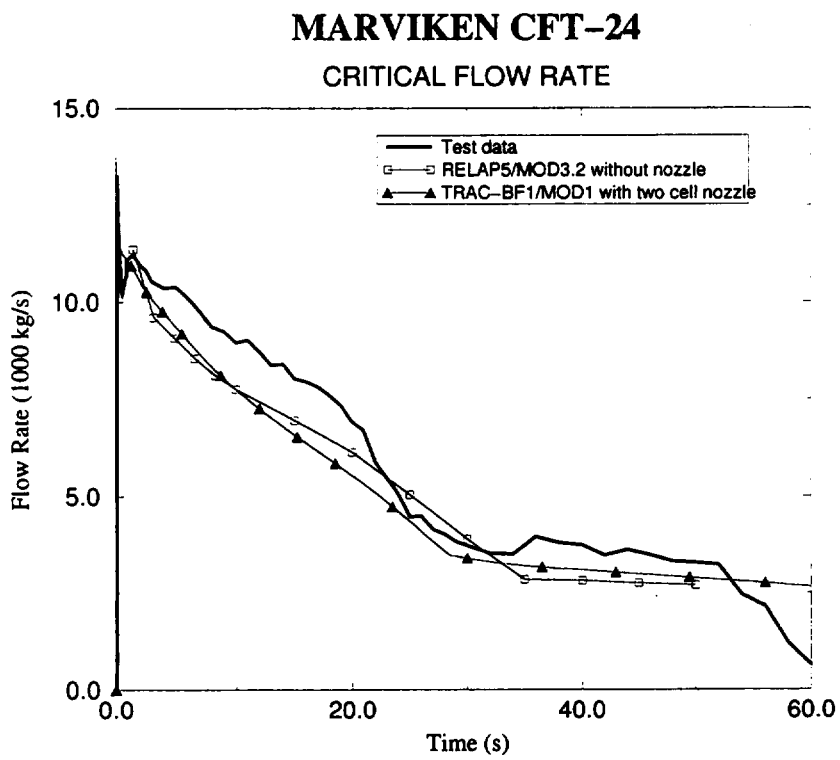

Figure 4.90: Mass flow at nozzle exit. Comparison between TRAC-BF1 and RELAP5/MOD3.2 results. Nozzle modeled as PIPE. CFT-24.

4.5.2 Comparison between TRAC-BF1 and RELAP5/MOD3.2 Results

The comparison between the simulations of CFT-24 with TRAC-BF1, RELAP5/MOD3.2 and the experimental data, Figure 4.90, shows that both codes give similar results as it was expected, because both have quite similar critical flow models implemented, with just small differences.

4.6 Results and Discussion of Boundary Condition Model (BCM). Henry-Fauske Model

The Henry-Fauske CFM has different model options than the Ransom-Trapp model:

- Henry-Fauske CFM does not depend on smooth/abrupt area change option,
- the homogeneous condition, $v_g = v_l$, is imposed in the model,
- there is only one discharge coefficient for all conditions (subcooled, two-phase and steam), and

- there is a new parameter in Henry-Fauske model, the disequilibrium parameter dp.

Apart from this, the assessment of RELAP5/MOD3.2.2beta with the Henry-Fauske model has been performed with several experiments, but only one Marviken CFT has been included (CFT-22, $L/D = 1.5$) among the selected experiments. Marviken CFT-22 does not cover all the different L/D relations for the nozzles. With this mind, three experiments (CFT-15, CFT-21 and CFT-24) have beeen selected for this assessment, which cover different thermo-hydraulic conditions at nozzle, subcooled and two-phase, and also different L/D relations for the nozzles (0.3, 1.5 and 3.3). The boundary conditions used in this analysis are shown in Figures 4.9 to 4.28.

The simulations have been performed with the nozzle modeled as a pipe and as junction (BCM-J, BCM-P), because as we have shown in the assessment of Ransom-Trapp model, sometimes modelling the nozzle as a junction is better than as a pipe.

The results show that the discharge flow rate, Figures 4.91 to 4.93, is better adjusted with:

- Subcooled conditions:
  - $L/D = 0.3$. Nozzle as a junction and $dp = 0.14$
  - $L/D = 1.5$. Nozzle as a pipe and $dp = 0.14$. The results with $dp = 0.01$ are not so good than $dp = 0.14$ but they are acceptable.
  - $L/D = 3.6$. Nozzle as a pipe and $dp = 0.01$
- Two-phase conditions:
  - $L/D = 0.3$. Nozzle as a junction and $dp = 0.01$
  - $L/D = 1.5$. Nozzle as a pipe and $dp = 0.01$. Similar results are obtained with $dp = 0.14$.
  - $L/D = 3.6$. Nozzle as a pipe and $dp = 0.01$

These results show that the advised dp value, $dp = 0.14$, in [MOR-98] is not adecuate for adjusting the simulated values to test data.

The inception of boiling is in accordance with the experimental data when the above dp values are used, see Figures 4.94 to 4.96. It must be remembered that when the simulation is performed with the Ransom-Trapp model and the nozzle is modeled as a pipe, the inception of boiling appears too early. So, the Henry-Fauske model gives better results, with respect to the inception of boiling, than the Ransom-Trapp model.

Several conclusions can be obtained from the above results:

- The best values of dp for adjusting the model are (in accordance with the results obtained in [LEV-82]),
  - $dp = 0.14$ for subcooled blowdown and $L/D < 1.5$
  - $dp = 0.01$ for $L/D > 1.5$
  - $dp = 0.01$ for saturated blowdown
- The best models for the different nozzles are:
  - Short nozzles $L/D \leq 0.3$ should be modeled as a junction.
  - Long nozzles $L/D \geq 1.5$ should be modeled as a pipe.
  - This assessment does not give enough information about the which is the best model for intermediate nozzles $1.5 > L/D > 0.3$.
- The inception of boiling is in accordance with the experimental data when Henry-Fauske model is used.

At present, only one dp value can be used for subcooled and two-phase periods. So, two disequilibrium parameters should be implemented in order to include the values mentioned above (one of them for the subcooled period and another for the two-phase one), and also the transition between them. This solution generates a problem because it implies a new degree of freedom, and therefore a negative consequence for the user effect.

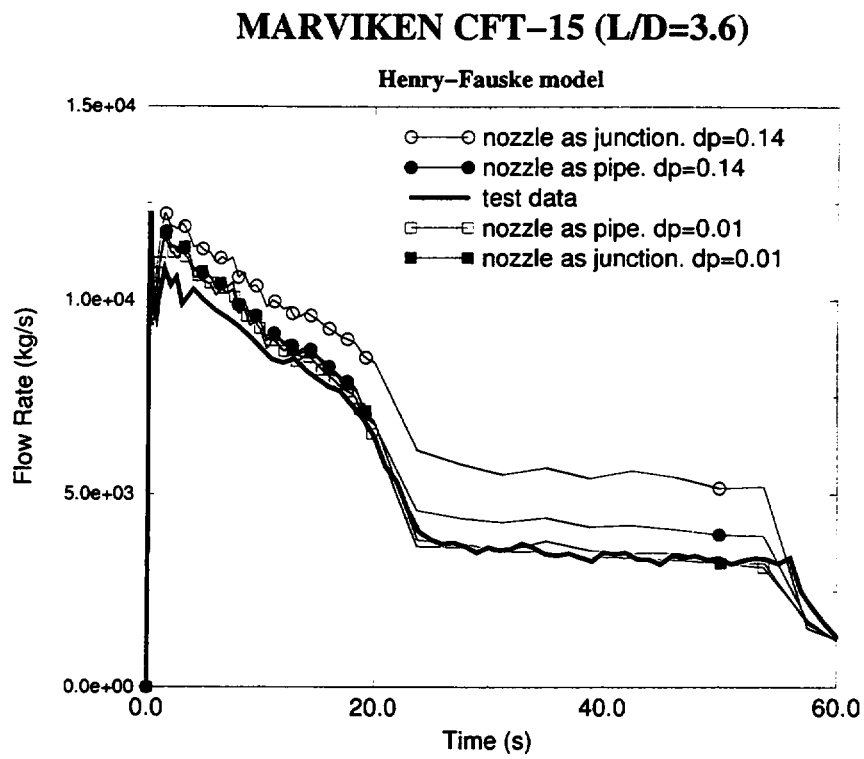

Figure 4.91: Mass flow at nozzle exit. Comparison between BCM-J and BCM-P with $dp = 0.14$ and 0.01. CFT-15.

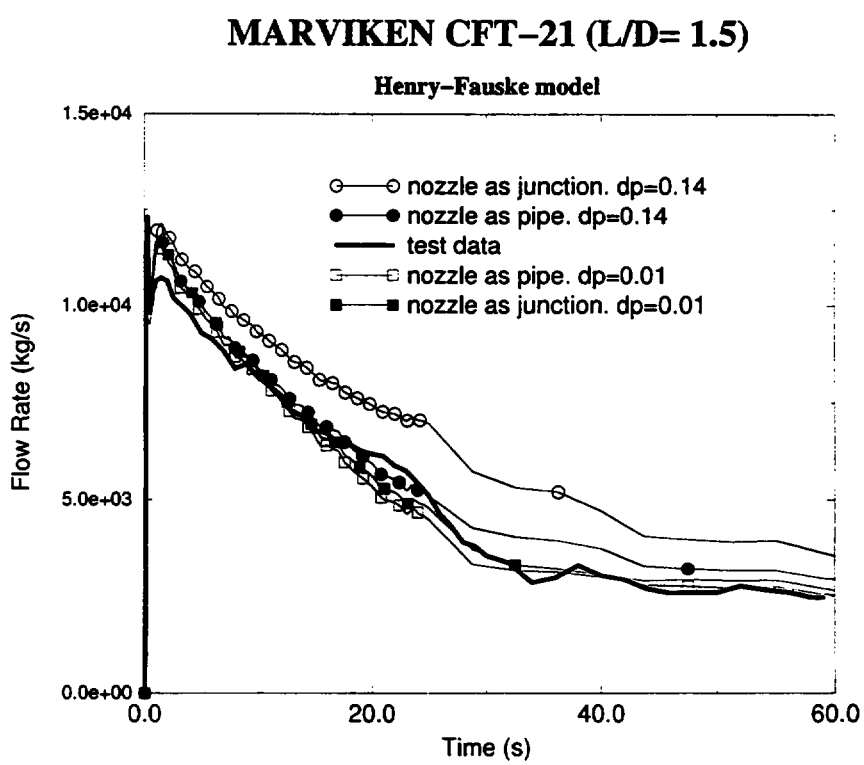

Figure 4.92: Mass flow at nozzle exit. Comparison between BCM-J and BCM-P with $dp = 0.14$ and 0.01. CFT-21.

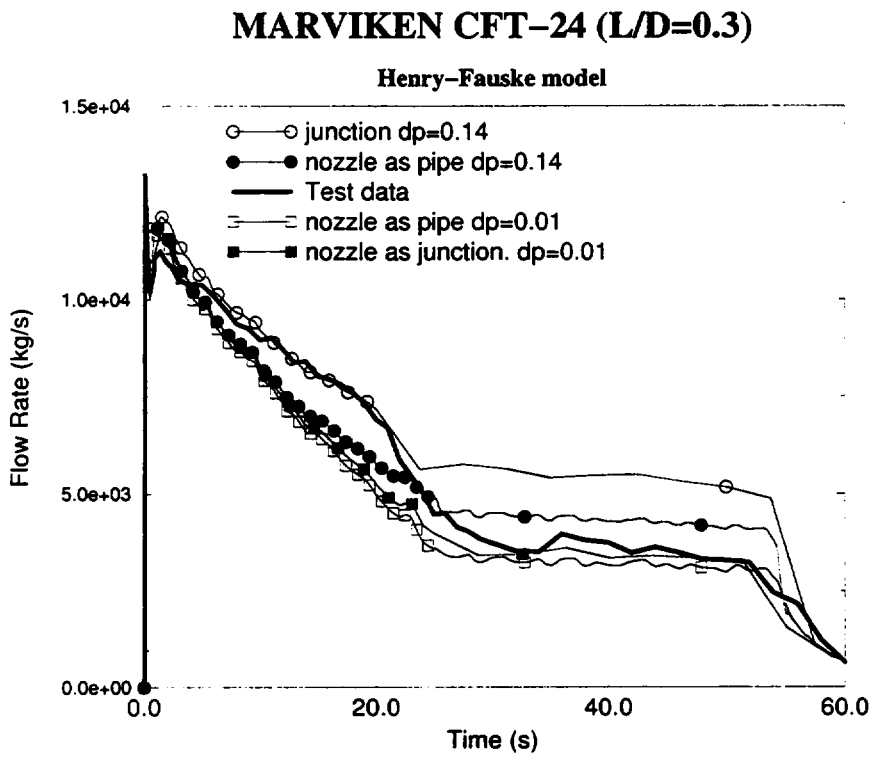

Figure 4.93: Mass flow at nozzle exit. Comparison between BCM-J and BCM-P with $dp = 0.14$ and 0.01. CFT-24.

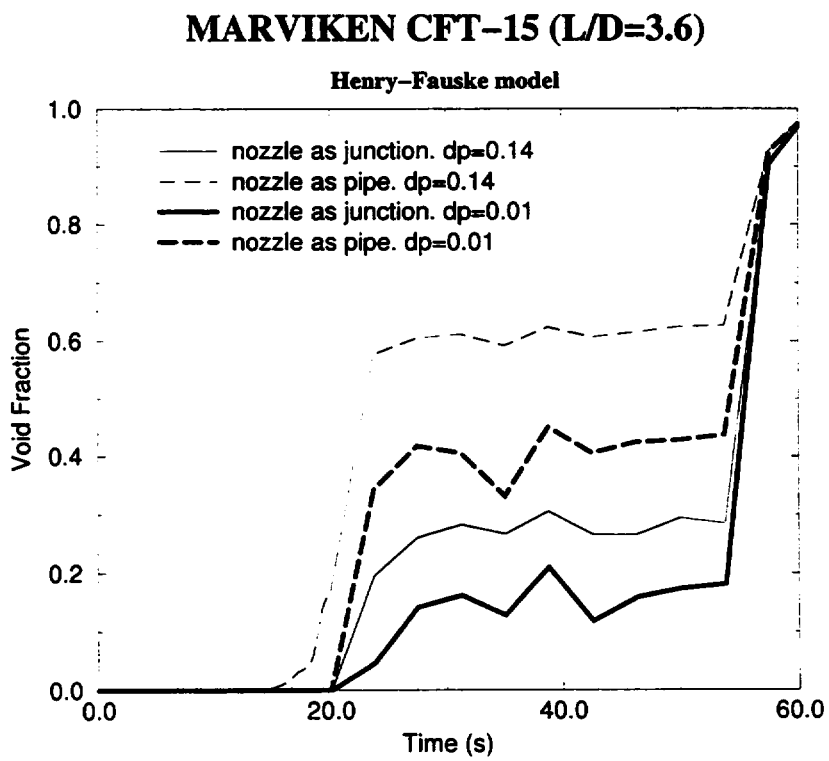

Figure 4.94: Void-fraction at nozzle exit. Comparison between BCM-J and BCM-P with $dp = 0.14$ and 0.01. CFT-15.

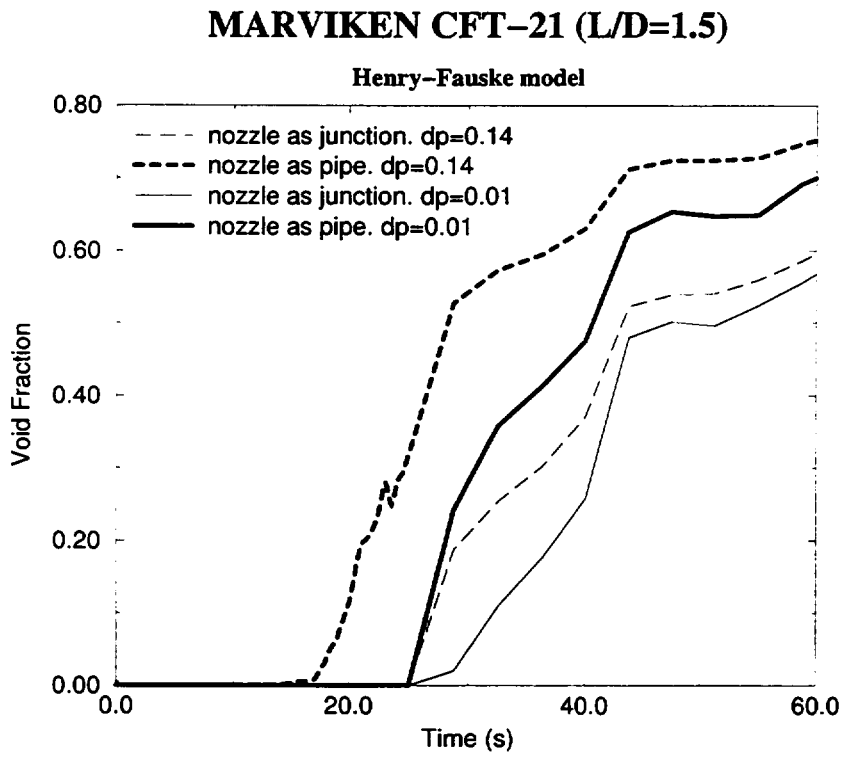

Figure 4.95: Void-fraction at nozzle exit. Comparison between BCM-J and BCM-P with $dp = 0.14$ and 0.01. CFT-21.

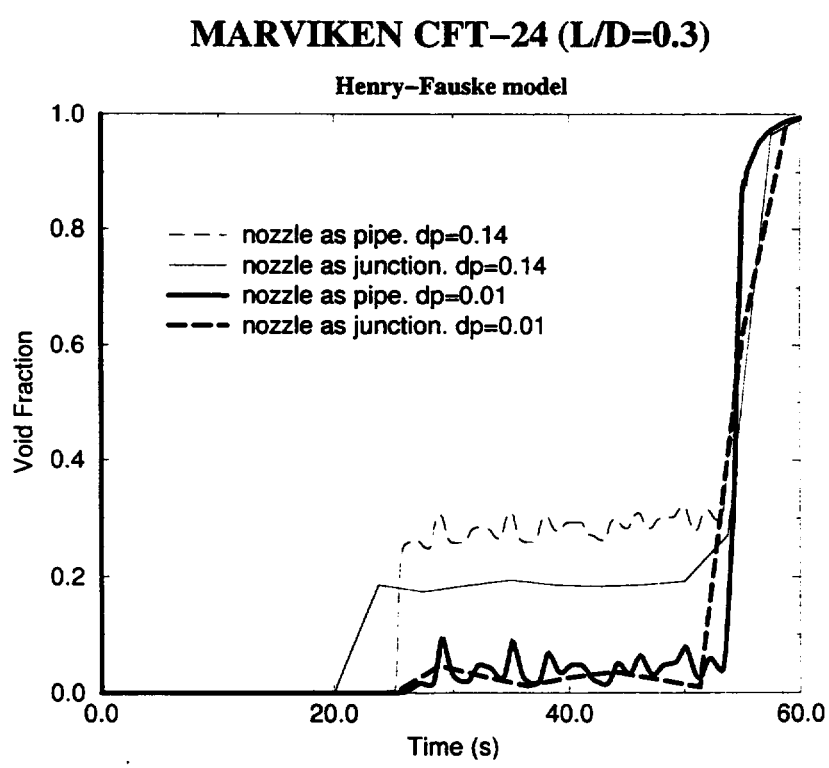

Figure 4.96: Void-fraction at nozzle exit. Comparison between BCM-J and BCM-P with $dp = 0.14$ and 0.01. CFT-24.

Chapter 5

Conclusions

The conclusions of this report are as follows:

1. The transition logic from CFM to Non-CFM for the default model (Ransom-Trapp) is not always adequate for changing from one model to the other correctly, as it is showed in Section 2.1.

2. The main conclusions of the sensitivity analysis of the Ransom-Trapp model are:

   - Subcooled. The behaviour is anomalous due to the transition logic from critical flow to non-critical flow. This problem only is important for large subcoolings.
   - Two-phase. The results show one or two maxima for the mass flow with pressures greater than 90 bar. This is not an expected behaviour and is not found in the literature. Oscillatory behaviour appears below 60 bar.
   - Energy loss coefficient. It must be used with care in junctions where critical mass flow is expected, because CFM does not depend on it, but non-CFM decreases with it.
   - Discharge Coefficients. From the results it can be concluded that the variation of the mass flow with the discharge coefficient has the same value than the discharge coefficient.
   - There are several other known problems with this model, that makes it necessary improving the model or the avoidance of its use.

3. The main conclusions of the sensitivity analysis of the Henry-Fauske model are:

- Subcooled. No problems were found with the transition logic from critical to non-critical flow.
- Two-phase. There are neither maxima for the mass flow nor oscillatory behaviour unlike in the Ransom-Trapp model.
- Energy loss coefficient. It must be used with care in junctions where critical mass flow is expected, because CFM does not depend on it, but non-CFM decreases with it.
- Disequilibrium parameter. Mass flow is strongly dependant on this parameter. In order to avoid the user effect, the value should be internally fixed or at least detailed user guidelines should be supplied.
- In general the model shows a good behaviour, but user guidelines should be supplied for the discharge coefficient and the disequilibrium parameter.

4. The following conclusions are obtained from the comparison of Ransom-Trapp model and Marviken tests:

   - In general, the mass flow simulated with CFM-off is always greater than with CFM on, except at the beginning of CFT-01, CFT-06 and CFT-17 (see Section 2.1, problems with the transition from CFM to Non-CFM). Also, CFM-off results do not adjust to experimental data and therefore the critical flow model is necessary.
   - When the nozzle is modeled as a single junction, better results are obtained with the abrupt area change option than with the smooth option. However, the differences between them are small for the Marviken experiments.
   - The subcooled period is apparently better reproduced with the nozzle modeled as a pipe than as a single junction (except in CFT-24), but it must be taken into account that the void fraction at the nozzle outlet is not null from the beginning of the transient with the nozzle modeled as a pipe, which is not in accordance with experimental data. So, the subcooled period is modeled with a two-phase critical flow model with non-null void fraction, which is wrong. This problem is not present when the nozzle is modeled as a SINGLE JUNCTION because that is equivalent to freezing the model.
   - The results obtained with both models during the two-phase period are quite similar to experimental data. CFT-06 and CFT-24 are better reproduced with the nozzle modeled as a junction.

- It should be better to choose the SINGLE JUNCTION model for the nozzle, since the subcooled period is better reproduced with the nozzle modeled as a SINGLE JUNCTION and for the two phase period both models seem to give similar results.
- The homogeneous option gives better results than the non-homogeneous one.
- SINGLE JUNCTION, trip-valve and motor valve models give similar results.
- The following conclusions are obtained from the discharge coefficient adjustment for BCM:
  - Nozzle modeled as SINGLE JUNCTION. A very good adjustment is achieved with the coefficients shown in Table 4.2.
  - Nozzle modeled as PIPE. The adjustment in the subcooled period is not so good as in the previous case. The reason is that when the subcooled discharge coefficients are fitted, the beginning of the boiling process is delayed. However, it can be observed that boiling is still starting too early with respect to the test data. Probably a delayed boiling model is needed in order to model the nozzle as a pipe.

    On the other hand, a good adjustment for the mass flow is achieved for the two-phase period, but the void fraction values are higher than with the nozzle modeled as a SINGLE JUNCTION.
  - The comparison of the discharge coefficient adjustment for both models, Table 4.2, shows that the discharge coefficients used with the nozzle modeled as a PIPE are higher than for SINGLE JUNCTION.

- The following conclusions are obtained from the discharge coefficient adjustment for the Initial Condition Model (ICM):
  - Nozzle modeled as SINGLE JUNCTION. In general, a good adjustment is achieved with the coefficients shown in Table 4.3, except in the subcooled period of CFT-21.
  - Nozzle modeled as PIPE. The fitting for the subcooled period for all cases is very poor, but on the other hand the adjustment is good for the two-phase period.
  - The comparison of the adjusted discharge coefficients for both models is shown in Table 4.3. The values are similar but, taking into account

that with the nozzle modeled as a PIPE the adjustment in the subcooled period is very poor, it seems to be better to model the nozzle as a SINGLE JUNCTION.

- The comparison between ICM and BCM results and their discharge coefficients, Table 4.4, shows that the values used to adjust the mass flow for ICM are always greater than for BCM. This problem may be caused by experimental errors or some constitutive relations or correlations not compatibles with the critical flow model, [ELI-94] (e.g. the $\Gamma_{flashing}$ model and the interfacial friction model).

5. The following conclusions are obtained from the comparison of Henry-Fauske model and Marviken tests:

   - The best values of dp for adjusting the model are (in accordance with the results obtained in [LEV-82]),
     - $dp = 0.14$ for subcooled blowdown and $L/D < 1.5$
     - $dp = 0.01$ for $L/D > 1.5$
     - $dp = 0.01$ for saturated blowdown
   - These results show that the advised dp value, $dp = 0.14$, in [MOR-98] is not adecuate for adjusting the simulated values to test data.
   - The best models for the different nozzles are:
     - Short nozzles $L/D \leq 0.3$ should be modeled as a junction.
     - Long nozzles $L/D \geq 1.5$ should be modeled as a pipe.
     - This assessment does not give enough information about the which is the best model for intermediate nozzles $1.5 > L/D > 0.3$.
   - The inception of boiling is in accordance with the experimental data when the Henry-Fauske model is used.
   - At present, only one dp value can be used for subcooled and two-phase periods. So, two disequilibrium parameters should be implemented in order to include the values mentioned above (one of them for the subcooled period and another for the two-phase one), and also the transition between them. This solution generates a problem because it implies a new degree of freedom, and therefore a negative consequence for the user effect.

6. Final Conclusions:

- The behaviour of the Henry-Fauske model is better than that of the Ransom-Trapp. In this sense, the new model is an improvement with respect to the Ransom-Trapp. On the other hand, the Henry-Fauske model is not a definitive solution for critical flow phenomena simulation, because it has several parameters (discharge coefficient and disequilibrium parameter) that are geometry dependent (i.e. L/D).
- It is necessary to have a critical flow model compatible with the constitutive relations and correlations of the code.
- In general, it is possible that any of the one-dimensional models could not simulate the critical flow phenomena in all conditions, due to the existence of two-dimensional effects. Anyway, the critical flow problem is not still solved, and new theoretical studies and experiments should be performed, with special emphasis in geometries and sizes similar to nuclear power plants.

Bibliography

[FOR-88] R. Pochard A. Forge, F. Steinhoff A. Porracchia (CEA). J. Miro, H.G. Sonnenburg, and V. Teschendorff (GRS). *Comparison of Thermal-Hydraulic Safety Codes for PWR Systems.* Graham and Trotman for the Commission of the European Communities, 1988.

[BAR-90] F. Barre and M. Bernard. The CATHARE code strategy and assessment. *Nuclear Engineering and Design*, 124:257–284, 1990.

[BES-90] D. Bestion. The physical closure laws in the CATHARE code. *Nuclear Engineering and Design*, 124:229–245, 1990.

[TRA-97] B.E. Boyack. TRAC-PF1/MOD2 adequacy assessment closure and special models. Technical Report LA-UR-97-232, LANL, 1997.

[SPI-90] M. Pellissier B. Spindler. Assessment of TRAC-PF1/MOD1 version 14.3 using separate effects critical flow and blowdown experiments. Technical Report NUREG/IA-023, US-NRC, 1990.

[TBD-85b] B.L. Charboneau. Overview of TRAC-BD1/MOD1 assessment studies. Technical Report NUREG/CR-4428, INEL, 1985.

[TRA-86] Safety Code Development Group. Energy Division. TRAC-PF1/MOD1: An advanced best-estimate computer program for pressurized water reactor thermal-hydraulic analysis. Technical Report NUREG/CR-3858. LA-10157-MS, LANL, 1986.

[TRA-81] T.D. Knight et al. TRAC-P1A independent assessment-1979. Technical Report NUREG/CR-1652. LA-8477-MS, LASL (LANL), 1981.

[TBD-85a] R.W. Shumway et al. TRAC-BD1/MOD1: An advanced best estimate computer program for boiling water reactor transient

analysis. volume 4: Developmental assessment. Technical Report NUREG/CR-3633, INEL, 1985.

[REL-90] K.E. Carlson et al. RELAP5/MOD3.2 code manual. volume III: Developmental assessment problems (draft). Technical Report NUREG/CR-5535, INEL, 1990.

[TRA-93] J.W. Spore et al. TRAC-PF1/MOD2. volume I: Theory manual. Technical Report LA-12031-M. NUREG/CR-5673, LANL, 1993.

[KAE-94] S.Y. Lee et al. Uncertainty quantification of RELAP5/MOD3/KAERI critical flow model using Marviken experimental data. Technical Report KAERI/TR-437/94, KAERI, 1994.

[KAE-95] T.S. Kwon et al. Quantification of realistic discharge coefficients for the critical flow model of RELAP5/MOD3/KAERI. *Journal of Korean Nuclear Society*, 27(5):701–709, 1995.

[CQS-97] C. Queral et al. Analysis and comparison of TRAC-BF1 and RELAP5/MOD3.2 critical flow models (in spanish). In SNE, editor, *XXIII Reunión SNE*, 1997.

[ELI-94] E. Elias and G. S. Lellouche. Two-phase critical flow. *Int. J. Multiphase Flow*, 20:91–168, 1994.

[REL-98] The Thermal Hydraulics Group. RELAP5/MOD3 code manual. volume VII: Summaries and reviews of independent code assessment reports. Technical Report NUREG/CR-5535 Volume VII. Revision 1, SCIENTECH, Inc., 1998.

[JOH-96] Gary Johnsen. RELAP5 code development status. In *CAMP-ESPAÑA*, 1996.

[TRA-80] J.F. Jackson and J.C. Vigil. Comparison of TRAC calculations with experimental data. Technical Report LA-UR-80-1267, LASL (LANL), 1980.

[KIM-92] K. Kim and H.J.Kim. Assessment of RELAP5/MOD2 critical flow with Marviken test 15 and 24. Technical Report NUREG/IA-086, US-NRC, 1992.

[TRA-84] T.D. Knight. TRAC-PD2 independent assessment. Technical Report NUREG/CR-3866. LA-10166-MS, LANL, 1984.

[GOM-98] E. Valero M. Gómez and I.E. Parra. Analysis of the critical flow model in TRAC-BF1. International agreement report, Department of Applied Mathematics and Statistics. Universidad Politécnica de Madrid, 1998.

[MOR-98] G.A. Mortensen. Critical flow model. RELAP5/MOD3.2.2Beta. In *CAMP. Idaho Falls, ID USA*, 1998.

[MAR-4-90] The Marviken Project. *The Marviken Full-Scale Critical-Flow Test*, volume 4 of *NUREG/CR-2671*, chapter Description of the Test Facility. EPRI-NP-2370, 1990.

[ROS-86] O. Rosdahl and D. Caraher. Assessment of RELAP5/MOD2 against critical flow data from Marviken tests JIT-11 and CFT-21. Technical Report NUREG/IA-007. STUDSVIK/NP-86/99, Swedish Nuclear Power Inspectorate, 1986.

[LAH-93] Jr. R.T. Lahey and F.J. Moody. *The Thermal-Hydraulics of a Boiling Water Nuclear Reactor.* American Nuclear Society, 1993.

[LEV-82] Inc. S. Levy. Critical flow data review and analysis. Technical Report EPRI-NP-2192, EPRI, 1982.

[TRA-83] M.S. Sahota and J.F. Lime. TRAC-PF1 choked-flow model. Technical Report LA-UR-82-1666, LANL, 1983.

[TRA-96] R.G. Steinke. A description of the test problems in the TRAC-P standard test matrix. Technical Report LA-UR-96-1475, LANL, 1996.

[STE-98] R.G. Steinke. Task completion report for update FXCFM. Technical Report LA-UR-98-1397, LANL, 1998.

[TRA-79] J.C. Vigil and K.A. Williams (Editors). TRAC-P1A developmental assessment. Technical Report NUREG/CR-1059. LA-8056-MS, LASL (LANL), 1979.

[REL-87] R.J. Wagner V.H. Ransom and G.W. Johnsen. RELAP5/MOD2 code manual. volume III: Developmental assessment problems. Technical Report EGG-TFM-7952, INEL, 1987.

[WEA-89] Walter L. Weaver. Improvements to the RELAP5/MOD3 choking model. International Agreement Report EGG-EAST-8822, EG&G Idaho, Inc., 1989.

Part I

Appendix: Subroutine JCHOKE flow logic

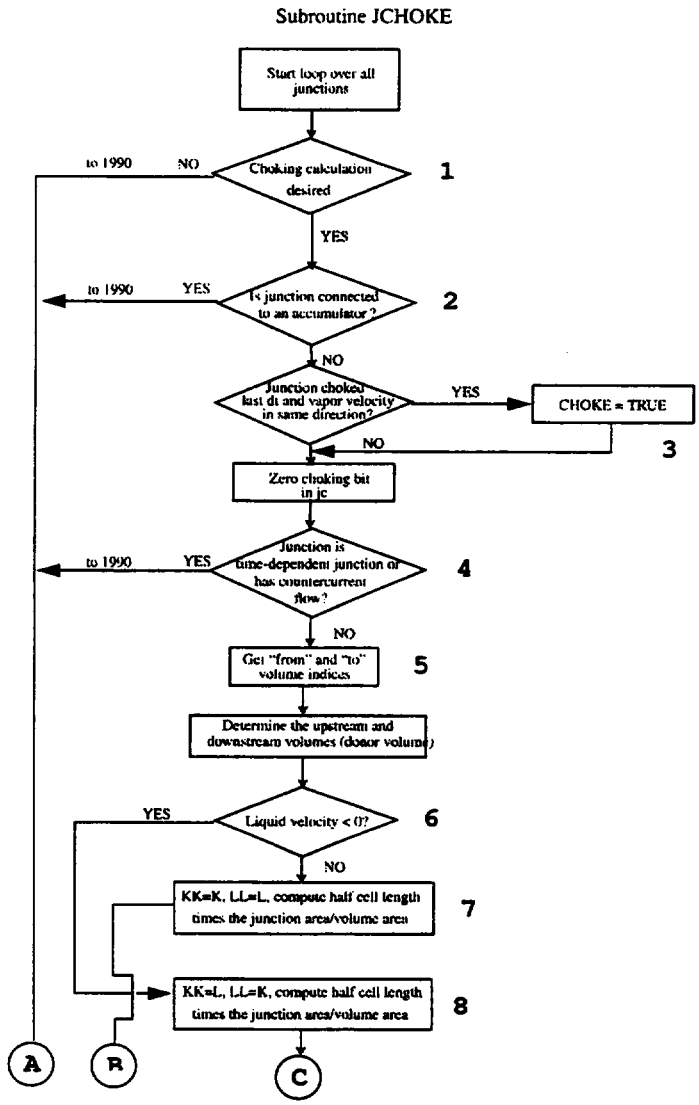

Figure 1: Subroutine JCHOKE flow logic.

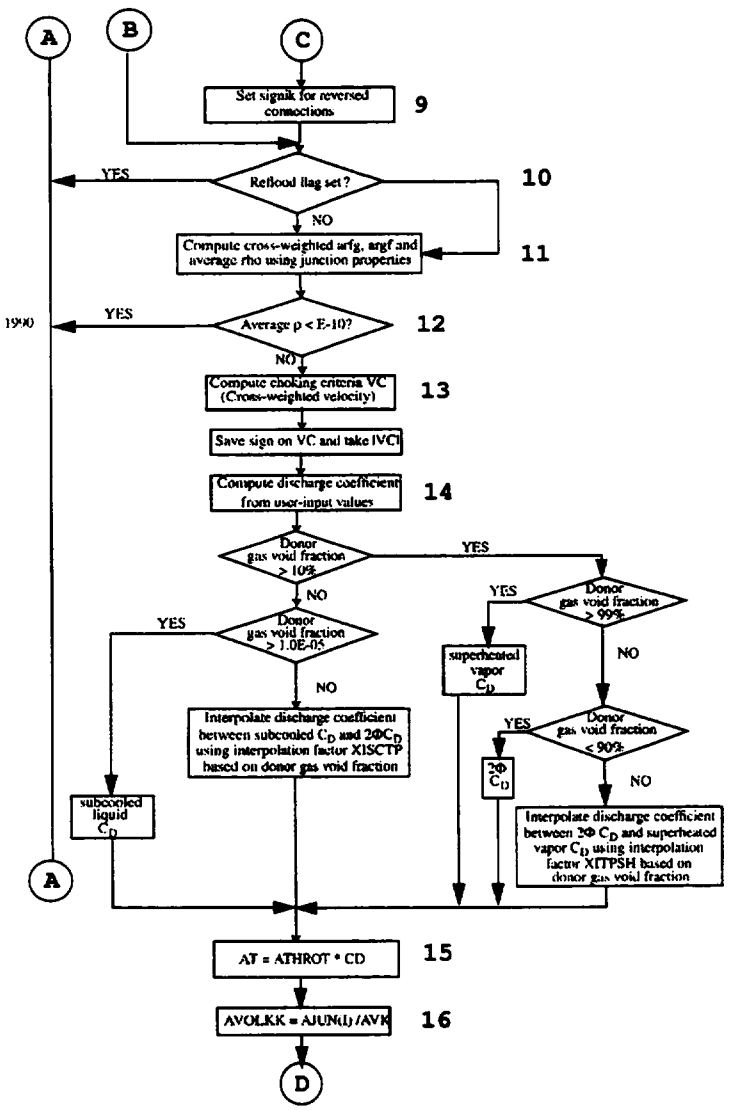

Figure 2: Subroutine JCHOKE flow logic (continued).

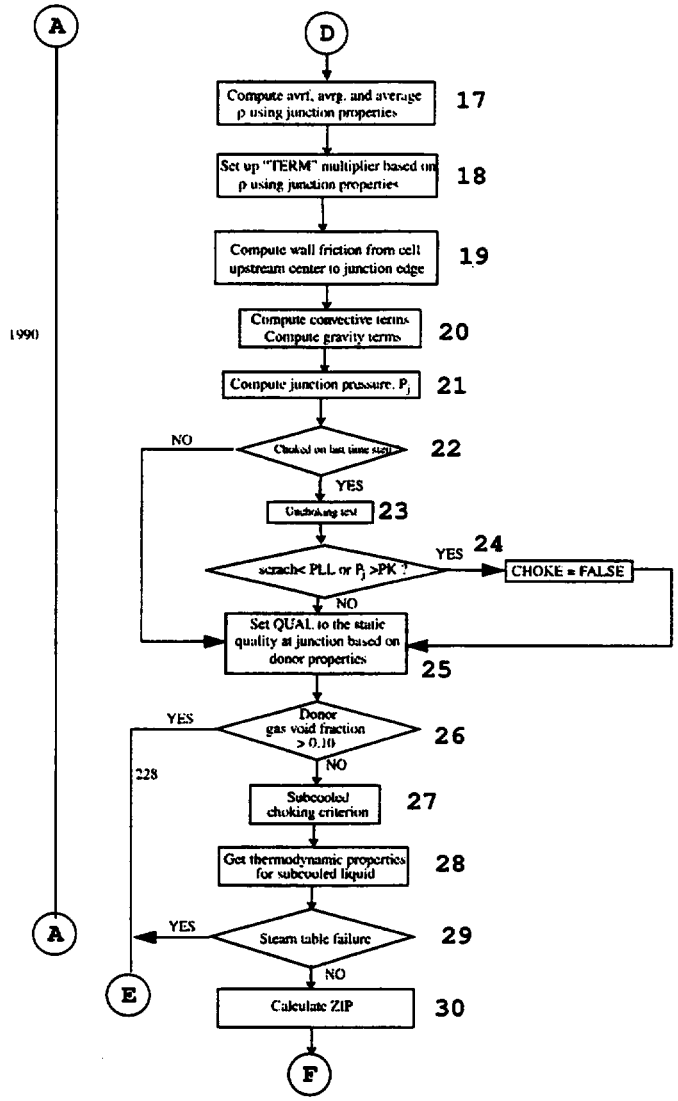

Figure 3: Subroutine JCHOKE flow logic (continued).

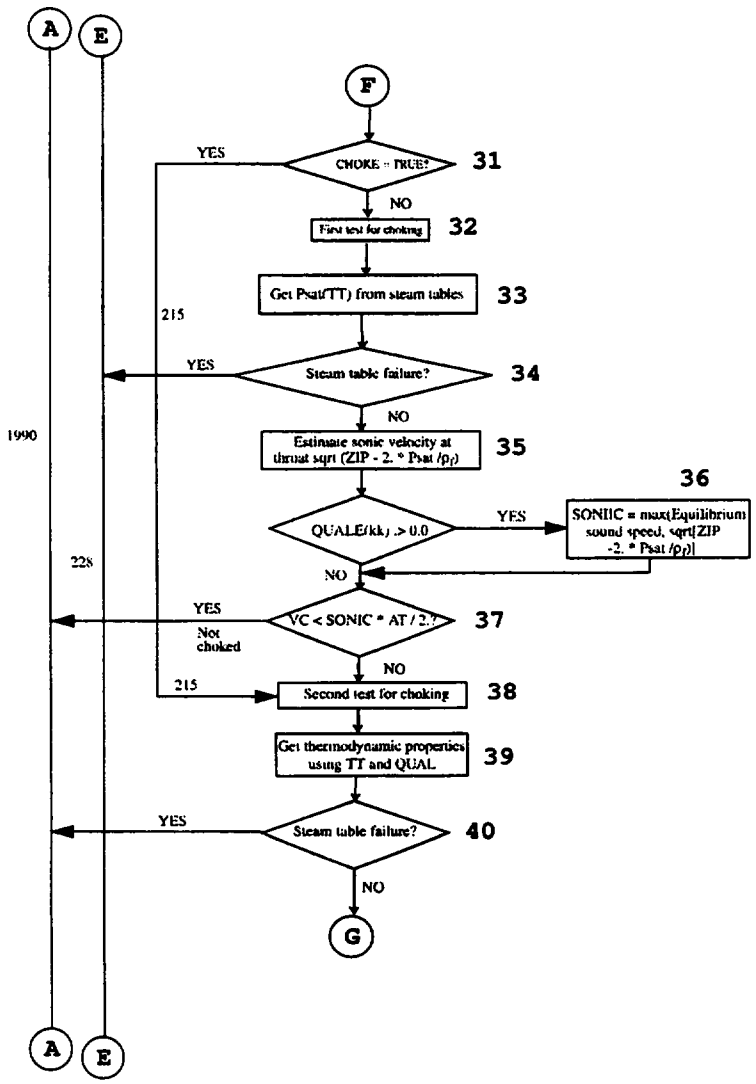

Figure 4: Subroutine JCHOKE flow logic (continued).

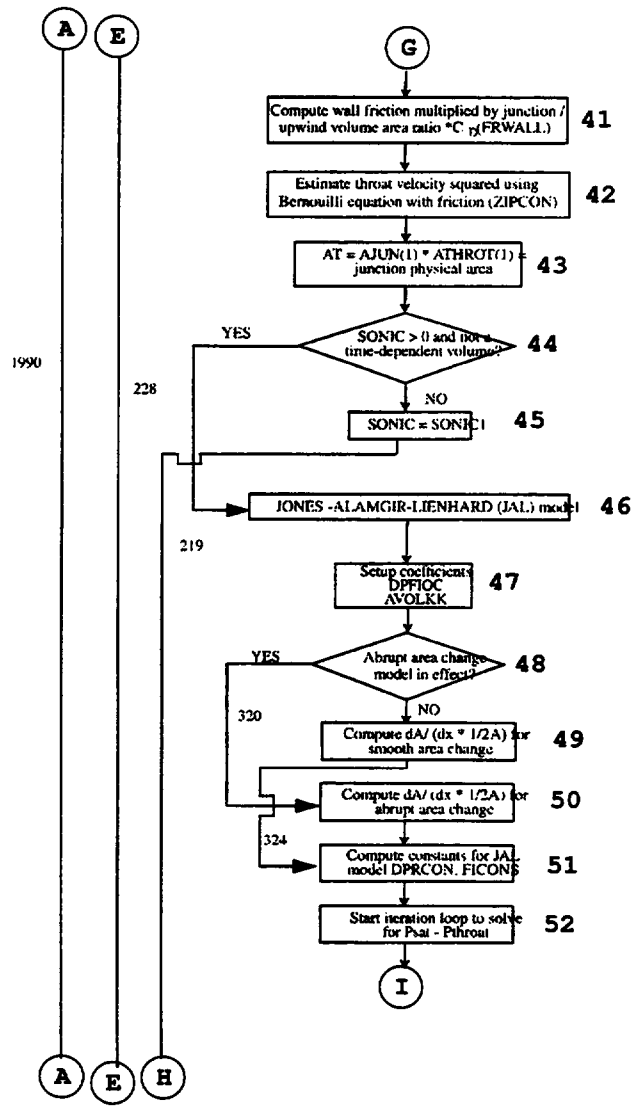

Figure 5: Subroutine JCHOKE flow logic (continued).

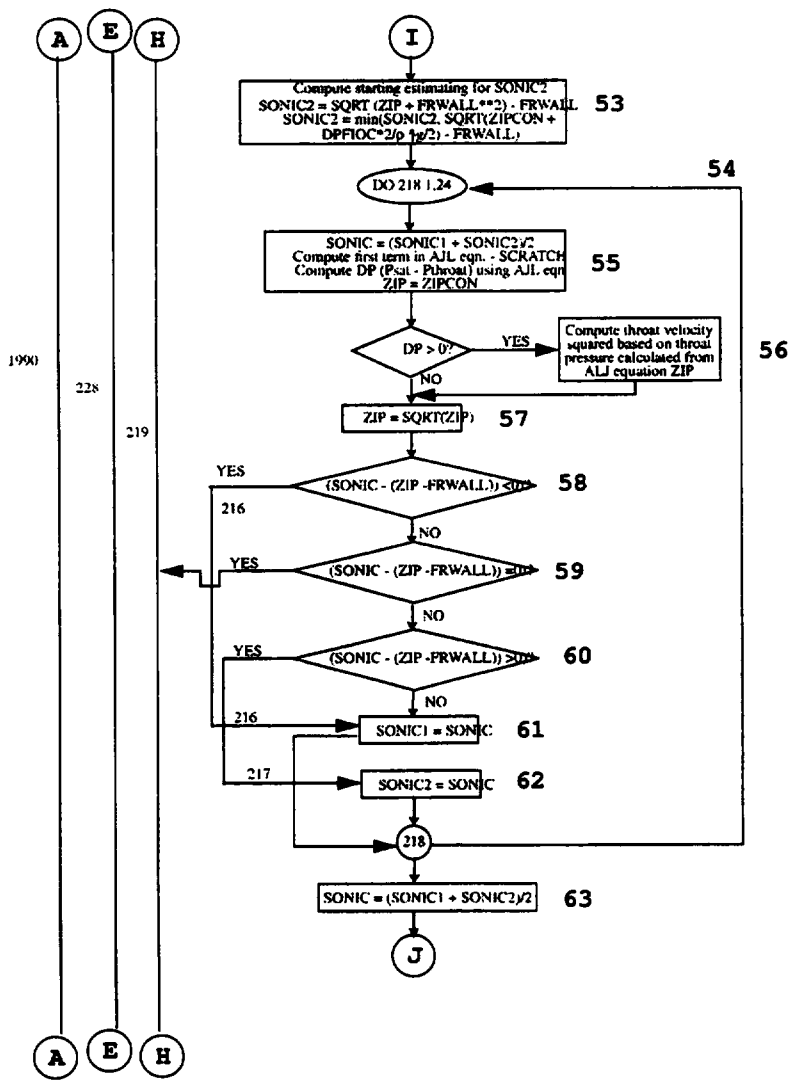

Figure 6: Subroutine JCHOKE flow logic (continued).

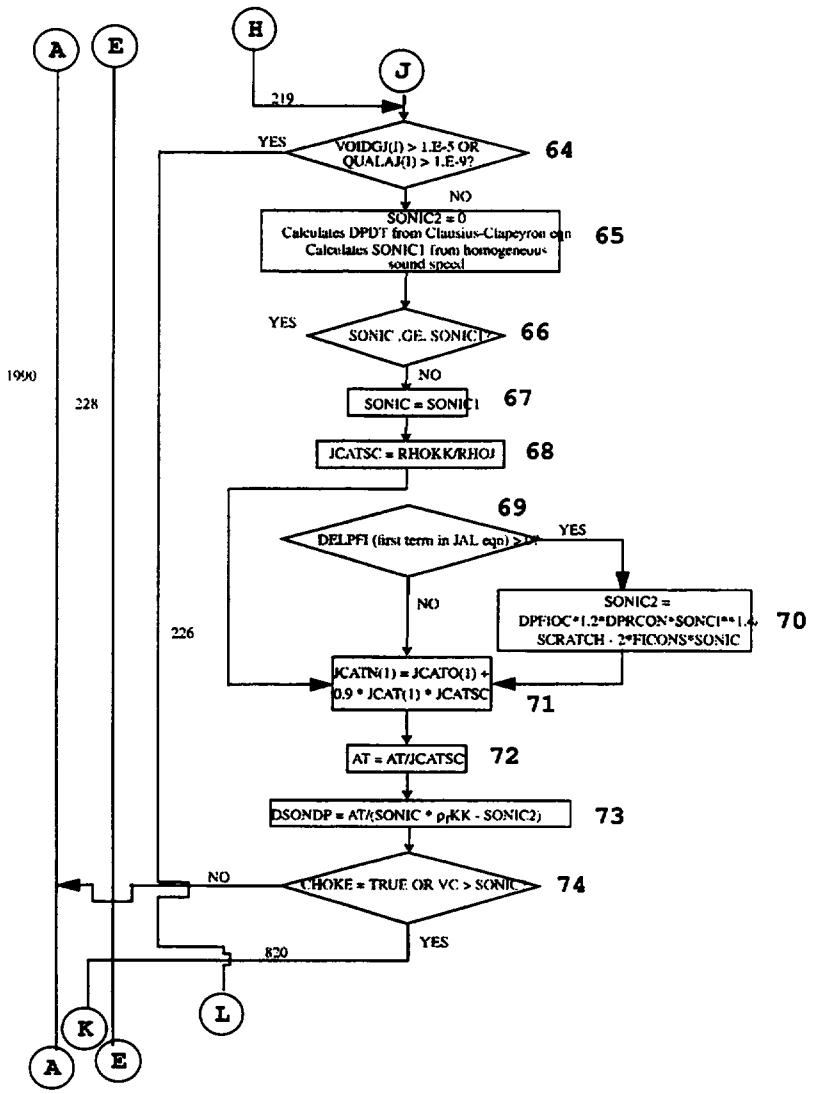

Figure 7: Subroutine JCHOKE flow logic (continued).

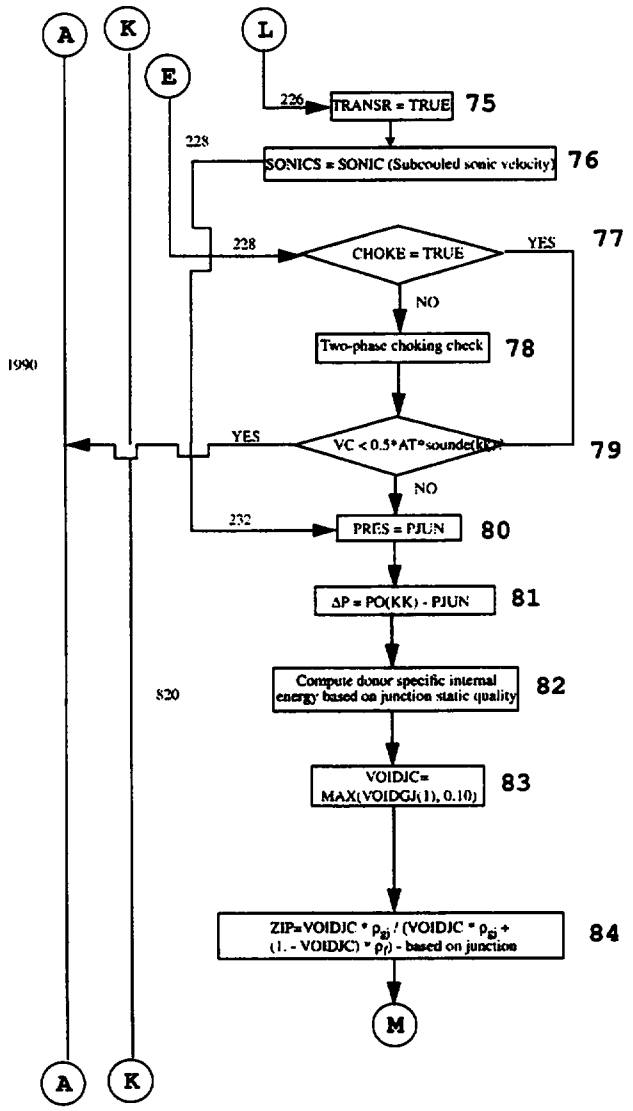

Figure 8: Subroutine JCHOKE flow logic (continued).

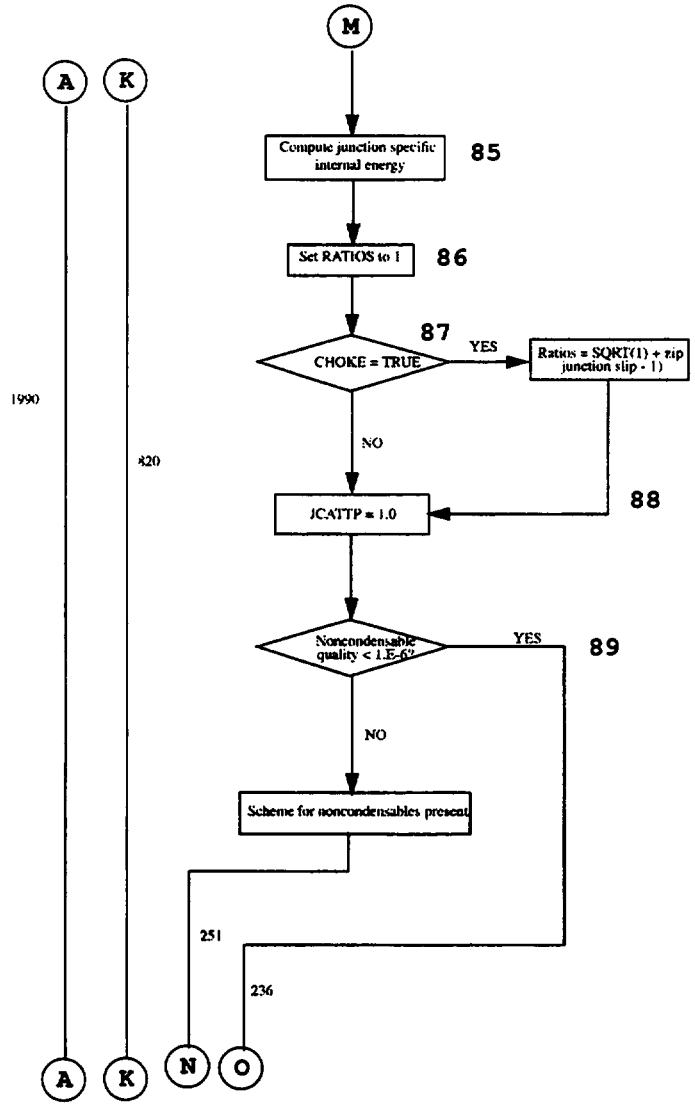

Figure 9: Subroutine JCHOKE flow logic (continued).

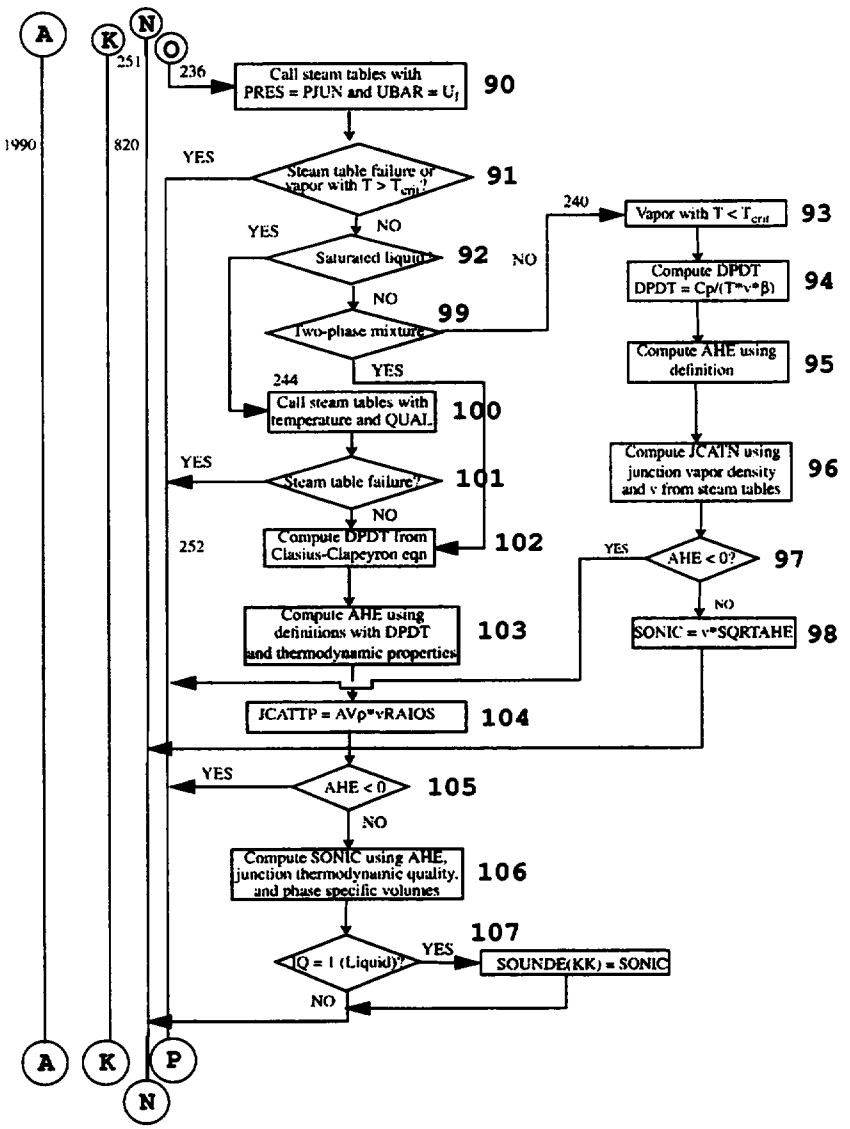

Figure 10: Subroutine JCHOKE flow logic (continued).

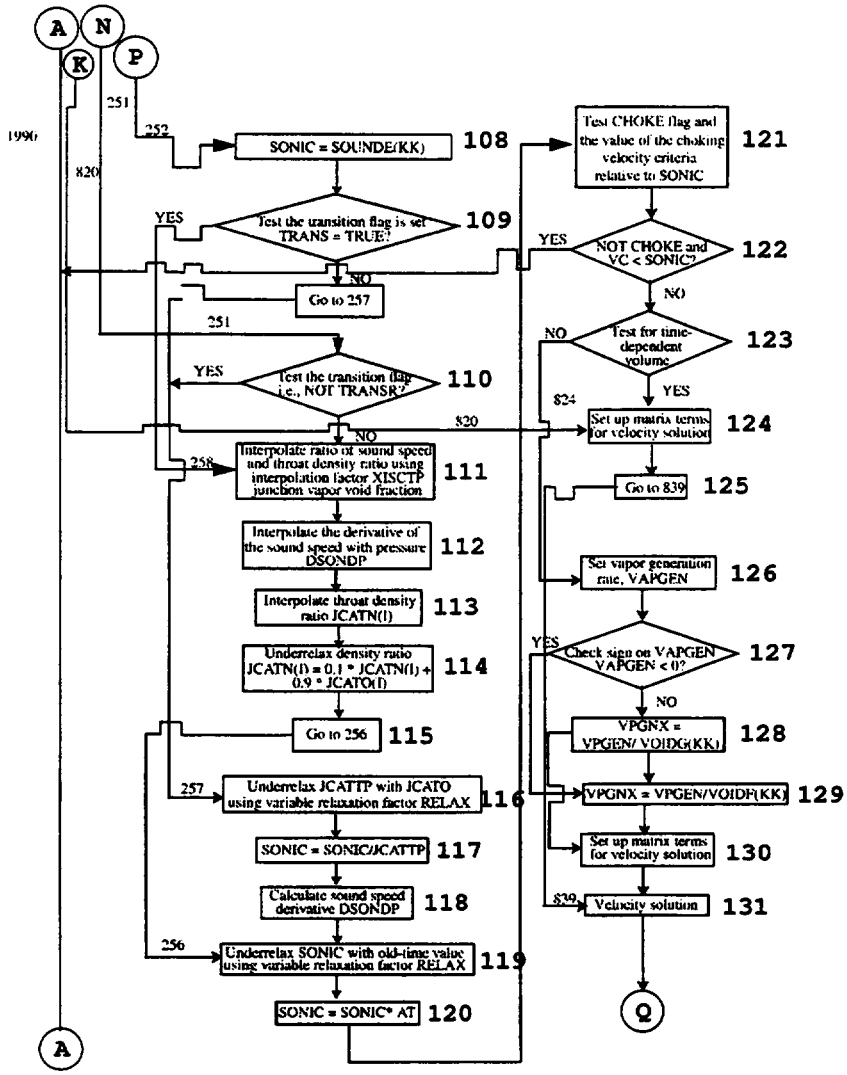

Figure 11: Subroutine JCHOKE flow logic (continued).

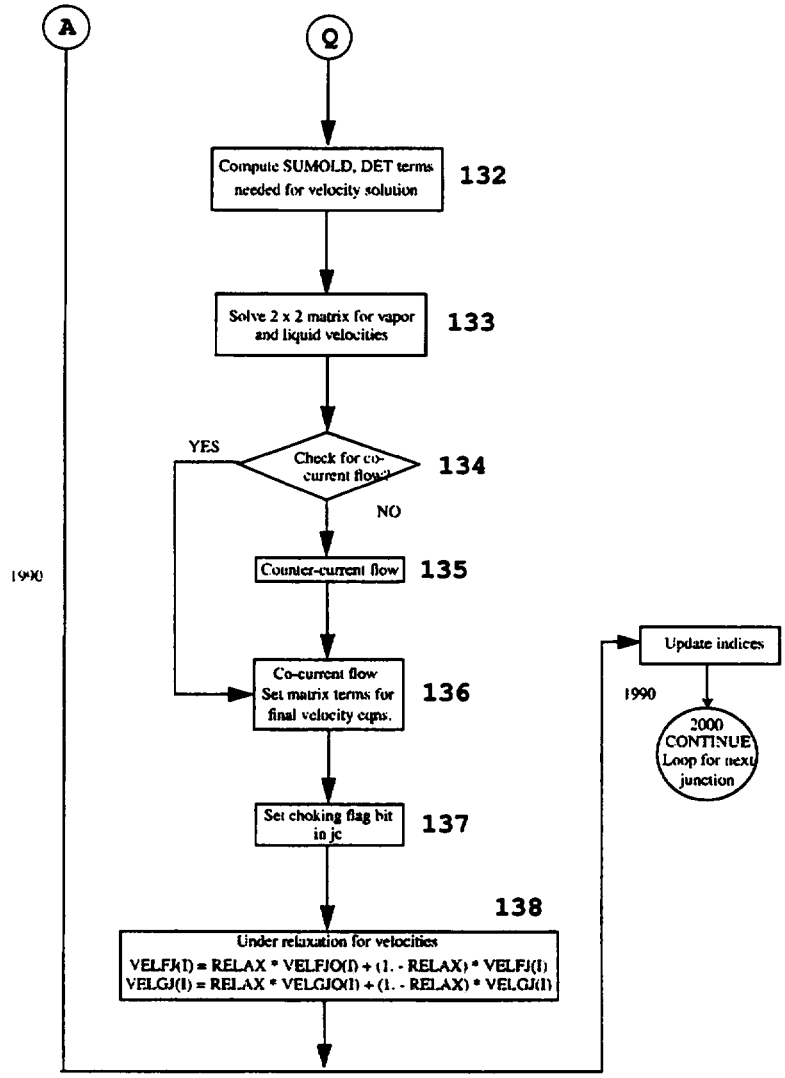

Figure 12: Subroutine JCHOKE flow logic (continued).

Part II

Appendix: Modified JCHOKE Subroutine

```
*deck jchoke
      subroutine jchoke
*in32 iprop
*in32 lprop
*in32end
c
c  $Id: jchoke.F,v 1.6.2.1 1995/09/15 16:23:35 rjw Exp $
c
c  Computation of choking theory.
c  These local variables had their names changed (4/12/95 gam)
c  a11    => c11
c  a12    => c12
c  a21    => c21
c  a22    => c22
c  avrf   => avrff
c  avrg   => avrgg
c  convf  => convff
c  convg  => convgg
c  diff   => difff
c  difg   => difgg
c  difold => difld
c  dx     => ddx
c  f2     => ff2
c  fricfj => frcfj
c  fricgj => frcgj
c  psld   => psldd
c  psmf   => psmff
c  psmg   => psmgg
c  sumf   => sumff
c  sumg   => sumgg
c  sumold => sumld
c  vpgen  => vpgenn
c  vpgnx  => vpgnxx
c  figj   => figjj
c  fifj   => fifjj
c  tt     => ttt
c  beta   => betaa
c  betaf  => betff
c  betag  => betgg
c  betags => betgs
c  cp     => cpp
c  cpf    => cppf
c  cpg    => cppg
c  ubar   => ubarr
c  qual   => quall
c  hbar   => hbarr
c  kapa   => kpa
c  kapaf  => kpaf
c  kapag  => kpag
c  kapags => kpags
c  pres   => press
c  vbar   => vbarr
c  vs     => vss
c  vsubf  => vsubff
c  vsubg  => vsubgg
c  us     => uss
c  usubf  => usubff
```

```
c  usubg  => usubgg
c  delpz  => delpzz
c
c  Cognizant engineer:  wlv.
c
$if def,impnon,1
      implicit none
*call comctl
*call contrl
*call fast
*call jundat
*call lpdat
*call machas
*call machns
*call machos
*call machss
*call scrtch
*call statec
*call stcblk
*call stcom
*call trnhlp
*call ufiles
*call voldat
c
c  Local variables.
      real a01,a02,c11,c12,c21,c22,ahe,aj,arfg,argf,arsm,at,atin,
     * avk,avolkk,avrff,avrgg,avrho,betaa,betf,betg,betgs,convff,
     * convfi,convgg,convgi,cpp,cppf,cppg,cvao,cvaq,dcva,delpfi,delpzz,
     * deltap,det,df1dps,df1dtg,df1dtt,df2dps,df2dtg,difff,difgg,difld,
     * dpdt,dpfioc,dprcon,dps,dsondp,dtg,dtt,dufdpt,dufdtt,dusdtt,ddx,
     & f1,
     * ff2,ficons,fjfg,frcfj,frcgj,frwall,hbarr,hsubf,hsubg,kpa,kpaf,
     * kpag,kpags,pa,pjun,pll,press,prop(36),psatt,psldd,psmff,psmgg,
     * qa,qair1,qara,qf,qs,quall,ra,ratios,rdet,rhofg,rhofin,rhoinv,
     * s(26),scrach,signik,signvc,sonic,sonic1,sonic2,sonics,sumff,
     & sumgg,
     * sumld,term,termz,toler,ttt,tg,tmaxl,vbarr,vc,vf,vff,vg,virmas,
     * vpgenn,vpgnxx,vss,vsubff,vsubgg,ua,ua1,uao,ubarr,uff,ujun,uss,
     & usubff,
     * usubgg,xe,zip,zipcon,c0,c1,figjj,fifjj,dummy,xintrp,relax,jcatsc,
     * jcattp,vgtpmn,vgtpmx,vgshmn,vgscmx,voidjc,avkxj,dxkxj,xisctp,
     * xitpsh,jcatsf,checkj,checkv,vfsave,vgsave,jcsave,qualty
      integer i,idg,ik,implt,in,ink,iq,is,isf,iskip,it,ix,
     & k,kk,kl,kx,kx2,ky,ky2,l,ll,lx,lx2,m,nredo
      logical err,choke,redo
c
c  State properties
      equivalence          ( prop( 1), ttt   ), ( prop( 2), press ),
     * ( prop( 3), vbarr ), ( prop( 4), ubarr ), ( prop( 5), hbarr ),
     * ( prop( 6), betaa ), ( prop( 7), kpa   ), ( prop( 8), cpp   ),
     * ( prop( 9), quall ), ( prop(10), psatt ), ( prop(11), vsubff),
     * ( prop(12), vsubgg), ( prop(13), usubff), ( prop(14), usubgg),
     * ( prop(15), hsubf ), ( prop(16), hsubg ), ( prop(17), betf  ),
     * ( prop(18), betg  ), ( prop(19), kpaf  ), ( prop(20), kpag  ),
     * ( prop(21), cppf  ), ( prop(22), cppg  )
$if def,newwtrp,3
      integer iprop(36)
```

```
      logical lprop(36)
      equivalence (prop(1),iprop(1),lprop(1))
c
      equivalence (rhofin,rhoinv),(ficons,fjfg),(ahe,aj)
      equivalence (frwall,vf),(pjun,vg)
      equivalence (deltap,sonic2,virmas),(zip,vpgenn)
      equivalence (xe,rhofg),(sonic1,dsondp)
      equivalence (avolkk,det,rdet,s(11)),(vff,vf,s(12)),
     * (delpfi,sumff,uff,s(13)),(dpfioc,sumgg,uss,s(14)),
     * (dprcon,sumld,vss,s(15)),(betgs,vpgnxx,zipcon,s(16)),
     * (difff,c11,df1dps,s(17)),(difgg,c12,df1dtg,s(18)), (term,scrach),
     * (difld,c21,df2dps,s(19)),(c22,df2dtg,s(20)),(a01,f1,s(21)),
     * (a02,ff2,s(22)),(dtg,s(25)),(dps,dtt,s(26)),(qs,s(7)),(qf,s(8))
c
      logical jstop,transr
c
c  Data statements.
      data iq/0/, toler/0.0025/
*call machaf
*call machnf
*call machof
*call machsf
c
c  Set flag for standard semi-implicit or 2-step implicit.
      implt = 0
      if (iand(print,128) .ne. 0) implt = 1
      iskip  = 0
      ix = ixjff
      is = ixsopr(issys)
c  Junction loop.
      i = lij(issys)
      do 2000 m = 1,lijn(issys)

c1 cqs   choking calculation desired

         if (chngno(52)) then
           jc(i) = iand(jc(i),not(1))
           go to 1990
         endif

c2 cqs  is junction connected to an accumulator?

        if (iand(jc(i),80) .ne. 0) go to 1990
         redo = .false.
 100     transr = .false.
         relax = 0.0

c3 cqs   junction choked last dt and vapor velocity in same direction

         choke = iand(jc(i),1).ne.0 .and. velgj(i)*velgjo(i).gt.0.0
         jc(i) = iand(jc(i),not(1))

c4 cqs   junction is timedependent junction or has countercurrent flow

         if (iand(jc(i),2).ne.0 .or. velfj(i)*velgj(i).le.0.0)
     &   go to 1990
```

```
c5 cqs   get the "from" and "to" volume indices

         k = ij1nx(i)
         kx = iand(ishft(jcex(i),-12),7)
         kx2 = k + kx
         kx = k + ishft(kx,-1)
         l = ij2nx(i)
         lx = iand(ishft(jcex(i),-9),7)
         lx2 = l + lx
         lx = l + ishft(lx,-1)

c  Define flow direction.

c6 cqs   liquid velocity >0 < 0

         if (velfj(i) .ge. 0.0) then

c7 cqs
           kk = k
           ky = kx
           ky2 = kx2
           ll = l
           ik = 1
           iq = 8192
           kl = 0
           avk = avkx(ix)
           ddx = dxkx(ix)*avk*0.5
         else

c8 cqs
           kk = l
           ky = lx
           ky2 = lx2
           ll = k
           ik = 2
           iq = 4096
           kl = 2
           avk = avlx(ix)
           ddx = dxlx(ix)*avk*0.5
         endif
         signik = 1.0

c9 cqs   set signik for reverse connections

         if (iand(jc(i),ik*4) .ne. 0) signik = -signik

c10 cqs  reflood flag set?

         if (iand(imap(ky),ishft(1,29)) .ne. 0) go to 1990
c
c  If current donor volume contains a different fluid from the last one,
c  call stcset.
         if (volmat(kk).ne.nfluid) call stcset (volmat(kk))
c
c  Set-up junction velocities for choke test.

c11 cqs  compute arfg,argf
```

```
        arfg = voidfj(i)*rhogj(i)
        argf = voidgj(i)*rhofj(i)
        arsm = arfg + argf

c12 cqs  average rho<E-10

        if (arsm .lt. 1.0e-10) go to 1990

c13 cqs  compute choking criteria vc

        vc = (arfg*velfj(i) + argf*velgj(i))/arsm
        signvc = sign(1.0,vc)
        vc = abs(vc)

c14 cqs  compute discharge cofficient from user input values

c  cqs *start of discharge coefficient calculation**********a
c  Discharge coefficient.**********************************
c  Define upper and lower bounds of transition region in void.
        vgscmx = 1.0e-05
        vgtpmn = 0.10
        xisctp = (voidgj(i) - vgscmx)/(vgtpmn - vgscmx)
        xisctp = max(0.0,min( 1.0,xisctp))
        xisctp = xisctp*xisctp*(3.0 - 2.0*xisctp)
        at = jdissc(i) + xisctp*(jdistp(i) - jdissc(i))
        vgtpmx = 0.90
        vgshmn = 0.99
        xitpsh = (voidgj(i) - vgtpmx)/(vgshmn - vgtpmx)
        xitpsh = max(0.0,min(1.0,xitpsh))
        xitpsh = xitpsh*xitpsh*(3.0 - 2.0*xitpsh)
        at = at + xitpsh*(jdissh(i) - jdistp(i))
c  cqs *end   of discharge coefficient calculation**********a

c15 cqs
        at = at*athrot(i)

c  General values needed in the calculation.

c16 cqs
        avolkk = ajun(i)/avk

c17 cqs  compute avrf, avrg ...

        avrff = voidfj(i)*rhofj(i)
        avrgg = voidgj(i)*rhogj(i)
        avrho = avrff+avrgg

c18 cqs
        term = 1.0
        if (iand(jc(i),iq) .ne. 0) term = 0.0
        termz = term

c19 cqs  compute wall friction from cell upstream center to junction edge

c  Wall frictions.
        frcfj = ddx*term*fwalf(ky)/(max(1.0e-5,voidfj(i))*rhofj(i))
```

```
        frcgj = ddx*term*fwalg(ky)/(max(1.0e-5,voidgj(i))*rhogj(i))

c20 cqs compute convective terms. compute gravity terms

c  Convective terms.
        if (redo) then
          atin = signvc*jcatn(i)/at**2
          convfi = atin*velfj(i)**2
          convgi = atin*velgj(i)**2
        else
          atin = signvc*jcato(i)/at**2
          convfi = atin*velfjo(i)**2
          convgi = atin*velgjo(i)**2
        endif
        convff = 0.5*(convfi - term*signvc*velf(ky)**2)
        convgg = 0.5*(convgi - term*signvc*velg(ky)**2)
        psmff = frcfj*avrff
        psmgg = frcgj*avrgg
c  Gravitational force.
        delpzz = gravcn*hydzc(ky2)*signik*term
        psldd = -(delpzz*avrho + avrff*convff + avrgg*convgg
     &          - pmpph(ix))

c21 cqs  compute junction pressure

        if (redo) then
         pjun = po(kk) + (psldd - psmff*velfj(i)
     &          - psmgg*velgj(i))*signvc
        else
         pjun = po(kk) + (psldd - psmff*velfjo(i)
     &          - psmgg*velgjo(i))*signvc
        endif

c   cqs  ***************************************************************************
c   cqs  * start of test for knowing if the flow is still choked in the new time step
c   cqs  ***************************************************************************
c22 cqs  choke on last time step?. See step 3

        if (choke) then

c23 cqs  Unchoking test.

          scrach = max(pjun,scvjck(ix))
          pll = po(kk) + scvtur(ix)*(po(ll) - po(kk))

c24 cqs   this is the test for knowing if the flow is still choked in the new time step

          if (chngno(42)) then
           if (pjun.gt.po(kk) .or. scvjck(ix).lt.pll) choke=.false.
          else
           if (scrach.lt.pll .or. pjun.gt.po(kk)) choke=.false.
          endif
        endif
c   cqs  ***************************************************************************
c   cqs  * end of  test for knowing if the flow is still choked in the new time step
c   cqs  ***************************************************************************
c
```

```
c25 cqs  set qual to the static quality at junction based on donor properties

         voidjc = min(vgscmx,voidgj(i))
         quall = voidjc*rhogj(i)
         quall = quall/(quall + (1.0 - voidjc)*rhofj(i))
         qualty = qualla

c26 cqs  donor gas void fraction >0.10? ("yes" go to 228, two-phase model, "no" continue with subcooled model)

         if (voidgj(i) .gt. vgtpmn) go to 228

         jcatsc = 1.0

c27 cqs  Subcooled choking criterion. This is only a comment of R5

cSSS
```

```
            if (err) go to 228

c35 cqs     estimate sonic velocity at throat

            sonic = sqrt(max(0.0,zip - psatt*rhofin))

c36 cqs      quale(kk) > 0.0

            if (quale(kk) .gt .0.0) sonic = max(sonic,sounde(kk))

c37 cqs     vc<sonic*at/2. First test for choking

            if (vc .lt. 0.5*at*sonic) go to 1990
         endif

c cqs ************************************************************
c cqs end   first test of choking. Subcooled model*****************b
c cqs ************************************************************


c38 cqs  this is only a comment
c  Second test of choking. The second test is at c74

c39 cqs  get thermodynamic properties

         if (nfluid .eq. 1) then
           call sth2x1 (fa(ndxstd),prop,err)
         elseif (nfluid .eq. 2) then
           call std2x1 (fa(ndxstd),prop,err)
$if def,newwtrp,3
         elseif (nfluid .eq. 12) then
           call stpu2t (fa(ndxstd),prop,36,1)
           err = lprop(32)
         else
           call  strtx (fa(ndxstd),prop,err)
         endif

c40 cqs steam table failure?

        if (err) go to 1990

c41 cqs  compute wall friction

         frwall = frcfj*at

c42 cqs  estimate throat velocity

         zipcon = zip + frwall**2 - psatt*rhofin

c43 cqs
         aj = ajun(i)*athrot(i)
         scrach = max(0.0,zipcon)
         sonic1 = max(0.0,sqrt(scrach) - frwall)

c44 cqs  sonic>0 and not a time dependent volume

         if (iand(vctrl(kk),1).ne.0 .or. sonic1.le.0.0) then
```

```
c  Time-dependent donor volume or negative Bernoulli extrapolated
c   velocity
           dpdt = (hsubg - hsubf)/(ttt*(vsubgg - vsubff))
           if (sonic1 .eq. 0.0) sonic1 = vsubff*dpdt
     &     *sqrt(ttt/(cppf - ttt*
     &     vsubff*dpdt*(2.0*betf - kpaf*dpdt)))

c45 cqs
           sonic = sonic1
           delpfi = 0.0
           go to 219
         endif

c cqs ************************************************************
c cqs start ALJ model ********************************************
c cqs ************************************************************

c  Get saturated liquid properties.


         press = pjun
         quall = qualty
         if (nfluid .eq. 1) then
           call sth2x2 (fa(ndxstd),prop,err)
         elseif (nfluid .eq. 2) then
           call std2x2 (fa(ndxstd),prop,err)
$if def,newwtrp,3
         elseif (nfluid .eq. 12) then
           call stpu2p (fa(ndxstd),prop,36,1)
           err = lprop(32)
         else
          call strpx (fa(ndxstd),prop,err)
         endif
         if (err) go to 1990

c  Constants for Jones-Alamgir-Lienhard correlation.

c47 cqs  setup coefficients dpfioc, avolkk

         dpfioc = (2.72958e9*(ttt*1.5448787e-3)**13.76)*sigma(kk)*
     &   sqrt(sigma(kk))*vsubgg/(vsubgg - vsubff)
         avolkk = min(aj*50.0,avolkk)
         scrach = avolkk - aj


         if (iand(jc(i),256) .eq. 0) then

c  Smooth junction.
           if ((kk.eq.k .and. iand(jc(i),8192).ne.0) .or.
     &     (kk.eq.l .and. iand(jc(i),4096).ne.0)) then
c  Upstream volume is cross flow volume.
             avkxj = 3.141592*diamv(ky)**2/4.
             dxkxj = diamv(ky)*0.5
             scrach = (avkxj - aj)/(dxkxj*aj)
           else
             scrach = 2.0*scrach/(dl(ky)*aj)
           endif
```

```
        else
          scrach = 0.1*scrach/(diamv(ky)*aj)
        endif

c51 cqs  compute constants for ALJ model

        dprcon = ((rhof(kk)*max(0.0,scrach))**0.8)*2.078e-8
        ficons =  (rhof(kk)*(aj/avolkk)**2)*6.9984e-2

c cqs    the constant 6.9984e-2 is 7.2e-2 in TRAC-BF1

c52 cqs start iteration loop. This is only a comment
c  Iteration solution for jones-alamgir-lienhard correlation.

c53 cqs  compute starting estimating for sonic2

        sonic2 = sqrt(zip + frwall**2) - frwall
        sonic2 = min(sonic2,sqrt(zipcon + dpfioc*rhofin*4.9) -
     &  frwall)

c54 cqs
        do 218 it = 1,24

c55 cqs
          sonic = (sonic1 + sonic2)*0.5
          scrach = sqrt(1.0 + dprcon*sonic**2.4)
          delpfi = dpfioc*scrach - ficons*sonic**2
          zip = zipcon

c56 cqs   compute throat velocity squared based on throat pressure calculated from ALJ equation ZIP

          if (delpfi.gt.0.0) zip = zip + delpfi*rhofin

c57 cqs
          zip = sqrt(max(zip,0.0))

c58,59,60 cqs

          if (sonic - max(0.0,zip - frwall)) 216,219,217

c61 cqs

  216     sonic1 = sonic
          go to 218

c62 cqs

  217     sonic2 = sonic
  218   continue

c cqs ************************************************************
c cqs end ALJ model ***********************************************
c cqs ************************************************************

c63 cqs  subcooled speed of sound

        sonic = (sonic1 + sonic2)*0.5
```

```
c64 cqs
c   cqs  vgscmx= 1.0e-5. If void>1.0e-5 or quality>1.0e-9 then we are in TRANSITION REGION
c   cqs  the program go on in the two phase region (c75).-------->>>>>TWO PHASE MODEL

  219    if (voidgj(i).gt.vgscmx .or. qualaj(i).gt.1.0e-9) go to 226

c*****************************************************************************************
c   cqs start HEM model for subcooled region  (void<1.0e-5) ****************************
c*****************************************************************************************

c   cqs We are in subcooled region. The maximun of ALJ and start of HEM(void=0.0) is used.
c   cqs it is necesary to calculate a_sound-HEM(void=0.0)

         jcatsf = avrho*(quall*vsubgg + (1.0 - quall)*vsubff)
         sonic2 = 0.0
         if (ttt .le. tcrit-7.0) then
c  Get saturated liquid-vapor properties of two-phase mixture.
           press = pjun
           quall = qualty
           ubarr = quall*ugj(i) + (1.0 - quall)*ufj(i)
           ubarr = ubarr + po(kk)*(quall*rhofj(i)
     &     + (1.0 - quall)*rhogj(i))/
     &     (rhogj(i)*rhofj(i)) - press*(quall*vsubgg +
     &     (1.0 - quall)*vsubff)
     &     - (delpzz+quall*(convgg - convff)+convff)*signvc

c cqs ubarr= u_mixture for calling steam-tables

           if (nfluid .eq. 1) then
             call sth2x6 (fa(ndxstd),prop,iq,err)
           elseif (nfluid .eq. 2) then
             call std2x6 (fa(ndxstd),prop,iq,err)
$if def,newwtrp,4
           elseif (nfluid .eq. 12) then
             call stpu2pu (fa(ndxstd),prop,36,1)
             iq = iprop(36)
             err = lprop(32)
           else
             call strpu1 (fa(ndxstd),prop,iq,err)
           endif

           if (err) then
             press = pjun
             quall = qualty
             if (nfluid .eq. 1) then
               call sth2x2 (fa(ndxstd),prop,err)
             elseif (nfluid .eq. 2) then
               call std2x2 (fa(ndxstd),prop,err)
$if def,newwtrp,3
             elseif (nfluid .eq. 12) then
               call stpu2p (fa(ndxstd),prop,36,1)
               err = lprop(32)
             else
               call strpx (fa(ndxstd),prop,err)
             endif
             if (err) go to 1990
```

```
            dpdt = (hsubg - hsubf)/(ttt*(vsubgg - vsubff))
            sonic1 = vsubff*dpdt*sqrt(ttt/(cppf - ttt*vsubff*dpdt*
     &      (2.0*betf - kpaf*dpdt)))

c cqs iq=2 two phase

          elseif (iq.eq.2) then

            dpdt = (hsubg - hsubf)/(ttt*(vsubgg - vsubff))
            ahe =  ttt/(quall*(cppg - ttt*vsubgg*dpdt*
     &                    (2.0*betg - kpag*dpdt))
     &      + (1.0 - quall)*(cppf - ttt*vsubff*dpdt*
     &                    (2.0*betf - kpaf*dpdt)))
            if (ahe .ge. 0.0) then
              sonic1 = vsubff*dpdt*sqrt(ahe)
            else
              press = pjun
              quall = qualty

              if (nfluid .eq. 1) then
                call sth2x2 (fa(ndxstd),prop,err)
              elseif (nfluid .eq. 2) then
                call std2x2 (fa(ndxstd),prop,err)
$if def,newwtrp,3
              elseif (nfluid .eq. 12) then
                call stpu2p (fa(ndxstd),prop,36,1)
                err = lprop(32)
              else
                call strpx (fa(ndxstd),prop,err)
              endif
              if (err) go to 1990

              dpdt = (hsubg - hsubf)/(ttt*(vsubgg - vsubff))
              sonic1 = vsubff*dpdt*sqrt(ttt/(cppf - ttt*vsubff*dpdt*
     &        (2.0*betf - kpaf*dpdt)))
            endif

c cqs iq=1 liquid

          elseif (iq.eq.1) then

            press = pjun
            quall = qualty

            if (nfluid .eq. 1) then
              call sth2x2 (fa(ndxstd),prop,err)
            elseif (nfluid .eq. 2) then
              call std2x2 (fa(ndxstd),prop,err)
$if def,newwtrp,3
            elseif (nfluid .eq. 12) then
              call stpu2p (fa(ndxstd),prop,36,1)
              err = lprop(32)
            else
              call strpx (fa(ndxstd),prop,err)
            endif
            if (err) go to 1990
```

```
c cqs ************************************
c cqs sound spped of HEM with void=0.0
c cqs this is the model that is normally used
c cqs in HEM model for subcooled liquid
c cqs ************************************

            dpdt = (hsubg - hsubf)/(ttt*(vsubgg - vsubff))
            sonic1 = vsubff*dpdt*sqrt(ttt/(cppf - ttt*vsubff*dpdt*
     &      (2.0*betf - kpaf*dpdt)))

c cqs iq=3 vapor

          elseif (iq.eq.3) then
            press = pjun
            quall = qualty

            if (nfluid .eq. 1) then
              call sth2x2 (fa(ndxstd),prop,err)
            elseif (nfluid .eq. 2) then
              call std2x2 (fa(ndxstd),prop,err)
$if def,newwtrp,3
            elseif (nfluid .eq. 12) then
              call stpu2p (fa(ndxstd),prop,36,1)
              err = lprop(32)
            else
              call strpx (fa(ndxstd),prop,err)
            endif
            if (err) go to 1990

            dpdt = (hsubg - hsubf)/(ttt*(vsubgg - vsubff))
            sonic1 = vsubff*dpdt*sqrt(ttt/(cppg - ttt*vsubgg*dpdt*
     &      (2.0*betg - kpag*dpdt)))
          endif


c*****************************************************************************
c   cqs end  of HEM model for subcooled region ***********************************
c*****************************************************************************

c  Set sonic velocity to maximum of equilibrium sound speed
c  and velocity needed to obtain required pressure drop.

c66 cqs
          if (sonic .lt. sonic1/jcatsf) then
c68 cqs
            jcatsc = jcatsf
c67 cqs
            sonic = sonic1
          else

c69,70 cqs
            if (delpfi .gt. 0.0) sonic2 = dpfioc*1.2*dprcon*
     &      sonic**1.4/scrach - 2.0*ficons*sonic
          endif
        endif
```

```
c73 cqs

         dsondp = at/(sonic*rhof(kk) - sonic2)
         xej(i) = 0.
         sonicj(i) = sonic/jcatsc

c cqs    jcat is relaxed with the value in the last time step

c71 cqs
         jcatn(i) = jcato(i) + 0.1*(jcatsc - jcato(i))
c72 cqs
         sonic = sonic/jcatsc
         dsondp = dsondp/jcatsc
         sonic = at*sonic

c cqs ** start write output ******************************************
         if (help .ne. 0) then
         if( iand(ihlppr(1),ishft(1,18)).ne.0 ) then
           if( iand(jcex(i),ishft(1,20)).ne.0 ) then
           if (iskip .eq. 0) then
             iskip = 1
             call helphd ('jchoke',7)
           endif
           write (output,1909) junno(i),ncount,timehy
 1909  format ('0From jchoke ',2i10,1p,e13.5)
           write (output,1910) voidgj(i),signvc
 1910  format (' Junction void fraction',2x,1p,e13.5,'flow direction',
     & 3x,e13.5)
           write (output,1908) psmff,psmgg,psldd,pjun,choke,press,psatt,
     &     po(kk),po(11)
 1908  format ('   psmff',9x,'psmgg',9x,'psldd',9x,'pjun',9x,'choke',
     & 8x,'press',8x,'psatt',8x,'po-up',8x,'po-dn'/' ',
     & 1p,4e13.5,113,4e13.5)
           write (output,1911) sounde(kk),sonic,dsondp,quale(kk),
     &     quals(kk),velfj(i),velgj(i),vc
 1911  format ('   sounde-up',4x,'sonic',8x,'dsondp',7x,'quale-up',
     & 5x,'qualso-up'   ,4x,'velfj(i)',5x,'velgj(i)',5x,'vc'/1p,8e13.5)
           endif
         endif
         endif
c cqs ** end write output ********************************************
c
c74 cqs
c   cqs  second choking criterion. Subcooled model

         if (choke .or. vc.ge.sonic) go to 820
         go to 1990

c*****************************************************************************
c   cqs end  of subcooled region ***********************************************
c*****************************************************************************

c75 cqs
c   cqs  the calculation in transition region (1.0e-5<void<0.1) go on in this point.
c   cqs  it comes from (c64)

  226    transr = .true.
```

```
         sonics = sonic

c76 cqs  go to two-phase flow-model

         go to 232


cTTT
```

```
c86 cqs set RATIOS to 1

        ratios = 1.0

c87 cqs
        if (choke) then
          if (redo) then
            ratios = sqrt(1.0 + max(zip*(velgj(i)/velfj(i) - 1.0),0.0))
          else
            ratios = sqrt(1.0 + max(zip*(velgjo(i)/velfjo(i) - 1.0),
     &      0.0))
          endif
        endif

c88 cqs

        jcattp = 1.0

c89 cqs  noncondensable quality < 1.E-6

        if (qualaj(i).lt.1.0e-6) go to 236

cNNN
```

```
c  Sonic velocity.
           sonic = sqrt(vbarr*pjun*(cvaq + ra)/cvaq)
           jcattp = rhogj(i)*vbarr
           go to 251
         endif
c  Calculation of equilibrium state.
c  Find saturation temperature of pjun to set up the upper limit.
         if (nfluid .eq. 1) then
           call psatpd (tmaxl,pjun,dpdt,2,err)
         elseif (nfluid .eq. 2) then
           call pstpd2 (tmaxl,pjun,dpdt,2,err)
$if def,newwtrp,5
         elseif (nfluid .eq. 12) then
           prop(2) = pjun
           call stpu00 (fa(ndxstd),prop,36,1,2)
           tmaxl = prop(1)
           dpdt = prop(3)
         else
           call strsat(fa(ndxstd),2,pjun,tmaxl,dpdt,err)
         endif
         if (err) tmaxl = tcrit
         tmaxl = tmaxl*0.9999
c  Initialize equilibrium temperature, ttt -- te.
         ttt = min(satt(kk),tmaxl)
         jstop = .false.
         do 260 it = 1,16
c  Get saturation vapor properties.
           if (nfluid .eq. 1) then
             call sth2x1 (fa(ndxstd),prop,err)
           elseif (nfluid .eq. 2) then
             call std2x1 (fa(ndxstd),prop,err)
$if def,newwtrp,3
           elseif (nfluid .eq. 12) then
             call stpu2t (fa(ndxstd),prop,36,1)
             err = lprop(32)
           else
             call strtx (fa(ndxstd),prop,err)
           endif
           if (err) go to 252
           dpdt = (hsubg - hsubf)/(ttt*(vsubgg - vsubff))
           dusdtt = cppg - vsubgg*(betg*press - (press*kpag -
     &     ttt*betg)*dpdt)
           uss = usubgg
           vss = vsubgg
           kpags = kpag
           betgs = betg
           pa = pjun-press
c  Call steam tables interpolation routine to get liquid properties from
c  temperature and pressure.
c  Note-liquid is subcooled.
           press = pjun
           if (nfluid .eq. 1) then
             call sth2x3 (fa(ndxstd),prop,iq,err)
           elseif (nfluid .eq. 2) then
             call std2x3 (fa(ndxstd),prop,iq,err)
$if def,newwtrp,4
           elseif (nfluid .eq. 12) then
```

```
            call stputp (fa(ndxstd),prop,36,1)
            err = lprop(32)
            iq = 1
          else
            call  strtp (fa(ndxstd),prop,iq,err)
          endif
          if (err .or. iq.ne.1) go to 252
          dufdtt = cpp - betaa*pjun*vbarr
c  Internal energy and specific heat*quala of air.
          term = max(ttt - tao,0.0)
          ua = cvao*ttt + 0.5*dcva*term**2+uao
          cvaq = (cvao + dcva*term)*qa
c  Values needed for newton iteration.
          term = vss*(ujun - qa*ua - qair1*ubarr)
          f1 = pa*term - qara*(uss - ubarr)*ttt
          df1dtt = term*(pa*(betgs - kpags*dpdt) - dpdt)- pa*vss*
     &    (cvaq + qair1*dufdtt) - qara*((uss - ubarr) + ttt*
     &    (dusdtt - dufdtt))
          if (jstop) go to 262
          dtt = f1/df1dtt
          ttt = max(min(ttt - dtt,tmaxl),ttrip)
          if (abs(dtt) .lt. toler*ttt) jstop = .true.
  260    continue
c  No solution after 15 iterations.
        go to 252
c  End of iteration.
  262    vff = vbarr
        dufdpt = vff*(pjun*kpa - ttt*betaa)
c  Calculation of equilibrium quality,xe.
        xe = (ujun - ubarr - qa*(ua - uss))/(uss - ubarr)
        if(xe .lt. qa) go to 252
        if (xe .gt. 1.005) go to 263
c  Calculation of equilibrium sound speed.
        qs = xe - qa
        qf = 1.0 - xe
        term = vss*(betgs - kpags*dpdt)
c  Set up the equation: a* (ddx/dp)s,(dt/dp)s =a0.
        c11 = uss-ubarr + pjun*(vss - vff)
        c12 = qf*(dufdtt + pjun*betaa*vff) + cvaq + qs*(dusdtt +
     &  pjun*term)
        c21 = pa*vss
        c22 = qs*(pa*term - dpdt*vss) - qara
        a01 = -qf*(dufdpt - kpa*vff*pjun)
        a02 = -qs*vss
c  Solution for (ddx/dp)s --dtt/det, (dt/dp)s -- dtg/det.
c  det = c11*c22-c12*c21
        dtt = a01*c22 - a02*c12
        dtg = a02*c11 - a01*c21
        vbarr = qf*vff + qs*vss
        jcattp = avrho*vbarr*ratios
c  ahe=-(dv/dp)s
        ahe = kpa*vff*qf - ((qf*vff*betaa + qs*term)*dtg +
     &  (vss - vff)*dtt)/(c11*c22 - c12*c21)
        if (ahe .le. 0.0) go to 252
        sonic = vbarr/sqrt(ahe)
        go to 251
c  Single phase vapor.
```

```
c  Initialize press and tg.
  263     tg = ttt
          press = pjun - pa
c  Newton iteration to find press,tg.
          jstop = .false.
          do 283 it = 1,16
c  Find psatt of tg.
            if (nfluid .eq. 1) then
              call sth2x0 (tg,psatt,err)
            else  if (nfluid .eq. 2 ) then
              call std2x0 (tg,psatt,err)
$if def,newwtrp,4
            elseif (nfluid .eq. 12) then
              prop(1) = tg
              call stpu0p (fa(ndxstd),prop,36,1)
              err = lprop(32)
            else
              call  strsat (fa(ndxstd),1,tg,psatt,dummy,err)
            endif
            if (.not.err) then
              if (press .ge. psatt) go to 268
            endif
c  Superheated vapor.
            ttt = tg
            if (nfluid .eq. 1) then
              call sth2x3 (fa(ndxstd),prop,iq,err)
            elseif (nfluid .eq. 2) then
              call std2x3 (fa(ndxstd),prop,iq,err)
$if def,newwtrp,4
            elseif (nfluid .eq. 12) then
              call stputp (fa(ndxstd),prop,36,1)
              err = lprop(32)
              iq = 3
            else
              call strtp (fa(ndxstd),prop,iq,err)
            endif
            if (err) go to 252
            if (iq .eq. 3) then
              usubgg = ubarr
              vsubgg = vbarr
              cppg = cpp
              kpag = kpa
              betg = betaa
              go to 270
            endif
c  Subcooled steam.
c  Extrapolation of vapor properties.
  268       if (nfluid .eq. 1) then
              call sth2x2 (fa(ndxstd),prop,err)
            elseif (nfluid .eq. 2) then
              call std2x2 (fa(ndxstd),prop,err)
            else
              call strpx (fa(ndxstd),prop,err)
            endif
            if (err) go to 252
            term = vsubgg
            vsubgg = term*(1.0 + betg*(tg - ttt))
```

```
          if (vsubgg .le. 0.0) go to 252
          usubgg = usubgg + (cppg - term*betg*press)*(tg - ttt)
          betg = betg*term/vsubgg
c  Internal energy and specific heat*quala of ideal gas.
  270     term = max(tg - tao,0.0)
          ua1 = cvao*tg + 0.5*dcva*term**2+uao
          cvaq = (cvao + dcva*term)*qa
c  Iteration parameters.
          pa = pjun - press
          f1 = pa *qair1*vsubgg - qara*tg
          ff2 = ujun - qa*ua1 - qair1*usubgg
          df1dps = -qair1*vsubgg*(1.0 +pa*kpag)
          df1dtg = pa*qair1*vsubgg*betg - qara
          df2dps = -qair1*vsubgg*(press*kpag - tg*betg)
          df2dtg = -cvaq - qair1*(cppg - press*vsubgg*betg)
          rdet = 1.0/(df1dps*df2dtg - df2dps*df1dtg)
          if (jstop) go to 286
          dps = rdet*(df2dtg*f1 - df1dtg*ff2)
          dtg = rdet*(df1dps*ff2 - df2dps*f1)
          press = max(min(press - dps,pjun),pmin)
          tg =   min(max(tg - dtg,ttrip),tcrit)
          if (max(abs(dps/press),abs(dtg/tg)) .lt. toler)
     &    jstop=.true.
  283    continue
c  No solution after 15 iterations.
         go to 252
  286    vbarr = qair1*vsubgg
         jcattp = rhogj(i)*vbarr
c  Calculation of single phase sound speed.
c  Set up the equation: a* (dps/dp)s,(dtg/dp)s =a0.
c  Note -- c11 and c12 are defined through equivalence to.
c    df1dps and df1dtg
c  a01 = -vbarr
         c21 = -vbarr*(tg*betg + pa*kpag)
         c22 = cvaq + qair1*cppg + pa*vbarr*betg
c  a02 = 0.0
c  Solution for (dps/dp)s -- dps/det, (dtg/dp)s -- dtg/det.
c*    det = c11*c22-c12*c21
c*    dps = a01*c22
c*    dtg = -a01*c21
c
c  ahe = a01/-(dv/dp)s
         ahe = (c12*c21 - c11*c22)/(betg*c21 + kpag*c22)
         if (ahe.le.0.0) go to 252
         sonic = sqrt(ahe)
         go to 251
c

cNNN
```

```
c90 cqs  call steam tables

  236    if (nfluid .eq. 1) then
           call sth2x6 (fa(ndxstd),prop,iq,err)
         elseif (nfluid .eq. 2) then
           call std2x6 (fa(ndxstd),prop,iq,err)
$if def,newwtrp,4
         elseif (nfluid .eq. 12) then
           call stpu2pu (fa(ndxstd),prop,36,1)
           iq = iprop(36)
           err = lprop(32)
         else
           call strpu1 (fa(ndxstd),prop,iq,err)
         endif

c91 cqs  steam table failure or vapor with T>Tcrit

         if (err .or. iq.eq.4) go to 252

c92 cqs

c cqs iq is calculated in sth2x6 (for nfluid=1, water)
c cqs selection of the model iq= 4 (T>Tcrit); 3 (vapor); 2 (two-phase); 1 (liquid)

         if (iq - 2) 244,248,240

c cqs    if vapor goto 240; two-phase 248; saturated liquid 244

cVVVVVVVVVVVVVVVVVVVVVVVVVVVVVVVVVVVVVVVVVVVVVVVVVVVVVVVVVVVVVVVVVVVVVVVVVVVV
c   cqs  start vapor model VVVVVVVVVVVVVVVVVVVVVVVVVVVVVVVVVVVVVVVVVVVVVVVVVVVV
cVVVVVVVVVVVVVVVVVVVVVVVVVVVVVVVVVVVVVVVVVVVVVVVVVVVVVVVVVVVVVVVVVVVVVVVVVVVV

c93 cqs  vapor with T<Tcrit
c94 cqs  compute dpdt

  240    dpdt = cpp/(ttt*vbarr*betaa)

c95 cqs  compute AHE

         ahe =  dpdt/(vbarr*(kpa*dpdt - betaa))

c96 cqs  compute JCATTP using junction vapor density and v from steam tables

         jcattp = rhogj(i)*vbarr

c97 cqs  AHE<0.0

         if (ahe .lt. 0.0) go to 252

c98 cqs
         sonic = vbarr*sqrt(ahe)

cVVVVVVVVVVVVVVVVVVVVVVVVVVVVVVVVVVVVVVVVVVVVVVVVVVVVVVVVVVVVVVVVVVVVVVVVVVVV
c   cqs  end   vapor model VVVVVVVVVVVVVVVVVVVVVVVVVVVVVVVVVVVVVVVVVVVVVVVVVVVV
cVVVVVVVVVVVVVVVVVVVVVVVVVVVVVVVVVVVVVVVVVVVVVVVVVVVVVVVVVVVVVVVVVVVVVVVVVVVV

         go to 251
```

```
cSSS
```

```
c109 cqs test the transition flag is set TRANS= TRUE?
         if (transr) go to 258
         go to 257

c110 cqs test the transition flag i.e. NOT TRANSR
c
  251    if (.not.transr) go to 257

c*********************************************************************
c   cqs  TRANSITION ZONE. 1.0e-5<void<0.1 . Interpolate SONIC and JCAT
c*********************************************************************

c111 cqs Interpolate ratio of sound spped and throat density ratio using interpolation factor XISCTP

  258    xintrp = xisctp

c    cqs transition between subcooled and two-phase models

         sonic = sonics/jcatsc + xintrp*(sonic/jcattp - sonics/
     &   jcatsc)

c112 cqs interpolate the derivative of the sound speed with pressure DSONDP

         dsondp = xintrp*0.15/(sounde(kk)*rho(kk)*jcattp) +
     &   (1.0 - xintrp)/(sonics*rhof(kk)*jcatsc)

c113 cqs interpolate throat density ratio

         jcatn(i) = jcatsc + xintrp*(jcattp - jcatsc)
         if (.not.redo) then

c114 cqs    underrelax density ratio JCATN

           jcatn(i) = jcato(i) + 0.1*(jcatn(i) - jcato(i))
         endif

c115 cqs --------------->>>>>>>> c119
         go to 256


c*******************************************************
c   cqs  start two-phase  ZONE. void>0.1. Underrelax JCAT
c*******************************************************

c116 cqs underrelax JCATTP with JCATO using variable relaxation factor RELAX
c
  257    if (redo) then
           jcatn(i) = jcatn(i) + 0.1*(jcattp - jcatn(i))
         else
           jcatn(i) = jcato(i) + 0.1*(jcattp - jcato(i))
         endif

c  In the two-phase region relax jcat.
c  ramp the old time weighting factor to ninety percent at a void
c  fraction fifty percent greater than the upper bound of the
c  transition region between the subcooled and two-phase regions.
```

```
c cqs vgtpmn=0.1

        xitpsh = (voidgj(i) - vgtpmn)/(0.5*vgtpmn)
        xitpsh = max(0.0,min(1.0,xitpsh))
        xitpsh = xitpsh*xitpsh*(3.0 - 2.0*xitpsh)
        relax = 0.9*xitpsh
        if (redo) then
          jcattp = jcattp + relax*(jcatn(i) - jcattp)
        else
          jcattp = jcattp + relax*(jcato(i) - jcattp)
        endif

c118 cqs calculate sound speed derivative DSONDP

        dsondp = 0.15/(sounde(kk)*rho(kk)*jcattp)

c117 cqs

        sonic = sonic/jcattp

c*****************************************************
c   cqs  end two-phase  ZONE. void>0.1. Underrelax JCAT
c*****************************************************

c*************************************************************
c   cqs  start two-phase and transition region. Underrelax sonic
c*************************************************************

c119 cqs underrelax SONIC with old time value using variable relaxation factor RELAX

c  In the transition region relax sonic
c  Ramp the old time weighting factor to ten percent at a void fraction
c  fifty percent greater than the upper bound of the
c  transition region between the subcooled and two-phase regions.

c cqs vgtpmn= 0.1. If voidgj(i) > 0.1 then xisctp=0.0 and relax=0.9

  256   xisctp = (voidgj(i) - vgtpmn)/(0.5*vgtpmn)
        xisctp = max(0.0,min(1.0,xisctp))
        xisctp = xisctp*xisctp*(3.0 - 2.0*xisctp)
        relax = 0.8*(1.e0 - xisctp) + 0.10
        if (sonicj(i).ne.0.0e0) sonic = sonic + relax*(sonicj(i) -
     &  sonic)
        sonicj(i) = sonic
        xej(i) = quall

c*************************************************************
c   cqs  end two-phase and transition region. Underrelax sonic
c*************************************************************

c120 cqs
        sonic = at*sonic
        dsondp = at*dsondp

c cqs ** start write output*****************************************
c
```

```
          if (help .ne. 0) then
          if( iand(ihlppr(1),ishft(1,18)).ne.0 ) then
            if( iand(jcex(i),ishft(1,20)).ne.0 ) then
            if (iskip .eq. 0) then
              iskip = 1
              call helphd ('jchoke',7)
            endif
            write (output,1909) junno(i),ncount,timehy
            write (output,1910) voidgj(i),signvc
            write (output,1908) psmff,psmgg,psldd,pjun,choke,press,psatt,
     &      po(kk),po(ll)
            write (output,1912) iq,sounde(kk),sonic,quale(kk),
     &      quals(kk),velfj(i),velgj(i),vc
 1912   format('    iq',2x,'sounde-up',4x,'sonic',8x,'quale-up',5x,
     &         'qualso-up',4x,'velfj(i)',5x,'velgj(i)',5x,'vc'/
     &         i6,1p,7e13.5)
c
            endif
          endif
          endif
c cqs ** end   write output*************************************************

c122 cqs NOT CHOKE and VC<SONIC?. number 953 is not used.
c cqs second test of choking criterion. Two-phase zone

  953     if (.not.choke .and. vc.lt.sonic) go to 1990

cTTT
```

```
        vpgenn = vapgno(kk)*ddx

c127 cqs check sign on VAPGEN

        if (vpgenn .ge. 0.0) then
c128 cqs
          vpgnxx = -vpgenn/max(1.0e-15,voidg(kk))
        else
c129 cqs
          vpgnxx = vpgenn/max(1.0e-15,voidf(kk))
        endif

c130 cqs set up matrix terms for velocity solution

        term = atin*(1.0 + jcatn(i)/jcato(i))*0.5
        f1 = term*velfjo(i)
        ff2 = term*velgjo(i)
        virmas = faaj(i)*avrho
        sumgg = (rhog(kk) + virmas)*ddx
        sumff = (rhof(kk) + virmas)*ddx
c  Incorporate fij(i), fxj(i) and c0j(i) into interphase
c  friction terms of momentum difference equation.
c  (figjj and fifjj now replace fjfg).
        c0 = c0j(i)
        c0 = min(1.33,max(1.0,c0))
        if (voidg(kk) .gt. 0.0) c0 = min(c0,1.0/voidg(kk))
        if (voidg(kk) .lt. 0.99999) then
          c1 = (1.0 - c0*voidg(kk))/(1.0 - voidg(kk))
        else
          c1 = ((voidg(kk) - 0.99999)+(1.0 - voidg(kk))*(1.0 -
     &    0.99999*c0)*1.0e5)*1.0e5
        endif
        figjj = (dl(ky)*(fij(i)*(abs(c1*velgjo(i) - c0*velfjo(i))*
     &  c1 + 0.01))*0.5 + fidxup(ix))/max(1.0e-20,voidgj(i)*
     &  voidfj(i))
        fifjj = (dl(ky)*(fij(i)*(abs(c1*velgjo(i) - c0*velfjo(i))*
     &  c0 + 0.01))*0.5 + fidxup(ix))/max(1.0e-20,voidgj(i)*
     &  voidfj(i))
        frcgj = frcgj*(1.0 - fxj(i))
        frcfj = frcfj*(1.0 - fxj(i))
c  Incorporate interphase friction terms fifjj and figjj into difff and
c  difgg.
        difgg = sumgg + (rhog(kk)*(frcgj + ff2) + figjj - vpgnxx)*dt
        difff = -sumff - (rhof(kk)*(frcfj + f1) + fifjj - vpgnxx)*dt
        difld = sumgg*velgjo(i) - sumff*velfjo(i) - ((rhog(kk) -
     &  rhof(kk))*delpzz + rhog(kk)*(convgg - convgi) - rhof(kk)*
     &  (convff - convfi))*dt

c131 cqs
c  Velocity solution.

c132 cqs compute SUMOLD, DET terms needed for velocity solution

  839   sumld = arsm*sonic*signvc
        det = 1.0/(difff*argf - difgg*arfg)
```

```
c133 cqs solve 2x2 matrix for vapor and liquid velocties

         vf = (difld*argf - difgg*sumld)*det
         vg = (difff*sumld - difld*arfg)*det
         if (err) relax = 0.9

c*********************************************************************
c cqs ** end   the calculation of vapor and liquid velocities***********
c*********************************************************************

c134 cqs check for cocurrent flow

         if (vg*vf .le. 0.0) then

c135 cqs   counter-current flow

           det = 1.0/(argf + arfg)
           vf = sumld*det
           vg = vf
           difff = 1.0
           difgg = -difff
           difld = 0.0
         endif

c136 cqs co-current flow. Set matrix terms for final velocity equations.

         if (implt .eq. 0) then
           velfj(i) = vf
           velgj(i) = vg
           scrach = dsondp*arsm*det
           vfdpk(ix+kl) = -difgg*scrach
           vgdpk(ix+kl) = difff*scrach
           vfdpl(ix-kl) = 0.0
           vgdpl(ix-kl) = 0.0
         else
           isf = jcnxd(i)
           idg = jcnxd(i+1)
           coefv(isf) = arfg
           coefv(isf+1) = argf
           sourcv(is) = sumld
           coefv(idg-1) = difff
           coefv(idg) = difgg
           sourcv(is+1) = difld
           sourcv(is) = relax*(arfg*velfjo(i) + argf*velgjo(i)) +
     &     (1.0 - relax)*sumld
           sourcv(is+1) = relax*(difff*velfjo(i) + difgg*velgjo(i)) +
     &     (1.0 - relax)*difld
           sumdpk(ix+kl) = dsondp*arsm
           difdpk(ix+kl) = 0.0
           sumdpl(ix-kl) = 0.0
           difdpl(ix-kl) = 0.0
         endif

c137 cqs set choking flag bit in jc

         jc(i) = ior(jc(i),1)
```

```
c cqs start write output*********************************
         if (help .ne. 0) then
         if( iand(ihlppr(1),ishft(1,18)).ne.0 ) then
           if( iand(jcex(i),ishft(1,20)).ne.0 ) then
             write (output,1914) junno(i),ncount,timehy,
     *       velfjo(i),velfj(i),velgjo(i),velgj(i)
           endif
         endif
         endif
 1914  format(' Final vel',2i10,1p,5e13.5)
c cqs end write output ********************************

c        Do calculations again if velocity or
c        density ratio have changed too much.
         if (chngno(43)) then
          if (redo) then
           checkj = abs((jcatn(i) - jcsave)/jcatn(i))
           checkv = voidfj(i)*abs((velfj(i) - vfsave)/velfj(i))
     &            + voidgj(i)*abs((velgj(i) - vgsave)/velgj(i))
          else
           checkj = abs((jcatn(i) - jcato(i))/jcatn(i))
           checkv = voidfj(i)*abs((velfj(i) - velfjo(i))/velfj(i))
     &            + voidgj(i)*abs((velgj(i) - velgjo(i))/velgj(i))
          endif
          if (checkj.gt.0.01 .or. checkv.gt.0.01) then
           vfsave = velfj(i)
           vgsave = velgj(i)
           jcsave = jcatn(i)
           if (redo) then
            nredo = nredo - 1
            if (nredo.gt.0) go to 100
           else
            redo = .true.
            nredo = 10
            go to 100
           endif
          endif
         endif

c138 cqs under relaxation for velocities

c  Under-relaxation treatment for choking.
         if (implt .eq. 0) then
           velfj(i) = velfjo(i) + (1.0 - relax)*(velfj(i) -
     &     velfjo(i))
           velgj(i) = velgjo(i) + (1.0 - relax)*(velgj(i) -
     &     velgjo(i))
c
           if (help .ne. 0) then
           if( iand(ihlppr(1),ishft(1,18)).ne.0 ) then
             if( iand(jcex(i),ishft(1,20)).ne.0 ) then
             write (output,1915) junno(i),ncount,
     &       timehy,relax,velfj(i),velgj(i)
             endif
           endif
           endif
  1915  format (' Under relax vel',2i10,1p,4e13.5)
```

```
c
          endif
 1990     ix = ix + scskp
          is = is + 2
          i = i + ijskp
 2000   continue
$if def,nanscr
c  Nan out scvtur, pmpph
        call nanscj(16,17)
$endif
        return
        end
```

NRC FORM 335
(2-89)
NRCM 1102,
3201, 3202

U.S. NUCLEAR REGULATORY COMMISSION

BIBLIOGRAPHIC DATA SHEET

(See instructions on the reverse)

1. REPORT NUMBER *(Assigned by NRC, Add Vol., Supp., Rev., and Addendum Numbers, if any.)*

NUREG/IA-0186

2. TITLE AND SUBTITLE

Analysis of the RELAP5/MOD3.2.2 Beta Critical Flow Models and Assessment Against Critical Flow Data From the Marviken Tests

3. DATE REPORT PUBLISHED

MONTH	YEAR
July	2000

4. FIN OR GRANT NUMBER

5. AUTHOR(S)

C. Queral, J. Mulas, C. G. de la Rua

6. TYPE OF REPORT

Technical

7. PERIOD COVERED *(Inclusive Dates)*

8. PERFORMING ORGANIZATION - NAME AND ADDRESS *(If NRC, provide Division, Office or Region, U.S. Nuclear Regulatory Commission, and mailing address; if contractor, provide name and mailing address.)*

Energy Systems Department
School of Mining Engineering
Polytechnic University of Madrid
SPAIN

9. SPONSORING ORGANIZATION - NAME AND ADDRESS *(If NRC, type "Same as above"; if contractor, provide NRC Division, Office or Region, U.S. Nuclear Regulatory Commission, and mailing address.)*

Division of Systems Analysis and Regulatory Effectiveness
Office of Nuclear Regulatory Research
U.S. Nuclear Regulatory Commission
Washington, DC 20555-0001

10. SUPPLEMENTARY NOTES

11. ABSTRACT *(200 words or less)*

In this report the critical flow models of RELAP5/MOD3.2.2 beta have been analyzed. First, an analysis of the implementation of the RELAP5/MOD3.2.2beta models have been performed in which it has been proved that the transition from the critical to the non-critical flow model is not well done for the Ransom-Trapp model. Second, a sensitivity analysis of both models (Ransom-Trapp and Henry-Fauske) in subcooled, two-phase and vapor conditions has been taken with respect to temperature, pressure, void-fraction, discharge coefficients, energy loss coefficient and disequilibrium parameter. Finally, seven Marviken tests have been simulated and compared with the experimental data in order to validate both models. As part of this assessment, an adjustment of the discharge coefficients for the Ransom-Trapp model with different nodalizations has been done and also it has been checked which are the best values of the disequilibrium parameter for the Henry-Fauske model in subcooled and two-phase conditions. Conclusions indicate that the behavior of the Henry-Fauske model is better than that of the Ransom-Trapp. In this sense, the new model is an improvement with respect to the Ransom-Trapp.

12. KEY WORDS/DESCRIPTORS *(List words or phrases that will assist researchers in locating the report.)*

RELAP5
Critical Flow

13. AVAILABILITY STATEMENT

unlimited

14. SECURITY CLASSIFICATION

(This Page)
unclassified

(This Report)
unclassified

15. NUMBER OF PAGES

16. PRICE

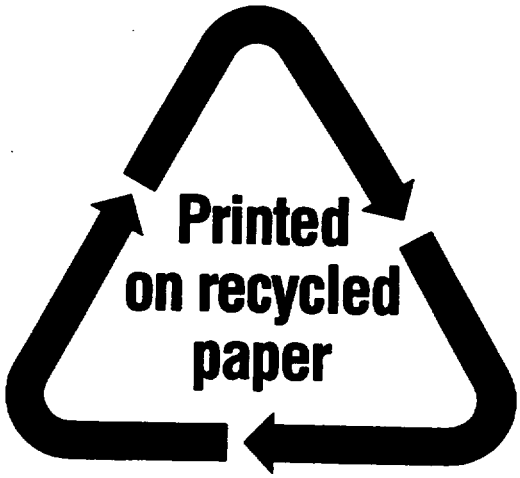

Federal Recycling Program

UNITED STATES
NUCLEAR REGULATORY COMMISSION
WASHINGTON, D.C. 20555-0001

1975 25 2000
years